1-1-2011

The Structural Basis of Flaviviridae Interaction with Antibodies and Receptors

Vincent Luca
Washington University in St. Louis

WASHINGTON UNIVERSITY

Division of Biology and Biomedical Sciences

Molecular Biophysics

Dissertation Examination Committee:
Daved Fremont, Chair
Adrianus Boon
Michael Diamond
Tom Ellenberger
Ted Hansen
Niraj Tolia

The Structural Basis for *Flaviviridae* Interaction with Antibodies and Receptors

By

Vincent Christopher Luca

A dissertation presented to the
Graduate School of Arts and Sciences
of Washington University in
partial fulfillment of the
requirements for the degree
of Doctor of Philosophy

December 2011

Saint Louis, Missouri

ABSTRACT OF THE DISSERTATION

The Structural Basis of *Flaviviridae* Interaction with Antibodies and Receptors

by

Vincent Christopher Luca

Doctor of Philosophy in Molecular Biophysics

Washington University in Saint Louis, 2011

Professor Daved H. Fremont, Chairperson

Flaviviridae are a family of enveloped, positive-stranded RNA viruses responsible for a variety of diseases including encephalitis, hemorrhagic fever and hepatocellular carcinoma. The envelope (E) proteins that coat the outer surface of these viruses provide the molecular machinery that drives receptor interaction and membrane fusion. The assignment of biological functions to specific structural elements of these E proteins has proven crucial to the understanding of viral entry into host cells. Clearance is dependent upon the presence of neutralizing antibodies that are able to disrupt several stages of this process. Given their fundamental role in the viral life cycle, we sought to determine the structural basis for envelope protein interaction with antibodies and receptors for human pathogens of the *Flaviviridae* family Japanese Encephalitis Virus, Hepatitis C Virus and St. Louis Encephalitis Virus.

Viruses of the *Flavivirus* genus within *Flaviviridae* are grouped into serocomplexes with similar clinical manifestations that are defined by cross-neutralization tests with polysera from heterologous infections. Japanese Encephalitis Virus (JEV) is the leading cause of viral encephalitis and prototypical member of the JEV

serocomplex. We determined the 2.1Å resolution crystal structure of the JEV E protein ectodomain to investigate whether structural features could contribute to our understanding of serocomplex-specific pathogenesis. JEV E possesses the three domains characteristic of flavivirus envelopes and epitope mapping of neutralizing antibodies revealed residues localized to the domain I lateral ridge, fusion loop, domain III lateral ridge and domain I-II hinge. The dimer interface, however, is remarkably small and lacks several contacts present in other flavivirus E homodimers. Uniquely conserved histidines of the JEV serocomplex suggest that pH-mediated structural transitions may be assisted by lateral interactions outside the dimer interface in the icosahedral virion. Our results suggest that variation of dimer structure and stability may influence the assembly, receptor interaction and uncoating of virions.

St. Louis Encephalitis Virus (SLEV) is another member of the JEV serocomplex with similar pathogenesis to JEV. We determined the 4.0 Å structure of the SLEV E protein in the post-fusion trimer conformation to compare it with E trimer structures from other serocomplexes. SLEV E crystallized as a trimer in the absence of lipids or detergents, requiring only low pH. However, its domain arrangement was nearly identical to other post-fusion structures. This suggests that viruses can alter dimer assembly but the structure of the activated, fusogenic conformation may be more strictly conserved.

The only member of *Flaviviridae* known to chronically infect humans is Hepatitits C Virus (HCV). HCV is blood borne and carried by roughly 3 percent of the world's population. Clinical manifestations include hepatitis, cirrhosis and hepatocellular carcinoma. HCV envelope protein E2 mediates interaction with host receptors CD81 and scavenger receptor BI (SR-BI) and is the primary target of neutralizing antibodies. To

elucidate detailed biochemical roles for these receptors' interactions with E2, we determined that the E2 ectodomain (sE2) interacts with soluble CD81 large extracellular loop (CD81-LEL) with 2:2 stoichiometry, and that this interaction inhibits subsequent engagement of SR-BI. We then evaluated the affinity and kinetics of sE2:CD81-LEL binding. Interaction between these proteins was enhanced by deletion of hypervariable region 1 (HVR1) of E2 and modulated by the genotype from which sE2 was generated. Furthermore, neutralization of HVR1-deleted HCV by a cross-reactive antibody was enhanced in a genotype-specific manner that correlated with sE2:CD81-LEL affinity measurements. Our results suggest that E2 cannot engage CD81 and SR-BI simultaneously, that HVR1 obscures conserved CD81 and antibody binding sites, and that genotypic variation influences HCV host receptor preference.

Acknowledgements

The creation of this thesis would not have been possible without the support of many wonderful colleagues, friends, and family. First, I would like to thank my thesis mentor Daved Fremont. He has shown enthusiasm at every stage of my career from his efforts in recruiting me to the biophysics program to his thoughtful commentary on my research. Daved has also provided tremendous resources and a stimulating laboratory environment that have allowed me to develop as an independent scientist. I also thank members of my thesis committee Ted Hansen, Mike Diamond, Niraj Tolia, Tom Ellenberger and Jacco Boon for their constructive commentary, guidance and encouragement. Mike Diamond was especially helpful in guiding my efforts when I was unsure how next to proceed.

I would also like to thank several collaborators and members of the Fremont lab. I am grateful to Chris Nelson, Tom Brett, Lawrence Yu and Bill McCoy, who have spent countless hours assisting me with nearly every experimental technique I have ever attempted. I have exchanged many thought and ideas with Kyle Austin and Megan Epperson, whose collective pleasant attitudes have kept my morale up throughout graduate school. Olga Lubman has been a confidant of mine since my earliest years in undergraduate research, and I am lucky to continue to work with her. Michelle Sabo has been my main scientific collaborator for many years, and her tireless work ethic led to production of many results and reagents that have proven essential to my work. The many friends I have made in the DBBS program are too many to list here, but the experiences I have shared with all of them have been invaluable.

Finally, I would like to thank my mother Dawn, my father Steve and my brother Alex for their love and support. They have taken great interest in my work, and their encouragement has kept me strong through the most difficult of times. With their help I have truly been able to pursue my dreams.

Table of Contents

Chapter 1:

Introduction to Japanese Encephalitis Virus

1.1 Abstract

Japanese Encephalitis Virus (JEV) is a mosquito borne pathogen that causes 30,000 to 50,000 cases of encephalitis and 10,000 deaths annually in Asia. There is no specific treatment for JEV infection and while multiple vaccines have been developed, licensing issues and safety concerns have restricted their availability in Asia. Consequently, generation of additional therapies and cost-effective cell culture vaccines is imperative. JEV belongs to the *Flavivirus* genus of the *Flaviviridae* family along with many other deadly human viruses including Dengue (DV), Yellow Fever (YFV) and West Nile (WNV). JEV is an enveloped virus with ~11kb positive-stranded genome that encodes a single polyprotein that is cleaved into 3 structural proteins and 7 non-structural proteins. Structural protein E is responsible for receptor interaction and membrane fusion. An icosahedral arrangement of E homodimers decorates the surface of the mature virion. However, a specific host receptor required for infection by JEV or any other flavivirus has not yet been identified. The humoral immune response, in particular the generation of neutralizing antibodies, is vital to clearance of JEV. Several studies have demonstrated that neutralization of flaviviruses is epitope-specific, with the most potent antibodies recognizing the lateral ridge of domain III of E. Further delineation of the molecular mechanisms of JEV interaction with antibodies and host receptors will therefore prove crucial to the control of this important human pathogen.

1.2 Transmission and clinical manifestations

JEV was first identified in 1934 as the causative agent of "summertime encephalitis" in Japan when it was isolated from the brain of a fatal human case[1,2]. The primary vector, the *Culex tritaeniorhynchus* mosquito[3], transmits the virus to pigs or wild birds that serve as amplifying hosts[4]. Humans may also become infected as dead-end hosts when bitten by carrier mosquitoes. The majority of infections are asymptomatic, but more severe clinical manifestations include flu-like symptoms, febrile illness and meningomyeloencephalitis[5]. While fewer than 2% of infections result in encephalitic illness[6], the fatality rate of these cases ranges from 20%-67%, with children and the elderly representing the most susceptible groups[7–9]. Approximately 30,000 to 50,000 cases of Japanese encephalitis are reported annually, although actual incidence has been estimated to be 175,000 due to substandard medical facilities and data reporting in affected regions[10].

1.3 Treatment and prevention

Therapy. Treatment of symptomatic infection with JEV is supportive. In more severe cases, this entails assisted feeding or breathing, anticonvulsants for seizure control, and osmotherapy for regulation of intracranial pressure. Currently, there is no specific antiviral therapy for JEV infection. Directed development of such an agent is unlikely given the relatively poor countries most severely affected by JEV, but it is possible that broad-spectrum antivirals designed to treat a more widespread, related virus such as Hepatitis C may be of greater interest to pharmaceutical companies[11].

Vaccines. Control of JEV and related encephalitic viruses such as West Nile Virus (WNV) and St. Louis Encephalitis Virus (SLEV) is most likely to be achieved by preventative approaches such as vaccination and regulation of vectors and amplifying hosts[2]. The first JEV vaccine was developed in Japan from the Nakayama reference strain and consisted of formalin-inactived virus isolated from mouse brains[12]. More recently, inactived cell culture derived and live attenuated vaccines from the SA-14-14-2 strain of JEV have been developed and utilized successfully in China[13], Nepal[14] and India[15]. However, despite the existence of these vaccines, they are not universally available in Asia due to cost, licensing issues and safety concerns[16–19].

1.4 JEV virology

***Genome organization of* Flaviviridae.** JEV is a member of the *Flaviviridae* family enveloped, positive-stranded RNA viruses. This family contains three genera, *Flavivirus, Hepacivirus,* and *Pestivirus.* A common feature of all members of *Flaviviridae* is the translation of the RNA genome into a single polyprotein that is cleaved into a series of structural and non-structural proteins by both host and viral proteases. However, the major differences between these viruses lie in the structural proteins located within the 5' region of the genome[20] (**Fig 1A-C**). Flaviviruses encode one envelope protein: E (**Fig 1A**), Hepaciviruses encode two: E1 and E2 (**Fig 1B**), and pestiviruses encode three: E^{rms}, E1 and E2 (**Fig 1C**).

Polyprotein processing. The *Flavivirus* genus of *Flaviviridae* contains JEV as well as related viruses WNV, Yellow Fever Virus (YFV) and Dengue Virus (DV). The genomes of these viruses encode a single polyprotein that is cleaved into 3 structural

proteins and 7 non-structural proteins[21]. The structural proteins are capsid (C), pre-membrane (prM) and envelope (E). C binds to viral RNA to form a nucleocapsid, prM prevents premature fusion with host membranes and E mediates cellular attachment and fusion[22]. The non-structural proteins are NS1, NS2A, NS2B, NS3, NS4A, NS4B and NS5[21] (**Fig 1A, 1D**). The NS1 protein is unique to flaviviruses and represents the only secreted protein encoded by any member of the *Flaviviridae* family. NS1 has multiple functions in the viral life cycle, serving as an inhibitor of complement activation[23] and a co-factor to the viral replication machinery[24,25]. NS2A contributes to viral assembly[26,27] and inhibits interferon-driven transcription[28]. NS3 is a dual-function protease/RNA-helicase[27,29], and NS2B is a co-factor for NS3 protease activity[30]. NS4A and NS4B both influence the interferon response[31,32] and NS5 is a methyltransferase[25] and RNA-polymerase[33].

1.5 Viral fusion proteins

Fusion protein overview. The major structural component of the JEV virion is the E protein. Flavivirus E proteins belong to a larger category of transmembrane viral fusion proteins that coat the outer surface of enveloped viruses. Viral fusion proteins serve as molecular machines that facilitate cellular attachment and fusion with the host membrane. While they vary dramatically in structure and sequence, the conserved mechanism by which they catalyze membrane fusion represents a remarkable example of convergent evolution[34]. The basic process by which this occurs involves a chemical or enzymatic activation event that triggers the formation of a trimer with exposed fusion peptides. The fusion peptides then insert into the host membrane and drag it together with the viral

membrane. Common examples of such an event are the acidic pH encountered in the endosome or cleavage by a host protease upon receptor binding or internalization. Differences in activation mechanism and three-dimensional structure, however, have led to the categorization of these proteins as class I[34–36], class II[36–38] or class III[39].

Class I fusion proteins. Defining features of class I fusion proteins include a predominantly helical structure and proteolytic cleavage of a precursor protein into a receptor-binding and fusion protein. Activation of class I proteins leads to formation of a trimeric, helical hairpin fusion structure that folds around a central coiled-coil[36]. The prototypical class I fusion protein is influenza hemagglutinin (HA). HA is first translated as a trimeric precursor HA0 that is cleaved during viral maturation by host proteases into receptor binding protein HA1 and fusion protein HA2[40–42] (**Fig 2A**). This cleavage event allows the resultant trimer of HA1:HA2 heterodimers to undergo a dramatic conformational change upon encountering acidic pH, leading to formation of helical hairpins[43] (**Fig 2B**). The hairpins with newly exposed fusion peptides are able to penetrate the host lipid bilayer and fuse it with the viral membrane, releasing its contents into the cytoplasm. Other notable human pathogen class I fusion glycoproteins include HIV gp41[44,45] and Ebola gp2[46,47].

Class II fusion proteins. Flavivirus E and alphavirus E1 proteins represent the class II fusion proteins[37]. Features that distinguish class II from class I proteins are a requisite dimer to trimer structural rearrangement prior to fusion and a distinct beta-strand rich, 3-domain architecture[34,36,37] (**Fig 2C**). Despite substantial differences in amino acid sequence, cellular processing and arrangement on the viral particle, structures of E and E1 are strikingly similar[43,48–52]. The conservation of these domains (the

structural details of which are described in 1.6 below) has been well established in crystal structures of flavivirus E ectodomains from Tick Borne Encephalitis Virus (TBEV)[48], DV[53] and WNV[54,55] as well as alphavirus E1 from Semliki Forest Virus (SFV)[49] and Chikungunya Virus (CV)[56]. E and E1 fusion loops are shielded by proteins prM and E2 respectively to prevent insertion into lipid bilayers during transport to the cell surface. prM and E2 are each cleaved by furin[57,58] prior to viral budding which generates an activated, mature virion capable of fusion after cellular uptake[59,60]. CryoEM reconstructions of mature WNV[61], DV[52] and SFV[51] revealed that E assembles into homodimers in flavivirus cryoEM models while SFV E1 and furin-cleaved E2 form trimers of heterodimers (**Fig 2C**). In both cases, this assembly results in burial of the fusion loop at the dimer interface, serving a protective role akin to uncleaved prM and E2 in immature particles. Upon endocytosis and subsequent exposure to the low pH environment of the endosome, E/E1 proteins on mature virions dissociate from their dimeric partners, undergo a conformational change and rearrange into a homotrimeric spike[43,50,62] (**Fig 2D**). This rearrangement brings three fusion loops together at the tip of the spike, allowing it to penetrate the endocytic membrane and drive the fusion process.

Class III fusion proteins. A third class of fusion protein was first identified upon determination of crystal structures of the Vesicular Stomatitis Virus (VSV) fusogenic G protein[63,64] and Herpes Simplex Virus 1 (HSV1) glycoprotein B (gB)[65]. G and gB have no detectable sequence similarity but adopted structurally homologous 5-domain folds previously unseen in viral fusion proteins, leading to their distinction as class III[39] (**Fig 2E**). Three of these domains, domain II, IV and the fusion-loop containing domain I, are primarily composed of beta-strands. However, domain III and V are helical, and domain

III possesses a helix that forms a trimeric coiled-coil characteristic of class I fusion proteins. Class III fusion proteins do not require proteolytic cleavage for activation or a capping protein for their fusion loop and remain trimeric in both the pre- and post-fusion conformations. Extensive structural reorganization accompanies the class III post-fusion transition. The most substantial motion involves the repositioning of domain I nearly 180° opposite its pre-fusion orientation, exposing its fusion loop[63,65] (**Fig 2F**).

1.6 JEV envelope glycoprotein structure

E domain architecture. JEV E possesses the three canonical domains characteristic of class II viral fusion proteins (**Fig 2C**). E proteins share ~35% amino acid sequence identity amongst flaviviruses[66] and are stabilized by 6 conserved disulfide bonds[67]. Domain I (DI) is a central beta-barrel flanked on opposite sides by domains II (DII) and III (DIII). An N-linked glycosylation site at ectodomain amino acid position 154 within DI is largely conserved and has been suggested to influence receptor interaction[68], neuroinvasion[69] and particle secretion[70]. Domain II is discontinuous, formed by two extended loops that protrude from domain I, and contains the hydrophobic fusion peptide at its apex[71,72]. C-terminal domain III is immunoglobulin-like and connected to DI by a flexible linker.

Structural rearrangements. Crystal structures of E bound to prM in the immature conformation[73], the pre-fusion dimer,[48,53,74] and post-fusion trimer[43,62] highlight its many structural rearrangements during the viral life cycle (**Fig 3A-C)**. These changes are driven by movements around two hinge regions that connect DI-DII and DI-DIII. Initially, the fusion loop of the immature E protein is capped by prM, with DI and DII

roughly in line with one another (**Fig 3A**). In this immature conformation, 3 E proteins assemble as trimeric spikes with a prM capping each fusion loop. When the virion encounters the low pH of the golgi, these trimers become E homodimers on the viral particle but are still associated with prM. Once prM is cleaved and released, DII kinks towards an opposing E subunit (**Fig 3B**), burying its fusion loop and facilitating the formation of a flat, antiparallel homodimer (**Fig 3B**). Upon encountering the acidic pH of the endosome, DIII undergoes a dramatic reorientation by swinging 70° toward domain II[43,59] (**Fig 3C**). The angle between DI and DII also shifts 30°, returning to a position similar to that observed in the prM-bound immature state[43]. This post-fusion trimeric "spike" brings the three fusion loops in close proximity at its tip, allowing for insertion into membranes.

Receptor interactions. Flaviviruses have been proposed to interact with a number of prospective cellular receptors, but there is little evidence that supports direct protein-protein binding or requirement for infection. αVβ3-integrin has been identified as a putative WNV and JEV receptor since antibodies raised against it are able to effectively inhibit infection in cell culture[75]. However, cell types lacking detectable expression of this integrin are still infectible[76–78]. Another tentative JEV receptor, heat shock protein 70 (Hsp70), was proposed based on inhibition of infection by anti-Hsp70 polyclonal antibodies but has only been evaluated for a single neuronal cell line (Neuro2a)[79]. Furthermore, lectins DC-SIGN and DC-SIGNR are considered attachment factors for DV[80] and WNV[77]. This attachment is mediated by N-linked glycans on the E protein and has been confirmed by the cryoEM structure of DV bound to the carbohydrate recognition domain of DC-SIGNR[81]. Despite the identification and characterization of

these many candidates, none are required for infection, leaving the nature of a "true" flavivirus receptor elusive.

Stem and transmembrane regions. The E ectodomain possesses a ~50aa C-terminal hydrophobic "stem" and transmembrane domain that contribute to membrane fusion[82,83]. The stem region lies flat along the viral membrane and is composed of two amphipathic helices. It is truncated from soluble E constructs so it is not present in available crystal structures[84]. However, modeling studies have suggested that it forms a "zipper" with a groove along the outer edge of domain II and to stabilize the post-fusion trimer[85]. Mutational analysis of the stem region has since confirmed that hydrophobic residues of the stem indeed interact with DII and affect trimer stability as well as fusion efficiency[83]. Flavivirus E is anchored to the viral membrane by a two-pass trasmembrane helix that is unique amongst viral fusion proteins. The two helices of this transmembrane hairpin have been demonstrated to interact with each other, promoting maximum trimerization and fusion efficiency[82].

1.7 Virion structure

Immature virion structure. There is currently no available JEV cryoEM structure. However, a series of elegant cryoEM studies have delineated the structures of both immature and mature structures of related viruses WNV and DV[52,60,86,86–88]. The cryoEM structure of immature DV particles at the neutral pH of the ER revealed a spiky decoration of irregular prM-E trimers on its surface. 180 copies of E and prM form these ~600Å diameter particles, which lack the T=3 quasi-symmetry expected of an icosahedral virion[86,87] (**Fig 4A**). An additional DV cryoEM structure has illuminated the structural

changes subviral particles undergo when they encounter the acidic (~6) pH of the golgi prior to maturation[60]. Pre-incubation of virus at pH 6.0 reduced DV particle diameter to ~530Å and arrangement of prM-E complexes shifted from trimeric spikes to flat dimers.[60] These dimers resembled those found in crystal structures[22,48,53,74] and mature virions[52,61] (**Fig 4B**). This reversible conformational change exposes regions of prM that allow for efficient furin cleavage prior to viral budding out of the cell[60].

Structure of mature virions After particles are trafficked out of the cell and prM is released, they undergo yet another conformational change. CryoEM structures of WNV and DV identified a herringbone-like assembly of E dimers[52,61]. Mature particles are ~500Å in diameter (**Fig 4C**), smaller than either immature form. These virions are geometrically unusual in that they display icosahedral symmetry but lack traditional T=3 symmetry[52]. The monomeric subunits that comprise the 90 E protein homodimers observed in cryoEM models are identical at 2, 3 and 5-fold axes of symmetry and thus do not have quasiequivalent environments (**Fig 4C**)[89]. The E proteins that lie at these axes do, however, differ in chemical and stoichiometric environments and can differentially interact with antibodies and receptors[90,91]. For instance, therapeutic monoclonal antibody (mAb) E16 neutralizes West Nile Virus by binding the putative receptor-binding DIII[92] at only the 2-and 3-fold axes but not at the 5-fold axis[91]. However, E16 neutralizes at a post-attachment stage of infection and allows for internalization of viral particles[93,94], suggesting that binding of a surface receptor could occur specifically at the 5-fold axis. While the reconstructed models of mature flaviviruses display uniform surfaces, it has been reported that a large population of infectious, partially mature "hybrid" particles are

released from cells[95,96]. Determination of the structure and geometry of these partially mature species presents a challenging problem due to their heterogeneous composition.

1.8 Antibody neutralization

Antibody neutralization models. Two models have been proposed to explain antibody-mediated neutralization of viruses. The maximum coating model suggests that neutralization is dependent only upon the number of antibodies binding to any site on a virus, with neutralization occurring when a critical number of sites become occupied[97,98]. This would imply that antibodies with the highest affinity for antigens would neutralize most potently. Alternatively, the functional inhibition model states that effective neutralization occurs through specific antibody-antigen interaction[98]. In this case, epitope specificity is of utmost importance: antibodies binding to locations on the virion that prevent distinct stages of the viral life cycle such as receptor interaction or membrane fusion will be more effective than high affinity antibodies binding to irrelevant regions. There is evidence to support both theories, and it is possible that antibody neutralization is virus-specific and can be a consequence of both mechanisms[97,98].

Serocomplex classification. Flavivirus infection elicits broadly cross-reactive antibodies, but polyclonal sera from infection with one virus only neutralize a subset of other viruses. The serocomplex system of classification for flaviviruses is based on this observation: membership in each serocomplex is defined by an ability to be cross-neutralized by polysera from heterologous infections[99]. Pathogenesis, tropism and clinical symptoms are generally conserved within serocomplexes. JEV is the prototypical member of the Japanese Encephalitis Virus serocomplex which includes SLEV and

WNV, viruses that all cause febrile illness, flu-like symptoms, acute or encephalitis[5,99]. DV, TBEV and YFV also represent three additional serocomplexes, each with distinct pathogeneses and tropisms.

Neutralization of flaviviruses. The humoral immune response plays a vital role in the control of flavivirus infection[100–102]. Understanding the precise molecular determinants of neutralization will provide new targets for therapeutic antibody and vaccine development such as proteins, domains or peptides. The majority of antibodies generated during infection with JEV or other flaviviruses recognize the E protein and neutralization is epitope-specific[91,93,103–105]. Identification of antibodies that bind neutralizing and non-neutralizing epitopes on E as well as mechanisms associated with recognition of these sites has allowed for the determination of structure-function relationships of domains, regions or individual residues. The most widely accepted neutralizing epitopes are the fusion loop of DII and the lateral ridge of DIII. However, antibody binding at the DI-DII hinge, DI-DIII linker, DI lateral ridge, DII lateral ridge, DII dimer interface and DII central interface have been associated with neutralization of JEV, DV and WNV [103,105–107] (**Fig 5**). The most potent neutralizing antibodies typically bind DIII and have been associated with blocking attachment and membrane fusion. Indirect evidence has implicated DIII in receptor interaction: an anti-DIII antibody, 3H5, prevents flavivirus binding to Vero cells[108,109]. However, WNV therapeutic antibody E16 allows for internalization of the virion but neutralizes by subsequently preventing fusion with the endosome[91,93,94]. Another class of broadly cross-reactive antibodies recognizes the conserved fusion loop epitope. These antibodies also prevent fusion and are generally less potent anti-DIII mAbs, potentially because the fusion loop is believed to be

inaccessible in mature virions. This so-called cryptic epitope may transiently become exposed as a result of E protein motions on the surface of the virion. Indeed, a cryoEM structure of an antibody bound to the fusion loop of mature WNV has been solved and captured a distorted viral particle, implying that these antibodies are able to access this obscured site in some capacity[110].

Antibody dependent enhancement of infection. An important concern in the design of therapeutic vaccines or antibodies for control of flaviviruses is the phenomenon of antibody dependent enhancement of infection (ADE). A neutralizing mAb will effectively prevent infection only upon occupying a critical number of sites on the virion. Sub-neutralizing concentrations of these antibodies[111,112] or coating by non-neutralizing antibodies[113] can promote uptake into cells by host Fc-receptors, leading to ADE. While JEV, TBEV, YFV and WNV are all susceptible to this phenomenon [114–117] it is most pronounced when DV infection of one serotype is followed by heterologous infection with a different DV serotype. The more severe symptoms associated with this second infection (such as a greater risk for hemorrhagic fever) are believed to be linked to ADE resulting from the circulation of antibodies generated against the previous serotype. It is postulated that these antibodies would be of lower affinity for the new virus and thus be present at sub-neutralizing concentrations capable of enhancing infection. The more severe clinical manifestations of DV linked to ADE along with the co-circulation of DV and JEV in Asia warrant serious consideration in future vaccine development.

1.9 Summary

JEV E is responsible for receptor interaction and membrane fusion, and antibody-mediated neutralization of the virus is dependent upon successful inhibition of these

functions. Given the presumed relationship between tropism and receptor interaction, I sought to investigate whether structural features of the JEV E protein could contribute to serocomplex-specific pathogenesis. No structure of a JEV serocomplex E protein has been determined in the dimeric or post-fusion trimeric conformation. Therefore, I solved the structure of the dimeric JEV E ectodomain. The results have revealed flavivirus evolutionary mechanisms for differential recognition of host ligands and highlight important differences in dimeric structures from several serocomplexes.

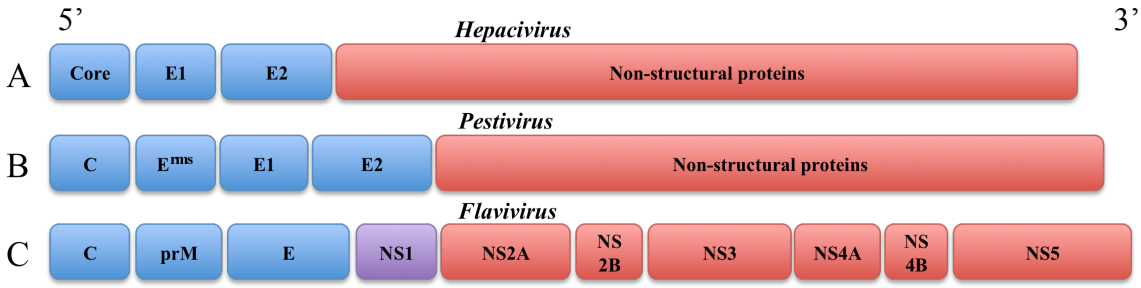

D

Protein	Localization	Primary functions
Capsid (C)	structural	Encapsulation of viral RNA
Pre-membrane (prM)	structural	Prevention of premature fusion during assembly and budding
Envelope (E)	structural	Receptor interaction, fusion with host membrane
NS1	secreted	Inhibition of complement activation, co-factor in replicase
NS2A	intracellular	Viral assembly, inhibition of interferon response
NS2B	intracellular	Co-factor for NS3 protease
NS3	intracellular	Protease, RNA-helicase
NS4A	intracellular	Modulates interferon response
NS4B	intracellular	Modulates interferon response
NS5	intracellular	Methyltransferase, RNA-polymerase

Figure 1: *Flavivirus* polyprotein processing and protein functions. Family *Flaviviridae* contains three genera with different structural proteins. A) Hepaciviruses have a core and two envelope proteins E1 and E2. B) Pestiviruses have capsid, E^{rns}, E1 and E2 proteins. C) Flaviviruses have a capsid, prM and E protein as well as 7 non-structural proteins. D) Summarized functional roles and localizations of the 10 flavivirus proteins.

Figure 2 Viral fusion protein structures.

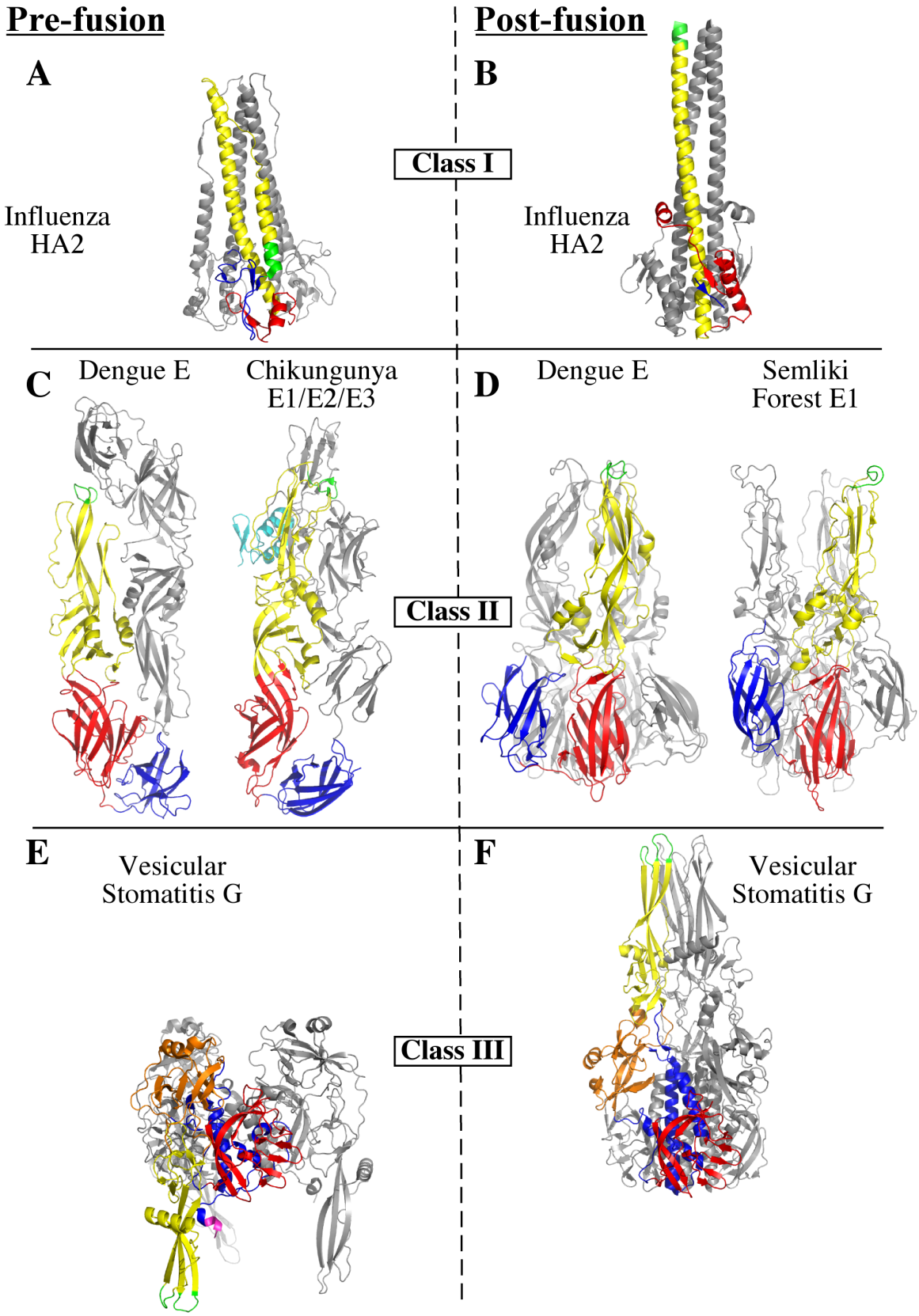

Figure 2 legend: Viral fusion protein structures. Structures of the pre-fusion (A) and post-fusion (B) conformations of class I Influenza HA2. The helical domain that elongates to expose the fusion peptide is colored yellow, fusion peptide green and N-terminal domains in red and blue. Other HA2 trimer subunits are colored grey. C) Structures of the pre-fusion class II flavivirus E homodimer and alphavirus E1-E2 heterodimer (C), and post fusion E/E1 trimers (D) DI is red, DII yellow and DIII blue. The opposing dimeric subunit of the E dimer and E2 of the E1-E2 heterodimer are colored grey, and the alphavirus E3 protein cyan. The post-fusion trimers (D) of E/E1 have a single subunit with colored domains and remaining subunits in grey. The exposed fusion loop at the tip of the spike is green. Structures of the pre-fusion (E) and post-fusion (F) class III VSV G protein. The DI lateral domain is red, DII trimerization domain blue, DIII PH domain orange, DIV fusion domain yellow, DV magenta and fusion peptide green. Only 1 of 3 trimeric subunits is colored in each panel.

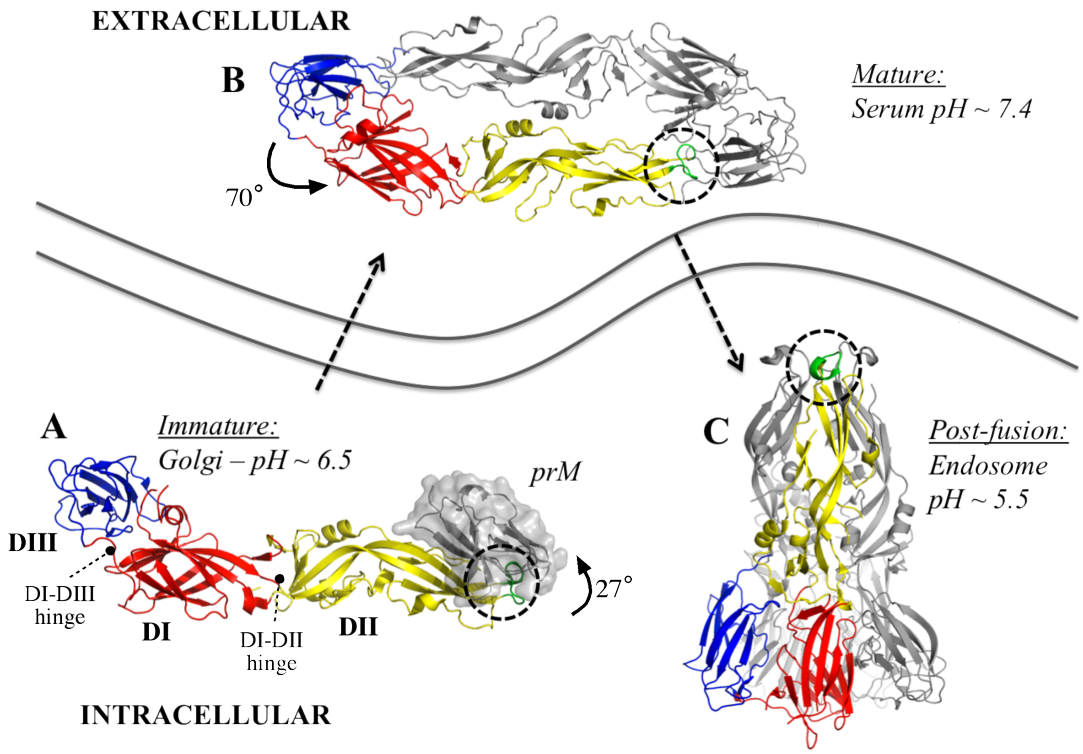

Figure 3. Conformational changes of the Flavivirus E protein. A) E protein in the immature conformation with fusion-loop (green) capped by prM (grey, space-filled). Domains I, II & III are colored red, yellow and blue respectively. The arrow and accompanying angle describe the movement of DII about the DI-DII hinge as E adopts the mature conformation. B) Mature E homodimer, with one protein colored as described in A) and the other in grey. The fusion loop is now capped by the DI/DIII cavity of the opposing subunit. The arrow in B) describes the movement of DIII about the DI-DIII hinge that accompanies formation of the post-fusion trimer. C) The fusion loop is exposed at the tip of the trimeric post-fusion spike. One subunit is colored while the other two are grey.

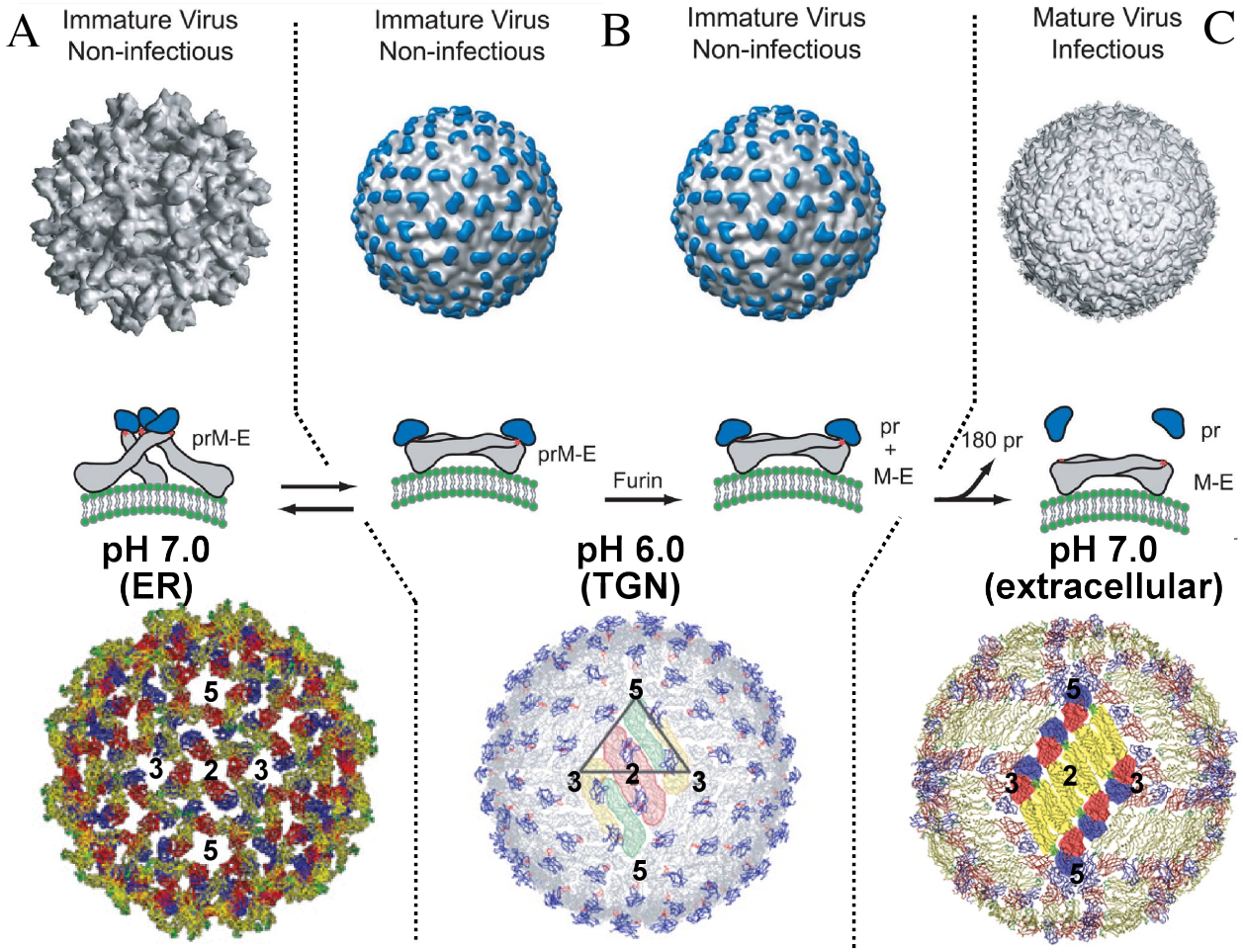

Figure 4: Flavivirus virion structures. The top panels display cryoEM densities of particles described, central panels are cartoons describing the conformation of E and bottom panels are atomic models generated by fitting E and prM into the cryoEM densities. A) Immature flavivirus particles assemble in the ER and are comprised of an icosahedral arrangement of E trimeric spikes with fusion loops capped by prM. B) As particles pass through the *trans*-golgi network prM is cleaved by furin and the lower pH causes them to settle into a dimeric arrangement. C) As the virus matures, the higher pH encountered upon secretion promotes the release of prM. In all reconstructions, axes of symmetry are labeled. Adapted from refs 22, 60 & 88.

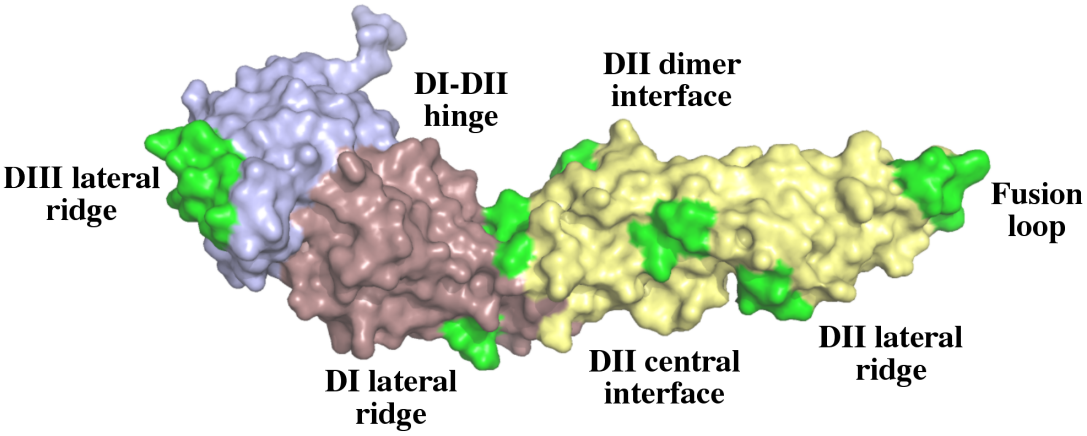

Figure 5: Neutralizing epitopes identified on the flavivirus E protein. Epitopes bound by antibodies neutralizing JEV, WNV or DV are highlighted in green and displayed on the surface of a JEV E protein. DI, DII and DIII are colored faded red, yellow and blue respectively.

1.10 References

1. Mitamura, T. *et al.* Study on Japanese encephalitis virus. Animal experiments and mosquito transmission experiments. *Kansai Iji 1* 260-261 (1936).
2. van den Hurk, A.F., Ritchie, S.A. & Mackenzie, J.S. Ecology and Geographical Expansion of Japanese Encephalitis Virus. *Annual Review of Entomology* **54**, 17-35 (2009).
3. HAMMON, W.M. & TIGERTT, W.D. Isolations of Japanese B encephalitis virus from naturally infected Culex tritaeniorhynchus collected in Japan. *Am J Hyg* **50**, 51-56 (1949).
4. BUESCHER, E.L. & SCHERER, W.F. Ecologic studies of Japanese encephalitis virus in Japan. IX. Epidemiologic correlations and conclusions. *Am. J. Trop. Med. Hyg.* **8**, 719-722 (1959).
5. Solomon, T. & Vaughn, D.W. Pathogenesis and clinical features of Japanese encephalitis and West Nile virus infections. *Curr. Top. Microbiol. Immunol* **267**, 171-194 (2002).
6. Vaughn, D.W. & Hoke, C.H., Jr The epidemiology of Japanese encephalitis: prospects for prevention. *Epidemiol Rev* **14**, 197-221 (1992).
7. Grossman, R.A., Edelman, R., Chiewanich, P., Voodhikul, P. & Siriwan, C. Study of Japanese encephalitis virus in Chiangmai valley, Thailand. II. Human clinical infections. *Am. J. Epidemiol.* **98**, 121-132 (1973).
8. Kono, R. & Kim, K.H. Comparative epidemiological features of Japanese encephalitis in the Republic of Korea, China (Taiwan) and Japan. *Bull. World Health Organ.* **40**, 263-277 (1969).

9. Parida, M. *et al.* Japanese Encephalitis Outbreak, India, 2005. *Emerging Infect. Dis.* **12**, 1427-1430 (2006).
10. Tsai, T.F. New initiatives for the control of Japanese encephalitis by vaccination: minutes of a WHO/CVI meeting, Bangkok, Thailand, 13-15 October 1998. *Vaccine* **18 Suppl 2**, 1-25 (2000).
11. Gould, E.A., Solomon, T. & Mackenzie, J.S. Does antiviral therapy have a role in the control of Japanese encephalitis? *Antiviral Res.* **78**, 140-149 (2008).
12. Shlim, D.R. & Solomon, T. Japanese encephalitis vaccine for travelers: exploring the limits of risk. *Clin. Infect. Dis.* **35**, 183-188 (2002).
13. Liu, W., Clemens, J.D., Yang, J.-ye & Xu, Z.Y. Immunization against Japanese encephalitis in China: a policy analysis. *Vaccine* **24**, 5178-5182 (2006).
14. Tandan, J.B. *et al.* Single dose of SA 14-14-2 vaccine provides long-term protection against Japanese encephalitis: a case-control study in Nepalese children 5 years after immunization. drjbtandan@yahoo.com. *Vaccine* **25**, 5041-5045 (2007).
15. Beasley, D.W.C., Lewthwaite, P. & Solomon, T. Current use and development of vaccines for Japanese encephalitis. *Expert Opin Biol Ther* **8**, 95-106 (2008).
16. Schiøler, K.L., Samuel, M. & Wai, K.L. Vaccines for preventing Japanese encephalitis. *Cochrane Database Syst Rev* CD004263 (2007).doi:10.1002/14651858.CD004263.pub2
17. Plesner, Arlien-Soborg & Herning Neurological complications to vaccination against Japanese encephalitis. *Eur. J. Neurol* **5**, 479-485 (1998).
18. Nothdurft, H.D. *et al.* Adverse reactions to Japanese encephalitis vaccine in travellers. *J. Infect* **32**, 119-122 (1996).

19. Takahashi, H., Pool, V., Tsai, T.F. & Chen, R.T. Adverse events after Japanese encephalitis vaccination: review of post-marketing surveillance data from Japan and the United States. The VAERS Working Group. *Vaccine* **18**, 2963-2969 (2000).
20. Thiel, H.J., Stark, R., Meyers, G., Weiland, E. & Rümenapf, T. Proteins encoded in the 5' region of the pestivirus genome--considerations concerning taxonomy. *Vet. Microbiol.* **33**, 213-219 (1992).
21. Chambers, T.J., Hahn, C.S., Galler, R. & Rice, C.M. Flavivirus genome organization, expression, and replication. *Annu. Rev. Microbiol.* **44**, 649-688 (1990).
22. Mukhopadhyay, S., Kuhn, R.J. & Rossmann, M.G. A structural perspective of the flavivirus life cycle. *Nat. Rev. Microbiol* **3**, 13-22 (2005).
23. Chung, K.M. *et al.* West Nile virus nonstructural protein NS1 inhibits complement activation by binding the regulatory protein factor H. *Proc. Natl. Acad. Sci. U.S.A.* **103**, 19111-19116 (2006).
24. Lindenbach, B.D. & Rice, C.M. trans-Complementation of yellow fever virus NS1 reveals a role in early RNA replication. *J. Virol.* **71**, 9608-9617 (1997).
25. Khromykh, A.A., Sedlak, P.L., Guyatt, K.J., Hall, R.A. & Westaway, E.G. Efficient trans-complementation of the flavivirus kunjin NS5 protein but not of the NS1 protein requires its coexpression with other components of the viral replicase. *J. Virol.* **73**, 10272-10280 (1999).
26. Leung, J.Y. *et al.* Role of nonstructural protein NS2A in flavivirus assembly. *J. Virol.* **82**, 4731-4741 (2008).
27. Liu, W.J., Chen, H.B. & Khromykh, A.A. Molecular and functional analyses of Kunjin virus infectious cDNA clones demonstrate the essential roles for NS2A in

virus assembly and for a nonconservative residue in NS3 in RNA replication. *J. Virol.* **77**, 7804-7813 (2003).

28. Liu, W.J., Chen, H.B., Wang, X.J., Huang, H. & Khromykh, A.A. Analysis of adaptive mutations in Kunjin virus replicon RNA reveals a novel role for the flavivirus nonstructural protein NS2A in inhibition of beta interferon promoter-driven transcription. *J. Virol.* **78**, 12225-12235 (2004).
29. Khromykh, A.A., Sedlak, P.L. & Westaway, E.G. cis- and trans-acting elements in flavivirus RNA replication. *J. Virol.* **74**, 3253-3263 (2000).
30. Chambers, T.J., Grakoui, A. & Rice, C.M. Processing of the yellow fever virus nonstructural polyprotein: a catalytically active NS3 proteinase domain and NS2B are required for cleavages at dibasic sites. *J. Virol.* **65**, 6042-6050 (1991).
31. Muñoz-Jordán, J.L. *et al.* Inhibition of alpha/beta interferon signaling by the NS4B protein of flaviviruses. *J. Virol.* **79**, 8004-8013 (2005).
32. Guo, J.-T., Hayashi, J. & Seeger, C. West Nile virus inhibits the signal transduction pathway of alpha interferon. *J. Virol.* **79**, 1343-1350 (2005).
33. Khromykh, A.A., Sedlak, P.L. & Westaway, E.G. trans-Complementation analysis of the flavivirus Kunjin ns5 gene reveals an essential role for translation of its N-terminal half in RNA replication. *J. Virol.* **73**, 9247-9255 (1999).
34. Harrison, S.C. Viral membrane fusion. *Nat Struct Mol Biol* **15**, 690-698 (2008).
35. Earp, L.J., Delos, S.E., Park, H.E. & White, J.M. The many mechanisms of viral membrane fusion proteins. *Curr. Top. Microbiol. Immunol.* **285**, 25-66 (2005).
36. Schibli, D.J. & Weissenhorn, W. Class I and class II viral fusion protein structures reveal similar principles in membrane fusion. *Mol. Membr. Biol.* **21**, 361-371 (2004).

37. Kielian, M. Class II virus membrane fusion proteins. *Virology* **344**, 38-47 (2006).

38. Kielian, M. & Rey, F.A. Virus membrane-fusion proteins: more than one way to make a hairpin. *Nat. Rev. Microbiol.* **4**, 67-76 (2006).

39. Backovic, M. & Jardetzky, T.S. Class III viral membrane fusion proteins. *Curr. Opin. Struct. Biol.* **19**, 189-196 (2009).

40. Bullough, P.A., Hughson, F.M., Skehel, J.J. & Wiley, D.C. Structure of influenza haemagglutinin at the pH of membrane fusion. *Nature* **371**, 37-43 (1994).

41. Wilson, I.A., Skehel, J.J. & Wiley, D.C. Structure of the haemagglutinin membrane glycoprotein of influenza virus at 3 A resolution. *Nature* **289**, 366-373 (1981).

42. Chen, J. *et al.* Structure of the hemagglutinin precursor cleavage site, a determinant of influenza pathogenicity and the origin of the labile conformation. *Cell* **95**, 409-417 (1998).

43. Modis, Y., Ogata, S., Clements, D. & Harrison, S.C. Structure of the dengue virus envelope protein after membrane fusion. *Nature* **427**, 313-319 (2004).

44. Weissenhorn, W., Dessen, A., Harrison, S.C., Skehel, J.J. & Wiley, D.C. Atomic structure of the ectodomain from HIV-1 gp41. *Nature* **387**, 426-430 (1997).

45. Buzon, V. *et al.* Crystal structure of HIV-1 gp41 including both fusion peptide and membrane proximal external regions. *PLoS Pathog.* **6**, e1000880 (2010).

46. Lee, J.E. *et al.* Structure of the Ebola virus glycoprotein bound to an antibody from a human survivor. *Nature* **454**, 177-182 (2008).

47. Weissenhorn, W., Carfí, A., Lee, K.H., Skehel, J.J. & Wiley, D.C. Crystal structure of the Ebola virus membrane fusion subunit, GP2, from the envelope glycoprotein ectodomain. *Mol. Cell* **2**, 605-616 (1998).

48. Rey, F.A., Heinz, F.X., Mandl, C., Kunz, C. & Harrison, S.C. The envelope glycoprotein from tick-borne encephalitis virus at 2 A resolution. *Nature* **375**, 291-298 (1995).

49. Roussel, A. *et al.* Structure and interactions at the viral surface of the envelope protein E1 of Semliki Forest virus. *Structure* **14**, 75-86 (2006).

50. Gibbons, D.L. *et al.* Conformational change and protein-protein interactions of the fusion protein of Semliki Forest virus. *Nature* **427**, 320-325 (2004).

51. Mancini, E.J., Clarke, M., Gowen, B.E., Rutten, T. & Fuller, S.D. Cryo-electron microscopy reveals the functional organization of an enveloped virus, Semliki Forest virus. *Mol. Cell* **5**, 255-266 (2000).

52. Kuhn, R.J. *et al.* Structure of dengue virus: implications for flavivirus organization, maturation, and fusion. *Cell* **108**, 717-725 (2002).

53. Modis, Y., Ogata, S., Clements, D. & Harrison, S.C. A ligand-binding pocket in the dengue virus envelope glycoprotein. *Proceedings of the National Academy of Sciences of the United States of America* **100**, 6986 -6991 (2003).

54. Kanai, R. *et al.* Crystal Structure of West Nile Virus Envelope Glycoprotein Reveals Viral Surface Epitopes. *J. Virol.* **80**, 11000-11008 (2006).

55. Nybakken, G.E., Nelson, C.A., Chen, B.R., Diamond, M.S. & Fremont, D.H. Crystal Structure of the West Nile Virus Envelope Glycoprotein. *J. Virol.* **80**, 11467-11474 (2006).

56. Voss, J.E. *et al.* Glycoprotein organization of Chikungunya virus particles revealed by X-ray crystallography. *Nature* **468**, 709-712 (2010).

57. Elshuber, S., Allison, S.L., Heinz, F.X. & Mandl, C.W. Cleavage of protein prM is necessary for infection of BHK-21 cells by tick-borne encephalitis virus. *J. Gen. Virol* **84**, 183-191 (2003).

58. Stadler, K., Allison, S., Schalich, J. & Heinz, F. Proteolytic activation of tick-borne encephalitis virus by furin. *J. Virol.* **71**, 8475-8481 (1997).

59. Allison, S.L. *et al.* Oligomeric rearrangement of tick-borne encephalitis virus envelope proteins induced by an acidic pH. *J. Virol* **69**, 695-700 (1995).

60. Yu, I.-M. *et al.* Structure of the Immature Dengue Virus at Low pH Primes Proteolytic Maturation. *Science* **319**, 1834-1837 (2008).

61. Mukhopadhyay, S., Kim, B.-S., Chipman, P.R., Rossmann, M.G. & Kuhn, R.J. Structure of West Nile virus. *Science* **302**, 248 (2003).

62. Nayak, V. *et al.* Crystal structure of dengue virus type 1 envelope protein in the postfusion conformation and its implications for membrane fusion. *J. Virol* **83**, 4338-4344 (2009).

63. Roche, S., Bressanelli, S., Rey, F.A. & Gaudin, Y. Crystal structure of the low-pH form of the vesicular stomatitis virus glycoprotein G. *Science* **313**, 187-191 (2006).

64. Roche, S., Rey, F.A., Gaudin, Y. & Bressanelli, S. Structure of the prefusion form of the vesicular stomatitis virus glycoprotein G. *Science* **315**, 843-848 (2007).

65. Heldwein, E.E. *et al.* Crystal structure of glycoprotein B from herpes simplex virus 1. *Science* **313**, 217-220 (2006).

66. Chambers, T.J., Maramorosch, K., Shatkin, A.J., Monath, T.P. & Murphy, F.A. *The Flaviviruses: Structure, Replication and Evolution*. (Academic Press: 2003).

67. Nowak, T. & Wengler, G. Analysis of disulfides present in the membrane proteins of the West Nile flavivirus. *Virology* **156**, 127-137 (1987).

68. Davis, C.W. *et al.* The location of asparagine-linked glycans on West Nile virions controls their interactions with CD209 (dendritic cell-specific ICAM-3 grabbing nonintegrin). *J. Biol. Chem* **281**, 37183-37194 (2006).

69. Shirato, K. *et al.* Viral envelope protein glycosylation is a molecular determinant of the neuroinvasiveness of the New York strain of West Nile virus. *Journal of General Virology* **85**, 3637 -3645 (2004).

70. Goto, A. *et al.* Role of the N-linked glycans of the prM and E envelope proteins in tick-borne encephalitis virus particle secretion. *Vaccine* **23**, 3043-3052 (2005).

71. Sultana, H. *et al.* Fusion loop peptide of the West Nile virus envelope protein is essential for pathogenesis and is recognized by a therapeutic cross-reactive human monoclonal antibody. *J. Immunol* **183**, 650-660 (2009).

72. Allison, S.L., Schalich, J., Stiasny, K., Mandl, C.W. & Heinz, F.X. Mutational Evidence for an Internal Fusion Peptide in Flavivirus Envelope Protein E. *J. Virol.* **75**, 4268-4275 (2001).

73. Li, L. *et al.* The flavivirus precursor membrane-envelope protein complex: structure and maturation. *Science* **319**, 1830-1834 (2008).

74. Modis, Y., Ogata, S., Clements, D. & Harrison, S.C. Variable Surface Epitopes in the Crystal Structure of Dengue Virus Type 3 Envelope Glycoprotein. *J. Virol.* **79**, 1223-1231 (2005).

75. Chu, J.J.-H. & Ng, M.-L. Interaction of West Nile virus with alpha v beta 3 integrin mediates virus entry into cells. *J. Biol. Chem* **279**, 54533-54541 (2004).

76. Medigeshi, G.R., Hirsch, A.J., Streblow, D.N., Nikolich-Zugich, J. & Nelson, J.A. West Nile virus entry requires cholesterol-rich membrane microdomains and is independent of alphavbeta3 integrin. *J. Virol.* **82**, 5212-5219 (2008).

77. Davis, C.W. *et al.* West Nile virus discriminates between DC-SIGN and DC-SIGNR for cellular attachment and infection. *J. Virol* **80**, 1290-1301 (2006).

78. Buttgereit, P. *et al.* Efficient gene transfer into lymphoma cells using adenoviral vectors combined with lipofection. *Cancer Gene Ther.* **7**, 1145-1155 (2000).

79. Das, S., Laxminarayana, S.V., Chandra, N., Ravi, V. & Desai, A. Heat shock protein 70 on Neuro2a cells is a putative receptor for Japanese encephalitis virus. *Virology* **385**, 47-57 (2009).

80. Tassaneetrithep, B. *et al.* DC-SIGN (CD209) mediates dengue virus infection of human dendritic cells. *J. Exp. Med.* **197**, 823-829 (2003).

81. Pokidysheva, E. *et al.* Cryo-EM reconstruction of dengue virus in complex with the carbohydrate recognition domain of DC-SIGN. *Cell* **124**, 485-493 (2006).

82. Fritz, R. *et al.* The unique transmembrane hairpin of flavivirus fusion protein E is essential for membrane fusion. *J. Virol.* **85**, 4377-4385 (2011).

83. Pangerl, K., Heinz, F.X. & Stiasny, K. Mutational analysis of the zippering reaction during flavivirus membrane fusion. *J. Virol.* **85**, 8495-8501 (2011).

84. Zhang, W. *et al.* Visualization of membrane protein domains by cryo-electron microscopy of dengue virus. *Nat. Struct. Biol.* **10**, 907-912 (2003).

85. Bressanelli, S. *et al.* Structure of a flavivirus envelope glycoprotein in its low-pH-induced membrane fusion conformation. *EMBO J* **23**, 728-738 (2004).

86. Zhang, Y., Kaufmann, B., Chipman, P.R., Kuhn, R.J. & Rossmann, M.G. Structure of immature West Nile virus. *J. Virol* **81**, 6141-6145 (2007).

87. Zhang, Y. *et al.* Structures of immature flavivirus particles. *EMBO J.* **22**, 2604-2613 (2003).

88. Perera, R. & Kuhn, R.J. Structural Proteomics of Dengue Virus. *Curr Opin Microbiol* **11**, 369-377 (2008).

89. CASPAR, D.L. & KLUG, A. Physical principles in the construction of regular viruses. *Cold Spring Harb. Symp. Quant. Biol.* **27**, 1-24 (1962).

90. Kaufmann, B. *et al.* Neutralization of West Nile virus by cross-linking of its surface proteins with Fab fragments of the human monoclonal antibody CR4354. *Proceedings of the National Academy of Sciences* doi:10.1073/pnas.1011036107

91. Nybakken, G.E. *et al.* Structural basis of West Nile virus neutralization by a therapeutic antibody. *Nature* **437**, 764-769 (2005).

92. Lee, J.W.-M., Chu, J.J.-H. & Ng, M.-L. Quantifying the specific binding between West Nile virus envelope domain III protein and the cellular receptor alphaVbeta3 integrin. *J. Biol. Chem* **281**, 1352-1360 (2006).

93. Oliphant, T. *et al.* Development of a humanized monoclonal antibody with therapeutic potential against West Nile virus. *Nat. Med* **11**, 522-530 (2005).

94. Thompson, B.S. *et al.* A therapeutic antibody against west nile virus neutralizes infection by blocking fusion within endosomes. *PLoS Pathog* **5**, e1000453 (2009).

95. Junjhon, J. *et al.* Influence of pr-M cleavage on the heterogeneity of extracellular dengue virus particles. *J. Virol* **84**, 8353-8358 (2010).

96. Rodenhuis-Zybert, I.A. *et al.* Immature dengue virus: a veiled pathogen? *PLoS Pathog* **6**, e1000718 (2010).

97. Burton, D.R., Saphire, E.O. & Parren, P.W. A model for neutralization of viruses based on antibody coating of the virion surface. *Curr. Top. Microbiol. Immunol.* **260**, 109-143 (2001).

98. Klasse, P.J. & Sattentau, Q.J. Mechanisms of virus neutralization by antibody. *Curr. Top. Microbiol. Immunol.* **260**, 87-108 (2001).

99. De Madrid, A.T. & Porterfield, J.S. The flaviviruses (group B arboviruses): a cross-neutralization study. *J. Gen. Virol* **23**, 91-96 (1974).

100. Diamond, M.S., Shrestha, B., Marri, A., Mahan, D. & Engle, M. B cells and antibody play critical roles in the immediate defense of disseminated infection by West Nile encephalitis virus. *J. Virol.* **77**, 2578-2586 (2003).

101. Gould, L.H. *et al.* Protective and therapeutic capacity of human single-chain Fv-Fc fusion proteins against West Nile virus. *J. Virol.* **79**, 14606-14613 (2005).

102. Tesh, R.B., Travassos da Rosa, A.P.A., Guzman, H., Araujo, T.P. & Xiao, S.-Y. Immunization with heterologous flaviviruses protective against fatal West Nile encephalitis. *Emerging Infect. Dis.* **8**, 245-251 (2002).

103. Oliphant, T. *et al.* Antibody recognition and neutralization determinants on domains I and II of West Nile Virus envelope protein. *J. Virol* **80**, 12149-12159 (2006).

104. Vogt, M.R. *et al.* Human monoclonal antibodies against West Nile virus induced by natural infection neutralize at a postattachment step. *J. Virol* **83**, 6494-6507 (2009).

105. Lin, C.-W. & Wu, S.-C. A functional epitope determinant on domain III of the Japanese encephalitis virus envelope protein interacted with neutralizing-antibody combining sites. *J. Virol* **77**, 2600-2606 (2003).

106. Goncalvez, A.P. *et al.* Humanized monoclonal antibodies derived from chimpanzee Fabs protect against Japanese encephalitis virus in vitro and in vivo. *J. Virol* **82**, 7009-7021 (2008).

107. Crill, W.D. & Chang, G.-J.J. Localization and Characterization of Flavivirus Envelope Glycoprotein Cross-Reactive Epitopes. *J Virol* **78**, 13975-13986 (2004).

108. Hiramatsu, K., Tadano, M., Men, R. & Lai, C.J. Mutational analysis of a neutralization epitope on the dengue type 2 virus (DEN2) envelope protein: monoclonal antibody resistant DEN2/DEN4 chimeras exhibit reduced mouse neurovirulence. *Virology* **224**, 437-445 (1996).

109. He, R.T. *et al.* Antibodies that block virus attachment to Vero cells are a major component of the human neutralizing antibody response against dengue virus type 2. *J. Med. Virol* **45**, 451-461 (1995).

110. Cherrier, M.V. *et al.* Structural basis for the preferential recognition of immature flaviviruses by a fusion-loop antibody. *EMBO J* **28**, 3269-3276 (2009).

111. Morens, D.M., Halstead, S.B. & Marchette, N.J. Profiles of antibody-dependent enhancement of dengue virus type 2 infection. *Microb. Pathog.* **3**, 231-237 (1987).

112. Pierson, T.C. *et al.* The stoichiometry of antibody-mediated neutralization and enhancement of West Nile virus infection. *Cell Host Microbe* **1**, 135-145 (2007).

113. Halstead, S.B. & O'Rourke, E.J. Dengue viruses and mononuclear phagocytes. I. Infection enhancement by non-neutralizing antibody. *J. Exp. Med.* **146**, 201-217 (1977).

114. Peiris, J.S. & Porterfield, J.S. Antibody-mediated enhancement of Flavivirus replication in macrophage-like cell lines. *Nature* **282**, 509-511 (1979).

115. Phillpotts, R.J., Stephenson, J.R. & Porterfield, J.S. Antibody-dependent enhancement of tick-borne encephalitis virus infectivity. *J. Gen. Virol* **66 (Pt 8)**, 1831-1837 (1985).

116. Gould, E.A. & Buckley, A. Antibody-dependent enhancement of yellow fever and Japanese encephalitis virus neurovirulence. *J. Gen. Virol* **70 (Pt 6)**, 1605-1608 (1989).

117. Mady, B.J., Erbe, D.V., Kurane, I., Fanger, M.W. & Ennis, F.A. Antibody-dependent enhancement of dengue virus infection mediated by bispecific antibodies against cell surface molecules other than Fc gamma receptors. *J. Immunol.* **147**, 3139-3144 (1991).

Chapter 2:

Crystal structure of Japanese Encephalitis Virus envelope protein

The research within this chapter consists of data that are published in the *Journal of Virology*.

Luca, VC, AbiMansour, JA, Nelson, CA, Fremont, DH. 2011. Crystal structure of the Japanese Encephalitis virus envelope protein. (In press).

This manuscript was written entirely by me. I carried out the crystal optimization, structure solution, model building, structural analysis, and multi-angle light scattering. Jad Abimansour purified the JEV E protein and assisted with crystallography, and Chris Nelson designed the JEV E DNA construct and established the protocol for refolding related E proteins.

2.1 Abstract

Japanese Encephalitis Virus (JEV) is the leading global cause of viral encephalitis. The JEV envelope protein (E) facilitates cellular attachment and membrane fusion and is the primary target of neutralizing antibodies. Herein, we have determined the 2.1Å resolution crystal structure of the JEV E ectodomain refolded from bacterial inclusion bodies. The E protein possesses the three domains characteristic of flavivirus envelopes and epitope mapping of neutralizing antibodies onto the structure reveals determinants that correspond to the domain I lateral ridge, fusion loop, domain III lateral ridge and domain I-II hinge. While monomeric in solution, JEV E assembles as an antiparallel dimer in the crystal lattice organized in a highly similar fashion as seen in cryoEM models of mature flavivirus virions. The dimer interface, however, is remarkably small and lacks many of the domain II contacts observed in other flavivirus E homodimers. Additionally, uniquely conserved histidines within the JEV serocomplex suggest that pH mediated structural transitions may be aided by lateral interactions outside the dimer interface in the icosahedral virion. Our results suggest that variation of dimer structure and stability may significantly influence the assembly, receptor interaction and uncoating of virions.

2.2 Acknowledgements

This work was supported in part by the Center for Structural Genomics of Infectious Diseases (CSGID) contract number HHSN272200700058C. We thank Mike Diamond, James Brien, Kelly Smith, Melissa Barrow and Kyle Austin for helpful discussions and experimental suggestions.

2.3 Introduction

Japanese Encephalitis Virus (JEV) is the leading cause of viral encephalitis worldwide, responsible for 30,000-50,000 cases and 10,000 deaths annually in eastern Asia. The virus is arthropod borne and naturally cycles between mosquitoes and pigs or wild birds but may also be transmitted to humans and horses[1]. There are multiple vaccines for JEV but they are not universally available in Asia due to cost, licensing issues and safety concerns[2–5]. JEV is a member of the *Flavivirus* genus along with several other viruses including West Nile Virus (WNV), Tick Borne Encephalitis Virus (TBEV) and Dengue Virus (DV).

Flaviviruses are positive-stranded RNA viruses with a 9-12kb genome that is translated as a single polyprotein that is cleaved by host and viral proteases into structural proteins capsid (C), pre-membrane (prM) and envelope (E) and 7 non-structural proteins. Capsid binds to viral RNA and forms a nucleocapsid that is enveloped by an ER derived membrane containing E and prM. E proteins are responsible for cellular attachment and possess a hydrophobic loop that mediates fusion of viral and host membranes[6–11].

During its life cycle, the JEV virion undergoes a maturation process that continuously shields the fusion peptide from premature insertion into the host cell membrane. In an immature virion, E forms irregular trimers with fusion loops capped by prM until it is cleaved in the *trans* Golgi prior to viral secretion[12–14]. E then rearranges into an icosahedral network of flat antiparallel homodimers that bury the loop at their interface[15,16]. Mature virions attach to cells and are taken up into the endosome where the acidic environment triggers an irreversible change from dimer to trimeric spikes[17–20]. This

process exposes the fusion loops that penetrate the endosome and drags together host and viral membranes, thereby releasing the nucleocapsid into the cell.

The majority of flavivirus neutralizing antibodies bind E and can inhibit several stages of the entry process including attachment and fusion[21–26]. Infection with a flavivirus results in the generation of broadly cross-reactive antibodies, but the polysera from a given infection will only neutralize a subset of other viruses. This phenomenon is the basis for the serocomplex system of classification in which flaviviruses are placed into groups defined by cross-neutralization tests with polysera from heterologous infections[27]. Clinical manifestations of infection are retained within a given serocomplex and range from febrile illness to hemorrhagic fever. The Japanese Encephalitis Virus serocomplex includes St. Louis Encephalitis Virus (SLEV), WNV and prototypical member JEV, all of which are known to cause flu-like symptoms, acute or fatal encephalitis[27,28]. The remaining serocomplexes also exhibit specific tropisms and pathogeneses, the most notable of which are represented by Tick Borne Encephalitis Virus, Yellow Fever Virus, and Dengue Virus.

Herein we have determined the crystal structure of the Japanese Encephalitis Virus E protein to investigate whether structural features could contribute to our understanding of serocomplex-specific pathogenesis. The E protein crystallized as the canonical head-to-tail flavivirus E protein dimer but with a notably small interface. The JEV E dimer has roughly half the buried surface area of any known flavivirus E structure and the majority of its contacts are between the fusion loop and Domain I-III pocket, not at the central dimerization region. We suggest that this smaller dimer interface may be

the preferred organization of E proteins from viruses in the JEV serocomplex and that it provides an effective atomic model for JEV E within mature virions.

2.4 Results

Bacterial expression and refolding of Japanese Encephalitis Virus E protein. Recombinant Japanese Encephalitis Virus E protein spanning residues 1-406 of the ectodomain was produced in *E. coli* as inclusion bodies and refolded by methods previously described for WNV E[29]. Briefly, inclusion bodies were solubilized in guanidine-HCl and β-mercaptoethanol and refolded by dilution into a buffer containing a 10:1 ratio of reduced to oxidized glutathione to allow for proper formation of disulfide bonds. Soluble E was then purified by size exclusion chromatography and anion exchange chromatography. Envelope proteins from JEV, WNV and SLEV were purified by this method, proving its effectiveness as a low-cost alternative for production of recombinant flavivirus E proteins.

Structure of Japanese Encephalitis Virus E protein. Crystals of the JEV ectodomain diffracted to 2.1Å and the structure was solved with an R_{work} of 22% and an R_{free} of 18% (data collection and refinement statistics in Table 1). Although it was refolded from bacterial inclusion bodies, JEV E retained the three-domain organization and all five disulfide bonds previously observed in other flavivirus E proteins (**Fig 1**)[16,30–34]. The central domain I is composed of a 9-stranded β-barrel located between the extended domain II and the globular domain III. Domain II is formed out of two extended loops that protrude from DI, the larger of which is stabilized by three disulfide bonds and contains the conserved fusion peptide at its tip. Domain III possesses an Ig-like fold and is found at the C-terminus of the ectodomain, connected to DI by a short peptide linker. The crystals only contained one molecule in the asymmetric unit, but application of the

orthorhombic symmetry operators allowed for the generation of the archetypal flavivirus envelope dimer.

N-linked glycosylation site. The location and presentation of the glycan linked to N^{154} has been linked to particle infectivity and interaction with putative cellular receptors DC-SIGN or DC-SIGNR[8,35,36]. Recombinant JEV E ectodomain was purified from bacterial inclusion bodies by oxidative refolding and therefore lacks this modification. In order to evaluate whether the E_o-F_0 loop region of JEV E is affected by glycosylation at N^{154}, it was was superimposed onto the glycosylated loop of the closely related West Nile Virus E structure. The main chain traces in this region overlay residues 144-164 with an overall RMSD of only 0.45, suggesting that glycosylation does not significantly affect the presentation of this region.

The Dimer Interface. The most unusual feature of the JEV E structure is its curiously small dimer interface. On the surface of the mature virion, flavivirus E proteins exist as an antiparallel dimer with the fusion peptide of DII nestled into a cavity formed by DI and DIII on the opposing subunit[15]. In the DV and TBEV E structures, there are extensive contacts across the DII-DII that stabilize this assembly. Several properties of the dimer from JEV, DV2, DV3 and TBEV envelope proteins were analyzed using the Protein Interfaces, Surfaces and Assemblies (PISA) server (Table 2)[37]. While the secondary and tertiary structure of JEV E is similar to those of other E proteins, it has only 44-56% of the buried surface area observed in other flavivirus E dimers (**Fig 2**). Additionally, it is not stabilized by any salt bridges and has far fewer hydrogen bonds across the assembly. The JEV E dimer has 843$Å^2$ of total buried surface area, while the lowest of any other structure is TBEV E with 1496$Å^2$. Further analysis revealed that the

largest disparity lies at the DII-DII interface. At this site JEV E only has 150Å^2 buried surface area, compared to 534Å^2 or greater for all of the other E proteins. The DI-DIII pocket that houses the fusion loop has relatively less buried surface area as well, but the difference at this surface is at most 0.4-fold, as compared to greater than 3-fold for the DII-DII interface. These values reinforce the conclusion that DII-DII contacts are deficient in the JEV dimer. The S_c across domain II of JEV E was only 0.372, a value below what is believed to signify a relevant protein-protein interaction. The other E proteins were found to have an S_c greater than 0.6, in line with other biologically significant interfaces. Interestingly, in all E structures the S_c of the fusion loop pocket was greater than the DII-DII region, suggesting that the precise fit of this peptide is of functional importance.

Domain I-II hinge angle. The angle between DI and DII varies substantially throughout the viral life cycle. The relative change in hinge angle between JEV E and that all other available pre-fusion E protein structures was calculated using Dyndom by individually superimposing JEV DI and DII onto those of WNV, DV2, DV3 and TBEV E proteins (**Fig 3**)[38]. The most closely related E protein, that of WNV (~75% identity), exhibited the largest difference at 16.0º, but this structure is monomeric and likely represents a pre-fusion conformation or intermediate that occurs during the trimer transition. Of the remaining E proteins, the JEV hinge most closely resembled that of TBEV, with a difference of only 3.4º. This was surprising since the two viruses are only 38% identical and that JEV E has only about 50% of the buried surface area relative to TBEV E. The differences in hinge for DV2 and DV3 E were found to be 8.7º and 9.6º respectively. While E molecules require flexibility to drive structural changes essential

for infection, it appears they also adjust to accommodate species-specific dimer arrangements.

Structural Contributions to the Interface. Several loops of the JEV E dimer subunits are devoid of contacts present in those of DV2, DV3 and TBEV (**Fig 4**). Three of these segments are specific to DV2 and DV3 E proteins. The first links strands B_o and C_o of DI and the second is the 'k-l' loop of DII (**Fig 4A**). In the DV2 and DV3 E structures, these peptides stretch across the assembly to pack against the 'i-j' loop from DII of the opposing subunit (**Fig 4A**). No residue in any of these regions contributes a dimer contact in JEV E and its 'k-l' loop actually angles up and away from the interface, in stark contrast to the conformation in DV2 E (**Fig 4C**). TBEV E, on the other hand, lacks the contacts found in the DV E proteins but possesses a 6-amino acid insertion between the f and g strands of DII (**Fig 4B**). Five of these six residues were identified as contacts in the TBEV E dimer. This insertion lies atop the 'b' and 'j' strands of the antiparallel proteins, so while TBEV has a similar hinge angle to that of JEV it buries additional surface area via this insertion. Sequence alignments of these regions of E proteins with known structures highlight their respective dimer contacts (**Fig 4D**).

JEV E Protein Stoichiometry. To assess the oligomeric state of the JEV E protein we utilized multi-angle light scattering. This technique directly determines absolute molecular weight from intrinsic scattering properties of proteins so it is advantageous over methods such as dynamic light scattering or SEC that extrapolate from hydrodynamic radius alone. Purified JEV E was loaded onto a SEC column at a concentration of 20μM and refractive index change and MALS were observed over the elution profile. JEV E eluted as a single peak with an experimentally determined

molecular weight of 45.3kD (**Fig 5A**). JEV E has a predicted molecular weight of 43.6kD, so while the soluble JEV E ectodomain packed as a crystallographic dimer, our observations demonstrate that it is predominantly monomeric in solution. The molecular weight of E proteins from WNV and SLEV were also determined in the same fashion. WNV E yielded a weight of 44.3kD (predicted 43.4kD) and SLEV yielded a weight of 39.6kD (predicted 44.2kD), both of which correspond to that of a monomer (**Fig 5B-C**). It has been previously reported that DV2, DV3 and TBEV were solution dimers, so we evaluated the oligomeric state of DV2 E to validate our assay (**Fig 5D**)[16,31,32,34]. Insect cell expressed DV2 E was utilized in these experiments as we have not been able to successfully refold DV E proteins from bacterial inclusion bodies. However, previous studies have indicated that insect cell expressed WNV E is monomeric in solution, suggesting that the single N-linked glycan does not play a significant role in the oligomeric state of the soluble ectodomain[33]. DV2 E indeed had a molecular weight of 90.3kD (predicted 45.4kD) corresponding to that of a dimer. Thus, E ectodomains from the Japanese Encephalitis Virus antigenic complex (JEV, SLEV, WNV) were all found to have monomeric molecular weights (**Fig 5A-C**), while the DV2 E protein exists predominantly as a dimer in solution (**Fig 5D**). The propensity of JEV E to remain as a solution monomer is consistent with the smaller dimer interface we observe relative to DV2 E.

Superimposition onto the Dengue Cryo-EM model. Determination of the cryoEM structures of DV and WNV revealed a framework of E protein dimers within the context of virion icosahedral symmetry[15,39]. In order to determine whether the conformation of JEV E found in our structure could, effectively reconstruct a mature icosahedral virion, we superimposed E subunits onto the main chain coordinates of DV2 E dimers from the cryoEM model. The JEV E crystal structure fits adequately into the arrangement with the only clash between main chains occurring in the b-c and h-i loops at the lateral edge of domain II at the two-fold axis (**Fig 6A**). This was unexpected given that fitting of other structures required the disassembly of E into domains and rigid body refinement[34]. Further analysis of the JEV model revealed the buried surface area between predicted dimers of the virion to be 469Å^2, yielding a difference of 364Å^2 when compared to the crystallographic dimer (**Fig 6C**). The buried dimer surface areas of other unliganded E proteins assembled into the virion were 404Å^2 for DV2 (pdb 1TG8), 424Å^2 for DV3 (pdb 1UZG) and 975Å^2 for TBEV (pdb 1SVB) (**Fig 6C**). Additionally, aligning entire dimers from the crystal structures onto the corresponding cryoEM dimers yielded RMSDs of 2.16 for JEV E, 2.43 for TBEV E, 3.35 for DV2E and 2.83 for DV3 E (**Fig 6B**). In conjunction with the BSA calculations, this RMSD suggests the JEV E structure provides an effective model for its assembly in the mature virion.

Localization of histidines. It has been suggested that protonation of histidines at acidic pH plays an important role in the flavivirus life cycle, especially during the structural transition that leads to membrane fusion. Proposed functions of these residues include homodimer dissociation, conformational changes of DIII and trimerization[40]. Mutation of broadly conserved H^{323} of TBEV E was shown to decrease infectivity but

substitution of each of the individual histidines of WNV E did not have an effect, suggesting that for some viruses they may act in concert[40,41]. In JEV E, most are found at the dimer interface, DI-III hinge and DI-II hinges, locations relevant to their proposed roles. Others, however, are situated along the lateral ridge on DII and DIII. Four histidines: His^{144}, His^{246}, His^{284} and His^{319}, are entirely conserved in flaviviruses and found at the dimer interface and inter-domain hinges. Three others: His^{81}, His^{395} and His^{397} are poorly represented in most flaviviruses but conserved within the JEV serocomplex and positioned at surfaces distal to the dimer interface (**Fig 7**). Protonation of the three serocomplex-specific histidines at this lateral edge would likely have an effect on the quaternary arrangement of adjacent subunits based on the modeling of JEV E into the DV cryo-EM reconstruction. The conservation at these positions may provide additional energy to stabilize JEV E within the icosahedral framework at neutral pH, possibly compensating for lost contributions at the dimer interface. At acidic pH, the protonation of these His residues outside the dimer interface may be an important mechanism for the regulation of viral uncoating.

Neutralizing epitopes. Mapping of antibodies onto the three-dimensional structures of the West Nile Virus and Dengue Virus E proteins has revealed the localization of dominant neutralizing epitopes[24]. Antibodies that neutralize flaviviruses localize to specific regions of the protein that span all three E protein domains, with the observation that many of the most potently neutralizing mAbs recognize the lateral ridge and 'A' strand of DIII[22,24,42–45]. Several studies have identified individual residues essential to recognition of JEV by neutralizing antibodies A3, B2, E3, NARMA3, 503, 4G2 and E3.3[26,46–50]. We have compiled and highlighted these residues on the crystal

structure and mature virion model of JEV E. These fall into four distinct regions: the DI-DII hinge, DI lateral ridge and DIII lateral ridge, which are exposed in the cryoEM structure, and the buried fusion loop (**Fig 8A**)[23,24]. Antibodies B2 (I^{126}), NARMA3 (Q^{52}) and 503 (Q^{52}, I^{126}, K^{136}, S^{275}) all bind exposed residues in the DI-DII hinge region (**Fig 8C**). Antibody A3 (K^{179}) maps to the DI lateral ridge (**Fig 8D**) and antibodies E3 (G^{302}) and E3.3 (I^{337}, F^{360}, R^{387}) recognize the DIII lateral ridge (**Fig 8E**). Broadly cross-reactive antibody 4G2 has been shown to weakly neutralize JEV and interacts with residues 104, 106 and 107 at the tip of the fusion loop (**Fig 8B**). The DI-DII hinge, DI and DIII lateral ridge epitopes are all largely exposed on the JEV mature virion, the exception being epitopes located where DIII packs at the at the inner 5-fold axis. It has been previously reported that antibodies binding WNV E at a similar epitope are also inaccessible[51]. The fusion loop epitope is commonly recognized by broadly cross-reactive antibodies and is partially buried in the JEV E model virion. This epitope is likely only transiently exposed due to motions of E proteins in the virion or in particles that contain E in the immature conformation.

2.5 Discussion

The structure of the JEV E ectodomain was determined to identify unique characteristics of this important pathogen. A notable feature of our high-resolution structure is the unusual dimeric interface of the E subunits. Measurements of homodimer buried surface area, shape complementarity, hydrogen bonds and salt bridges each indicate a less substantial interface relative to those of TBEV, DV2 and DV3. We determined the oligomeric state of JEV, SLEV and WNV E proteins and found that all were solution monomers consistent with our JEV structure as well as two independent crystal structures of monomeric WNV E[30,33]. Our results suggest that flavivirus evolution has modulated the E homodimer interface and dimeric affinity, which may substantially affect recognition by antibodies and cellular receptors.

Cryo-EM structures of mature WNV and DV have revealed a tightly packed "herringbone" arrangement of E proteins in which the dimer interface as well as lateral ridges of all three domains support a stable icosahedral framework[15,39]. E protein homodimerization has been thought to be a primary building block of the mature flavivirus virion, so it was surprising to find that JEV E and related serocomplex proteins were solution monomers. An explanation for the disparate dimer properties of the JEV envelope could be that it relies upon quaternary contacts among dimers rather than the dimer interface per se as principal load-bearing points in the viral chassis. Consistent with this hypothesis is the location of the JEV serocomplex's uniquely conserved histidines at the outer edges of the E protein where quaternary contacts would be made with other E dimer rafts. While mutation of individual histidine residues does not have a significant effect on West Nile Virus infectivity, it has been proposed that protonation of multiple

histidines in concert may drive E homodimer dissociation as an essential step in the series of conformational changes that lead to membrane fusion[40,41]. Strikingly, three of nine histidines conserved in the JEV serocomplex (**Fig 7)** are found on the lateral edge of E rather than at hinge regions or the dimer interface, suggesting that these viruses may utilize pH to regulate structural transitions by breaking non-dimer interfaces.

Analysis of contact residues across E proteins revealed specific structural differences between the JEV homodimer and that of DV or TBEV. Two DII loops, 'k-l' of DV2/3 and 'f-g' of TBEV, make contributions to the interface that are entirely absent in JEV E. The 'k-l' loop angles forward in one structure of DV2 E (1OKE) and creates a pocket that the hydrophobic ligand *n*-octyl-β-D-glucoside was observed to bind crystallographically[31]. In the JEV E structure, this loop is splayed away from the interface but opens a channel ~15Å in diameter where these contacts would be made in DV2 E (**Fig 2**). These channels are large enough to accommodate the insertion of a host ligand, raising the possibility that their presence or absence could influence viral tropism by modulating receptor interaction. Alternatively, the major contributor of E dimer contacts present in TBEV but not JEV is the 'f-g' loop of DII. In TBEV, 'f-g' contains a 6-amino acid insertion that positions itself atop 'b' and 'j' strands from the opposing DII and appears to latch the subunits together. Other TBEV E serocomplex members Powassan Virus and Langat Virus also share this insertion. Notably, a histidine residue H^{208} is conserved at the apex of the loop so protonation at low pH could provide energy to repel the molecules apart.

While our comparison of E proteins has highlighted differences between the crystal structures, serological data suggests that E may adopt a continuum of distinct

conformations on the surface of the virion. Structural proteins from flaviviruses, picornaviruses, nodaviruses and rhinoviruses are all believed to exhibit flexibility within their icosahedral organization[43,52–55]. Evidence that has arisen from the study of both DIII and fusion loop-specific neutralizing antibodies strongly suggests that the cage of flavivirus E proteins ratchet through conformations specific to the virus that encodes them. It has been reported that high temperature pre-incubation of Dengue Virus with an anti-DIII Fab resulted in an unusual, distorted cryo-EM structure in which E was locked into a previously unobserved icosahedral assembly[55]. The antibody recognizes an epitope of DIII that is partially masked in mature virions, yet the Fab managed to bind the virion and capture this unusual conformation. The West Nile specific antibody E16, on the other hand, binds a similar epitope and does not cause any significant changes in the mature arrangement upon binding[22]. The range of motion of E proteins within a mature virion could thus be influenced by the packing of the dimer. Another class of antibodies bind the fusion loop epitope that is buried in the cryo-EM model of the mature virus particle, implying that it must be at least transiently exposed during its life-cycle[24,46]. Unexpectedly, many of these fusion loop antibodies are broadly cross-reactive but do not cross-neutralize. JEV and TBEV in particular were found to have a poor correlation between the antibody affinity for their recombinant E proteins and neutralization titer, strongly suggesting that exposure of this conserved epitope differs from one viral species to the next[56]. One fusion-loop antibody, E53, has even been reported to preferentially recognize the E protein spikes that occur in immature virions[29]. Indeed, partially mature virions would be predicted to have the propensity for unique assembly based on the number and location of uncleaved prM[29,57,58]. The resulting permuted distortions of the E

protein network likely results in arrangements not represented by the icosahedral geometry of reported cryo-EM models.

It is becoming increasingly clear that the distinct arrangement of flavivirus E protein subunits can affect antibody recognition and neutralization. Recent evidence has described a neutralizing Fab with a paratope that cross-links two independent E proteins on the surface of the virion.[59]. While this antibody bound icosahedral axes outside of the dimer interface, its discovery supports the notion that specific organization of JEV, DV and TBEV E proteins can influence molecular recognition events of the virion. Additional factors that may influence E presentation on the particle surface are the transmembrane and stem-loop regions not present in the crystal structures[60]. However, their influence does not oppose the hypothesis that quaternary organization or flexibility could be distinct for individual flaviviruses.

In conclusion, the structure of the JEV E ectodomain has revealed a uniquely small dimer interface that may play a role in flavivirus stabilization, immunorecogntion and pathogenesis. Features of the protein including its monomeric solution state, relatively low buried surface area and location of serocomplex-conserved histidines suggest that it is representative of its native state in the virion. Superimposition of JEV E onto the DV cryoEM structure of the mature virion results in only a single clash and did not require the separation of domains to effectively reconstruct a JEV particle. This model also highlights the residues recognized by several classes of neutralizing antibody, indicating both surface exposed and buried epitopes. As both clearance and enhancement of flavivirus infections strongly depend on antibody recognition of complex E protein

epitopes, continued evaluation of intricate structural features of these proteins is essential to the design of future therapeutics and vaccines.

2.6 Materials and Methods

Cloning, Expression and Purification of soluble JEV E, SLEV E and WNV E.

A cDNA encoding ectodomain residues 1-406 of the JEV E from the SA-14-14-2 strain protein and those of WNV and SLEV E were cloned into the bacterial expression vector Pet21a (+). This vector was transformed into BL21-DE3 (RIL) cells (Stratagene), grown in a large-scale 4L culture and induced at an optical density 400nm of 0.8 with 1mM isopropyl β-D-1-thiogalactopyranoside (IPTG). After 4 hours the cells were centrifuged and pellets were suspended in 50mL solution buffer (50mM Tris pH 8.0, 25% sucrose, 10mM DTT) and then an equal amount of lysis buffer (50mM Tris pH 8.0, 1% TritonX-100, 100mM NaCl, 10mM DTT) was added. The mixture was treated with 0.8mg/mL lysozyme and sonicated three times for 15 seconds to disrupt cell membranes. Next, the lysate was centrifuged at 10,000xg and the pellet containing the protein inclusion bodies was washed 3x with 50mL wash buffer (50mM Tris pH 8.0, 0.5% TritonX-100, 100mM NaCl, 1mM DTT) and then once in wash buffer without TritonX-100. Purified inclusion body pellets were resuspended in 20mL TE buffer (10mM Tris pH 8.0, 1mM EDTA) and 2mL aliquots of this slurry were each solubilized in 10mL of 6M guanidine-HCl, 10mM Tris pH 8.0 and 20mM β-mercaptoethanol. These aliquots were rapidly diluted by adding 1mL every 30 minutes drop-wise into a rapidly stirring 1L reservoir of oxidative refolding buffer (400mM non-detergent sulfobetaine-201 (NDSB-201), 100mM Tris pH 8.0, 0.5mM oxidized glutathione and 5mM reduced glutathione) for overnight refolding. The refolded protein was concentrated to a volume of 10mL using an Amicon 400 concentrator with 30kD cutoff membrane and purified on a S200 size exclusion chromatography (SEC) column. It was isolated from eluted fractions corresponding to a

predicted molecular weight of 20kD, suggesting it interacts with the sephadex beads of the column since the purified protein was full-length. This material was further purified on a MonoQ anion exchange column.

Expression and Purification of DV2 E. Residues 1-394 of Dengue Virus 2 E ectodomain with an N-terminal honeybee melittin signal sequence were cloned into the baculovirus transfer vector pAcUW51. The DV2 E encoding transfer vector was then co-transfected into SF9 cells grown in serum free Sf-900 II media (Invitrogen) with the Flashbac Gold bacmid (Oxford Expression Technologies) to allow homologous recombination to generate recombinant baculoviruses. The virus was then amplified by passaging the supernatant at ratios of 1:10 into fresh SF9 cultures until titer was sufficient for large-scale expression. 5 liters of hi-five cells grown in Express Five (Invitrogen) serum free media were then infected with recombinant virus to drive expression of secreted DV2 E. The supernatant from the large-scale infection was then filtered with a 0.2μm cutoff bottle-top filter, concentrated and buffer exchanged into nickel binding buffer (300mM sodium citrate, 150mM NaCl and 50mM NaPO4 pH 8.0) using a Cetramate tangential flow concentrator with 30kD cutoff membrane. This supernatant was then purified by nickel and size-exclusion chromatography.

Crystallization of JEV E. Soluble JEV E protein was crystallized at 20°C by hanging drop vapor diffusion. Drops containing 0.5μL of protein at a concentration of 10mg/mL were combined with 0.5μL of mother liquor containing 0.1M Tris pH 8.0, 16% polyethylene glycol (PEG) 3350 and 0.2M sodium citrate and diffraction-quality crystals grew in 3 days. The crystals were cryoprotected by transferring them briefly into a drop containing 10% PEG 3350, 25% glycerol, 0.2M sodium citrate, 0.1M Tris pH 8.0 and

then cooling them in liquid nitrogen. Data were collected at the Advanced Photon Source (APS) beamline 21-ID-F. The data set was processed, integrated, scaled and merged using HKL2000[61]. JEV E crystallized in space group I222 with unit cell dimensions a=61.1 Å, b=62.4Å, c=243.0Å and contains one molecule per asymmetric unit.

Structure Determination. The structure of JEV E was solved using molecular replacement. The West Nile Virus E protein (pdb ID 2HG0/2I69) was used as a model in Phaser via the PHENIX graphical user interface[62]. Mutation of amino acid side chains and model building was done in Coot[63]. The model was refined to 2.1Å resolution in several steps using PHENIX refine. Initially rigid body refinement of each of the three domains was performed followed by atomic refinement and automated addition of waters. Coordinates were then uploaded to the TLSID server to obtain domain predictions for translation liberation screw (TLS) refinement[64,65]. The resultant structure has a final R_{work} of 18.0% and an R_{free} of 22.1% and a total of 214 waters. The N-terminal 403 of 406 amino acids of the E protein construct were built into the model.

Multi-Angle Light Scattering. JEV, WNV, SLEV and DV2 E proteins (200µg) were loaded in sizing buffer (150mM sodium chloride, 20mM HEPES pH 7.4, 0.01% sodium azide) onto a size exclusion chromatography column set up in series with a Dawn Helios II multi-angle light scattering detector (Wyatt), Optilab rEX (Wyatt) differential refractive index detector and photodiode array detector 996 (Waters). The light scattering, refractive index change and UV absorbance were each observed over the elution profile. The data was then analyzed with the Astra V macromolecular characterization software package (Wyatt) to calculate the molecular weight of each protein from the light scattering and refractive index change.

2.6.6 Protein structure accession number.

The coordinates for JEV E have been deposited in the RCSB Protein Data Bank (accession code 3P54).

Table 1: X-ray data collection and refinement statistics for JEV E protein ectodomain

Data collection	
Space group	I222
Cell dimensions	a=61.11 Å, b=62.40 Å, c=243.04 Å
Resolution (high res shell)	50.0-2.10 Å (2.18-2.10 Å)
Completeness	99.24% (99.8%)[a]
Redundancy	4.3 (4.4)
I/σ	12.1 (2.0)
R-merge (I)	0.07 (0.427)
Refinement	
Resolution (high res shell)	30.2-2.10 Å (2.17–2.10 Å)
R-work reflections[b] (*F>0)*	25663 (2470)[a]
R-free reflections	1284 (136)
R-work	0.1811 (0.2037)
R-free	0.2242 (.2294)
JEV E residues (atoms)	403 (3045)
Solvent atoms	210
Estimated coordinate error	0.230
Wilson B-factor	27.62 $Å^2$
R.m.s.d. bond lengths	0.009 Å
R.m.s.d. bond angles	1.098°

[a] Values in parentheses are for data in the highest resolution shell
[b] Statistics as defined in Phenix

Table 2: Analysis of E protein dimer interfaces

E	BSA ($Å^2$)	BSA D13-D2 ($Å^2$)	BSA DII-DII ($Å^2$)	S_C: total	S_C: D13-D2	S_C D2-D2	Interface residues	H-bonds	Salt Bridges
JEV (3P54)	843.1	346.8	149.4	0.786	0.799	0.372	38	2	0
DV2-βOG (1OKE)	1929.2	577.5	825.2	0.719	0.766	0.655	62	17	4
DV2 (1TG8)	1703.0	557.5	613.9	0.735	0.790	0.612	57	20	5
DV3 (1UZG)	1593.2	533.6	534.6	0.654	0.629	0.602	51	12	2
TBE (1SVB)	1496.2	412.8	672.1	0.702	0.754	0.633	49	8	2

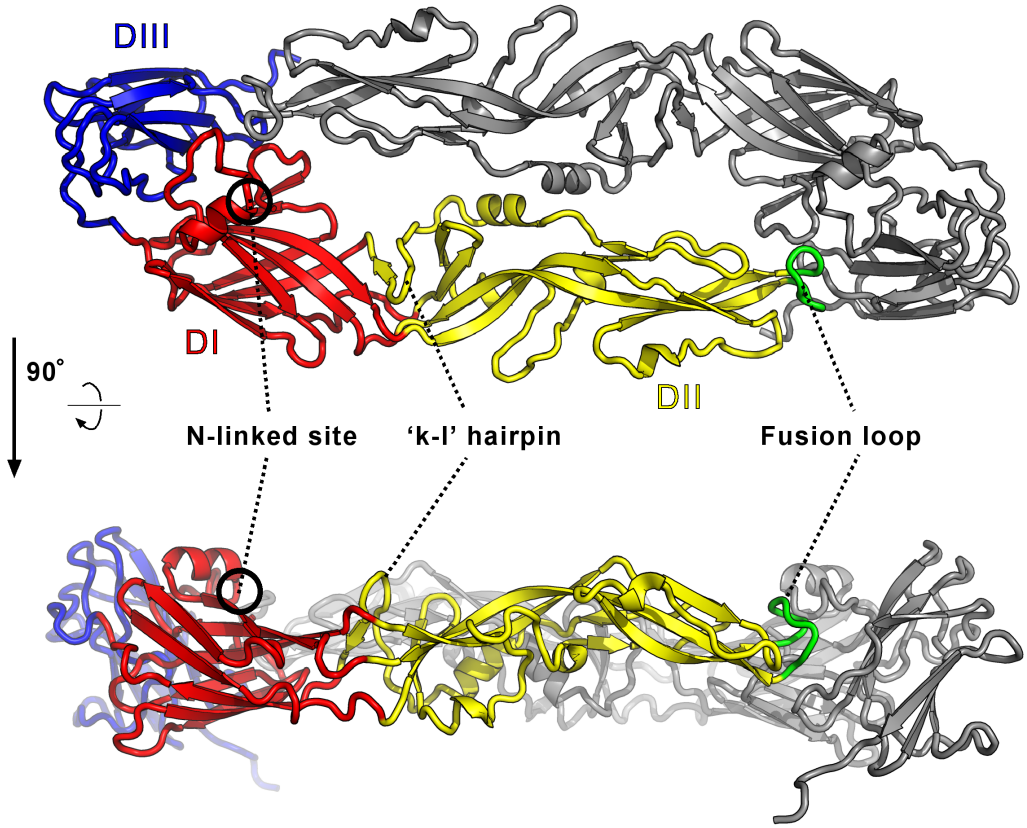

Figure 1: Crystal structure of JEV E ectodomain. JEV E possesses the three domains characteristic of flavivirus E with symmetry operators that allow for generation of the canonical E dimer. JEV E cartoon representation crystal structure with domain I highlighted in red, domain II in yellow, domain III in blue and crystallographic dimer generated from orthorhombic symmetry in grey. The structure is also shown rotated 90° into the page. The fusion loop is colored green and the 'k-l' loop and glycosylation site are indicated in both structures.

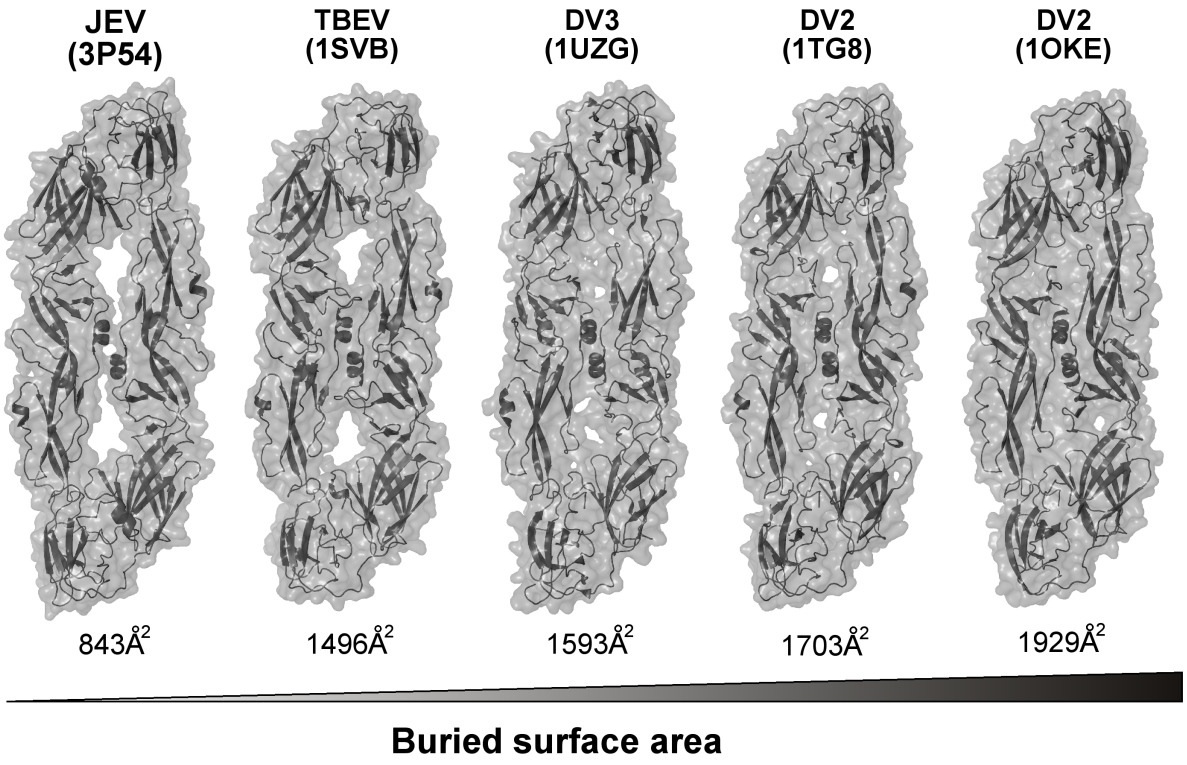

Figure 2: Relative buried surface area of dimeric flavivirus E protein structures. JEV E has a small dimer interface relative to other E crystal structures. Surface representations of known dimeric E protein crystal structures are displayed arranged in ascending order of buried surface area. Note the that JEV E and TBEV E have visible solvent channels between subunits at the dimer interface, and that these channels are absent in DV E dimers with greater buried surface area.shrinking channels between the subunits as buried surface area decreases.

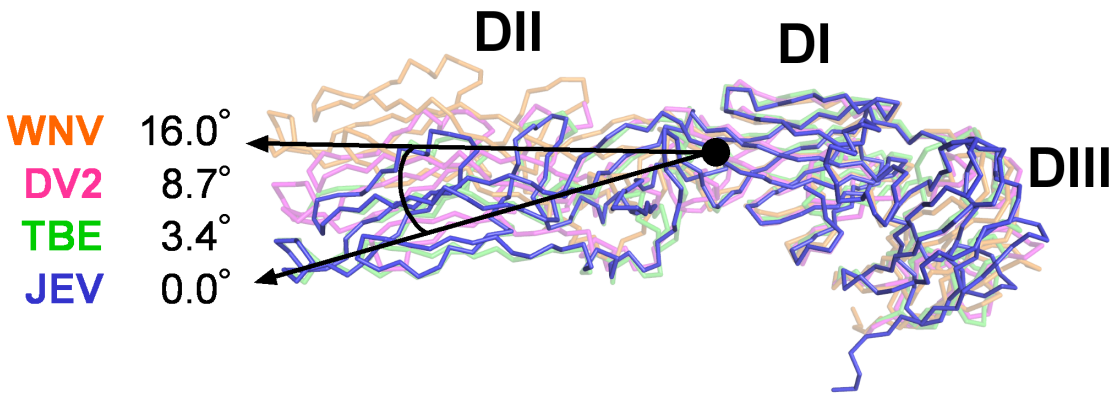

Figure 3: Comparison of E protein DI-DII hinge angles. The DI-DII hinge angle of JEV E is most similar to that of TBEV E. Various crystal structures of E were superimposed onto DI of JEV E and the relative angle between DI and DII was determined using Dyndom. Proteins are colored according to virus of origin and the numbers on the left indicate the difference in angle between DI and DII of each E protein and JEV E. The DV3 E protein was omitted for clarity and because it varies by less than 1 degree from that of DV2 E.

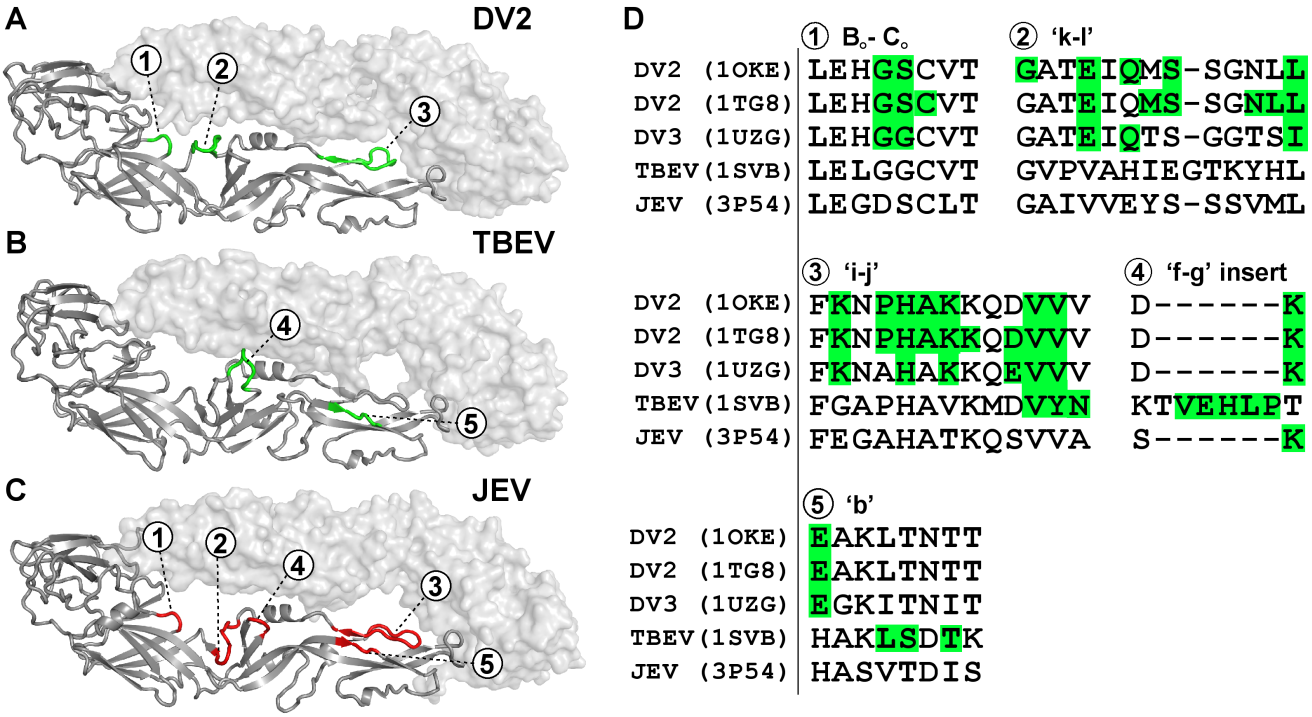

Figure 4: Dimeric contact residues in E proteins from DV, TBEV and JEV serocomplexes. Multiple loops of domains I and II have dimer contacts in TBEV and DV E that are lacking in JEV E. **A.** Loops colored green contribute to dimer contacts in the Dengue Virus and **B.** Tick Borne Encephalitis E proteins but not in JEV E. **C.** The equivalent loops are colored red in the JEV E structure. **D.** The sequences corresponding to the numbered loops are aligned for all known dimeric E protein structures, with dimer contact residues highlighted in green. The parent virus of the E protein its pdb id are shown left to the left of each sequence.

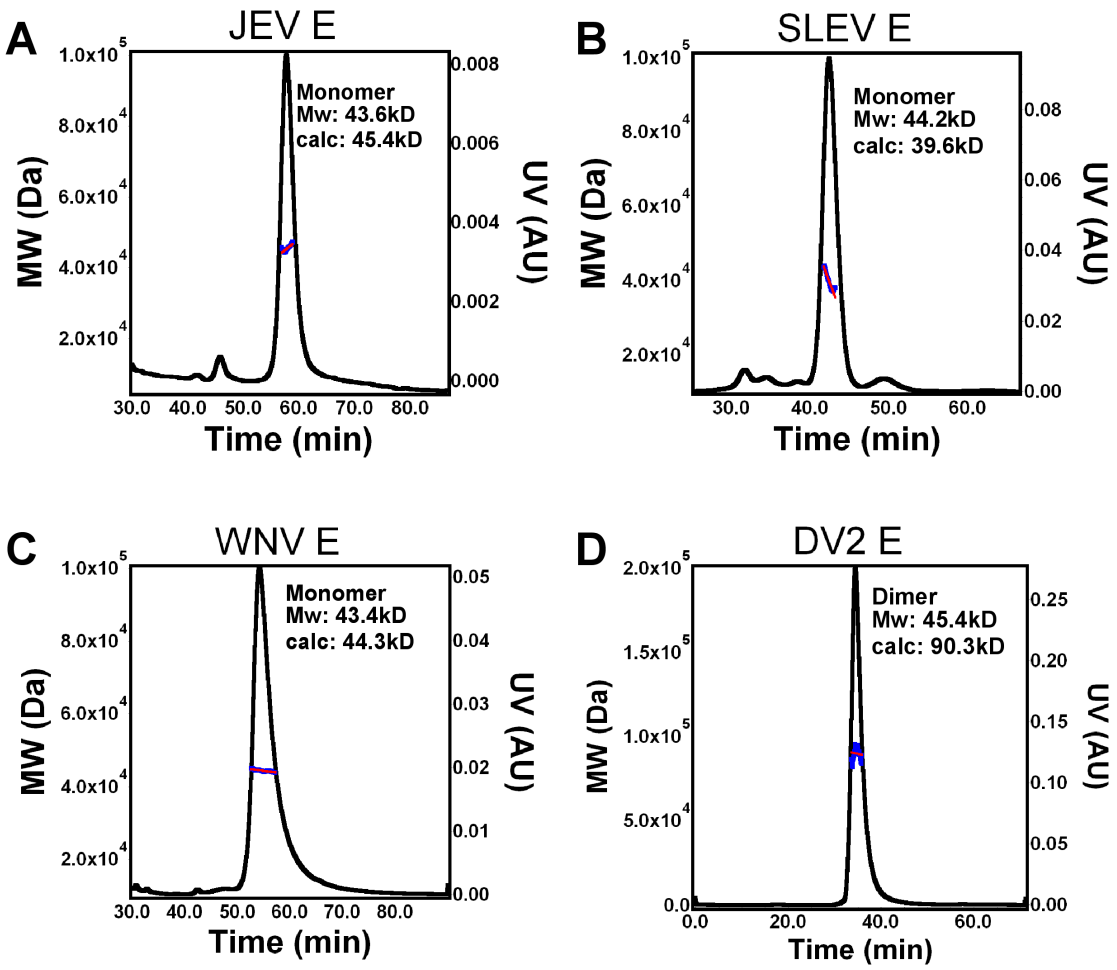

Figure 5: Multi-angle light scattering evaluation of E protein solution oligomeric state. E proteins from viruses of the JEV E serocomplex favor a monomeric solution state. Multi-angle light scattering was utilized to calculate the solution molecular weight (MW) of JEV E (**A**), SLEV E (**B**), WNV E (**C**) and DV2 E (**D**) over their elution profile on a S200 sizing column. JEV E, SLEV E and WNV E had MW corresponding to that of monomers while DV2 E was that of a dimer. The UV absorbance trace is colored black, molar mass calculation in blue and fitted molar mass in red.

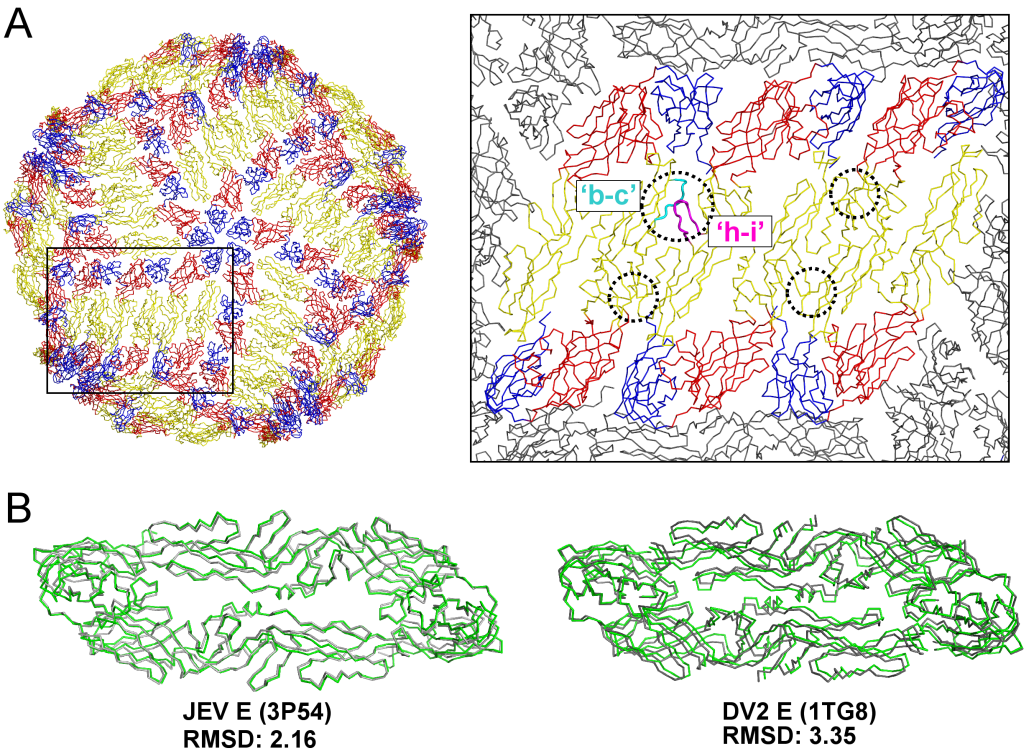

C

	Buried surface area (crystal) Å^2	Buried surface area (cryoEM) Å^2	RMSD crystal dimer: cryoEM dimer
JEV E	843	469	2.16
TBEV E	1496	975	2.43
DV2 E	1703	404	3.35
DV3 E	1593	424	2.83

Figure 6: Comparison of E protein crystal structures to DV2 cryo-EM model. A. JEV E monomers were superimposed onto E proteins from the DV2 cryoEM reconstruction. The enlarged window of E proteins at the 2-fold axis shows the only clashing main-chain loops, 'b-c' and 'h-i', in cyan and magenta respectively. **B.** JEV E and DV2 E crystal structure backbones (green) are overlaid onto artificially generated dimers created by superimposing monomers from the crystal structure onto Dengue E dimers of the cryoEM model (grey). **C.** The table describes the buried surface areas from the crystal structures, the cryoEM model dimers and the RMSD obtained by aligning the crystal structure dimers onto the cryoEM models.

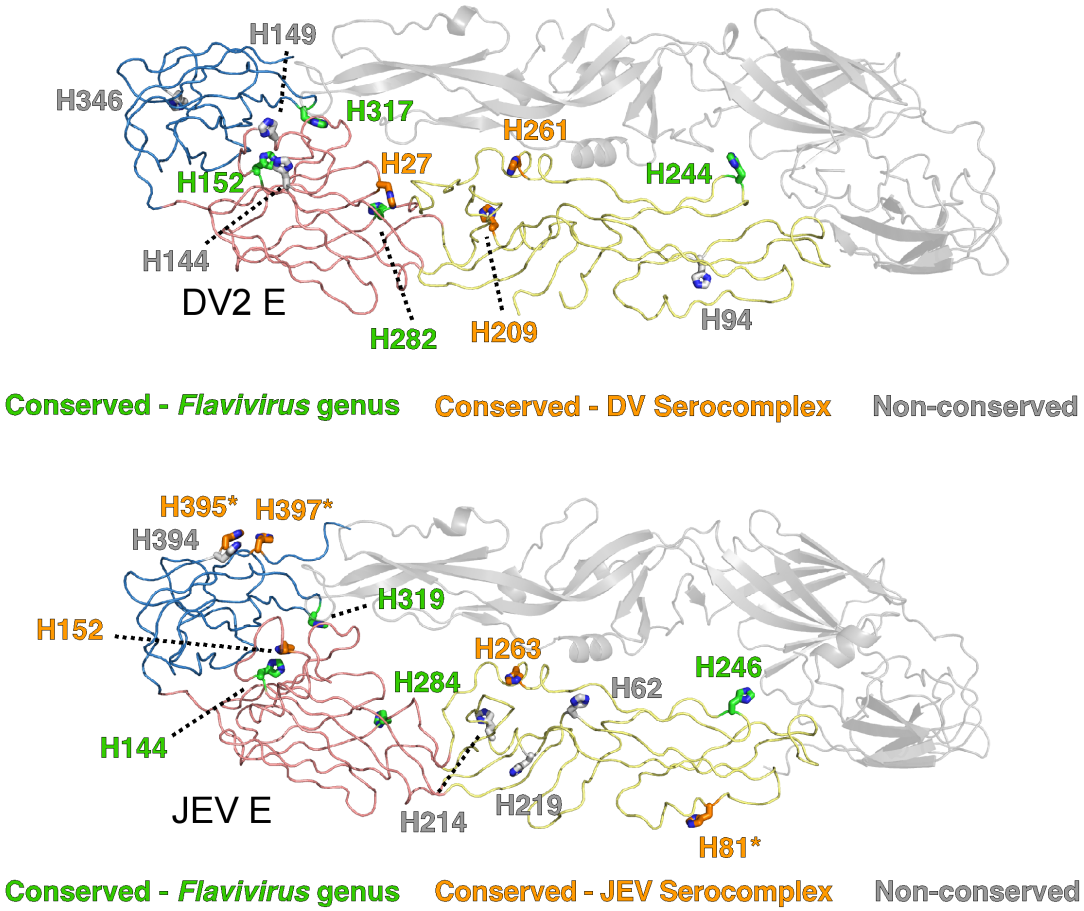

Figure 7: Conservation and localization of histidines of E proteins from the JEV and DV serocomplexes. Histidines on the lateral edge of DII and DIII are poorly represented in flaviviruses but conserved in the JEV serocomplex. Histidines of the DV2 E and JEV E proteins are shown in stick representation on one dimer subunit and labeled with their residue number for the given virus. Those colored green represent those conserved in all flaviviruses, orange are conserved in only the DV2 (top) or JEV serocomplex (bottom) and grey are not broadly conserved. Histidines fully conserved in the JEV serocomplex but not in other flaviviruses are found on the outer edge of the dimer and marked with an asterisk.

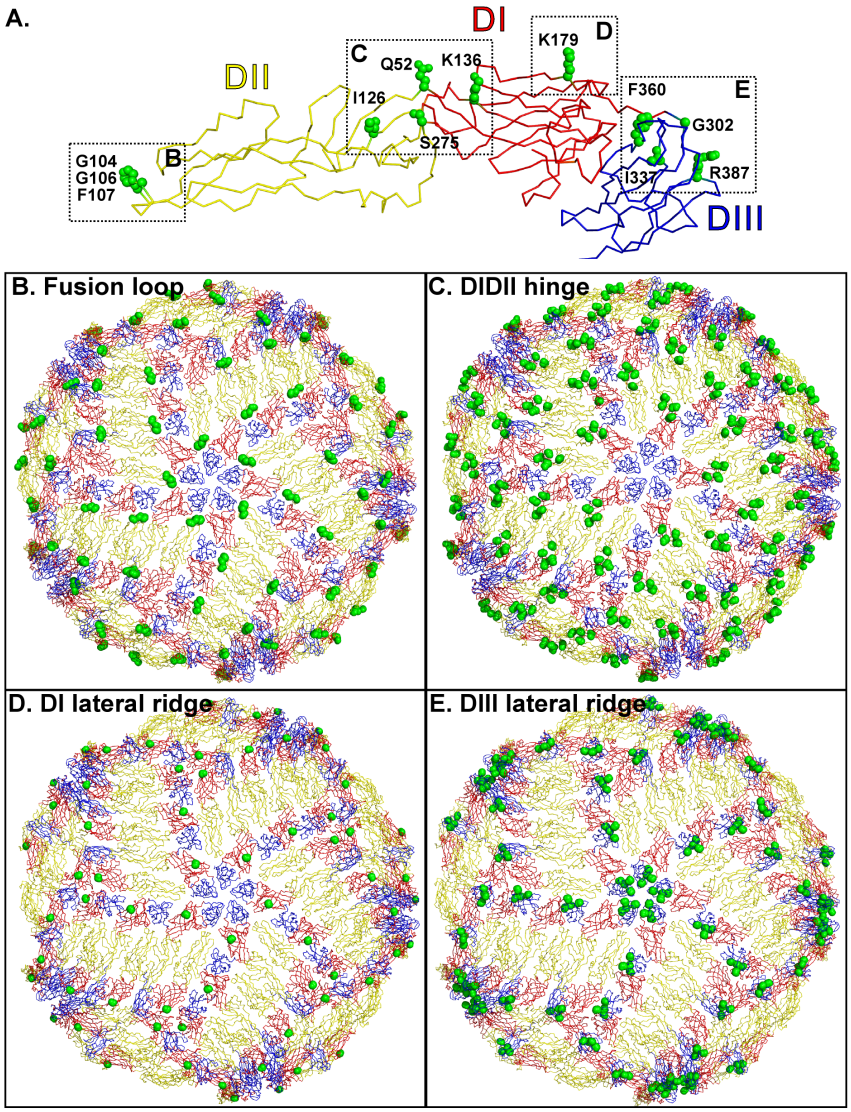

Figure 8: Mapping of neutralizing epitopes onto the JEV E protein and reconstructed virion. JEV E neutralizing epitopes are found at the DI-DII hinge, DI lateral ridge, DIII lateral ridge and fusion loop. **A.** Side chains of residues critical for binding by previously identified JEV neutralizing antibodies are colored green and in spherical representation. **B.** 4G2 (G^{104}, G^{106}, L^{107}) maps to the fusion loop. **C.** B2 (I^{126}), NARMA3 (Q^{52}) and 503 (Q^{52}, I^{126}, K^{136}, S^{275}) map to the DI-DII hinge. **D.** A3 (K^{179}) maps to the DI lateral ridge (panel D). **E.** E3 (G^{302}) and E3.3 (I^{337}, F^{360}, R^{387}) map to the DIII lateral ridge. The regions described above have also been mapped onto the model of the JEV virion to reveal their arrangement and accessibility in the icosahedral assembly.

2.7 References

1. Konno, J., Endo, K., Agatsuma, H. & Ishida, N. Cyclic outbreaks of Japanese encephalitis among pigs and humans. *Am. J. Epidemiol* **84**, 292-300 (1966).
2. Nothdurft, H.D. *et al.* Adverse reactions to Japanese encephalitis vaccine in travellers. *J. Infect* **32**, 119-122 (1996).
3. Plesner, Arlien-Soborg & Herning Neurological complications to vaccination against Japanese encephalitis. *Eur. J. Neurol* **5**, 479-485 (1998).
4. Schiøler, K.L., Samuel, M. & Wai, K.L. Vaccines for preventing Japanese encephalitis. *Cochrane Database Syst Rev* CD004263 (2007).doi:10.1002/14651858.CD004263.pub2
5. Takahashi, H., Pool, V., Tsai, T.F. & Chen, R.T. Adverse events after Japanese encephalitis vaccination: review of post-marketing surveillance data from Japan and the United States. The VAERS Working Group. *Vaccine* **18**, 2963-2969 (2000).
6. Allison, S.L., Schalich, J., Stiasny, K., Mandl, C.W. & Heinz, F.X. Mutational Evidence for an Internal Fusion Peptide in Flavivirus Envelope Protein E. *J. Virol.* **75**, 4268-4275 (2001).
7. Chu, J.J.-H. & Ng, M.-L. Interaction of West Nile virus with alpha v beta 3 integrin mediates virus entry into cells. *J. Biol. Chem* **279**, 54533-54541 (2004).
8. Davis, C.W. *et al.* West Nile virus discriminates between DC-SIGN and DC-SIGNR for cellular attachment and infection. *J. Virol* **80**, 1290-1301 (2006).
9. Huang, C.Y.-H. *et al.* The dengue virus type 2 envelope protein fusion peptide is essential for membrane fusion. *Virology* **396**, 305-315 (2010).

10. Lee, J.W.-M., Chu, J.J.-H. & Ng, M.-L. Quantifying the specific binding between West Nile virus envelope domain III protein and the cellular receptor alphaVbeta3 integrin. *J. Biol. Chem* **281**, 1352-1360 (2006).
11. Navarro-Sanchez, E. *et al.* Dendritic-cell-specific ICAM3-grabbing non-integrin is essential for the productive infection of human dendritic cells by mosquito-cell-derived dengue viruses. *EMBO Rep* **4**, 723-728 (2003).
12. Elshuber, S., Allison, S.L., Heinz, F.X. & Mandl, C.W. Cleavage of protein prM is necessary for infection of BHK-21 cells by tick-borne encephalitis virus. *J. Gen. Virol* **84**, 183-191 (2003).
13. Stadler, K., Allison, S., Schalich, J. & Heinz, F. Proteolytic activation of tick-borne encephalitis virus by furin. *J. Virol.* **71**, 8475-8481 (1997).
14. Yu, I.-M. *et al.* Structure of the Immature Dengue Virus at Low pH Primes Proteolytic Maturation. *Science* **319**, 1834-1837 (2008).
15. Kuhn, R.J. *et al.* Structure of dengue virus: implications for flavivirus organization, maturation, and fusion. *Cell* **108**, 717-725 (2002).
16. Rey, F.A., Heinz, F.X., Mandl, C., Kunz, C. & Harrison, S.C. The envelope glycoprotein from tick-borne encephalitis virus at 2 A resolution. *Nature* **375**, 291-298 (1995).
17. Allison, S.L. *et al.* Oligomeric rearrangement of tick-borne encephalitis virus envelope proteins induced by an acidic pH. *J. Virol* **69**, 695-700 (1995).
18. Bressanelli, S. *et al.* Structure of a flavivirus envelope glycoprotein in its low-pH-induced membrane fusion conformation. *EMBO J* **23**, 728-738 (2004).

19. Modis, Y., Ogata, S., Clements, D. & Harrison, S.C. Structure of the dengue virus envelope protein after membrane fusion. *Nature* **427**, 313-319 (2004).
20. Nayak, V. *et al.* Crystal structure of dengue virus type 1 envelope protein in the postfusion conformation and its implications for membrane fusion. *J. Virol* **83**, 4338-4344 (2009).
21. He, R.T. *et al.* Antibodies that block virus attachment to Vero cells are a major component of the human neutralizing antibody response against dengue virus type 2. *J. Med. Virol* **45**, 451-461 (1995).
22. Nybakken, G.E. *et al.* Structural basis of West Nile virus neutralization by a therapeutic antibody. *Nature* **437**, 764-769 (2005).
23. Oliphant, T. *et al.* Development of a humanized monoclonal antibody with therapeutic potential against West Nile virus. *Nat. Med* **11**, 522-530 (2005).
24. Oliphant, T. *et al.* Antibody recognition and neutralization determinants on domains I and II of West Nile Virus envelope protein. *J. Virol* **80**, 12149-12159 (2006).
25. Thompson, B.S. *et al.* A therapeutic antibody against west nile virus neutralizes infection by blocking fusion within endosomes. *PLoS Pathog* **5**, e1000453 (2009).
26. Wu, K.-P. *et al.* Structural basis of a flavivirus recognized by its neutralizing antibody: solution structure of the domain III of the Japanese encephalitis virus envelope protein. *J. Biol. Chem* **278**, 46007-46013 (2003).
27. De Madrid, A.T. & Porterfield, J.S. The flaviviruses (group B arboviruses): a cross-neutralization study. *J. Gen. Virol* **23**, 91-96 (1974).

28. Solomon, T. & Vaughn, D.W. Pathogenesis and clinical features of Japanese encephalitis and West Nile virus infections. *Curr. Top. Microbiol. Immunol* **267**, 171-194 (2002).

29. Cherrier, M.V. *et al.* Structural basis for the preferential recognition of immature flaviviruses by a fusion-loop antibody. *EMBO J* **28**, 3269-3276 (2009).

30. Kanai, R. *et al.* Crystal Structure of West Nile Virus Envelope Glycoprotein Reveals Viral Surface Epitopes. *J. Virol.* **80**, 11000-11008 (2006).

31. Modis, Y., Ogata, S., Clements, D. & Harrison, S.C. A ligand-binding pocket in the dengue virus envelope glycoprotein. *Proceedings of the National Academy of Sciences of the United States of America* **100**, 6986 -6991 (2003).

32. Modis, Y., Ogata, S., Clements, D. & Harrison, S.C. Variable Surface Epitopes in the Crystal Structure of Dengue Virus Type 3 Envelope Glycoprotein. *J. Virol.* **79**, 1223-1231 (2005).

33. Nybakken, G.E., Nelson, C.A., Chen, B.R., Diamond, M.S. & Fremont, D.H. Crystal Structure of the West Nile Virus Envelope Glycoprotein. *J. Virol.* **80**, 11467-11474 (2006).

34. Zhang, Y. *et al.* Conformational changes of the flavivirus E glycoprotein. *Structure* **12**, 1607-1618 (2004).

35. Davis, C.W. *et al.* The location of asparagine-linked glycans on West Nile virions controls their interactions with CD209 (dendritic cell-specific ICAM-3 grabbing nonintegrin). *J. Biol. Chem* **281**, 37183-37194 (2006).

36. Hanna, S.L. *et al.* N-linked glycosylation of west nile virus envelope proteins influences particle assembly and infectivity. *J. Virol* **79**, 13262-13274 (2005).

37. Krissinel, E. & Henrick, K. Inference of macromolecular assemblies from crystalline state. *J. Mol. Biol* **372**, 774-797 (2007).

38. Hayward, S. & Berendsen, H.J. Systematic analysis of domain motions in proteins from conformational change: new results on citrate synthase and T4 lysozyme. *Proteins* **30**, 144-154 (1998).

39. Mukhopadhyay, S., Kim, B.-S., Chipman, P.R., Rossmann, M.G. & Kuhn, R.J. Structure of West Nile virus. *Science* **302**, 248 (2003).

40. Fritz, R., Stiasny, K. & Heinz, F.X. Identification of specific histidines as pH sensors in flavivirus membrane fusion. *The Journal of Cell Biology* **183**, 353 -361 (2008).

41. Nelson, S., Poddar, S., Lin, T.-Y. & Pierson, T.C. Protonation of individual histidine residues is not required for the pH-dependent entry of west nile virus: evaluation of the "histidine switch" hypothesis. *J. Virol* **83**, 12631-12635 (2009).

42. Brien, J.D. *et al.* Genotype-specific neutralization and protection by antibodies against dengue virus type 3. *J. Virol* **84**, 10630-10643 (2010).

43. Delaet, I. & Boeyé, A. Monoclonal antibodies that disrupt poliovirus only at fever temperatures. *J. Virol* **67**, 5299-5302 (1993).

44. Sánchez, M.D. *et al.* Characterization of neutralizing antibodies to West Nile virus. *Virology* **336**, 70-82 (2005).

45. Sultana, H. *et al.* Fusion loop peptide of the West Nile virus envelope protein is essential for pathogenesis and is recognized by a therapeutic cross-reactive human monoclonal antibody. *J. Immunol* **183**, 650-660 (2009).

46. Crill, W.D. & Chang, G.-J.J. Localization and Characterization of Flavivirus Envelope Glycoprotein Cross-Reactive Epitopes. *J Virol* **78**, 13975-13986 (2004).

47. Goncalvez, A.P. *et al.* Humanized monoclonal antibodies derived from chimpanzee Fabs protect against Japanese encephalitis virus in vitro and in vivo. *J. Virol* **82**, 7009-7021 (2008).

48. Kobayashi, Y., Hasegawa, H. & Yamauchi, T. Studies on the antigenic structure of Japanese encephalitis virus using monoclonal antibodies. *Microbiol. Immunol* **29**, 1069-1082 (1985).

49. Morita, K. *et al.* Locus of a virus neutralization epitope on the Japanese encephalitis virus envelope protein determined by use of long PCR-based region-specific random mutagenesis. *Virology* **287**, 417-426 (2001).

50. Vogt, M.R. *et al.* Human monoclonal antibodies against West Nile virus induced by natural infection neutralize at a postattachment step. *J. Virol* **83**, 6494-6507 (2009).

51. Kaufmann, B. *et al.* West Nile virus in complex with the Fab fragment of a neutralizing monoclonal antibody. *Proceedings of the National Academy of Sciences* **103**, 12400 -12404 (2006).

52. Bothner, B., Dong, X.F., Bibbs, L., Johnson, J.E. & Siuzdak, G. Evidence of viral capsid dynamics using limited proteolysis and mass spectrometry. *J. Biol. Chem* **273**, 673-676 (1998).

53. Delaet, I. & Boeyé, A. Capsid destabilization is required for antibody-mediated disruption of poliovirus. *J. Gen. Virol* **75 (Pt 3)**, 581-587 (1994).

54. Lewis, J.K., Bothner, B., Smith, T.J. & Siuzdak, G. Antiviral agent blocks breathing of the common cold virus. *Proc. Natl. Acad. Sci. U.S.A* **95**, 6774-6778 (1998).

55. Lok, S.-M. *et al.* Binding of a neutralizing antibody to dengue virus alters the arrangement of surface glycoproteins. *Nat Struct Mol Biol* **15**, 312-317 (2008).

56. Stiasny, K., Kiermayr, S., Holzmann, H. & Heinz, F.X. Cryptic Properties of a Cluster of Dominant Flavivirus Cross-Reactive Antigenic Sites. *J. Virol.* **80**, 9557-9568 (2006).

57. Junjhon, J. *et al.* Influence of pr-M cleavage on the heterogeneity of extracellular dengue virus particles. *J. Virol* **84**, 8353-8358 (2010).

58. Rodenhuis-Zybert, I.A. *et al.* Immature dengue virus: a veiled pathogen? *PLoS Pathog* **6**, e1000718 (2010).

59. Kaufmann, B. *et al.* Neutralization of West Nile virus by cross-linking of its surface proteins with Fab fragments of the human monoclonal antibody CR4354. *Proceedings of the National Academy of Sciences* doi:10.1073/pnas.1011036107

60. Kiermayr, S., Stiasny, K. & Heinz, F.X. Impact of quaternary organization on the antigenic structure of the tick-borne encephalitis virus envelope glycoprotein E. *J. Virol* **83**, 8482-8491 (2009).

61. Minor, W. & Otwinowski, Z. Processing of X-ray diffraction data collected in oscillation mode. *Methods in Enzymology* **276**, 307-326 (1997).

62. Adams, P.D. *et al.* PHENIX: building new software for automated crystallographic structure determination. *Acta Crystallogr. D Biol. Crystallogr* **58**, 1948-1954 (2002).

63. Kleywegt, G.J. *et al.* The Uppsala Electron-Density Server. *Acta Crystallogr. D Biol. Crystallogr* **60**, 2240-2249 (2004).

64. Merritt, E.A. & Painter, J. TLSMD web server for the generation of multi-group TLS models. *Journal of Applied Crystallography* **39**, 109-111

65. Painter, J. & Merritt, E.A. Optimal description of a protein structure in terms of multiple groups undergoing TLS motion. *Acta Crystallogr D Biol Crystallogr* **62**, 439-450 (2006).

Chapter 3:

The St. Louis Encephalitis Virus envelope fusogenic trimer

3.1 Abstract

St. Louis Encephalitis Virus (SLEV) is a member of the JEV serocomplex of flaviviruses and can cause febrile illness, nausea and encephalitis. We determined the 4.0 Å structure of its E protein in the post-fusion trimer conformation to compare it with E trimer structures from other serocomplexes. SLEV E crystallized as a trimer in the absence of lipids or detergents, requiring only low pH. However, its domain arrangement was nearly identical to other post-fusion structures. This suggests that viruses can alter dimer assembly but the structure of the activated, fusogenic conformation may be more strictly conserved.

3.2 Cloning, purification and crystallization of SLEV E

Cloning and purification of SLEV E was carried out as described in 2.5.1. After successful refolding, SLEV E was buffer exchanged into 50mM sodium acetate pH 5.5 and concentrated to ~5mg/mL. SLEV E protein was crystallized at 20°C by hanging drop vapor diffusion. Drops containing 0.5μL of protein at a were combined with 0.5μL of mother liquor containing 0.1M sodium acetate pH 5.5, 3% polyethylene glycol (PEG) 8000 and 2% ethylene glycol. Diffraction-quality crystals grew in 3-7 days (**Fig 1A**). Crystals were cryoprotected by transferring them briefly into a drop containing 10% PEG 8000, 25% ethylene glycol and 0.1M sodium acetate pH 5.5 and then cooling them in liquid nitrogen. Data were collected at the Advanced Photon Source (APS) beamline ID19. The data set was processed, integrated, scaled and merged using HKL2000[1]. SLEV E crystallized in space group I23 with unit cell dimensions a = b = c = 177.34 Å and contains one molecule per asymmetric unit.

3.3 Structure determination

The structure of SLEV E was solved using molecular replacement. The sequence of SLEV E was threaded onto the structure of the post-fusion E trimer from Dengue 2[2] (pdb ID 1OK8) using Phyre2[3]. This model was then used for molecular replacement using Phaser within the PHENIX graphical interface[4]. An additional model of SLEV E was generated by threading SLEV E onto the JEV E crystal structure (pdb ID 3P54) and manually superimposing domains I, II and III onto those molecular replacement solution. SLEV has greater sequence identity with JEV E than DV E, so this model was used as a reference model during refinement. The structure was refined to 4.0Å resolution in

PHENIX by rigid body refinement followed by several rounds of atomic refinement with reference model and secondary structure restraints was performed and yielded an R_{work} of 32% and R_{free} of 34% (Table 1).

3.4 SLEV E post-fusion trimer

The preliminary crystal structure of SLEV E was determined at refined to 4.0Å resolution. The R_{work} and R_{free} were 32 and 34% respectively, and 383 out of 406 residues were built into the model. The loops spanning residues 146-164 was not visible in the density. The residues of this loop are also disordered in both post-fusion structures of DV E proteins, so this is not unusual[2,5]. SLEV E adopted the 3-domain architecture previously observed in E proteins[6]. DI is an 8-stranded β-barrel, DII is formed out of two extended loops protruding from DI and DIII is a 6-stranded Ig-like domain (**Fig 1A**). Crystals were grown at pH 5.5 and E was found in the post-fusion conformation. There was a single E protein in the asymmetric unit, but application of cubic symmetry allowed for generation of the trimer (**Fig 1A**). When DI of SLEV E was superimposed onto DI of the DV2 E trimer, the most significant differences were visible in DII, while DIII from SLEV E did not vary substantially in orientation relative to DV2 DIII (**Fig 1B**). Further analysis will be carried out upon further refinement, as we do not wish to over-interpret our results given the low resolution of the structure.

3.5 Discussion and future directions

We have solved the first structure of a post-fusion E protein from the JEV serocomplex. It was originally believed that E protein trimerization required both acidic

pH and the presence of membranes[7]. However, the post-fusion structure of DV1 E was recently solved in the absence of detergent[5]. Interestingly, DV2 E[2] and TBEV E[8] crystals grown in presence of lipids or detergents diffracted to high resolution (2.0 and 2.7 Å). DV1 E[5] and SLEV E structures, on the other hand, are relatively low-resolution (3.5 Å and 4.0 Å), implying insertion into membranes provides additional stabilization.

Attempts to improve the resolution of the SLEV E crystals have been unsuccessful. The crystals have a high solvent content (~80%) that was apparent upon inspection of the large solvent channels that permeate the lattice (**Fig 2**). The fusion loops are completely buried within a pocket formed by DI-DIII from 3 different E proteins that each belong to a separate trimer (**Fig 3)**. Attempts to dehydrate crystals have failed thus far. Our next attempt to improve diffraction will be to pursue crystallization of SLEV E in the presence of stabilizing lipids or detergents. We obtained a 4.0 Å resolution SAD data set with selenomethionine-derived SLEV E and the additional phase information will be utilized to improve our model. Future efforts will focus on the comparison of a fully refined SLEV E structure to the structures of other class II fusion proteins in the post-fusion conformation.

Table 1: Data collection and refinement statistics

Data collection	
Space group	I23
Cell dimensions	a=b=c=177.34Å
Resolution (high res shell)	50.0-4.00 Å (4.07-4.00 Å)
Completeness	99.56% (99.5%)[a]
Redundancy	11.7 (11.7)
I/σ	30.5 (7.0)
R-merge (I)	0.07 (0.488)
Refinement	
Resolution (high res shell)	37.8-4.03 Å (4.17–4.03 Å)
R-work reflections[b] (*F>0)*	7383 (698)[a]
R-free reflections	388 (36)
R-work	0.3254 (0.3503)
R-free	0.3433 (.4021)
SLEV E residues (atoms)	381 (2917)
Wilson B-factor	131.70 $Å^2$
R.m.s.d. bond lengths	0.009 Å
R.m.s.d. bond angles	1.544°

[a] Values in parentheses are for data in the highest resolution shell
[b] Statistics as defined in Phenix

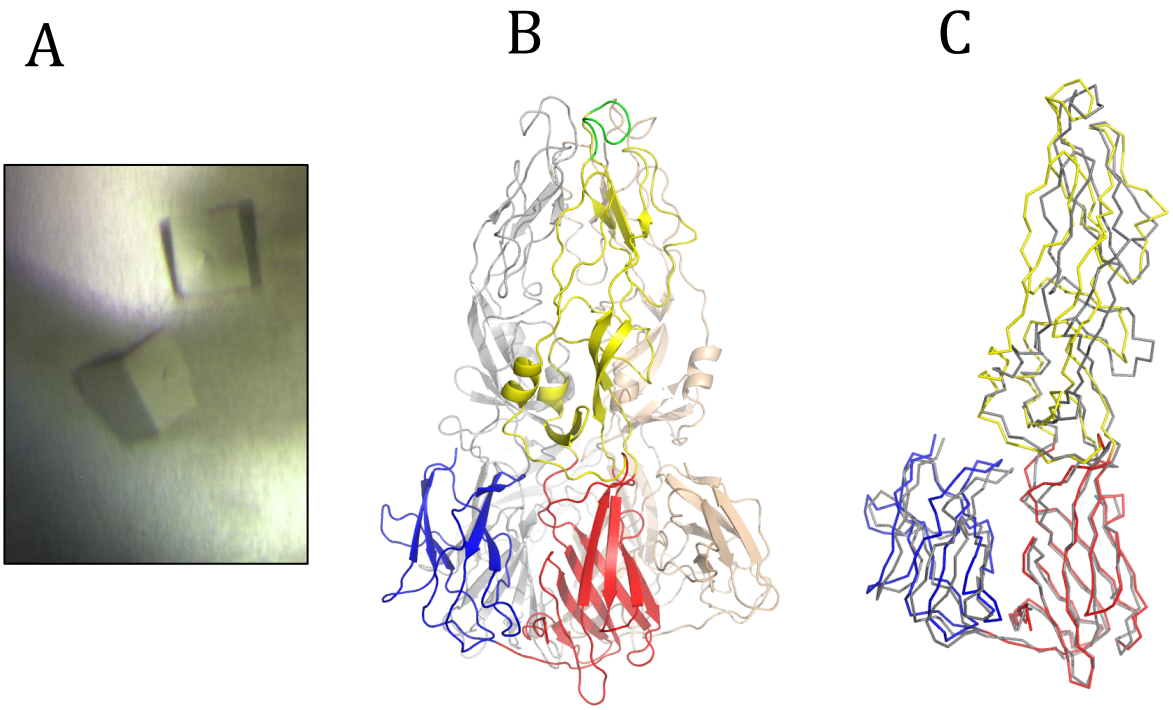

Figure 1: Crystal structure of SLEV E. A) Cubic crystals grew in 3% PEG 8000, 2% ethylene glycol, 0.1M sodium acetate pH 5.5 after 3-7 days. B) SLEV E trimer. DI is colored red, DII yellow, DIII blue and fusion loop green. Application of cubic symmetry allowed generation of the trimer, with additional subunits colored grey and wheat. C) Least-squares superimposition of DI of SLEV E onto DI of DV2 E (grey). Slight differences in the angles of DII and DIII relative to DI are visible.

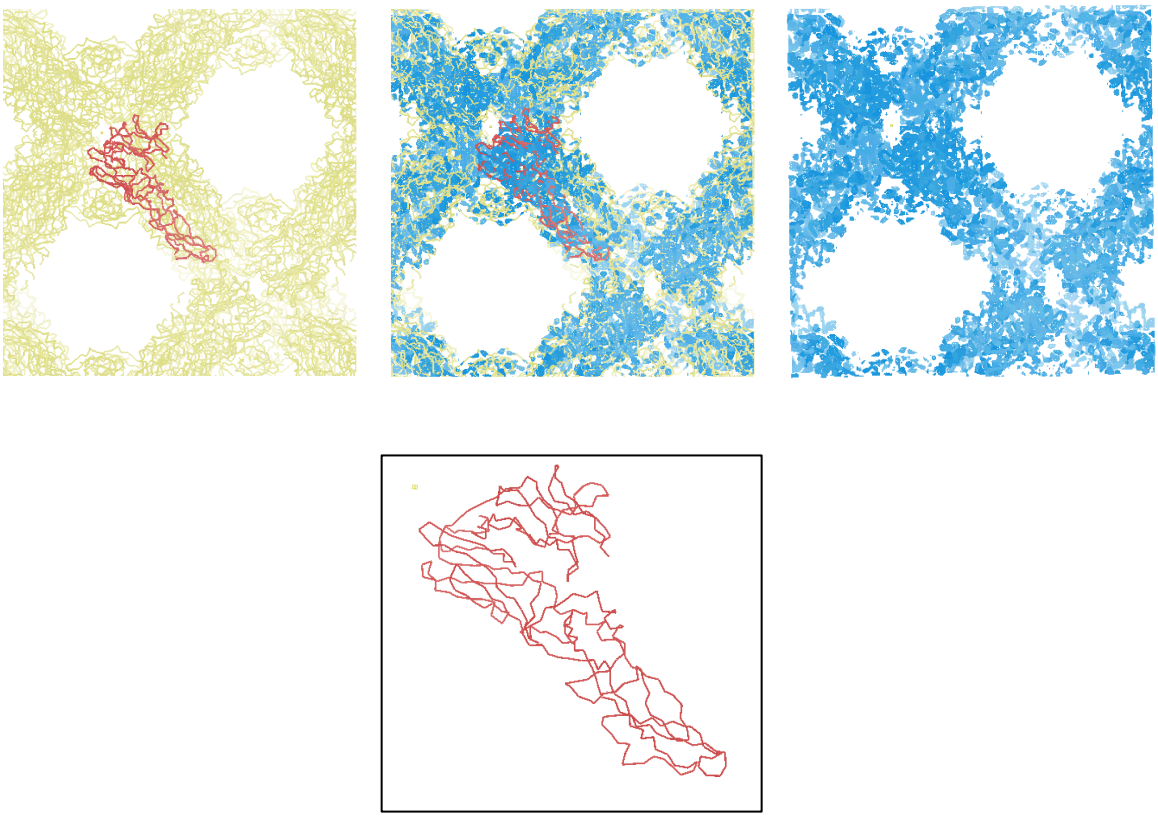

Figure 2: SLEV E packing and solvent channels. The SLEV E trimer was formed by application of cubic symmetry and packed into a lattice with large solvent channels between trimers. A single E subunit is displayed below (outlined box, red ribbon structure). The top left panel shows only the E packing arrangement, the right panel shows the density and the center panel is the two merged.

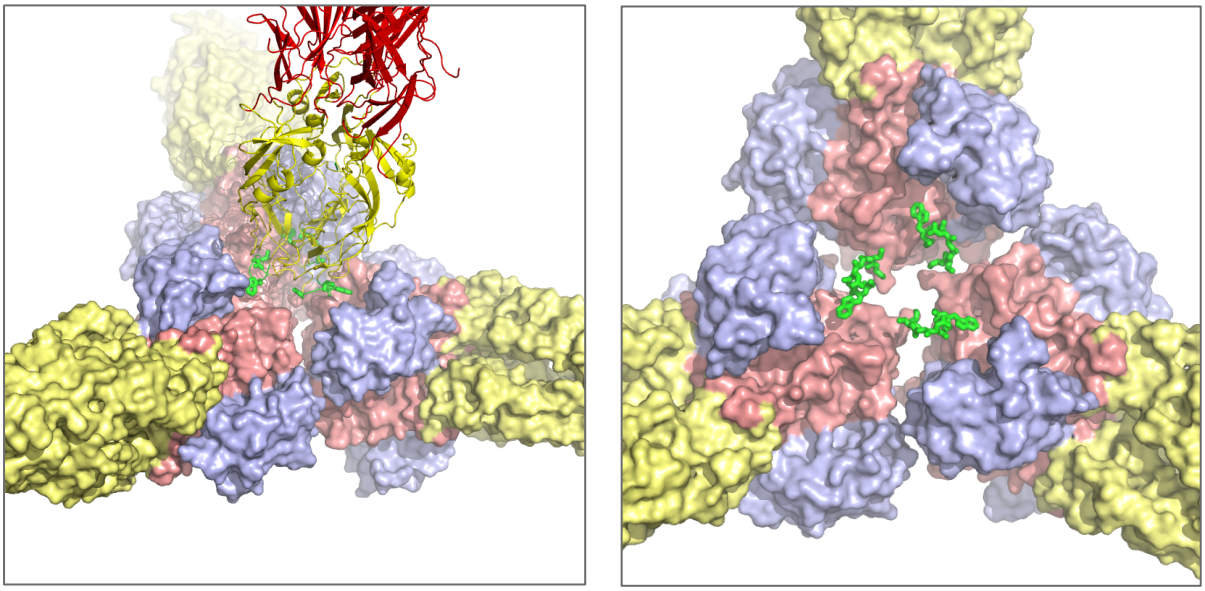

Figure 3: Fusion loop burial. A) In the absence of detergent, the fusion loops of SLEV E packed into a pocket formed by DI and DIII of three E monomers that each belong to a separate trimer assembly. DI is shown in red, DII in yellow and DIII in blue. The trimer with inserted fusion loop (green) is shown in cartoon representation. DIII is omitted from the cartoon representation for clarity. B) The stick representation of the 3 fusion loops is displayed.

3.6 References

1. Minor, W. & Otwinowski, Z. Processing of X-ray diffraction data collected in oscillation mode. *Methods in Enzymology* **276**, 307-326 (1997).
2. Modis, Y., Ogata, S., Clements, D. & Harrison, S.C. Structure of the dengue virus envelope protein after membrane fusion. *Nature* **427**, 313-319 (2004).
3. Kelley, L.A. & Sternberg, M.J.E. Protein structure prediction on the Web: a case study using the Phyre server. *Nat Protoc* **4**, 363-371 (2009).
4. Adams, P.D. *et al.* PHENIX: building new software for automated crystallographic structure determination. *Acta Crystallogr. D Biol. Crystallogr* **58**, 1948-1954 (2002).
5. Nayak, V. *et al.* Crystal structure of dengue virus type 1 envelope protein in the postfusion conformation and its implications for membrane fusion. *J. Virol* **83**, 4338-4344 (2009).
6. Rey, F.A., Heinz, F.X., Mandl, C., Kunz, C. & Harrison, S.C. The envelope glycoprotein from tick-borne encephalitis virus at 2 A resolution. *Nature* **375**, 291-298 (1995).
7. Stiasny, K., Allison, S.L., Marchler-Bauer, A., Kunz, C. & Heinz, F.X. Structural requirements for low-pH-induced rearrangements in the envelope glycoprotein of tick-borne encephalitis virus. *J. Virol.* **70**, 8142-8147 (1996).
8. Bressanelli, S. *et al.* Structure of a flavivirus envelope glycoprotein in its low-pH-induced membrane fusion conformation. *EMBO J* **23**, 728-738 (2004).

Chapter 4:

Introduction to Hepatitis C Virus

4.1 Abstract

Hepatitis C virus (HCV) is a blood borne pathogen that chronically infects roughly 3% of the global population. Clinical manifestations include hepatitis, cirrhosis and hepatocellular carcinoma. HCV is a member of the *Flaviviridae* family, a group of enveloped, positive-stranded RNA viruses. The current therapy for HCV is a combination of interferon-α and ribavirin. This treatment only succeeds in ~50% of cases and often leads to more detrimental side effects than those of the disease. The inability to develop a preventative vaccine has been linked to many features that shield the virus from antibody recognition, including extensive glycosylation and sequence variability of envelope proteins E1 and E2. Entry is mediated by direct interaction between E2 and receptors CD81 and scaveng3er receptor BI. However, virions also associate with lipoproteins that allow for hijacking of the lipoprotein transport machinery to facilitate infection. There is no crystal structure for E1 or E2 and their organization on mature virions is unknown. Determination of the structural and biophysical basis for HCV receptor interaction should illuminate new targets for the rational design of antivirals and antibodies that can inhibit HCV at vulnerable stages of the entry process.

4.2 Discovery and epidemiology

Hepatitis C was first isolated as the causative agent of non-A, non-B viral hepatitis in 1989[1], but genetic "molecular clock" approaches estimate the virus first appeared in humans as many as 1,000 years ago[2]. Transmission of HCV occurs from contact with infected blood. The majority of cases have resulted from needle sharing during injected drug use or blood transfusions that occurred prior to screening for the virus in 1990[3]. Sexual transmission of HCV is possible but rare[4]. Up to 75% of those infected proceed to chronic infection, although the virus has been deemed the "silent epidemic" because a high percentage these individuals clinical symptoms may be delayed for several years[5,6]. There are 8,000-10,000 annual deaths[7] linked to HCV infection, a relatively small number relative to the 1.5 to 3 million deaths caused by HIV[8]. However, it has been estimated that 170 million people are chronically infected with HCV[9], which is ~5 times that of those carrying HIV. Therefore, progression of liver disease HCV-positive individuals poses a massive public health problem.

4.3 Clinical manifestations and treatment

Symptoms of chronic infection. Many chronic HCV infections are asymptomatic, and in some cases their manifestation of clinical symptoms does not occur for 20 or more years[10]. The most common symptoms that do occur include jaundice, fatigue, cirrhosis, hepatitis, and hepatocellular carcinoma[11]. However, even those with asymptomatic infection are at risk for progressive liver damage. HCV is currently the leading cause of adult liver transplantation in the U.S., but if the antiviral therapy is not able to clear the virus prior to the transplant, re-infection will occur.

Antiviral therapy. The current treatment for HCV is a combination of pegylated interferon-α and ribavirin[12]. Viral clearance as a result of this combination therapy is ~50%, but depends upon the HCV genotype being treated[13]. Genotype 1 is most prevalent in the U.S. and is the most resistant[14]. Side effects of this lengthy 48-week regimen occur in 50% or more patients and range from flu-like symptoms to depression. The severity of these side effects relative to the typically mild short-term symptoms of HCV infection results in a large degree of patient non-compliance and thus discontinuation of treatment[15]. Promising results have been achieved with an antiviral that specifically inhibits the HCV NS2-3A viral protease. In clinical trials, combination therapy that included this protease, interferon-α and ribavirin inhibitor resulted in a sustained virologic response in 72% of patients[16]. Several other drugs that specifically target other non-structural proteins are also in clinical trials, forecasting a promising future for control of HCV[17].

Vaccine development. Development of a prophylactic or therapeutic HCV vaccine has been unsuccessful to date. This is largely because of the extensive sequence diversity amongst strains or generation of quasispecies within a single host[18–20]. The only preventative vaccine to be evaluated in clinical trials consisted of recombinant HCV E1 and E2 envelope proteins[21]. This vaccine was well tolerated and generated neutralizing antibodies against HCV. However, this approach is unlikely to succeed given the results of several previous studies. For example, it has been established that chronically infected individuals often possess high titers of neutralizing antibodies,[22] and that E1-E2 vaccines tested on chimpanzees do not prevent infection with heterologous strains[23]. Future prophylactic approaches are likely to focus on the use of virus-like particles (VLPs) or

inactivated virus, but immunization with these agents still does not address the issue of sequence variability. A potentially more promising approach involves complementation of the antiviral regimen with a therapeutic vaccine. Augmentation of the immune system by recombinant interferon-α is essential to this treatment, so it is apparent that boosting the host response can be a successful strategy[24]. Therapeutic vaccines utilizing recombinant HCV E1[25], core[26,27] or non-structural proteins[28,29] have been developed with and administered with several different delivery systems but none are particularly effective[30].

4.4 Virology

HCV is a member of the *Flaviviridae* family and is the lone representative of genus *Hepacivirus.* There are six major genotypes of HCV, each of which differ by 30-35% in sequence at the nucleotide level[31]. HCV is an enveloped, positive-stranded RNA virus that possesses a ~9.6kb genome. The genome encodes for a single polyprotein is cleaved by viral and host proteases into 3 structural and 7 non-structural (NS) proteins[32] (**Fig 1**). Core binds to viral RNA and forms the nucleocapsid and been implicated in the inhibition of interferon signalling[33]. Envelope protein 1 and 2 (E1/E2) are transmembrane proteins that coat the surface of the HCV virion. These proteins are primarily involved in functions that mediate cellular entry such as attachment, receptor interaction and membrane fusion[34]. The p7 non-structural protein is a dual-pass transmembrane protein that exhibits ion-channel activity in vitro[35,36]. NS2 is a membrane protein involved in the replication complex and is essential for cleavage at the NS2/3 junction in the polyprotein[37]. NS3 is a multi-function protein with an N-terminal cysteine protease

domain and a C-terminal RNA-helicase[38]. NS4A is co-factor for NS3 and associates with the ER through its transmembrane domain[39]. NS4B is a 4-pass transmembrane protein that induces a membranous web involved in formation and budding of HCV virions[40–42]. NS5A is a membrane-associated phosphoprotein that binds to viral RNA[43] and NS5B and is essential for replication. NS5B is also membrane associated and serves as a low fidelity RNA polymerase[44,45].

4.5 HCV envelope glycoproteins

The surface of the mature HCV virion is decorated with transmembrane envelope glycoproteins E1 and E2 that facilitate attachment and membrane fusion. E1 and E2 have been proposed to operate as class II fusion proteins (refer to 1.5.3) based on predictions that their secondary structure consists primarily of β-strands, and has similar genomic organization to flaviviruses. However, their sequences are divergent from any known class II protein, and a group of class III fusion proteins rich in β-strand content have also been recently discovered[46], so this presumption is highly speculative. The majority of host neutralizing antibodies recognize E2, however neutralizing anti-E1 antibodies have been reported. While E1 and E2 have been studied extensively, several basic features including their oligomeric state and assembly in the native virion, membrane topology and localization of a fusion peptide remain unclear.

E1 biochemistry, membrane topology and putative functions. E1 is a 162aa (polyprotein aa 192-353) transmembrane protein with poorly understood function. The ectodomain of E1 contains 4 N-linked glycosylation sites and the protein has 6 cysteine residues that form disulfide bonds (**Fig 2A**). A proposed function of E1 is to serve as a

chaperone for folding of E2[47], but several studies have verified that soluble E2 constructs adopt a functional fold in the absence of E1 co-expression[48,49]. Several regions of E1 have been suggested to contain the HCV fusion peptide. Perhaps most intriguing is the hydrophobic central region of E1 that spans polyprotein residues 272-298. This region has been proposed by some to serve as a fusion peptide[50] and by others a central transmembrane domain[51]. Indeed, there is conflicting evidence that supports both a two-pass and single-pass transmembrane topology model of E1. Antibodies that bind residues 313-327 can neutralize HCV, suggesting the region immediately C-terminal to 272-298 is exposed on the virion and argues that E1 has a lone transmembrane domain at its C-terminus[52]. On the other hand, the same C-terminal region recognized by these antibodies also binds the HCV core protein, which is enveloped by the viral membrane and inaccessible to host antibodies[51]. This second finding implies that E1 possesses a transmembrane helix at 272-298 as well as its C-terminus. It is possible, especially given that HCV envelope protein organization in viral particles is unclear, that these conflicting data may be reconciled by the existence of two distinct forms of E1 with one or two transmembrane domains. E1 also can potentially mediate HCV entry by associating with apolipoproteins B and E (ApoB, ApoE) to direct interaction with the low-density lipoprotein receptor (LDL-R)[53].

E2 biochemistry. E2 is a 363aa transmembrane protein (polyprotein aa 384-743) responsible for direct interaction with HCV receptors CD81[54,55] and SR-BI[56,57] and is the primary target of neutralizing antibodies. E2 contains 11 N-linked glycosylation sites, all of which have been confirmed to be modified by host cells[58], and 18 conserved cysteines that stabilize its structure by forming disulfide bonds[59] (**Fig 2B**). Lines of evidence

supporting the hypothesis that E2 is a class II viral fusion protein are anecdotal and based entirely on its localization in the genome and secondary structure content. E2 has no significant sequence similarity to any known protein, making structural prediction difficult. Regardless of these limitations, a computational model of E2 generated through the threading of its sequence onto domains I and II of a flavivirus E protein has been published[60]. Mutation of polyprotein residues 416-430 and 600-620 led to defects in HCV pseudoparticle fusion[61] and are thus considered candidates for the viral fusion peptide. However, in the absence of structural information it is difficult to differentiate peptides that physically penetrate host membranes from those that assist in conformational changes prior to fusion.

E2 soluble ectodomain. C-terminal truncation of E2 prior to its hydrophobic stem and transmembrane regions results in the secretion of a soluble form of its ectodomain[48]. This recombinant, soluble E2 (sE2), spanning polyprotein residues 384-660, has been critical to the discovery of HCV receptors CD81[55] and SR-BI[57], monoclonal antibody generation[56] and biochemical studies of envelope protein function. Production of sE2 leads to the secretion of a monomeric form along with disulfide-linked aggregates[48]. I have reproduced this expression pattern by generating sE2 through recombinant baculovirus infection of Hi-Five cells and it is the main protein reagent used in the HCV portion of my thesis. Methods described for this purification can be found in 4.7.1. Briefly, sE2 secreted into insect cell supernatants was purified by nickel and size exclusion chromatography (SEC), and the monomeric fraction obtained from the SEC purification was collected and utilized for subsequent experiments (**Fig 3**). Monomeric sE2 is believed to resemble the native E2 ectodomain based on its ability to directly bind

host receptors CD81[62] and SR-BI[57] and inhibit HCV infection when bound to hepatocytes[49]. There is also evidence that HCV particles contain disulfide-linked E2 aggregates, but soluble forms of these aggregates do not bind CD81[63] and few studies have investigated their relevance otherwise.

Hypervariable region 1. The most genetically diverse region of the HCV genome is located at the N-terminus of E2 and deemed hypervariable region 1[64] (HVR1). Despite its sequence variability, the length and physiochemical properties of HVR1 are conserved[65], suggesting it retains structural elements or functional utility (**Fig 4**). Indeed, HVR1 has been implicated in binding to hepatocytes and evasion of the humoral immune response. HVR1 binds to heparin sulfate through electrostatic interaction with basic residues and this binding may be competitively inhibited by the heparin-binding V3 variable loop of HIV[66,67]. Furthermore, deletion mutants of E2 lacking HVR1 lose the ability to bind SR-BI[57], highlighting its importance for interaction with at least two attachment factors. HVR1 was one of the first identified neutralizing epitopes on the HCV structural proteins[68]. Based on this discovery, it was demonstrated that treatment of chimpanzees with anti-HVR1 polysera was able to prevent infection with homologous strains[23]. This protection reinforced the biological importance of HVR1 but its variability makes it an inherently poor vaccine candidate. HCV lacking HVR1 has increased susceptibility to neutralizing antibodies and captures increased amounts of soluble CD81 in pull-down assays, suggesting it may also play a role in concealing conserved protein surfaces from antibodies[69].

Oligomeric state and disulfide connectivity in recombinant E1/E2. Understanding of envelope protein arrangement in native HCV virions has been

complicated because of substantial differences in the properties of recombinant versus virus-incorporated envelope proteins. While there is little structural information available for these proteins, the connectivity of the disulfide bonds formed in both E1 and E2 has been established. Those formed by E1 were sequential[70], with each cysteine forming an intramolecular bond with an adjacent cysteine (**Fig 2A**). The E2 disulfides contained sequential and non-sequential linkages, implying they play a role in stabilization of tertiary structure[59] (**Fig 2B**). Early assessments of the oligomeric state of transiently expressed E1 and E2 observed the formation of a non-covalent heterodimer[71]. However, the story grew more complex upon evaluation of E1 and E2 association in infectious particles. These studies revealed a barely detectable fraction of monomeric E1 and E2 and large quantities of disulfide-linked oligomers, suggesting a web of cross-linked E1 and E2 proteins encase the native virion[72]. Furthermore, cell-culture derived virus requires reduced (unpaired) cysteine residues in E1 and E2 for infection[73]. These data indicate the disulfide mapping of recombinant E1 and E2 does not recapitulate what is present in infectious virus. The poor comprehension of HCV envelope protein assembly presents a major concern for the selection of effective immunogens for vaccination.

4.6 The HCV virion

The HCV virion is composed of C, the RNA genome and a host derived lipid membrane containing E1 and E2. These particles are roughly spherical and measure ~50nm across[74]. The association of HCV with lipoproteins such as ApoB, ApoE or HDL results in a low particle buoyant density relative to other small RNA viruses[75]. These lipoprotein-associated forms of HCV are referred to as lipoviroparticles. Infection of

hepatocytes by lipoviroparticles may be mediated by direct interaction between E1 and E2 with a variety host entry factors, or by indirect interaction between lipoproteins and cellular lipoprotein receptors[76–79].

4.7 Host entry factors

A multitude of candidate receptors and attachment factors important for HCV infection have been identified (**Fig 5**). Most of these host factors may be assigned to three categories: 4 transmembrane tetraspanins (CD81) and tight-junction proteins (claudins 1/6/9, occludin), lipoprotein receptors (SR-BI, LDL-receptor), and carbohydrates/carbohydrate recognition proteins (heparin sulfate, DC-SIGN, L-SIGN). While direct interaction with HCV has only been demonstrated for a subset of these molecules, many are still required for productive infection of hepatocytes.

CD81. The first identified HCV receptor was tetraspanin CD81[62]. Tetraspanins are a family of 4 transmembrane domain proteins that interact with one another to stabilize membranes and participate in signaling. CD81 is also a member of the B-cell receptor complex, and HCV can infect B-cells along with hepatocytes[80,81]. There are two extracellular loops in between the transmembrane helices of CD81, the second of which is deemed the large-extracellular loop (LEL). The crystal structure of this loop revealed a 5-helix arrangement and two molecules in the asymmetric unit forming what is presumed to be a homodimer[82]. The interaction of E2 and CD81 has been mapped to the LEL, specifically to residue F185 situated on opposite ends of the homodimer[83] (**Fig 6**). Protein determinants of E2:CD81 binding have also been mapped to discontinuous regions of E2 including W420, G436-Y443, Y527, W529, G530 and D535[84,85] (**Fig 2B**). CD81 likely

serves as a post-attachment receptor since anti-CD81 mAbs neutralize HCV regardless of whether they are applied before or after virus is bound to hepatocytes[55]. Interaction of HCV with CD81 also serves to prime the virus for membrane fusion[86].

Scavenger receptor BI. Scavenger receptor BI is required for HCV infection and directly interacts with E2[57]. SR-BI is a two-pass transmembrane protein with N- and C-termini oriented towards the cytosol. It has a single, ~400aa glycosylated extracellular loop and is involved in lipid and cholesterol transport through binding of lipoproteins and uptake of foreign substances or organisms. Ligands that interact with the extracellular loop are typically negatively charged and include high-density lipoprotein (HDL)[87], ApoB and ApoE[87,88]. HCV is often found in serum as a "lipoviroparticle" associated with ApoB and ApoE. Therefore, it has been proposed that HCV hijacks the SR-BI transport machinery to gain entry into cells, either by engaging SR-BI with E2[57] or associated ApoE[76,78]. HCV infection is also enhanced by the presence of HDL[89,77,90], providing further evidence for this mechanism. Unlike what is observed for interaction with CD81, binding of HCV to SR-BI occurs at an early stage of infection and specifically involves amino acids 70-87 and E210 in the N-terminal half of the extracellular loop[91]. Deletion of HVR1 from E2 ablates SR-BI binding[57], indicating it contains at least part of the molecular determinants for this interaction. Interestingly, both SR-BI and CD81 are also involved in *Plasmodium falciparum* (causative agent of malaria) infection of hepatocytes[92], suggesting they may be part of a conserved portal for pathogen entry.

Tight junction proteins. Claudins 1, 6 and 9 (CLN1, CLN6, CLN9)[93,94] and occludin (OCLN)[95] are tight junction proteins necessary for HCV infection. These proteins function as cellular adhesion molecules and each has a 4-transmembrane

topology similar to CD81. CLN1/6/9 and OCLN do not directly bind HCV, but appear to co-localize with other receptors[96] and can facilitate direct cell-to-cell transmission[97]. Antibodies that bind CLN1 block HCV infection[98], implying it is in proximity to the virus during entry. Indeed, complexes of CD81 and CLN1 have been identified and appear to associate with HCV[96]. OCLN may also indirectly associate with HCV, as it co-precipitates with E2 from infected cells[99]. The specific determinants within CLN1 and OCLN required for HCV infection have been identified and include the first extracellular loop of CLN1[93] and second extracellular loop of OCLN[95]. While the exact role of tight junction molecules in HCV infection is unclear, discovery of OCLN as an entry factor led to the development of the first immunocompetent HCV mouse model. Transgenic mice expressing human CD81 and OCLN are susceptible to a single cycle of HCV infection[100], reinforcing the importance of OCLN for HCV infection despite its inability to directly bind virus.

Other candidate attachment and entry factors. Additional molecules implicated in HCV infection are the LDL-receptor[76,101], heparin sulfate[66,67] and mannose-binding lectins DC-SIGN and L-SIGN[102]. The LDL-receptor likely interacts with HCV in a manner similar to SR-BI in which indirect interactions with virion-associated lipoproteins facilitates entry[76]. Binding of HCV to heparin sulfate occurs through interactions with HVR1 and enhances viral attachment to hepatocytes[67]. DC-SIGN and L-SIGN bind carbohydrates on E2, allowing HCV to disseminate to proximal hepatocytes upon infection of a cell[102]. However, several different viruses attach to cells through non-specific interactions with heparin sulfate and mannose-binding lectins, so these are typically considered attachment factors and not true receptors.

4.8 Role of antibodies in chronic infection

The role of neutralizing antibodies in acute and chronic HCV infection is unclear. Early experiments were met with paradoxical results: most individuals chronically infected with HCV had high titers of neutralizing antibodies but acute infections were associated with low titers[22]. More recent studies, however, reported that spontaneous clearance of HCV is consistently linked to rapid induction of neutralizing antibodies during the acute phase of infection while those with a delayed response progress to chronic infection[103,104]. It is therefore likely that once a poor initial response allows HCV to establish infection, its many immune evasion strategies allow it to persist in the presence of neutralizing antibodies.

4.9 Antibody evasion mechanisms

Genetic variation and hypervariable region 1. HCV employs a variety of strategies to evade recognition and clearance by antibodies. Perhaps the most effective is the ability of HCV to rapidly vary its sequence due to the low fidelity of RNA polymerase NS5B[45]. In infected patients, a population of quasispecies will emerge[18–20] and a high degree of diversity amongst these species during early infection is predictive of a chronic infection[105]. The most diverse region of HCV is HVR1, a variable region that serves a role in cellular attachment[67] as well as antibody evasion[69]. Antibodies that bind HVR1 neutralize HCV but do not lead to clearance, presumably due to its frequent mutation[106]. Furthermore, HVR1 is able to obscure conserved neutralizing epitopes from recognition[69].

Glycosylation of E2. Viral N-linked glycans are believed to be flexible and structurally indistinguishable from host carbohydrates, so they are rarely targeted exclusively by neutralizing antibodies. The presence of several glycans on the surface of a virion could therefore sterically inhibit antibody access to protein epitopes. Mutation of N-linked glycans at sites N417, N423, N448, N532 and N645 of E2 (**Fig 2C**) each leads to increased neutralization sensitivity[107], indicating they are able to shield protein surfaces from recognition. All E2 glycans also exhibit microheterogeneity[58], meaning modification at a single site may is not consistent. This implies that even neutralizing antibodies able to recognize carbohydrate epitopes would not effectively bind all available sites on viral particles.

Cell to cell transmission. HCV is able to spread directly from cell to cell upon infection of hepatoma and B-cell lines[108,109]. This means of transmission is independent of CD81[109] but still requires CLN1 and OCLN[109,108], suggesting the virus may pass through tight junctions. Cell-to-cell transfer from infected cell lines to uninfected cells occurs despite the presence of neutralizing antibodies, representing yet another mechanism utilized by HCV to evade the humoral immune response.

4.10 Neutralizing epitopes

Several neutralizing antibodies have been mapped to specific sites on E1 and E2. Some of the first identified were found to recognize the C-terminal half of HVR1 and functioned by blocking cellular attachment. In our own studies, we isolated neutralizing antibodies that bind C-terminal residues of HVR1 G397, F403, G406 as well as residue R572 within the intergenotypic variable region (igVR)[110] and block infection at a post-

attachment step[56]. This mapping suggests these two variable regions are within close spatial proximity in the structure of E2 (**Fig 2C**). Additional conserved linear and discontinuous neutralizing epitopes have been determined for several antibodies, and are most commonly located within E2 polyprotein residue ranges 412-424 or 523-550[111–114]. Binding determinants for CD81 are also located within these regions[85], implying that HCV cross-neutralization may be achieved through generation of antibodies that recognize this site. For unclear reasons, no neutralizing antibodies that bind residues of E2 C-terminal to the igVR have been isolated. The epitopes of two anti-E1 monoclonals that neutralize HCV have been identified (**Fig 2A**). The first is located at the non-conserved N-terminus of E1. This epitope is recognized by antibody H-111, which neutralized HCV pseudoparticles by preventing attachment[115]. The other spans conserved residues 313-327 near the C-terminus of E1[116]. Antibodies that recognize this region are able to cross-neutralize several HCV genotypes, which warrants consideration of E1 for future vaccine or therapeutic development.

4.11 Generation and characterization of a panel of anti-E2 antibodies

In order to study the structural basis for antibody neutralization of HCV, I took part in a collaborative effort that led to production of a large panel anti-E2 monoclonal antibodies[56]. I played a significant role in the generation and characterization of these antibodies, so the associated publication containing detailed methods and my specific contributions is attached (**Appendix 1)**. However, the neutralization mechanisms defined in this work guided subsequent experiments in my thesis so they are summarized below.

The goal of our work was to generate neutralizing monoclonal antibodies, map them to specific regions of E2 and correlate structural features with neutralization mechanism. To initiate this study, I produced sE2 from genotype 1 and 2 for immunization of mice (**Fig 3**). I then generated yeast-displayed E2 constructs for screening of hybridoma supernatants. By this method, we isolated a total of 79 monoclonal antibodies that reacted with E2. I also generated yeast display constructs expressing E2 from genotypes 1-6 as well as two C-terminal truncations of $E2^{117}$. The yeast were utilized to evaluate cross-reactivity and map antibodies to one of three regions of E2 (**Fig 7**). Experiments performed by collaborators identified 7 neutralizing antibodies, mapped them to individual residues of E2 and determined their ability to inhibit E2 interaction with CD81 and SR-BI.

Our results revealed that the most potent neutralizing antibodies bound region 1 of E2 and recognized broadly conserved epitopes or HVR1 (**Table 1**). One antibody, H77.39, blocked interaction with both CD81 and SR-BI. These findings suggested CD81 and SR-BI could share an overlapping binding site on E2. My subsequent investigation of this possibility and the role of HVR1 were inspired by these findings and became a major focus of this thesis (Chapter 4).

4.12 Summary

Despite the identification of a wide array of HCV receptors and entry factors, many essential structural and biophysical details accompanying these interactions have not been determined. Therefore, I sought to clarify several aspects of the interplay between E2, CD81 and SR-BI. I elucidated the stoichiometry of sE2 and CD81-LEL

alone and in complex. I was able to determine the kinetics and affinity of this interaction as well as the ability of HVR1 to modulate E2 binding to CD81 and SR-BI. Perhaps most interestingly, I established that sE2:CD81-LEL complexes are unable able to engage SR-BI, suggesting they share a binding site on E2. Future directions will focus on the crystallization of E2 in hopes of understanding the structural basis for HCV attachment, entry and fusion.

Table 1: Summary of neutralizing anti-E2 mAbs. Adapted from ref. 56, Sabo *et al.*

	Region bound	EC_{50} (µg/uL)	Cross-reactivity	Inhibition of CD81 binding	Inhibition of SR-BI binding	Loss of binding residues
H39	**I**	**1.09**	**123456**	+++	+++	**N415, N417**
J36	**I/HVR1**	**1.95**	**2**	+	+++	**F403, G406, G397+R572**
H16	**I**	**3.44**	**123456**	-	+++	**G406+G530, G406, N410, I411,**
J103	**I/HVR1**	**7.05**	**2**	-	+++	**F403, G406, G397/ R572**
H28	**II**	**13.88**	**25**	-	-	**R543**
H56	**III**	**19.23**	**2346**	-	-	**C552**
H31	**II**	**38.20**	**2**	+++	+	**W529, G530, D533**

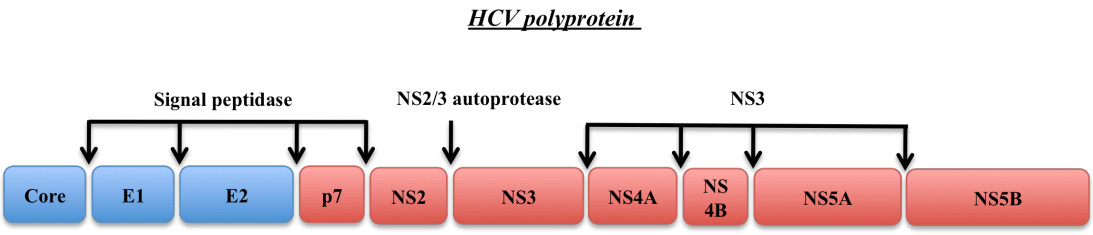

Protein	Localization	Primary functions
Core	structural	Encapsulation of viral RNA
E1	structural	Facilitates entry by binding ApoE
E2	structural	Interacts with CD81, SR-BI, heparin sulfate
p7	intracellular	Putative ion channel
NS2	intracellular	Replication complex, NS3 cofactor
NS3	intracellular	Dual-function protease/helicase
NS4A	intracellular	ER-associated NS3 co-factor
NS4B	intracellular	Induces membranous web for particle assembly and budding
NS5A	intracellular	Phosphoprotein, co-factor for NS5B replication of RNA
NS5B	intracellular	Low fidelity RNA polymerase

Figure 1: The HCV polyprotein. Structural proteins are colored blue in the schematic, non-structural proteins are colored red. Protease cleavage sites are indicated by arrows and the host or viral protease that cleaves a given site is listed above each site.

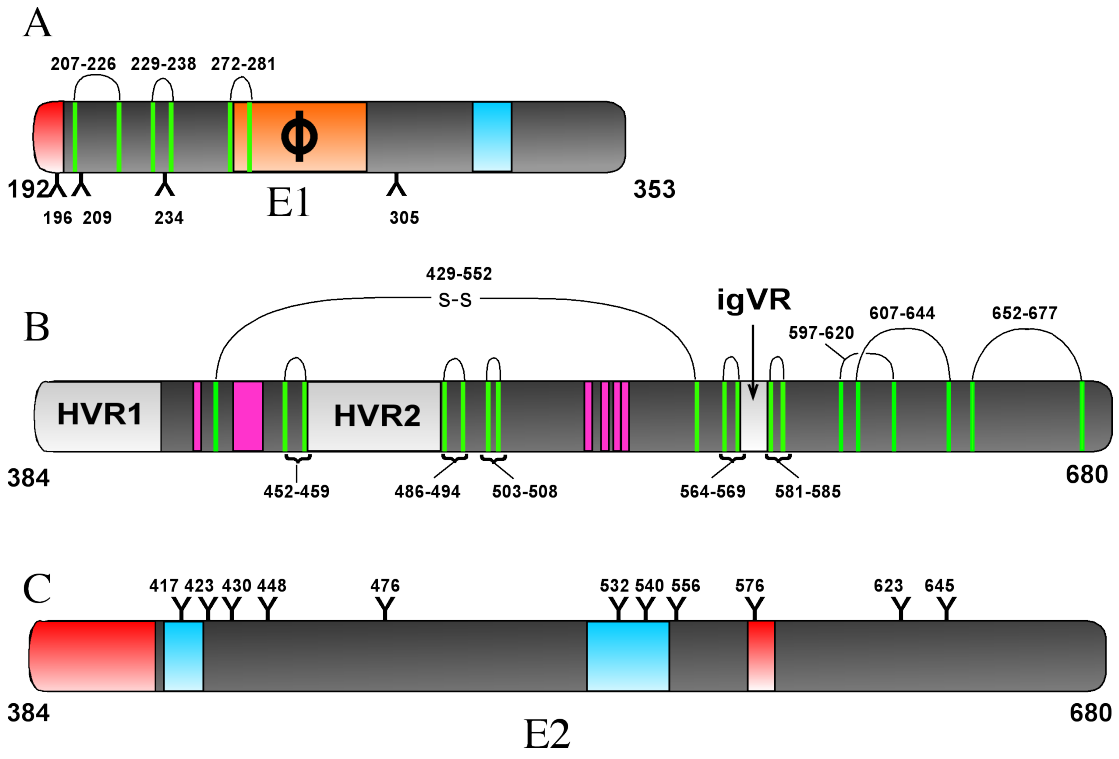

Figure 2: HCV E1 and E2. A) A schematic of E1 indicating disulfide linkages (green bars connected by black lines), glycans (black Y-shaped protrusions), conserved neutralizing epitope (blue, spans 412-424 and 523-550), non-conserved neutralizing epitope (red) and hydrophobic region (orange with phi). Polyprotein residues corresponding to the termini, disulfides and N-linked sites are labeled. B) Schematic of E2 that indicates disulfide linkages (green bars connected by black lines), CD81 binding regions (magenta bars) and variable regions (light grey). C) Schematic indicating conserved (blue, spans 412-424 and 523-550) and non-conserved (red, spans 384-410 and 570-580) neutralizing epitopes believed to be within spatial proximity on the E2 surface. Glycans are shown as black Y-shaped protrusions . Polyprotein residues corresponding to the N-linked sites, cysteines and termini are displayed in B) and C).

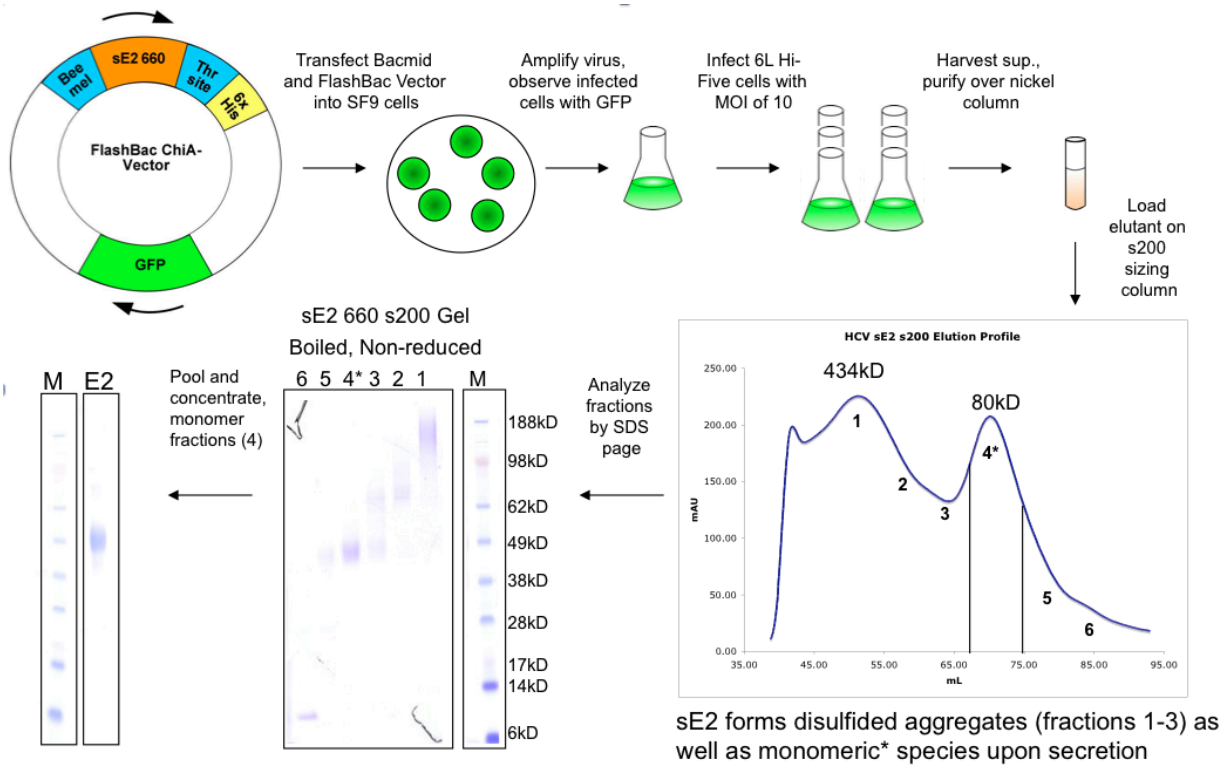

Figure 3: Purification of soluble E2. The steps of sE2 purification including transfection, recombinant baculovirus amplification, affinity chromatography and size exclusion chromatography are described. Each arrow indicates a purification or purity assessment step. Infected insect cells were tracked and titered by GFP fluorescence given the transfer vector utilized encoded a GFP on a second promoter. The SEC profile is displayed in the bottom right corner, and fractions corresponding to the numbering across the profile were loaded in non-reducing buffer on an SDS-PAGE gel. Disulfide linked aggregates are found in fractions 1-3 and therefore only the monomeric sE2 found in peak labeled 4 was collected.

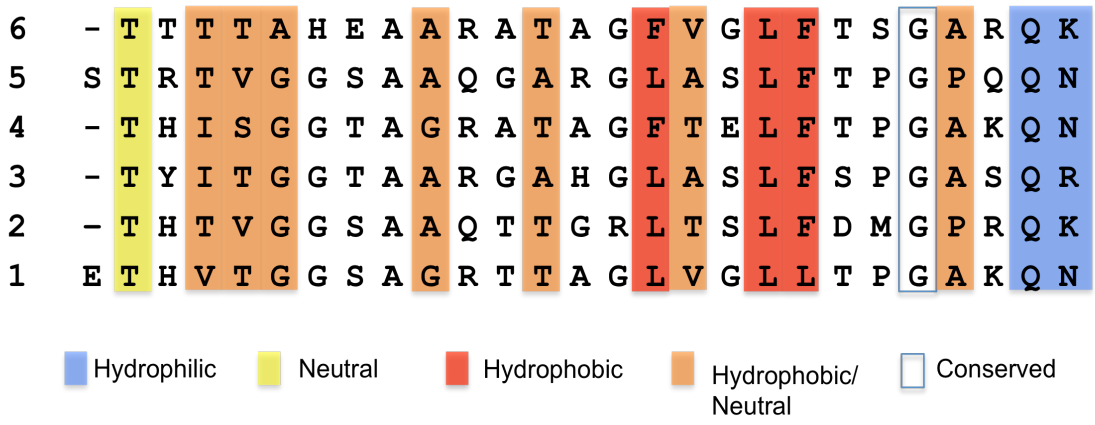

Figure 4: Conservation of physiochemical properties within HVR1. Several residues of HVR1 have specific chemical characteristics[65], indicated by the coloring above.

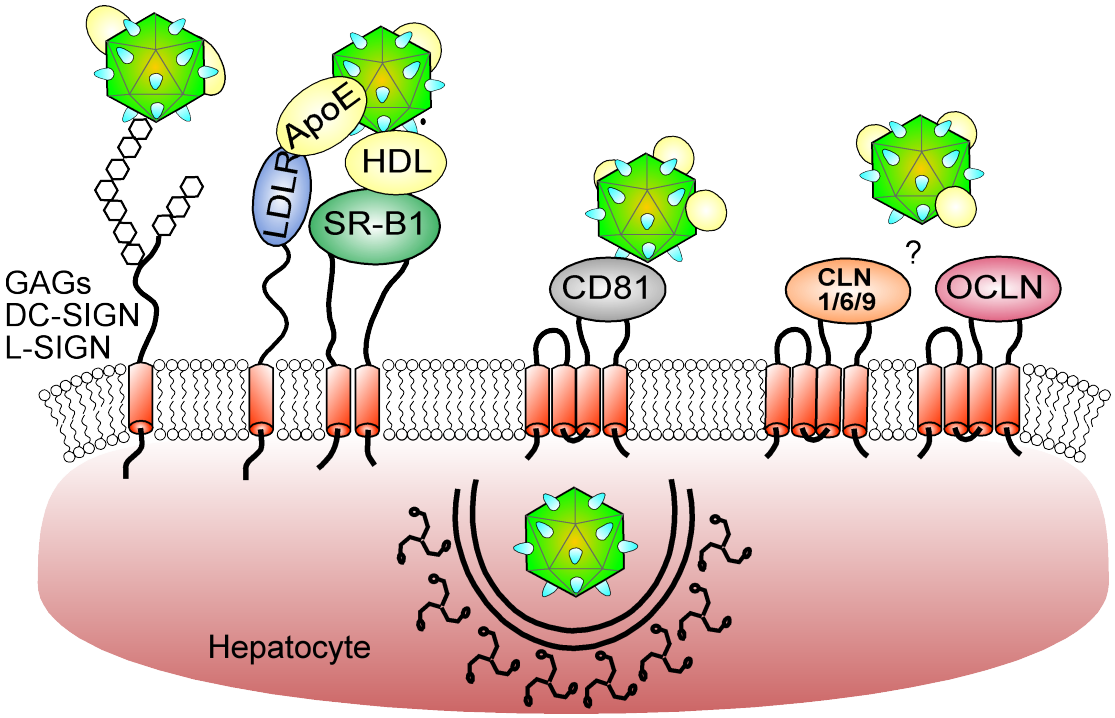

Figure 5: HCV receptors. A cartoon representation of HCV entry, HCV lipoviroparticles are green with blue spikes. HCV binds attachment factors GAGs, DC-SIGN or L-SIGN prior to directly or indirectly interacting with lipoprotein receptors LDL-R or SR-BI. E2 directly binds to CD81. Tight-junction proteins CLN1/6/9 and OCLN are required for infection but their exact role is unclear. Upon some combination of associations with these receptors, the HCV virion is taken into cells by clathrin-mediated endocytosis.

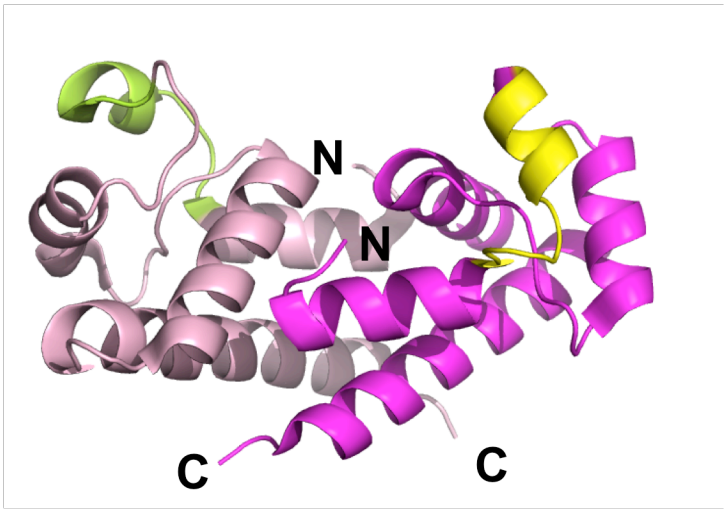

Figure 6: Crystal structure and E2 binding determinants of CD81-LEL. Subunits of the CD81-LEL dimer are colored magenta and light pink. Helices containing E2 binding determinants are colored yellow and green respectively. The plasma membrane is approximately oriented along the plane of the page.

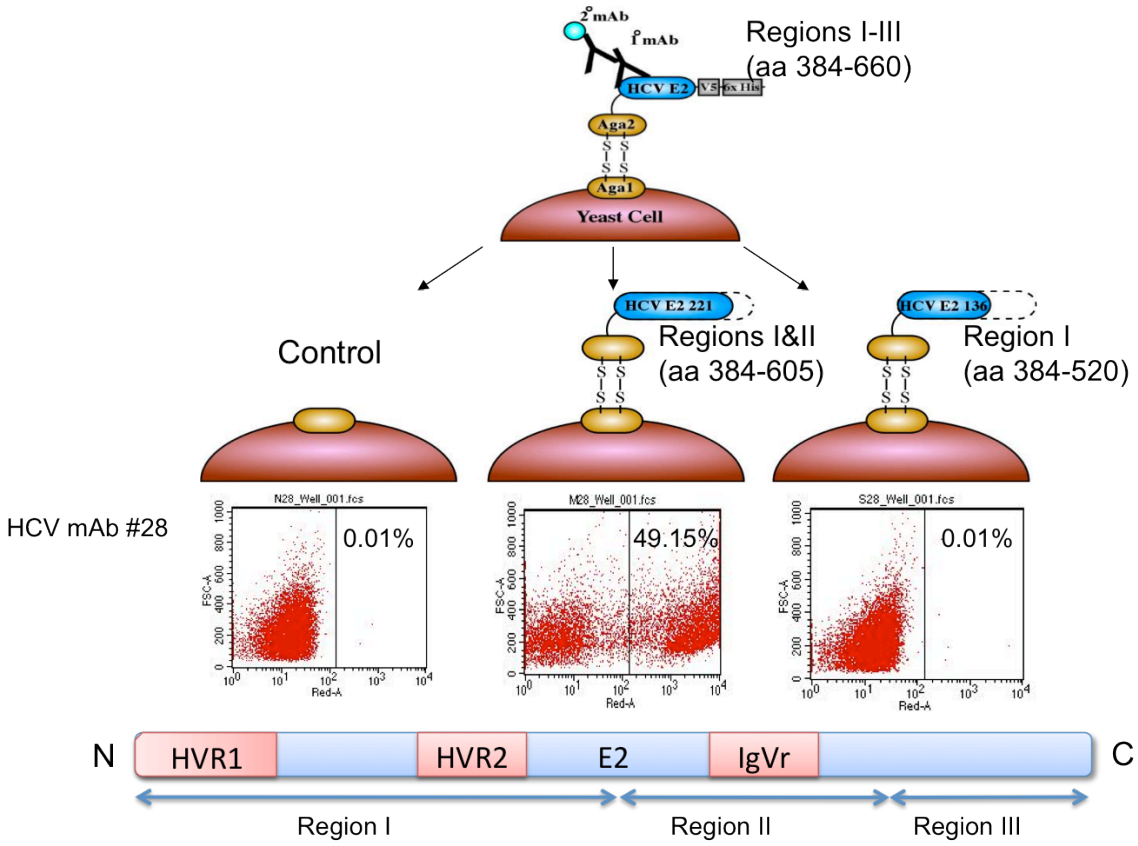

Figure 7: Yeast surface display constructs of E2. Yeast displayed E2 is linked at the N-terminus to cell wall protein Aga2, tethering it to the surface. Yeast expressing region I (E2 residues 384-520), regions I and II (E2 residues 384-605) or regions I-III (E2 residues 384-660) were used to map antibody recognition regions by exclusion. An example is displayed for antibody H77.28. Dot plots indicate a shift in the yeast population when an antibody is able to bind; in this case it requires regions I and II. E2 (residues 384-660) from genotypes 1-6 were also successfully displayed.

4.13 References

1. Choo, Q.L. *et al.* Isolation of a cDNA clone derived from a blood-borne non-A, non-B viral hepatitis genome. *Science* **244**, 359-362 (1989).
2. Pybus, O.G. *et al.* Genetic history of hepatitis C virus in East Asia. *J. Virol.* **83**, 1071-1082 (2009).
3. Heintges, T. & Wands, J.R. Hepatitis C virus: epidemiology and transmission. *Hepatology* **26**, 521-526 (1997).
4. Cavalheiro, N. de P. Sexual transmission of hepatitis C. *Rev. Inst. Med. Trop. Sao Paulo* **49**, 271-277 (2007).
5. Lauer, G.M. & Walker, B.D. Hepatitis C virus infection. *N. Engl. J. Med.* **345**, 41-52 (2001).
6. Hoofnagle, J.H. Course and outcome of hepatitis C. *Hepatology* **36**, S21-29 (2002).
7. Alter, M.J. Epidemiology of hepatitis C. *Hepatology* **26**, 62S-65S (1997).
8. UNAIDS report for 2003: most deaths and new infections ever; some good news. *AIDS Treat News* 3 (2003).
9. Hepatitis C: global prevalence. *Wkly. Epidemiol. Rec.* **72**, 341-344 (1997).
10. Pellicano, R. *et al.* The epidemiology of hepatitis C virus infection. An update for clinicians. *Minerva Gastroenterol Dietol* **50**, 1-7 (2004).
11. Marcellin, P. Hepatitis C: the clinical spectrum of the disease. *J. Hepatol.* **31 Suppl 1**, 9-16 (1999).
12. Ferguson, M.C. Current therapies for chronic hepatitis C. *Pharmacotherapy* **31**, 92-111 (2011).

13. Soriano, V., Peters, M.G. & Zeuzem, S. New therapies for hepatitis C virus infection. *Clin. Infect. Dis.* **48**, 313-320 (2009).
14. Manns, M.P. *et al.* Peginterferon alfa-2b plus ribavirin compared with interferon alfa-2b plus ribavirin for initial treatment of chronic hepatitis C: a randomised trial. *Lancet* **358**, 958-965 (2001).
15. Kraus, M.R. *et al.* Compliance with therapy in patients with chronic hepatitis C: associations with psychiatric symptoms, interpersonal problems, and mode of acquisition. *Dig. Dis. Sci.* **46**, 2060-2065 (2001).
16. Sherman, K.E. *et al.* Response-guided telaprevir combination treatment for hepatitis C virus infection. *N. Engl. J. Med.* **365**, 1014-1024 (2011).
17. Lin, K. Development of novel antiviral therapies for hepatitis C virus. *Virologica Sinica* **25**, 246-266 (2010).
18. Martell, M. *et al.* Hepatitis C virus (HCV) circulates as a population of different but closely related genomes: quasispecies nature of HCV genome distribution. *J. Virol.* **66**, 3225-3229 (1992).
19. Fishman, S.L. & Branch, A.D. The Quasispecies Nature and Biological Implications of the Hepatitis C Virus. *Infect Genet Evol* **9**, 1158-1167 (2009).
20. Bukh, J., Miller, R.H. & Purcell, R.H. Genetic heterogeneity of hepatitis C virus: quasispecies and genotypes. *Semin. Liver Dis.* **15**, 41-63 (1995).
21. Frey, S.E. *et al.* Safety and immunogenicity of HCV E1E2 vaccine adjuvanted with MF59 administered to healthy adults. *Vaccine* **28**, 6367-6373 (2010).
22. Logvinoff, C. *et al.* Neutralizing antibody response during acute and chronic hepatitis C virus infection. *Proc. Natl. Acad. Sci. U.S.A.* **101**, 10149-10154 (2004).

23. Choo, Q.L. *et al.* Vaccination of chimpanzees against infection by the hepatitis C virus. *Proceedings of the National Academy of Sciences* **91**, 1294 -1298 (1994).

24. Bailly, F., Si, N., Si, A. & Trepo, C. Treatment of HCV liver disease by recombinant interferon alpha. *Nephrol. Dial. Transplant.* **11 Suppl 4**, 56-57 (1996).

25. Leroux-Roels, G. *et al.* A candidate vaccine based on the hepatitis C E1 protein: tolerability and immunogenicity in healthy volunteers. *Vaccine* **22**, 3080-3086 (2004).

26. Alvarez-Lajonchere, L. *et al.* Immunogenicity of CIGB-230, a therapeutic DNA vaccine preparation, in HCV-chronically infected individuals in a Phase I clinical trial. *J. Viral Hepat.* **16**, 156-167 (2009).

27. Drane, D. *et al.* Priming of CD4+ and CD8+ T cell responses using a HCV core ISCOMATRIX vaccine: a phase I study in healthy volunteers. *Hum Vaccin* **5**, 151-157 (2009).

28. El-Gogo, S., Staib, C., Lasarte, J.J., Sutter, G. & Adler, H. Protective vaccination with hepatitis C virus NS3 but not core antigen in a novel mouse challenge model. *J Gene Med* **10**, 177-186 (2008).

29. Jirmo, A.C. *et al.* Monocytes transduced with lentiviral vectors expressing hepatitis C virus non-structural proteins and differentiated into dendritic cells stimulate multi-antigenic CD8(+) T cell responses. *Vaccine* **28**, 922-933 (2010).

30. Halliday, J., Klenerman, P. & Barnes, E. Vaccination for hepatitis C virus: closing in on an evasive target. *Expert Rev Vaccines* **10**, 659-672 (2011).

31. Simmonds, P. *et al.* Consensus proposals for a unified system of nomenclature of hepatitis C virus genotypes. *Hepatology* **42**, 962-973 (2005).

32. Grakoui, A., Wychowski, C., Lin, C., Feinstone, S.M. & Rice, C.M. Expression and identification of hepatitis C virus polyprotein cleavage products. *J. Virol.* **67**, 1385-1395 (1993).

33. Lin, W. *et al.* Hepatitis C virus core protein blocks interferon signaling by interaction with the STAT1 SH2 domain. *J. Virol.* **80**, 9226-9235 (2006).

34. Voisset, C. & Dubuisson, J. Functional hepatitis C virus envelope glycoproteins. *Biol. Cell* **96**, 413-420 (2004).

35. Pavlović, D. *et al.* The hepatitis C virus p7 protein forms an ion channel that is inhibited by long-alkyl-chain iminosugar derivatives. *Proc. Natl. Acad. Sci. U.S.A.* **100**, 6104-6108 (2003).

36. Griffin, S.D.C. *et al.* The p7 protein of hepatitis C virus forms an ion channel that is blocked by the antiviral drug, Amantadine. *FEBS Lett.* **535**, 34-38 (2003).

37. Reed, K.E., Grakoui, A. & Rice, C.M. Hepatitis C virus-encoded NS2-3 protease: cleavage-site mutagenesis and requirements for bimolecular cleavage. *J. Virol.* **69**, 4127-4136 (1995).

38. Kim, D.W., Gwack, Y., Han, J.H. & Choe, J. C-terminal domain of the hepatitis C virus NS3 protein contains an RNA helicase activity. *Biochem. Biophys. Res. Commun.* **215**, 160-166 (1995).

39. Wölk, B. *et al.* Subcellular localization, stability, and trans-cleavage competence of the hepatitis C virus NS3-NS4A complex expressed in tetracycline-regulated cell lines. *J. Virol.* **74**, 2293-2304 (2000).

40. Egger, D. *et al.* Expression of hepatitis C virus proteins induces distinct membrane alterations including a candidate viral replication complex. *J. Virol.* **76**, 5974-5984 (2002).

41. Hügle, T. *et al.* The hepatitis C virus nonstructural protein 4B is an integral endoplasmic reticulum membrane protein. *Virology* **284**, 70-81 (2001).

42. Lundin, M., Monné, M., Widell, A., Von Heijne, G. & Persson, M.A.A. Topology of the membrane-associated hepatitis C virus protein NS4B. *J. Virol.* **77**, 5428-5438 (2003).

43. Pawlotsky, J.M. & Germanidis, G. The non-structural 5A protein of hepatitis C virus. *J. Viral Hepat.* **6**, 343-356 (1999).

44. Behrens, S.E., Tomei, L. & De Francesco, R. Identification and properties of the RNA-dependent RNA polymerase of hepatitis C virus. *EMBO J.* **15**, 12-22 (1996).

45. Argentini, C., Genovese, D., Dettori, S. & Rapicetta, M. HCV genetic variability: from quasispecies evolution to genotype classification. *Future Microbiol* **4**, 359-373 (2009).

46. Backovic, M. & Jardetzky, T.S. Class III viral membrane fusion proteins. *Curr. Opin. Struct. Biol.* **19**, 189-196 (2009).

47. Brazzoli, M. *et al.* Folding and dimerization of hepatitis C virus E1 and E2 glycoproteins in stably transfected CHO cells. *Virology* **332**, 438-453 (2005).

48. Michalak, J.P. *et al.* Characterization of truncated forms of hepatitis C virus glycoproteins. *J. Gen. Virol.* **78 (Pt 9)**, 2299-2306 (1997).

49. Whidby, J. *et al.* Blocking Hepatitis C Virus Infection with Recombinant Form of Envelope Protein 2 Ectodomain. *J Virol* **83**, 11078-11089 (2009).

50. Bruni, R. *et al.* A computational approach identifies two regions of Hepatitis C Virus E1 protein as interacting domains involved in viral fusion process. *BMC Struct Biol* **9**, 48 (2009).

51. Nakai, K. *et al.* Oligomerization of hepatitis C virus core protein is crucial for interaction with the cytoplasmic domain of E1 envelope protein. *J. Virol.* **80**, 11265-11273 (2006).

52. Meunier, J.-C. *et al.* Isolation and characterization of broadly neutralizing human monoclonal antibodies to the e1 glycoprotein of hepatitis C virus. *J. Virol.* **82**, 966-973 (2008).

53. Mazumdar, B., Banerjee, A., Meyer, K. & Ray, R. Hepatitis C virus E1 envelope glycoprotein interacts with apolipoproteins in facilitating entry into hepatocytes. *Hepatology* **54**, 1149-1156 (2011).

54. Nakajima, H., Cocquerel, L., Kiyokawa, N., Fujimoto, J. & Levy, S. Kinetics of HCV envelope proteins' interaction with CD81 large extracellular loop. *Biochem. Biophys. Res. Commun.* **328**, 1091-1100 (2005).

55. Cormier, E.G. *et al.* CD81 is an entry coreceptor for hepatitis C virus. *Proc. Natl. Acad. Sci. U.S.A.* **101**, 7270-7274 (2004).

56. Sabo, M.C. *et al.* Neutralizing monoclonal antibodies against hepatitis C virus E2 protein bind discontinuous epitopes and inhibit infection at a postattachment step. *J. Virol.* **85**, 7005-7019 (2011).

57. Scarselli, E. *et al.* The human scavenger receptor class B type I is a novel candidate receptor for the hepatitis C virus. *EMBO J.* **21**, 5017-5025 (2002).

58. Iacob, R.E., Perdivara, I., Przybylski, M. & Tomer, K.B. Mass spectrometric characterization of glycosylation of hepatitis C virus E2 envelope glycoprotein reveals extended microheterogeneity of N-glycans. *J. Am. Soc. Mass Spectrom.* **19**, 428-444 (2008).

59. Krey, T. *et al.* The Disulfide Bonds in Glycoprotein E2 of Hepatitis C Virus Reveal the Tertiary Organization of the Molecule. *PLoS Pathog* **6**, (2010).

60. Yagnik, A.T. *et al.* A model for the hepatitis C virus envelope glycoprotein E2. *Proteins* **40**, 355-366 (2000).

61. Lavillette, D. *et al.* Characterization of Fusion Determinants Points to the Involvement of Three Discrete Regions of Both E1 and E2 Glycoproteins in the Membrane Fusion Process of Hepatitis C Virus. *J Virol* **81**, 8752-8765 (2007).

62. Pileri, P. *et al.* Binding of hepatitis C virus to CD81. *Science* **282**, 938-941 (1998).

63. Patel, A.H., Wood, J., Penin, F., Dubuisson, J. & McKeating, J.A. Construction and characterization of chimeric hepatitis C virus E2 glycoproteins: analysis of regions critical for glycoprotein aggregation and CD81 binding. *J. Gen. Virol.* **81**, 2873-2883 (2000).

64. Bukh, J., Miller, R.H. & Purcell, R.H. Genetic heterogeneity of hepatitis C virus: quasispecies and genotypes. *Semin. Liver Dis.* **15**, 41-63 (1995).

65. Penin, F. *et al.* Conservation of the conformation and positive charges of hepatitis C virus E2 envelope glycoprotein hypervariable region 1 points to a role in cell attachment. *J. Virol.* **75**, 5703-5710 (2001).

66. Barth, H. *et al.* Cellular binding of hepatitis C virus envelope glycoprotein E2 requires cell surface heparan sulfate. *J. Biol. Chem.* **278**, 41003-41012 (2003).

67. Basu, A., Beyene, A., Meyer, K. & Ray, R. The hypervariable region 1 of the E2 glycoprotein of hepatitis C virus binds to glycosaminoglycans, but this binding does not lead to infection in a pseudotype system. *J. Virol.* **78**, 4478-4486 (2004).

68. Kato, N. *et al.* Humoral immune response to hypervariable region 1 of the putative envelope glycoprotein (gp70) of hepatitis C virus. *J. Virol.* **67**, 3923-3930 (1993).

69. Bankwitz, D. *et al.* Hepatitis C virus hypervariable region 1 modulates receptor interactions, conceals the CD81 binding site, and protects conserved neutralizing epitopes. *J. Virol.* **84**, 5751-5763 (2010).

70. Depraetere, S., Depla, E., Verheyden, G. & Bosman, A. HCV E1 comprising specific disulfide bridges. (2008).at <http://www.google.com/patents/about/7413741_HCV_E1_comprising_specific_disul.html?id=s8msAAAAEBAJ>

71. Dubuisson, J. *et al.* Formation and intracellular localization of hepatitis C virus envelope glycoprotein complexes expressed by recombinant vaccinia and Sindbis viruses. *J. Virol.* **68**, 6147-6160 (1994).

72. Vieyres, G. *et al.* Characterization of the envelope glycoproteins associated with infectious hepatitis C virus. *J. Virol.* **84**, 10159-10168 (2010).

73. Fraser, J., Boo, I., Poumbourios, P. & Drummer, H.E. Hepatitis C virus (HCV) envelope glycoproteins E1 and E2 contain reduced cysteine residues essential for virus entry. *J. Biol. Chem.* **286**, 31984-31992 (2011).

74. Yu, X. *et al.* Cryo-electron microscopy and three-dimensional reconstructions of hepatitis C virus particles. *Virology* **367**, 126-134 (2007).

75. Bradley, D. *et al.* Hepatitis C virus: buoyant density of the factor VIII-derived isolate in sucrose. *J. Med. Virol.* **34**, 206-208 (1991).

76. Owen, D.M., Huang, H., Ye, J. & Gale, M., Jr Apolipoprotein E on hepatitis C virion facilitates infection through interaction with low-density lipoprotein receptor. *Virology* **394**, 99-108 (2009).

77. Voisset, C. *et al.* High density lipoproteins facilitate hepatitis C virus entry through the scavenger receptor class B type I. *J. Biol. Chem.* **280**, 7793-7799 (2005).

78. Hishiki, T. *et al.* Infectivity of hepatitis C virus is influenced by association with apolipoprotein E isoforms. *J. Virol.* **84**, 12048-12057 (2010).

79. Maillard, P. *et al.* The interaction of natural hepatitis C virus with human scavenger receptor SR-BI/Cla1 is mediated by ApoB-containing lipoproteins. *FASEB J.* **20**, 735-737 (2006).

80. Fornasieri, A. *et al.* Hepatitis C virus (HCV) in lymphocyte subsets and in B lymphocytes expressing rheumatoid factor cross-reacting idiotype in type II mixed cryoglobulinaemia. *Clin. Exp. Immunol.* **122**, 400-403 (2000).

81. Machida, K. *et al.* Hepatitis C virus (HCV)-induced immunoglobulin hypermutation reduces the affinity and neutralizing activities of antibodies against HCV envelope protein. *J. Virol.* **82**, 6711-6720 (2008).

82. Kitadokoro, K. *et al.* CD81 extracellular domain 3D structure: insight into the tetraspanin superfamily structural motifs. *EMBO J.* **20**, 12-18 (2001).

83. Higginbottom, A. *et al.* Identification of amino acid residues in CD81 critical for interaction with hepatitis C virus envelope glycoprotein E2. *J. Virol.* **74**, 3642-3649 (2000).

84. Drummer, H.E., Boo, I., Maerz, A.L. & Poumbourios, P. A conserved Gly436-Trp-Leu-Ala-Gly-Leu-Phe-Tyr motif in hepatitis C virus glycoprotein E2 is a determinant of CD81 binding and viral entry. *J. Virol.* **80**, 7844-7853 (2006).

85. Owsianka, A.M. *et al.* Identification of conserved residues in the E2 envelope glycoprotein of the hepatitis C virus that are critical for CD81 binding. *J. Virol.* **80**, 8695-8704 (2006).

86. Sharma, N.R. *et al.* Hepatitis C virus is primed by CD81 protein for low pH-dependent fusion. *J. Biol. Chem.* **286**, 30361-30376 (2011).

87. Hoekstra, M., Berkel, T.J.V. & Eck, M.V. Scavenger receptor BI: A multi-purpose player in cholesterol and steroid metabolism. *World J Gastroenterol* **16**, 5916-5924 (2010).

88. Li, X., Kan, H.-Y., Lavrentiadou, S., Krieger, M. & Zannis, V. Reconstituted discoidal ApoE-phospholipid particles are ligands for the scavenger receptor BI. The amino-terminal 1-165 domain of ApoE suffices for receptor binding. *J. Biol. Chem.* **277**, 21149-21157 (2002).

89. Bartosch, B. *et al.* An interplay between hypervariable region 1 of the hepatitis C virus E2 glycoprotein, the scavenger receptor BI, and high-density lipoprotein promotes both enhancement of infection and protection against neutralizing antibodies. *J. Virol.* **79**, 8217-8229 (2005).

90. Dreux, M. *et al.* High density lipoprotein inhibits hepatitis C virus-neutralizing antibodies by stimulating cell entry via activation of the scavenger receptor BI. *J. Biol. Chem.* **281**, 18285-18295 (2006).

91. Catanese, M.T. *et al.* Role of scavenger receptor class B type I in hepatitis C virus entry: kinetics and molecular determinants. *J. Virol.* **84**, 34-43 (2010).

92. Yalaoui, S. *et al.* Scavenger receptor BI boosts hepatocyte permissiveness to Plasmodium infection. *Cell Host Microbe* **4**, 283-292 (2008).

93. Evans, M.J. *et al.* Claudin-1 is a hepatitis C virus co-receptor required for a late step in entry. *Nature* **446**, 801-805 (2007).

94. Zheng, A. *et al.* Claudin-6 and claudin-9 function as additional coreceptors for hepatitis C virus. *J. Virol.* **81**, 12465-12471 (2007).

95. Ploss, A. *et al.* Human occludin is a hepatitis C virus entry factor required for infection of mouse cells. *Nature* **457**, 882-886 (2009).

96. Bonander, N. *et al.* Structural characterization of CD81-Claudin-1 hepatitis C virus receptor complexes. *Biochem. Soc. Trans.* **39**, 537-540 (2011).

97. Brimacombe, C.L. *et al.* Neutralizing antibody-resistant hepatitis C virus cell-to-cell transmission. *J. Virol.* **85**, 596-605 (2011).

98. Krieger, S.E. *et al.* Inhibition of hepatitis C virus infection by anti-claudin-1 antibodies is mediated by neutralization of E2-CD81-claudin-1 associations. *Hepatology* **51**, 1144-1157 (2010).

99. Liu, S. *et al.* Tight junction proteins claudin-1 and occludin control hepatitis C virus entry and are downregulated during infection to prevent superinfection. *J. Virol.* **83**, 2011-2014 (2009).

100. Dorner, M. *et al.* A genetically humanized mouse model for hepatitis C virus infection. *Nature* **474**, 208-211 (2011).

101. Monazahian, M. *et al.* Low density lipoprotein receptor as a candidate receptor for hepatitis C virus. *J. Med. Virol.* **57**, 223-229 (1999).

102. Cormier, E.G. *et al.* L-SIGN (CD209L) and DC-SIGN (CD209) mediate transinfection of liver cells by hepatitis C virus. *Proc. Natl. Acad. Sci. U.S.A.* **101**, 14067-14072 (2004).

103. Pestka, J.M. *et al.* Rapid induction of virus-neutralizing antibodies and viral clearance in a single-source outbreak of hepatitis C. *Proc. Natl. Acad. Sci. U.S.A.* **104**, 6025-6030 (2007).

104. Dowd, K.A., Netski, D.M., Wang, X.-H., Cox, A.L. & Ray, S.C. Selection pressure from neutralizing antibodies drives sequence evolution during acute infection with hepatitis C virus. *Gastroenterology* **136**, 2377-2386 (2009).

105. Farci, P. *et al.* The outcome of acute hepatitis C predicted by the evolution of the viral quasispecies. *Science* **288**, 339-344 (2000).

106. Kurosaki, M., Enomoto, N., Marumo, F. & Sato, C. Rapid sequence variation of the hypervariable region of hepatitis C virus during the course of chronic infection. *Hepatology* **18**, 1293-1299 (1993).

107. Helle, F. *et al.* The neutralizing activity of anti-hepatitis C virus antibodies is modulated by specific glycans on the E2 envelope protein. *J. Virol.* **81**, 8101-8111 (2007).

108. Valli, M.B. *et al.* Transmission in vitro of hepatitis C virus from persistently infected human B-cells to hepatoma cells by cell-to-cell contact. *J. Med. Virol.* **78**, 192-201 (2006).

109. Witteveldt, J. *et al.* CD81 is dispensable for hepatitis C virus cell-to-cell transmission in hepatoma cells. *J. Gen. Virol.* **90**, 48-58 (2009).

110. McCaffrey, K., Boo, I., Poumbourios, P. & Drummer, H.E. Expression and characterization of a minimal hepatitis C virus glycoprotein E2 core domain that retains CD81 binding. *J. Virol.* **81**, 9584-9590 (2007).

111. Law, M. *et al.* Broadly neutralizing antibodies protect against hepatitis C virus quasispecies challenge. *Nat. Med.* **14**, 25-27 (2008).

112. Owsianka, A. *et al.* Monoclonal antibody AP33 defines a broadly neutralizing epitope on the hepatitis C virus E2 envelope glycoprotein. *J. Virol.* **79**, 11095-11104 (2005).

113. Owsianka, A.M. *et al.* Broadly neutralizing human monoclonal antibodies to the hepatitis C virus E2 glycoprotein. *J. Gen. Virol.* **89**, 653-659 (2008).

114. Angus, A.G.N. & Patel, A.H. Immunotherapeutic potential of neutralizing antibodies targeting conserved regions of the HCV envelope glycoprotein E2. *Future Microbiol* **6**, 279-294 (2011).

115. Keck, Z.-Y. *et al.* Human monoczlonal antibody to hepatitis C virus E1 glycoprotein that blocks virus attachment and viral infectivity. *J. Virol.* **78**, 7257-7263 (2004).

116. Meunier, J.-C. *et al.* Isolation and characterization of broadly neutralizing human monoclonal antibodies to the e1 glycoprotein of hepatitis C virus. *J. Virol.* **82**, 966-973 (2008).

117. Martinez-Donato, G. *et al.* Expression and processing of hepatitis C virus structural proteins in Pichia pastoris yeast. *Biochem. Biophys. Res. Commun.* **342**, 625-631 (2006).

Chapter 5:

Hepatitis C E2 interaction with CD81 inhibits binding to Scavenger Receptor BI and is modulated by genotype and hypervariable region 1

5.1 Abstract

Hepatitis C Virus (HCV) infects roughly 3% of the global population and is the leading cause of liver disease in adults in the United States. Infection of hepatocytes requires the presence of several candidate cellular receptors, the most thoroughly characterized of which are scavenger receptor B1 (SR-BI) and tetraspanin CD81. To elucidate the detailed biochemical roles of these receptors' interactions with the HCV envelope protein E2, we first determined that soluble E2 ectodomain (sE2) interacts with CD81 large extracellular loop (CD81-LEL) with a 2:2 stoichiometry, and that this interaction inhibits subsequent engagement of SR-BI. Affinity and kinetics of sE2:CD81-LEL binding were then measured by surface plasmon resonance. Affinity of sE2 for CD81-LEL was enhanced by deletion of hypervariable region 1 (HVR1) of E2 and acidic pH, and modulated by the HCV genotype from which sE2 was produced. Furthermore, neutralization of HVR1-deleted HCV by a broadly cross-reactive antibody was enhanced in a genotype-specific manner that correlated with sE2:CD81-LEL affinity measurements. Taken together, our results suggest that E2 alone cannot simultaneously engage both CD81 and SR-BI, that HVR1 obscures CD81 and antibody binding sites, and that genotypic variation substantially influences HCV host receptor preference.

5.2 Acknowledgements

Work contained within this chapter is a manuscript in progress. Contributing authors include Michelle S. Sabo Jannick Prentoe and Jens Bukh and Michael S. Diamond. Sabo and Diamond contributed with thoughtful discussions and suggestions and experimental contributions. Prentoe and Bukh performed the neutralization assays with HVR1-deleted HCV.

5.3 Introduction

Hepatitis C Virus (HCV) is a blood borne pathogen carried by roughly 3% of the global population[1]. Symptoms associated with chronic infection include cirrhosis, hepatitis and hepatocellular carcinoma. Currently, there is no vaccine for HCV and treatment is a combination of pegylated interferon-α[2,3] and ribavirin[4], which results in a sustained virologic response in only ~45% of cases[5]. However, this 48-week regimen is associated with severe side effects, resulting in a large degree of patient non-compliance and thus premature discontinuation of therapy. Recent clinical trials that incorporated an inhibitor of HCV protease NS2/3 have reported an increased rate of viral clearance[6,7], suggesting that development of additional antivirals for a cocktail-based approach is a promising strategy for future therapies.

HCV is a member of *Flaviviridae*, a family of enveloped viruses with a single-stranded positive-sense RNA genome. The genome encodes for a polyprotein that is cleaved into 3 structural and 7 non-structural proteins by host and viral proteases[8,9]. The core, envelope 1 (E1), and envelope 2 (E2) proteins represent the HCV structural proteins. Core binds to the RNA genome and is enveloped by a host lipid membrane that contains transmembrane proteins E1 and E2 to comprise the infectious virion. E2 has been implicated in receptor interaction and is the primary target for neutralizing antibodies[10–13], while the function of E1 is poorly understood. The oligomeric state and disulfide organization of E1 and E2 in the mature virion are also unclear. Initial studies reported a heterodimeric E1-E2 complex,[14] while other more recent work suggests a complex network of monomers and disulfide linked oligomers[15]. A recombinant, soluble form of E2 lacking the transmembrane domain and C-terminal stem region (sE2) is

believed to adopt a fold similar to full-length E2 and has been a valuable tool in functional and biochemical studies[16,17].

Distinct features of the E1 and E2 are able to complicate HCV recognition by the adaptive immune system. Extensive glycosylation of both envelope proteins is believed to reduce accessibility of neutralizing epitopes[18–20]. E1 and E2 possess 4 and 11 N-linked glycosylation sites respectively and mutation of several N-linked residues has been linked to increased susceptibility to neutralizing antibodies[18,20]. Additionally, E2 encodes for 3 regions that exhibit considerable sequence variability. The inter-genotype variable region (igVR) diverges across each of the 7 or more HCV genotypes[21] while hypervariable regions 1 and 2 (HVR1, HVR2) display variability between isolates and can even contribute to the emergence of quasispecies within a single host[22–25]. HVR1 consists of the N-terminal 27 amino acids of E2 and is a dominant neutralizing epitope[22,25,26]. Despite its high mutation rate, certain features of HVR1 including its length and physiochemical properties are conserved[27], suggesting it may retain structural elements or biological roles important for the viral life cycle. Such roles include mediating viral attachment via binding to heparin sulfate[28,28] and, along with certain E2 glycans[19,20], concealment of conserved receptor and antibody binding sites[26,29].

A series of host factors are implicated in HCV infection, the most thoroughly characterized of which are tetraspanin CD81[11,30] and the HDL-binding scavenger receptor BI (SR-BI)[10]. Other candidate receptors are tight-junction molecules claudins 1/6/9[31,32] and occludin[33], mannose-binding lectins DC-SIGN and L-SIGN[34], LDL-receptor[35] and heparin sulfate[28,36]. Direct interaction between E2 with CD81[26,37] and SR-BI has been demonstrated in several assays[38,39], and antibodies that bind either receptor potently

inhibit HCV infection[40,41]. Conserved discontinuous regions and residues of E2 are involved in CD81 interaction[42,43], while the non-conserved HVR1 represents the putative SR-BI binding site[44,45]. Understanding of the specific kinetic and functional contributions of CD81, SR-BI and other receptors in during infection is currently limited. CD81 is believed to function at a post-attachment step in the entry process[46] and primes the virion for membrane fusion[47]. SR-BI, on the other hand, is involved in cellular attachment[38] and is able to facilitate HDL mediated enhancement of infection[48].

Herein, we have deconvoluted the relationship between E2 and receptors CD81 and SR-BI. Kinetics and affinity between several E2 constructs and CD81 were determined to evaluate the impact of genotype, pH and hypervariable region 1 on this interaction. Deletion of HVR1 resulted in genotype specific enhancement of binding to CD81-LEL, suggesting that the degree by which it obscures this binding site may vary substantially between isolates. We also experimentally determined the solution oligomeric state of sE2, CD81-LEL and the sE2:CD81 complex to further elucidate this crucial stage of HCV infection. Furthermore, CD81-LEL interaction with sE2 prevented subsequent engagement to SR-BI, suggesting the presence of a shared binding site for both receptors.

5.4 Results

Stoichiometry of sE2:CD81 interaction. Direct biochemical interaction between sE2 to CD81-LEL has been demonstrated in several studies[11,37,42,43], yet the solution oligomeric state of these molecules alone or in complex have not been resolved. We utilized multi-angle light scattering (MALS) to determine the molecular weight (MW) of sE2 and CD81-LEL over individual peaks resolved by a size exclusion column. This direct measurement of MW is advantageous over methods such as dynamic light scattering or size-exclusion chromatography that determine molecular weight based on extrapolation from hydrodynamic radius alone. The predicted MW of sE2 in the absence of glycosylation is 32.1kD (**Fig 1A**). We determined that MW of sE2 was 36.1kD, corresponding to that of a monomer (**Fig 1B**). This larger value was to be expected given that sE2 has 11 N-linked glycan sites of unknown or heterogeneous composition that could not be accounted for in the calculation. The predicted MW of the recombinant CD81-LEL construct is 13.8kD and the experimental value was that of a dimer (28.5kD). To obtain the stoichiometry of the sE2:CD81-LEL complex, we mixed CD81-LEL with 5-fold molar excess sE2 and then determined the MW of the two resultant peaks individually. The MW of the first peak to elute from the column was 34.0kD, corresponding to monomeric sE2, as it was expected to be in excess, and the MW of the second peak was calculated at 101.8kD (**Fig 1C**). This value corresponds to a 2:2 interaction and can be explained by addition of the experimental MW of 2 molecules of sE2 (72.2kD) and one dimer of CD81-LEL (28.5kD) that would yield a predicted experimental MW of 100.7kD. Also supporting this stoichiometry is the non-crystallographic homodimeric crystal structure of CD81-LEL[49]. Residues implicated in

E2 interaction are located on opposite faces of the dimer[50] so it is unlikely that a single E2 protein could encircle the entire CD81 assembly and contact both sides simultaneously.

Effects of genotype, HVR1 deletion, pH, and enzymatic deglycosylation on kinetics & affinity of sE2:CD81 interaction. In order to thoroughly establish the biochemical relationship between E2 and human CD81, we utilized surface plasmon resonance (SPR) to measure affinity and kinetics of interaction under a variety of conditions. Elucidation of the stoichiometry of interaction between the two proteins allowed for proper orientation on the sensor chip. This entailed immobilization of dimeric CD81-LEL as opposed to monomeric sE2 to avoid avidity effects that artificially inflate K_D values when passing multimeric proteins over an immobilized ligand. The data were fitted to a 1:1 kinetic model in accordance with our MALS results that suggested each subunit of the CD81-LEL dimer interacts with one sE2 molecule.

Since it has been proposed that HVR1 obscures the CD81 binding site of E2[29], we evaluated binding of both genotype 1 (H77) and genotype 2 (J6) sE2 and ΔHVR1 sE2 constructs over immobilized CD81-LEL (**Fig 2A**). The K_D of interaction for genotype 1 sE2 was 1.01×10^{-7} M and for genotype 2 was 1.75×10^{-6} M (**Fig 2B**). In this case, genotypic variation alone was responsible for a 17-fold difference in affinity. Deletion of HVR1 from genotype 1 sE2 resulted in a 2.2-fold increase in K_D while deletion of HVR1 from genotype 2 sE2 yielded a more substantial 8.8-fold enhancement (**Fig 2B**). This difference implies that the extent that HVR1 obscures recognition is modulated by viral genotype. The kinetic basis for this change was an increase in on-rate (k_a), supporting the notion that deletion of HVR1 exposes the CD81 binding site and allows for more rapid

engagement by E2. Fitting individual curves corresponding to each sE2 concentration revealed no significant increase or decrease in k_d (data not shown), indicating that while CD81-LEL has two sE2 binding sites there was no evidence for cooperativity.

Binding experiments were performed as a function of pH in an attempt to observe affinity changes that may result as HCV passes through the endosome during its life cycle. At pH 6.4 (early endosome) the K_D of genotype 1 sE2 for CD81-LEL increased by 2.9-fold relative to pH 7.4 (**Fig 2B**). The relative affinity increased further at pH 5.4 (late endosome) to 4.4-fold (**Fig 2B**). At pH 5.4, the enhancement in K_D resulted from an increase in on-rate but also was accompanied by a more rapid off-rate and therefore a decrease in half-life. The biological relevance of this more rapid dissociation could be attributed to the consideration that HCV virions likely require disengagement from CD81 prior to initiating fusion events with the host membrane.

Enzymatically deglycosylated sE2 was also evaluated for kinetics and affinity of interaction with CD81-LEL relative to untreated sE2. A series of three enzymes, Endo F1/F3 and PngaseF were used to deglycosylate native sE2. First, sE2 was treated with Endo F1/F3, then buffer exchanged into optimal conditions for PngaseF treatment prior to addition of this third enzyme. The untreated sE2 construct has a predicted MW of ~31kD but runs as a diffuse band at ~54kD on a 4-12% SDS gel due to the extensive glycosylation (**Fig 2C**). Upon treatment with these enzymes, sE2 runs at ~38kD, indicating a reduction of approximately 60% (16kD) of the glycosylation MW (**Fig 2C**). To control for possible effects of the pH 5.5 buffer required for Endo F1/F3 cleavage, sE2 used for comparison in kinetics and affinity measurements was treated with the equivalent buffers in the absence of EndoF1/F3/PngaseF. Removal of these glycans only

had a small effect on kinetics of affinity of CD81 interaction, increasing 2.3-fold relative to the sE2 incubated with buffer alone.

Enhancement of HCVcc neutralization by a cross-reactive mAb upon HVR1 deletion. HCV-neutralizing antibodies are significantly less potent relative to those that neutralize other members of *Flaviviridae*[39,51–53]. This disparity is potentially due to concealment of neutralizing epitopes by the variable regions and glycans of E2. We have demonstrated that deletion of HVR1 from sE2 resulted in an enhancement of affinity for receptor CD81 that was modulated by the genotype from which it was produced. These results led us to conclude that HVR1 obscures the CD81 binding site and neutralizing epitopes to different degrees based on properties of the isolate it originated from. To evaluate the extent in which HVR1 contributes to this inhibition in the context of the HCV virion, we performed neutralization assays using a broadly cross-neutralizing antibody H77.39 on both genotype 1 and 2 HCVcc +/- HVR1. This antibody recognizes a conserved region of E2 and inhibits CD81 and SR-BI binding. The antibody was more potent in both HVR1 deletion viruses, with EC50 increases of 55-fold for the genotype 1 virus and 253-fold for the genotype 2 virus (**Fig 3**). This greater enhancement of neutralization potential for HVR1 deleted genotype 2 HCV relative to genotype 1 correlates with the increase in affinity displayed by genotype 2 ΔHVR1 sE2 binding to CD81-LEL relative to genotype 1. The fold-change in K_D is substantially lower than that of the EC50 value, but this is expected given there are many copies of E2 per virion and HVR1 could contribute to lateral quaternary interactions with these additional E2 molecules.

CD81-LEL inhibition of sE2:SR-BI interaction. We have previously demonstrated that certain HCV-neutralizing antibodies inhibit sE2 interaction with both CD81 and SR-BI[39]. We therefore hypothesized that these receptors may share an overlapping binding site. To evaluate whether sE2 is able to bind SR-BI and CD81 simultaneously, we incubated sE2 with various concentrations of CD81-LEL and observed the effect on interaction with CHO cell-expressed SR-BI. Indeed, equimolar or greater concentrations of CD81-LEL potently inhibited subsequent engagement with SR-BI. Bound sE2 was detected by flow cytometry with a fluorescently labeled secondary antibody specific to a C-terminal 6x His tag and should not interfere with CD81 or SR-B1 binding (**Fig 4A-B**). To control for the possibility that sE2 binding to both receptors simply caused steric inhibition of the secondary antibody, we stained sE2 to CHO cells in the presence or absence of excess CD81-LEL, washed away excess protein, lysed the cells and then performed a western blot to detect the bound sE2. In this experiment, the proteins are denatured and separated following staining of the cells and unbound sE2 was detected with a non-conformational antibody, eliminating the possibility that recognition by the secondary antibody was impeded by the dual engagement of both receptors (**Fig 4C**). Staining of wild-type CHO cells with sE2+/- CD81-LEL resulted in a small background E2 band, but sE2 staining of SR-BI expressing CHO cells was reduced in the presence of CD81-LEL. Our results reinforced the original flow cytometry data and support the conclusion that a single E2 molecule does not efficiently bind SR-BI while in complex with CD81.

Neutralizing antibodies J6.36 and J6.103 bind the C-terminus of HVR1. Previous reports indicate that antibodies that bind the C-terminus of HVR1 are able to

neutralize HCVpp[26,54]. While the detailed mechanism for their neutralization is unclear, it has been reported that they are able to prevent attachment to multiple hepatocyte cell lines[55]. We previously characterized antibodies J6.36 and J6.103 for genotype cross-reactivity, epitope recognition and inhibition of sE2 interaction with receptors CD81 and SR-BI[39]. Each was specific for genotype 2 (J6) E2 and lost binding upon mutation of residues G397+R572, F403 and G406. Neither mAb cross-reacted with other HCV genotypes and two of four residues bound lie within HVR1; thus, we anticipated that their dominant epitope would lie within this region. We evaluated J6.36 and J6.103 for binding to GST-fusion constructs that spanned the full HVR1 (residues 385-410 of the E2 polyprotein) as well as truncations consisting of residues 385-397, 391-403 and 398-410. Indeed, both reacted with full length HVR1. Neither bound the N-terminal residues 385-397. J6.103 recognized the C-terminal 398-410 segment and central 391-403 peptides with comparable signal as the full length HVR1. J6.36, on the other hand, gave a robust signal for the C-terminal 398-410 peptide but yielded a much lower signal for 391-403 (**Fig 5**).

Deletion of HVR1 ablates sE2 binding to CHO cell expressed SR-BI but not CD81. Several studies have demonstrated that HVR1 interacts with SR-BI[10,45,56]. In order to evaluate whether our ΔHVR1 sE2 was properly folded, CHO cells expressing human SR-BI or CD81 with E2 from two different genotypes +/- HVR1 (**Fig 6**). Indeed, deletion of HVR1 from both H77 and J6 sE2 reduced binding to SR-BI dramatically. However, we did not observe an increase in binding of ΔHVR1 sE2 to CD81 as was detected in our SPR experiments. This may be explained by the fact that the enhanced

affinity of ΔHVR1 sE2 for CD81-LEL was primarily due to an increase in on-rate, while increased cell staining is attributed to half-life, which is linked to the kinetic off-rate.

5.5 Discussion

In our study, we ascertained the binding stoichiometry, kinetics and affinity of the soluble E2 ectodomain for the CD81 large extracellular loop. By utilizing a variety of modified sE2 constructs and solution conditions, we determined that genotype and deletion of HVR1 had the most substantial effects on E2:CD81 affinity, and that acidic pH and the enzymatic removal of sE2 glycans played a more modest role. In vitro experiments with HVR1 deletion viruses resulted in a dramatic increase in the neutralization potency of a broadly cross-reactive antibody that blocks E2:CD81 interaction, supporting our biochemical results that indicated HVR1 obscures the CD81 binding site. Deletion of HVR1 from also resulted in ablation of sE2 binding to SR-BI. Additionally, we observed that binding of sE2 to recombinant CD81-LEL potently inhibits subsequent engagement of SR-BI expressed on the surface of CHO cells, suggesting the binding site for these receptors may overlap on the E2 protein.

An essential step in HCV infection is direct binding of E2 to receptor CD81. Several protein determinants that contribute to this interaction have been identified, but the oligomeric state of the CD81:E2 complex has not been resolved. Using multi-angle light scattering we were able to determine that sE2 and CD81-LEL interact as a 2:2 complex. A CD81 residue, F185, is critical to E2 interaction[50] and maps to opposite ends of the LEL homodimer[49]. Two E2 monomers would be able to engage this residue with little possibility for steric inhibition, and so its location on the CD81-LEL crystal

structure is supportive of our stoichiometric data. Analysis of the sE2: CD81-LEL affinity measurements did not indicate cooperative binding, so it is yet to be determined whether HCV infection requires or is enhanced through bivalent CD81 interaction with E2. Arenavirus GP1 represents an example of a viral surface protein that recognizes opposing ends of a dimeric receptor (transferring receptor 1) with 2:2 stoichiometry[57] but kinetic information that would allow for biophysical comparisons of these interactions has not been determined.

A suggested role for HVR1 is the concealment of the conserved CD81 binding site of E2[24,26]. However, the specific role of HVR1 in the energetics accompanying the E2:CD81 interaction remains unclear. Elucidation of the solution oligomeric states of sE2 and CD81-LEL allowed us to properly orient them in SPR experiments in order to accurately determine their single-site K_D. The K_D for sE2 from H77 and J6 strains were 101nM and 1750nM respectively. These values fall within the range observed for envelope protein-receptor interactions from unrelated viruses such as HIV[58] and Measles[59]. Deletion of HVR1 from sE2 constructs enhanced this affinity, confirming that the region indeed obscures the CD81 binding site. However, this increase varied substantially between the H77 (~2-fold increase) and J6 (~9-fold increase) strains indicating both wild-type affinity for CD81 and the extent to which HVR1 affects this interaction are genotype-specific. A more pronounced effect was observed in the neutralization of HVR1-deleted HCV by H77.39, an antibody that blocks CD81-E2 interaction. The EC50 of H77.39 was increased 55-fold and 253-fold for H77 and J6 respectively, suggesting that HVR1 concealment is genotype-specific in HCV virions as well. This large increase in neutralization potential of H77.39 relative to minor increases

in sE2:CD81-LEL affinity may be due to amplification resulting from the absence of several HVR1 peptides or stabilizing effects exerted by HVR1 in the quaternary structure of the virion.

Both CD81 and SR-BI bind directly to E2 and are necessary for productive HCV infection[10,11]. Given this requirement, our finding that sE2 engagement of CD81-LEL precludes SR-BI binding gives rise to multiple possible models for utilization of these two receptors. One model would suggest that the virion interacts with both receptors through coordination of two separate E2 proteins, each of which binds only one receptor. While this mode of synchronized interaction of viral envelope proteins has not (to our knowledge) been previously reported, there is no obvious physical limitation that excludes this option. Alternatively, HCV may require a viral or host co-factor that mediates interaction of a single E2 protein with CD81 and SR-BI. E1 might fill this role, however no soluble, properly folded E1 construct has been reported and previous studies with E1-E2 captured from lysates did not observe a substantial increase in CD81-LEL binding relative to E2 alone[37]. Other candidates include host lipoproteins apolipoprotein E (ApoE), low-density or high-density lipoprotein (LDL or HDL). Infectious HCV may be found as lipoviroparticles associated with ApoE[60] and LDL[61], and HCV infectivity is enhanced in the presence of HDL[48]. Another feasible scenario is that the acidic pH of the endosome or receptor-binding triggers a conformational change that enables one E2 protein to interact with CD81 and SR-BI. Several viral envelope proteins are primed in this fashion, but this mechanism is most notably exemplified by the interaction of HIV gp120 with host receptor CD4. Attachment of gp120 to CD4 alters the structure of gp120 and potentiates subsequent binding to host chemokine receptors[58,62–64]. Our affinity

measurements indicated mild enhancement of sE2:CD81-LEL affinity at low pH so these molecules do not likely disengage in the endosome. It is possible that E2 releases from SR-BI at acidic pH but we have not been able to test this due to the lack of a soluble form of the receptor.

Several determinants of CD81 and SR-BI interaction with E2 have been identified. Known CD81 binding regions are discontinuous and include residues W420, Y527, W529, G530, D535[42] and a hydrophobic peptide spanning G436-Y443[43]. Prior studies, as well as results of our staining SR-BI expressing cells with ΔHVR1 sE2 indicate that HVR1 is necessary for E2 to engage SR-BI. However, pre-incubation of sE2 with CD81-LEL potently inhibited SR-BI interaction, suggesting these two receptors may partially share a binding site on E2. Indirect evidence for the location of this shared site may be garnered from the epitope mapping of antibody H77.39 that inhibits E2 binding to both receptors. This antibody mapped to residues N415 and N417, which lie directly between the C-terminus of HVR1 (polyprotein residue 410) and CD81 binding residue W420. Based on the location of the H77.39 epitope, we speculate that the conserved region of E2 C-terminal to HVR1 may comprise a portion of this overlapping site. Alanine scanning reports have established that mutation of N415[42] or N417[19] did not substantially reduce E2:CD81 binding, but W420 or the 436-433 peptide represent other candidate residues in this region.

As ongoing studies illuminate the antibody evasion strategies employed by HCV envelope proteins, it is important to note the many parallels that have emerged to those utilized by HIV. Unlike large, chronic DNA viruses such as Herpes Simplex Virus-1 that encode for an array of immunomodulatory proteins, HCV and HIV are small RNA

viruses with limited genomic space reserved for this purpose. Common features include modulation of affinity for host receptors through sequence variation[58,62,65] and shielding of important envelope protein interfaces from antibody recognition with variable loops or glycans[20,29,66–68]. HIV gp120 can utilize CD4 or either of chemokine receptors CXCR4/CCR5 for infection[58,62]. While gp120 from most HIV strains binds CD4, mutations in the V3 loop have allowed monospecific variants to utilize just a single chemokine receptor[69,70]. HCV is believed to require both SR-BI and CD81, but our results indicate that affinity of the E2-CD81 interaction can differ by at least 17-fold across genotypes. This divergence may represent an evolutionary response to immune pressure or a strain-specific fluctuation in HCV preference for receptors akin to what has been described for HIV. Given the limited number of HCV strains amenable to cell-culture production, it is entirely possible that undiscovered strains have distinct receptor requirements. The HCV HVR1 and HIV V3 variable regions can also bind with heparin sulfate to augment cellular attachment[28,36,71,72] and are targeted by neutralizing antibodies[26,54,65,72]. By utilizing variable regions for important functional roles, these viruses can retain structural integrity while evading antibody recognition.

In conclusion, we have resolved several previously unknown biochemical and molecular details of the interplay between E2, CD81 and SR-BI. Delineation of the 2:2 binding stoichiometry of the E2:CD81 complex has clarified an important aspect of HCV attachment and entry. Furthermore, we have resolved the kinetics and affinity of this interaction and established that concealment of receptor- and antibody-binding sites by HVR1 is genotype dependent. We have also determined that sE2 engagement of CD81-LEL prevents subsequent interaction with SR-BI, suggesting that these receptors share an

E2 binding site. Alternately, HCV may sequentially engage its receptors in stages as it becomes internalized. If HCV E2 indeed possesses an overlapping binding site for these receptors, it presents an intriguing target for inhibitor, therapeutic antibody or vaccine development. Taken together, our findings raise the question of whether HCV, like HIV, has strain-specific preferences for receptor interaction. Given the limited number of HCV isolates that replicate in cell culture, it is possible that undiscovered strains do not require all of the established receptors. As structural information emerges on the HCV envelope proteins, it is expected that many of these questions will be resolved and stimulate the development of novel therapeutics.

5.6 Materials and methods

Cloning expression and purification of sE2 and ΔHVR1 sE2. Residues 384-661 of genotype 1 (H77) or residues 385-661 of genotype 2 (J6) E2 ectodomain with an N-terminal honeybee melittin signal sequence were cloned into the baculovirus transfer vector pAcUW51. Since the yield of H77 sE2 was initially poor for this construct, a mutation of unpaired cysteine C652 to serine was introduced to increase secretion from insect cells (REF). HVR1 deletion constructs (ΔHVR1 sE2) spanning these same regions of the H77 and J6 isolates but lacking residues 387-410 (H77) or 388-410 (J6) were also generated. Residues 384-386 and 385-387 of these constructs were retained to allow for proper cleavage of the signal peptide by signal peptidase. The E2 encoding transfer vectors were co-transfected into SF9 cells grown in Sf-900 II media (Invitrogen) with the Flashbac Gold bacmid (Oxford Expression Technologies) to permit homologous recombination for production of recombinant baculoviruses. The virus was then

amplified by passaging the supernatant at ratios of 1:10 into fresh SF9 cultures until titer was sufficient for large-scale expression. 5 liters of Hi-five cells grown in Express Five (Invitrogen) media were infected with recombinant virus to drive expression of secreted sE2. The supernatants from the large-scale infections were then filtered with a 0.2μm cutoff bottle-top filter, concentrated and buffer exchanged into nickel binding buffer (300mM sodium citrate, 150mM NaCl and 50mM NaPO4 pH 8.0) using a Centramate tangential flow concentrator with 30kD cutoff membrane. The supernatants were finally purified by nickel and size-exclusion chromatography.

Cloning expression and purification of CD81-LEL. Residues 114-203 of human CD81 were cloned from a cDNA into a Pet28a(+) vector modified with a thrombin cleavable C-terminal BirA biotinylation sequence and 6x His tag. This bacterial expression vector was transformed into BL21-DE3 (RIL) cells (Stratagene), grown in a large-scale 6L culture of luria broth (LB) supplemented with 50mg/L kanamycin and induced at an optical density 400nm of 0.8 with 1mM isopropyl β-D-1-thiogalactopyranoside (IPTG). After 4 hours of induction the cells were centrifuged and pellets suspended in solution buffer (50mM Tris pH 8.0, 25% sucrose, 10mM DTT). Next, an equal amount of lysis buffer (50mM Tris pH 8.0, 1% TritonX-100, 100mM NaCl, 10mM DTT) was added. The lysate was supplemented with 0.8mg/mL lysozyme and sonicated to disrupt cell membranes. The lysate was then centrifuged; the supernatant was discarded and the inclusion body pellet was washed 3x with wash buffer (50mM Tris pH 8.0, 0.5% TritonX-100, 100mM NaCl, 1mM DTT) and once in wash buffer without TritonX-100. Purified inclusion bodies were solubilized in 6M guanidine-HCl, 10mM Tris pH 8.0 and 20mM β-mercaptoethanol. Aliquots of this solution were

diluted in oxidative refolding buffer containing 400mM L-arginine, 100mM Tris pH 8.0, 0.5mM oxidized glutathione and 5mM reduced glutathione for overnight refolding. The refolded protein was concentrated using an Amicon 400 concentrator with 10kD cutoff membrane and purified on a S200 size exclusion column.

Enzymatic deglycosylation of sE2. 1mg of H77 sE2 was buffer exchanged into Endo F digestion buffer (0.1M acetate pH 5.5) and protease inhibitor cocktail (Sigma) was added to a final concentration of 1x in a total volume of 100μL. 1 unit of Endo F1 and Endo F3 (Sigma) were each added to the digestion, which was allowed to proceed for 6 hours at room temperature. Next, 20uL of 1M Tris-HCl pH 8.0 was added to the reaction along with 2500 units of Pngase F and incubated at room temperature overnight. sE2 was subsequently purified by nickel chromatography to remove the glycosidases.

Cloning expression and purification of GST-HVR1 fusion proteins. HVR1 peptides spanning residues 385-410, 385-397, 391-403 and 398-410 of the J6 isolate were cloned into the PGEX-4T-1 vector which encodes for an N-terminal GST tag. DNA inserts were generated by ordering complementary, overalapping primers (IDT) with BamHI and XhoI sites encoded at the 5' and 3' ends (relative to the coding region of the sequence) respectively. Double-stranded inserts were generated by boiling equimolar concentrations of each primer mixed together and letting the solution cool to room temperature. PGEX-4T-1 was cleaved at BamHI and XhoI, restriction sites allowing for in frame cloning of the HVR1 inserts, gel purified and ligated with the various HVR1 constructs.

GST-HVR1 peptides were expressed as soluble fusion proteins in 1L cultures of BL21 DE3 (RIL) cells (Stratagene) by inducton with 1mM IPTG upon reaching an OD of

1.0. Expression was allowed to proceed for 4 hours after induction, after which cells were lysed in B-PER lysis buffer (Pierce), clarified by centrifugation at 10,000g for 30 minutes and purified by affinity chromatography with glutathione linked agarose.

Multi-angle light scattering. CD81-LEL or sE2 protein (200μg) was individually injected onto an HPLC and flowed over a sizing column while multiple parameters were measured. The light scattering, refractive index change and UV absorbance were observed over the elution profile via the Dawn Helios II multi-angle light scattering detector (Wyatt), Optilab rEX (Wyatt) differential refractive index detector and photodiode array detector 996 (Waters) respectively. These data were analyzed with Astra V macromolecular characterization software (Wyatt) to calculate the molecular weight (MW) of each protein from the light scattering and refractive index change. In order to determine the MW of the sE2:CD81-LEL complex, 100μg CD81-LEL was mixed with 500μg of sE2 and each of the two resultant peaks in the elution profile (representative of excess sE2 and complex) was processed as described above.

Surface plasmon resonance. CD81-LEL was coupled to a CM5 sensor chip using standard amine chemistry to a level of 200 response units (RU). Various concentrations of sE2 +/- HVR1 from genotypes 1 and 2 were passed over the chip at 60μL/min until reaching equilibrium. This required 240 seconds for genotype 1 and 60 seconds for genotype 2. All curves were reference subtracted from a control flow cell containing 200 RU of amine coupled murine anti-K^b antibody to account for non-specific interaction. The chip was regenerated with 0.1M glycine pH 2.7 after sE2 binding to remove any protein that remained bound. This regeneration condition did not result in any observable loss of subsequent binding during the runs. Binding experiments were performed on a

Biacore T-100 instrument in *HBS-EP* buffer pH 7.4 (10mM Hepes, 150mM NaCl, 3mM EDTA, 0.005% Tween-20). When varying pH conditions to measure its effects on kinetics of genotype 1 sE2:CD81-LEL interaction, HBS-EP was adjusted to pH 6.4 or 5.4 with 1N hydrochloric acid. For each experiment, a minimum of 5 curves were fitted to a 1:1 kinetic binding model in order to determine k_a, k_d and K_D using the Biacore T-100 evaluation software.

Neutralization of HCVcc and ΔHVR1 HCVcc. Neutralization of chimeric viruses +/- HVR1 with genotype 1a(H77)-2a(J6) specific core-NS2 sequences was assessed by focus forming unit assay: 50 to 400 $TCID_{50}$ of HCV were incubated 1 h at 37°C with MAb H77.39 or an isotype control and then incubated with cells for 3 h. After 48 h cells were immunostained for NS5A as previously described [54]. FFU counting was automated using ImmunoSpot Series 5 UV Analyzer [58]. Percent neutralization was calculated by relating FFU counts to mean of six-replicates incubated in the absence of antibody (virus only). Neutralization data were analyzed as variable slope dose-response curves using GraphPad Prism 4.0 and IC_{50}-values were interpolated by the software.

ELISA for detection of antibody binding to HVR1. 200ng of each GST-HVR1 fusion protein were diluted into 100µL of coating buffer (0.5 M carbonate bicarbonate buffer, pH 9.6), loaded into a 96-well Maxisorp plate (Nunc) and allowed to incubate overnight at 4°C. Wells were washed 3x with PBS + 0.05% Tween and blocked for 1 hour at 37°C with PBS + 1% BSA, then washed 3x again. Wells containing a GST-HVR1 protein or BSA alone were then incubated with 500ng of either J36 or J103 antibody in 100µL PBS + 1% BSA for 30 minutes at 4°C. Wells were next washed 3x and treated with a peroxidase conjugated anti-mouse Fc polyclonal antibody for 30 minutes at 4°C

for secondary detection. Finally, wells were washed 3x to remove excess secondary antibody and developed with 150µL of 3, 3′ ,5 ,5′-Tetramethylbenzidine (TMB) substrate for 5 minutes at room temperature. This experiment was performed in duplicate three independent days and a representative experiment was reported.

E2 binding to receptor-expressing CHO cells. To assess whether CD81-LEL could inhibit binding of sE2 to SR-BI, CHO cells expressing SR-BI were detached with PBS supplemented with 4 mM EDTA and 10% FBS and washed three times in medium. Cells (10^5) were pelleted in a V-bottom plate and incubated with 0.5µM of genotype 1 (H77) sE2 pre-mixed with varying concentrations of CD81-LEL (0-16 µM). Cells were washed, incubated with an Alexa Fluor 647-labeled penta-His antibody (Qiagen) for 20 min on ice, washed again, and binding analyzed on a FACSArray flow cytometer (Becton-Dickinson) using FloJo software (Tree Star). Binding of 1µM sE2 and ΔHVR1 sE2 was detected using the same staining protocol in the absence of CD81-LEL.

Statistical analysis. All data were analyzed using Graphpad Prism software (version 4.0) **.**

Western blot for detection of E2 binding to SRB1 expressing CHO cells. 10^5 wild type CHO cells as well as those expressing human CD81, SR-BI or no recombinant receptor were stained with 4µM H77 sE2 alone or pre-mixed with 32 µM human CD81-LEL in PBS+1% BSA. Cells were washed three times with PBS, resuspended in 50µL PBS+1% Tween-20 and 50µL SDS loading buffer + 10mM 2-mercaptoethanol and lysed by sonication. 30µL samples were loaded onto a 4-15% precast polyacrylamide gel (Biorad) and then transferred to a PVDF membrane using the iBlot system (Invitrogen). The membrane was blocked with PBS+0.1% Tween-20 containing 5% non-fat dry milk

(Biorad) for 30 minutes and then non-conformational murine anti-E2 antibody H77.36 was added to a concentration of 10μg/mL and incubated for 30 minutes. The membrane was then washed three times in PBS+0.1% Tween-20 and stained with goat anti-mouse Fc peroxidase-conjugated secondary antibody (Sigma) for 30 minutes at a 1:25,000 dilution. The blot was again washed 3 times, dried and samples were detected using the ECL western blotting detection reagent (GE Healthcare) after a 30 second exposure on CL-Xposure film (Pierce).

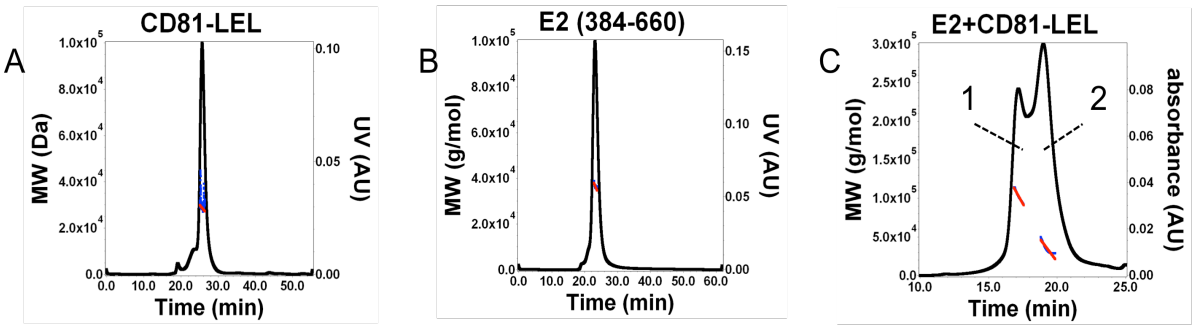

	MW-predicted	Mw-calculated	Oligomeric state
CD81-LEL	13.8kD	28.5kD	Dimer
sE2 (384-660)	32.1kD	36.1kD	Monomer
sE2 (peak 2, "C")	32.1kD	34.0kD	Monomer
CD81-LEL+sE2 (peak 1, "C")	NA	101.8kD	2:2

Figure 1: Oligomeric state of sE2 and CD81-LEL alone and in complex. Solution molecular weight of CD81-LEL (A), sE2 (B) and the two proteins in complex (C) were determined by multi-angle light scattering over their elution profiles from a size-exclusion column. In panel "C", each peak was evaluated independently. The molecular weight of peak 1 corresponded to a 2:2 CD81-LEL:sE2 complex and peak 2 is corresponded to sE2, which was in excess. The black trace represents UV absorbance, red and blue represent the molar mass and fitted molar mass across the peaks.

A

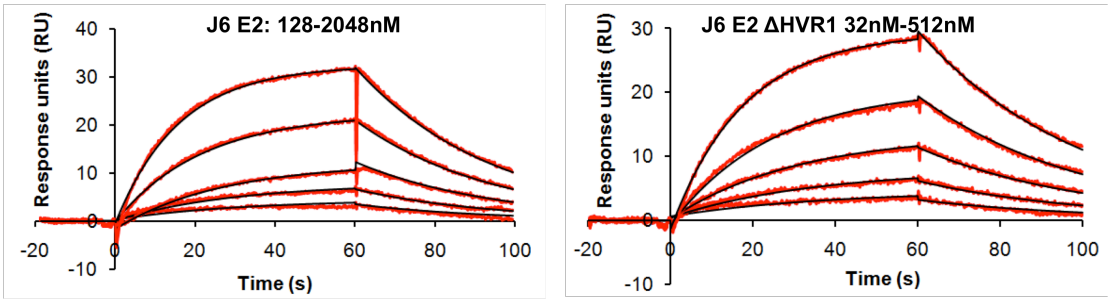

	k_a (1/Ms)	k_d (1/s)	K_D (M)	$t_{1/2}$ (s)	Fold change from wt K_D
J6 E2	$1.66x10^4$	$2.90x10^{-2}$	$1.75x10^{-6}$	24.9	-
J6 E2 delta HVR1	$1.24x10^5$	$2.47x10^{-2}$	$1.99x10^{-7}$	28.1	8.8
H77 E2 pH 7.4	$2.78x10^4$	$2.81x10^{-3}$	$1.01x10^{-7}$	246	-
H77 E2 delta HVR1	$4.59x10^4$	$2.11x10^{-3}$	$4.60x10^{-8}$	328	2.2
H77 E2 pH 6.4	$6.82x10^4$	$2.41x10^{-3}$	$3.54x10^{-8}$	288	2.9
H77 E2 pH 5.4	$1.95x10^5$	$4.52x10^{-3}$	$2.31x10^{-8}$	153	4.4
H77 E2 (deglyc ctrl)	$1.77x10^4$	$3.62x10^{-3}$	$2.04x10^{-7}$	191	
H77 E2-deglyc	$2.30x10^4$	$2.03x10^{-3}$	$8.80X10^{-8}$	341	2.3

B

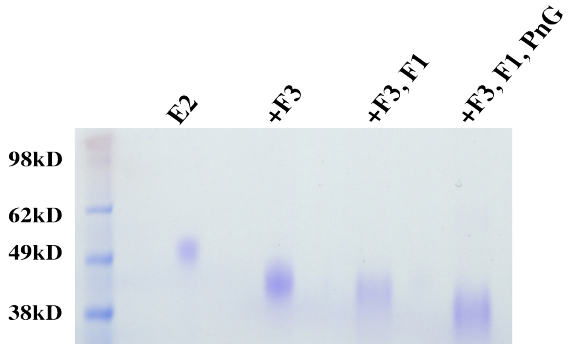

Figure 2: Affinity and kinetics of sE2:CD81-LEL interaction. A) Selected sensograms are displayed, red curves are the raw data and the black curves are 1:1 kinetic fits. CD81-LEL was immobilized on a sensor chip and H77 or J6 sE2 +/- HVR1 was flowed over the surface to evaluate kinetics and affinity. H77 sE2 was also tested at pH 6.4 and 5.4, and after deglycosylation. The row designated H77 E2 (deglyc ctrl) contains the parameters for sE2 exposed to the equivalent buffers conditions as the enzymatically treated protein. B) SDS-page gel analysis of untreated sE2 or sE2 treated by EndoF3 alone, Endo F1 and F3, or Endo F1, F3 and PngaseF.

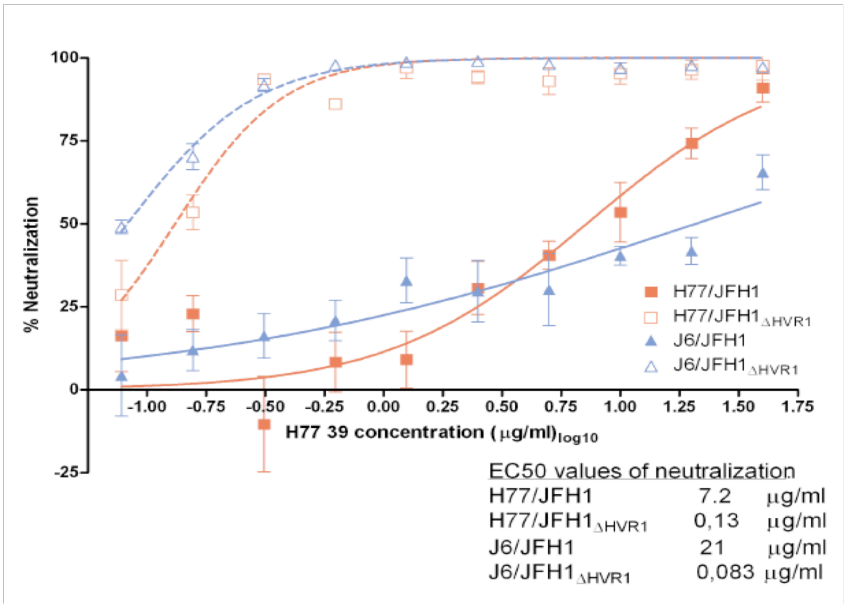

Figure 3: Neutralization of J6 and H77 HCVcc +/- HVR1 by a broadly cross-reactive antibody. Broadly cross-reactive antibody H77.39 blocks sE2 interaction with CD81 and was tested for neutralization of H77 and J6 virus +/- HVR1. Bracketed values to the right of the chart of EC50 values represent increase fold-increase over the neutralization of ΔHVR1 virus over wild-type virus.

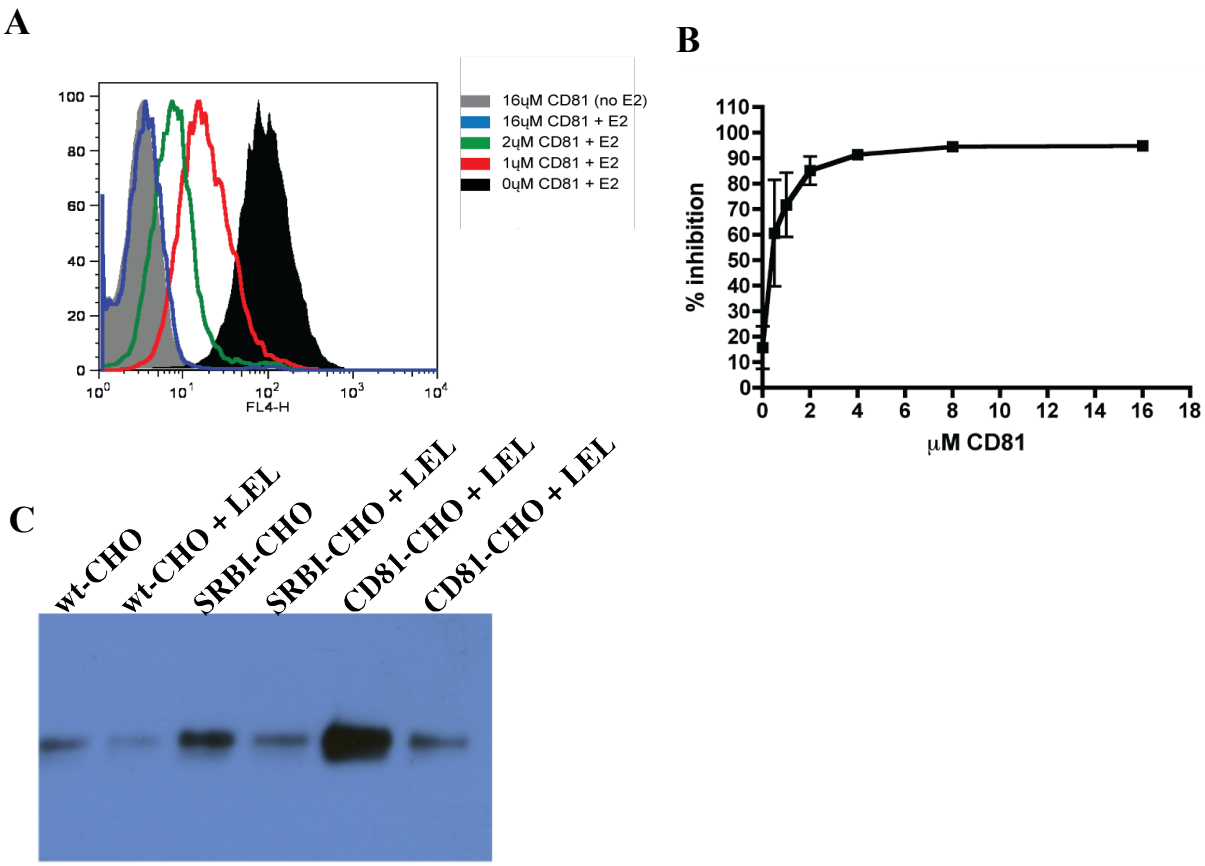

Figure 4: Soluble CD81-LEL inhibits sE2 engagement of SR-BI. A) Inhibition of sE2 binding to CHO cells expressing SR-BI was tested by staining in the presence of various concentrations of CD81-LEL and detecting by flow cytometry. B) Data from (A) is expressed as percent inhibition of sE2 binding to SR-BI expressing cells v. concentration of CD81-LEL. C) Western blot of lysates from WT CHO cells or CHO cells expressing CD81 or SR-BI stained with sE2 or sE2 + CD81-LEL (designated by +LEL). Bound sE2 was detected with non-conformational anti-E2 antibody H77.36.

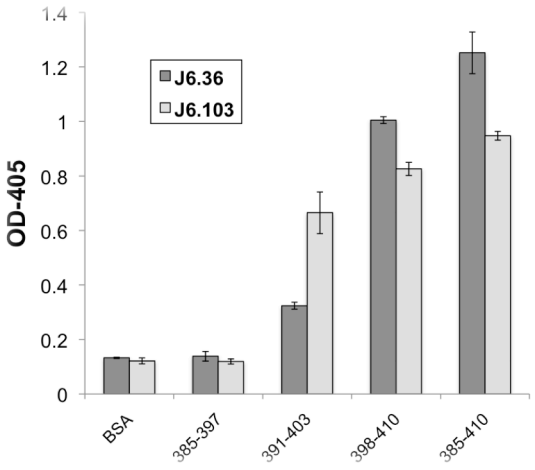

Figure 5: Neutralizing antibody recognition of HVR1. HVR1 or truncations of HVR1 were fused to GST was detected by monoclonal antibodies J6.36 or J6.103. BSA alone served as a negative control.

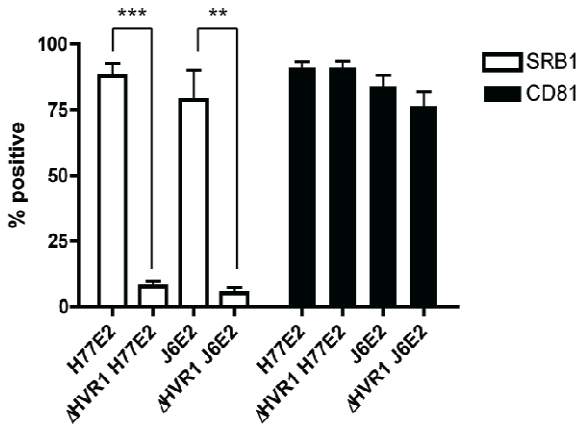

Figure 6: Binding of sE2 and ΔHVR1 sE2 to CD81 and SR-BI. CHO cells expressing SR-BI or CD81 were stained with sE2 or ΔHVR1 sE2 from H77 or J6 strains. Bound sE2 was detected with an anti-6x His antibody.

5.7 References

1. Shepard, C.W., Finelli, L. & Alter, M.J. Global epidemiology of hepatitis C virus infection. *Lancet Infect Dis* **5**, 558-567 (2005).
2. Hoofnagle, J.H. *et al.* Treatment of chronic non-A,non-B hepatitis with recombinant human alpha interferon. A preliminary report. *N. Engl. J. Med.* **315**, 1575-1578 (1986).
3. Ferenci, P. Historical treatment of chronic hepatitis B and chronic hepatitis C. *Gut* **34**, S69-S73 (1993).
4. Reichard, O., Andersson, J., Schvarcz, R. & Weiland, O. Ribavirin treatment for chronic hepatitis C. *Lancet* **337**, 1058-1061 (1991).
5. Bailly, F., Si, N., Si, A. & Trepo, C. Treatment of HCV liver disease by recombinant interferon alpha. *Nephrol. Dial. Transplant.* **11 Suppl 4**, 56-57 (1996).
6. Sherman, K.E. *et al.* Response-guided telaprevir combination treatment for hepatitis C virus infection. *N. Engl. J. Med.* **365**, 1014-1024 (2011).
7. Kwong, A.D., Kauffman, R.S., Hurter, P. & Mueller, P. Discovery and development of telaprevir: an NS3-4A protease inhibitor for treating genotype 1 chronic hepatitis C virus. *Nat. Biotechnol.* **29**, 993-1003 (2011).
8. Grakoui, A., Wychowski, C., Lin, C., Feinstone, S.M. & Rice, C.M. Expression and identification of hepatitis C virus polyprotein cleavage products. *J. Virol.* **67**, 1385-1395 (1993).
9. Moradpour, D., Penin, F. & Rice, C.M. Replication of hepatitis C virus. *Nat. Rev. Microbiol.* **5**, 453-463 (2007).

10. Scarselli, E. *et al.* The human scavenger receptor class B type I is a novel candidate receptor for the hepatitis C virus. *EMBO J.* **21**, 5017-5025 (2002).
11. Pileri, P. *et al.* Binding of hepatitis C virus to CD81. *Science* **282**, 938-941 (1998).
12. Bartosch, B. *et al.* In vitro assay for neutralizing antibody to hepatitis C virus: evidence for broadly conserved neutralization epitopes. *Proc. Natl. Acad. Sci. U.S.A.* **100**, 14199-14204 (2003).
13. Kaplan, M., Gawrieh, S., Cotler, S.J. & Jensen, D.M. Neutralizing antibodies in hepatitis C virus infection: a review of immunological and clinical characteristics. *Gastroenterology* **125**, 597-604 (2003).
14. Dubuisson, J. *et al.* Formation and intracellular localization of hepatitis C virus envelope glycoprotein complexes expressed by recombinant vaccinia and Sindbis viruses. *J. Virol.* **68**, 6147-6160 (1994).
15. Vieyres, G. *et al.* Characterization of the envelope glycoproteins associated with infectious hepatitis C virus. *J. Virol.* **84**, 10159-10168 (2010).
16. Michalak, J.P. *et al.* Characterization of truncated forms of hepatitis C virus glycoproteins. *J. Gen. Virol.* **78 (Pt 9)**, 2299-2306 (1997).
17. Whidby, J. *et al.* Blocking Hepatitis C Virus Infection with Recombinant Form of Envelope Protein 2 Ectodomain. *J Virol* **83**, 11078-11089 (2009).
18. Helle, F. *et al.* Role of N-linked glycans in the functions of hepatitis C virus envelope proteins incorporated into infectious virions. *J. Virol.* **84**, 11905-11915 (2010).
19. Falkowska, E., Kajumo, F., Garcia, E., Reinus, J. & Dragic, T. Hepatitis C virus envelope glycoprotein E2 glycans modulate entry, CD81 binding, and neutralization. *J. Virol.* **81**, 8072-8079 (2007).

20. Helle, F. *et al.* The neutralizing activity of anti-hepatitis C virus antibodies is modulated by specific glycans on the E2 envelope protein. *J. Virol.* **81**, 8101-8111 (2007).
21. McCaffrey, K., Boo, I., Poumbourios, P. & Drummer, H.E. Expression and characterization of a minimal hepatitis C virus glycoprotein E2 core domain that retains CD81 binding. *J. Virol.* **81**, 9584-9590 (2007).
22. Hijikata, M. *et al.* Hypervariable regions in the putative glycoprotein of hepatitis C virus. *Biochem. Biophys. Res. Commun.* **175**, 220-228 (1991).
23. Kurosaki, M., Enomoto, N., Marumo, F. & Sato, C. Rapid sequence variation of the hypervariable region of hepatitis C virus during the course of chronic infection. *Hepatology* **18**, 1293-1299 (1993).
24. Rispeter, K. *et al.* Hepatitis C virus variability: sequence analysis of an isolate after 10 years of chronic infection. *Virus Genes* **21**, 179-188 (2000).
25. Kato, N. *et al.* Humoral immune response to hypervariable region 1 of the putative envelope glycoprotein (gp70) of hepatitis C virus. *J. Virol.* **67**, 3923-3930 (1993).
26. Vieyres, G., Dubuisson, J. & Patel, A.H. Characterization of antibody-mediated neutralization directed against the hypervariable region 1 of hepatitis C virus E2 glycoprotein. *J Gen Virol* **92**, 494-506 (2011).
27. Penin, F. *et al.* Conservation of the conformation and positive charges of hepatitis C virus E2 envelope glycoprotein hypervariable region 1 points to a role in cell attachment. *J. Virol.* **75**, 5703-5710 (2001).

28. Basu, A., Beyene, A., Meyer, K. & Ray, R. The hypervariable region 1 of the E2 glycoprotein of hepatitis C virus binds to glycosaminoglycans, but this binding does not lead to infection in a pseudotype system. *J. Virol.* **78**, 4478-4486 (2004).
29. Bankwitz, D. *et al.* Hepatitis C virus hypervariable region 1 modulates receptor interactions, conceals the CD81 binding site, and protects conserved neutralizing epitopes. *J. Virol.* **84**, 5751-5763 (2010).
30. Flint, M. *et al.* Characterization of hepatitis C virus E2 glycoprotein interaction with a putative cellular receptor, CD81. *J. Virol.* **73**, 6235-6244 (1999).
31. Evans, M.J. *et al.* Claudin-1 is a hepatitis C virus co-receptor required for a late step in entry. *Nature* **446**, 801-805 (2007).
32. Zheng, A. *et al.* Claudin-6 and claudin-9 function as additional coreceptors for hepatitis C virus. *J. Virol.* **81**, 12465-12471 (2007).
33. Ploss, A. *et al.* Human occludin is a hepatitis C virus entry factor required for infection of mouse cells. *Nature* **457**, 882-886 (2009).
34. Cormier, E.G. *et al.* L-SIGN (CD209L) and DC-SIGN (CD209) mediate transinfection of liver cells by hepatitis C virus. *Proc. Natl. Acad. Sci. U.S.A.* **101**, 14067-14072 (2004).
35. Monazahian, M. *et al.* Low density lipoprotein receptor as a candidate receptor for hepatitis C virus. *J. Med. Virol.* **57**, 223-229 (1999).
36. Barth, H. *et al.* Cellular binding of hepatitis C virus envelope glycoprotein E2 requires cell surface heparan sulfate. *J. Biol. Chem.* **278**, 41003-41012 (2003).

37. Nakajima, H., Cocquerel, L., Kiyokawa, N., Fujimoto, J. & Levy, S. Kinetics of HCV envelope proteins' interaction with CD81 large extracellular loop. *Biochem. Biophys. Res. Commun.* **328**, 1091-1100 (2005).

38. Catanese, M.T. *et al.* Role of scavenger receptor class B type I in hepatitis C virus entry: kinetics and molecular determinants. *J. Virol.* **84**, 34-43 (2010).

39. Sabo, M.C. *et al.* Neutralizing monoclonal antibodies against hepatitis C virus E2 protein bind discontinuous epitopes and inhibit infection at a postattachment step. *J. Virol.* **85**, 7005-7019 (2011).

40. Catanese, M.T. *et al.* High-avidity monoclonal antibodies against the human scavenger class B type I receptor efficiently block hepatitis C virus infection in the presence of high-density lipoprotein. *J. Virol.* **81**, 8063-8071 (2007).

41. Meuleman, P. *et al.* Anti-CD81 antibodies can prevent a hepatitis C virus infection in vivo. *Hepatology* **48**, 1761-1768 (2008).

42. Owsianka, A.M. *et al.* Identification of conserved residues in the E2 envelope glycoprotein of the hepatitis C virus that are critical for CD81 binding. *J. Virol.* **80**, 8695-8704 (2006).

43. Drummer, H.E., Boo, I., Maerz, A.L. & Poumbourios, P. A conserved Gly436-Trp-Leu-Ala-Gly-Leu-Phe-Tyr motif in hepatitis C virus glycoprotein E2 is a determinant of CD81 binding and viral entry. *J. Virol.* **80**, 7844-7853 (2006).

44. Dreux, M. *et al.* High density lipoprotein inhibits hepatitis C virus-neutralizing antibodies by stimulating cell entry via activation of the scavenger receptor BI. *J. Biol. Chem.* **281**, 18285-18295 (2006).

45. Bartosch, B. *et al.* An interplay between hypervariable region 1 of the hepatitis C virus E2 glycoprotein, the scavenger receptor BI, and high-density lipoprotein promotes both enhancement of infection and protection against neutralizing antibodies. *J. Virol.* **79**, 8217-8229 (2005).
46. Cormier, E.G. *et al.* CD81 is an entry coreceptor for hepatitis C virus. *Proc. Natl. Acad. Sci. U.S.A.* **101**, 7270-7274 (2004).
47. Sharma, N.R. *et al.* Hepatitis C virus is primed by CD81 protein for low pH-dependent fusion. *J. Biol. Chem.* **286**, 30361-30376 (2011).
48. Voisset, C. *et al.* High density lipoproteins facilitate hepatitis C virus entry through the scavenger receptor class B type I. *J. Biol. Chem.* **280**, 7793-7799 (2005).
49. Kitadokoro, K. *et al.* CD81 extracellular domain 3D structure: insight into the tetraspanin superfamily structural motifs. *EMBO J.* **20**, 12-18 (2001).
50. Higginbottom, A. *et al.* Identification of amino acid residues in CD81 critical for interaction with hepatitis C virus envelope glycoprotein E2. *J. Virol.* **74**, 3642-3649 (2000).
51. Nybakken, G.E. *et al.* Structural basis of West Nile virus neutralization by a therapeutic antibody. *Nature* **437**, 764-769 (2005).
52. Oliphant, T. *et al.* Development of a humanized monoclonal antibody with therapeutic potential against West Nile virus. *Nat. Med.* **11**, 522-530 (2005).
53. Law, M. *et al.* Broadly neutralizing antibodies protect against hepatitis C virus quasispecies challenge. *Nat. Med.* **14**, 25-27 (2008).

54. Li, C., Candotti, D. & Allain, J.P. Production and characterization of monoclonal antibodies specific for a conserved epitope within hepatitis C virus hypervariable region 1. *J. Virol.* **75**, 12412-12420 (2001).

55. Zibert, A., Schreier, E. & Roggendorf, M. Antibodies in human sera specific to hypervariable region 1 of hepatitis C virus can block viral attachment. *Virology* **208**, 653-661 (1995).

56. Dao Thi, V.L., Dreux, M. & Cosset, F.-L. Scavenger receptor class B type I and the hypervariable region-1 of hepatitis C virus in cell entry and neutralisation. *Expert Rev Mol Med* **13**, e13 (2011).

57. Abraham, J., Corbett, K.D., Farzan, M., Choe, H. & Harrison, S.C. Structural basis for receptor recognition by New World hemorrhagic fever arenaviruses. *Nat. Struct. Mol. Biol.* **17**, 438-444 (2010).

58. Myszka, D.G. *et al.* Energetics of the HIV gp120-CD4 binding reaction. *Proc. Natl. Acad. Sci. U.S.A.* **97**, 9026-9031 (2000).

59. Santiago, C., Björling, E., Stehle, T. & Casasnovas, J.M. Distinct kinetics for binding of the CD46 and SLAM receptors to overlapping sites in the measles virus hemagglutinin protein. *J. Biol. Chem.* **277**, 32294-32301 (2002).

60. Jiang, J. & Luo, G. Apolipoprotein E but not B is required for the formation of infectious hepatitis C virus particles. *J. Virol.* **83**, 12680-12691 (2009).

61. Nielsen, S.U. *et al.* Association between hepatitis C virus and very-low-density lipoprotein (VLDL)/LDL analyzed in iodixanol density gradients. *J. Virol.* **80**, 2418-2428 (2006).

62. Moore, J.P. Coreceptors: implications for HIV pathogenesis and therapy. *Science* **276**, 51-52 (1997).

63. Rizzuto, C.D. *et al.* A conserved HIV gp120 glycoprotein structure involved in chemokine receptor binding. *Science* **280**, 1949-1953 (1998).

64. Feng, Y., Broder, C.C., Kennedy, P.E. & Berger, E.A. HIV-1 entry cofactor: functional cDNA cloning of a seven-transmembrane, G protein-coupled receptor. *Science* **272**, 872-877 (1996).

65. Svicher, V. *et al.* Identification and structural characterization of novel genetic elements in the HIV-1 V3 loop regulating coreceptor usage. *Antiviral Therapy* **16**, 1035-1045 (2011).

66. Laakso, M.M. *et al.* V3 loop truncations in HIV-1 envelope impart resistance to coreceptor inhibitors and enhanced sensitivity to neutralizing antibodies. *PLoS Pathog.* **3**, e117 (2007).

67. Helle, F., Duverlie, G. & Dubuisson, J. The hepatitis C virus glycan shield and evasion of the humoral immune response. *Viruses* **3**, 1909-1932 (2011).

68. Wei, X. *et al.* Antibody neutralization and escape by HIV-1. *Nature* **422**, 307-312 (2003).

69. Lin, G., Lee, B., Haggarty, B.S., Doms, R.W. & Hoxie, J.A. CD4-Independent Use of Rhesus CCR5 by Human Immunodeficiency Virus Type 2 Implicates an Electrostatic Interaction between the CCR5 N Terminus and the gp120 C4 Domain. *J Virol* **75**, 10766-10778 (2001).

70. Endres, M.J. *et al.* CD4-independent infection by HIV-2 is mediated by fusin/CXCR4. *Cell* **87**, 745-756 (1996).

71. Crublet, E., Andrieu, J.-P., Vivès, R.R. & Lortat-Jacob, H. The HIV-1 envelope glycoprotein gp120 features four heparan sulfate binding domains, including the co-receptor binding site. *J. Biol. Chem.* **283**, 15193-15200 (2008).

72. Harrop, H.A., Coombe, D.R. & Rider, C.C. Heparin specifically inhibits binding of V3 loop antibodies to HIV-1 gp120, an effect potentiated by CD4 binding. *AIDS* **8**, 183-192 (1994).

Chapter 6:

Conclusions and future directions

6.1 Abstract

The focus of this thesis was the establishment of a structural basis for antibody and receptor interactions with *Flaviviridae* Japanese Encephalitis Virus and Hepatitis C Virus. To this end, I determined the high-resolution dimeric crystal structure of JEV E, which provided insight into the mechanisms of serocomplex-specific pathogenesis in flaviviruses. Additionally, I was able to resolve several biochemical features of the interplay between HCV envelope protein E2, antibodies and host receptors CD81 and SR-BI. Studies of these interactions indicated that E2 cannot simultaneously engage both receptors and that sequence diversity within E2 may contribute to receptor preference. Future studies will focus on identification of specific residues involved in the putative shared CD81/SR-BI binding site on E2 and determination of the kinetics and affinity of E2 interaction and membrane-bound receptors. I speculate that crystallization of E2 will require generation of new constructs that more closely resemble its conformation in the native virion. Finally, I have discussed the need for new therapeutics and reviewed antivirals that have been garnered from advances in the understanding of virus structure and entry.

6.2 Conclusions and summary: JEV E structure

JEV is an important human pathogen and the leading global cause of viral encephalitis. Cross-neutralization tests have allowed for classification of flaviviruses into serocomplexes[1] with specific tropisms and pathogeneses. Our results have illuminated structural and biophysical features of flavivirus E proteins that may contribute to serocomplex-specific pathogenesis. The high-resolution crystal structure of JEV E revealed a dimer interface that is remarkably small relative to those of other known dimeric E structures. This interface had only ~50% of the buried surface area found between other E homodimers. JEV E lacks many of the contacts found at the central DII-DII dimerization region of other E structures. The surface area it does bury is almost exclusively within the DI-DIII pocket that houses the fusion-loop, highlighting the evolutionary requirement to shield this peptide from prematurely inducing fusion.

Given the sparse JEV E dimer interface and monomeric crystal structure of WNV E[2,3], we hypothesized that reduced dimerization propensity may be serocomplex-specific. Indeed, we found that JEV E, WNV E and SLEV E were predominantly monomeric in solution while DV2 E was dimeric. We resolved the oligomeric states of these proteins by multi-angle light scattering, which allows for direct experimental determination of molecular weight. Utilization of this technique was of particular importance since oligomeric state determination by techniques such as SEC and crystallography has yielded inaccurate results for E proteins. Our own JEV E crystallized as a dimer but favored monomers in solution, and extrapolations based on molecular weight standards using SEC have been unreliable[3].

Quaternary interactions between E proteins on the surface of virions can influence binding of antibodies and cellular receptors. The epitope of WNV-neutralizing antibody CR4354 is found across two adjacent E proteins, indicating that the specific assembly of E on the virion can contribute to immune recognition[4]. DIII is believed to play a role in flavivirus attachment and entry[5,6] and packs in 3 distinct chemical environments on the mature virion[7]. However, anti-DIII antibody E16 binds only 2 of these 3 environments but allows for virion attachment and entry[8,9]. This implies that only a pentameric arrangement of DIII at the 5-fold axis is required for receptor interaction at the cell surface.

It has become increasingly clear that E protein organization plays a significant role in host recognition of flaviviruses. Our findings therefore implicate the assembly and dimerization affinity of E proteins in serocomplex-specific pathogenesis.

6.3 Conclusions and summary: HCV receptor interaction

Extensive characterization of a large panel of anti-E2 antibodies has provided insight towards mechanisms of effective neutralization of HCV. The most potent neutralizing antibodies bound the N-terminal region I of E2, could be cross-reactive or strain-specific and were able to inhibit interaction with CD81, SR-BI or both[10]. These findings led us to further investigate the specific molecular determinants responsible for E2 interaction with these two receptors.

Since our H77.39 antibody was able to strongly inhibit sE2 binding to both CD81 and SR-BI, we wanted to investigate whether these receptors may share a binding site on E2. We pre-bound sE2 to CD81-LEL and were indeed able to block subsequent binding

to SR-BI. Currently we are only able to speculate as to where on E2 the binding sites of SR-BI and CD81 may overlap. Our own work and that of several others have identified HVR1 (E2 residues 384-410) as a requirement for SR-BI interaction[11,12]. Residues W420 and 529-535 are required for E2:CD81 interaction[13], so reasonable prediction is that the W420 or other conserved residues in close proximity to HVR1 may comprise the shared site. Another possibility is that an event accompanying HCV entry, such as a receptor- or acid-induced conformational change, allows E2 to link both receptors or disengages it from one so it may bind the other. We are in the process of investigating whether the reverse of our findings, pre-binding of E2 to SR-BI, will block CD81:E2 interaction.

While direct binding of E2 to CD81 has been extensively characterized, some basic biochemical features of this interaction are unknown. We determined the solution oligomeric state of sE2, CD81-LEL and the sE2:CD81 complex. CD81-LEL formed a homodimer that was engaged by 2 monomeric sE2 proteins to form a 2:2 complex. This stoichiometric information allowed us to properly orient the two proteins in SPR experiments that measured the kinetics and affinity of this interaction. Binding was non-cooperative, and CD81-LEL and sE2 bound with an affinity comparable to that observed for other viral envelope proteins with cellular receptors. The interaction was strengthened mildly by low pH (5.4) and enzymatic removal of glycans from sE2, but these increases are unlikely to be of biological relevance.

Two of our neutralizing antibodies bound HVR1 of E2, a region that plays several roles in the HCV life cycle. Deletion of HVR1 from sE2 led to enhancement of CD81-LEL binding, and this increase in affinity was genotype specific. Additionally, neutralization of HVR1-deleted virus by our broadly cross-reactive mAb H77.39 was

enhanced and correlated with the genotype-specific increase in affinity observed in our SPR experiments. Taken together, these results indicate that the extent that HVR1 conceals the CD81 binding site and conserved neutralizing epitopes varies across HCV genotypes.

6.4 Future directions: HCV receptor interaction

Kinetics and affinity of sE2 interaction with membrane bound receptors. While our results have clarified some aspects of E2 interaction with receptors, several questions remain. The 2:2 complex of sE2 and CD81-LEL formed in solution, but it is unclear whether bivalent engagement of CD81 by HCV in a cellular system is necessary for infection. Furthermore, the interaction of E2 with full-length CD81 or SR-BI in cell membranes may not be identical to what is observed in solution. In the immediate future, it is realistic to believe we can determine the affinity of sE2 for SR-BI and CD81 captured from cell lysates to better recapitulate the native interaction. This could be achieved by biolayer interferometry because the technique bypasses the sensitive fluidics of SPR instruments.

Purification of E1-E2 complexes. A major concern in studies of HCV entry is the inability to generate a soluble E1-E2 complex with properties similar to E1-E2 in wild-type virus. Little is known about the function of E1, including its influence on E2 receptor binding. Even basic features of E1 such as its membrane topology are unclear. Unfortunately, the oligomeric state of E1 and E2 virions is also poorly understood so development of a functional E1-E2 complex will likely require a trial and error approach with truncations, leucine-zippered heterodimers or linkers. Another potential strategy

would be to purify E1 and E2 with trypsin treatment of virus grown in serum-free media (to eliminate contaminating lipoproteins associated with particles). This approach has been used successfully in purification of TBEV E[14], but the relatively low titer of cell-culture produced HCV could hamper such efforts.

Identification of individual E2 residues involved in SR-BI interaction. CHO cells expressing SR-BI allowed us to test our anti-E2 antibodies for inhibition of E2:SR-BI binding, but will also provide us with an excellent tool to identify the molecular determinants of this interaction in future experiments. While HVR1 has been proposed to bind SR-BI[11], HVR1 peptide alone is not sufficient for E2:SR-BI binding (data not shown). Staining of these SR-BI expressing CHO cells with mutants of sE2 known to have null CD81 binding activity may allow us to identify residues involved in an overlapping binding site. One ideal example is a mutant of the W420 residue only 10aa upstream of HVR1 in primary sequence and ablates CD81 binding[15]. The specific SR-BI binding determinants within HVR1 are also undefined. Our antibodies J6.36 and J6.103 each block this interaction and map to G397, F403 and G406 of E2[10], providing a series of candidate residues for mutation.

6.5 Future directions: *Flaviviridae* and structural biology

Flavivirus structures. The structural biology of flaviviruses has been studied extensively. Currently, there are available crystal structures of one immature E protein bound to prM[16], 5 in the pre-fusion conformation[3,17–19] and 3 in the post-fusion conformation[20–22]. Also, cryoEM structures and constructions have been determined for immature viruses at neutral[23,24] and acidic[25] pH and mature viruses alone[7,26], bound to

antibodies[27,27] and bound to the DC-SIGN attachment factor[28]. The final frontier in regards to structure determination of whole flavivirus virions will most likely be the result of advances in technology that allow for single molecule reconstruction at near-atomic resolution[29]. A large percentage of particles released by infected cells are partially mature, meaning they incorporate uncleaved prM proteins[30]. A single-particle reconstruction that reveals the structure a partially mature virion, or even the structure of a single fully mature particle could resolve many unanswered questions in the realm of flavivirus structural biology. For example, such a reconstruction may finally explain how neutralizing antibodies recognize buried epitopes such as the fusion loop. The discovery of a true cellular receptor that interacts with E would also generate new avenues for co-crystallization studies, but the requirement or existence of such a molecule is speculative.

Determination of HCV envelope protein structures. Many of my efforts were directed toward the crystallization of HCV E1 and E2 but were met with little success. While crystallization of a given protein is never guaranteed, one can provide several arguments based on the available literature as to why no group has succeeded in determining a structure of E1 or E2. The paradigm for envelope glycoprotein crystallization was established by Kwong *et al.* and led to successful determination of the HIV gp120[31]. The techniques were directed at minimizing the degrees of heterogeneity and conformational flexibility inherent to viral fusion proteins. Deletion of variable loops, mutation of N-linked glycosylation sites, enzymatic removal of glyans and stabilization with Fabs are the main strategies used to accomplish this goal. While mutation of more than a single N-linked glycosylation site on E2 was found to dramatically reduce yield, I was able to produce HVR1-deleted sE2, enzymatically

remove ~70% of its glycan molecular weight and complex it with Fab. Screening sE2 modified or complexed by these methods did not yield protein crystals. These methods were popularized many years ago, and have utilized in attempts to crystallize E2 by many groups besides our own; so it would seem there are additional complicating factors that prevent crystallization.

One hypothesis to explain no group has successfully crystallized E2 is that sE2 may be secreted as a heterogeneous population with varying degrees of unpaired and paired cysteines. Constructs of E2 span residues 384-660 and have been disulfide mapped to reveal the connectivity between the cysteines of purified sE2 monomers[32]. However, it has been determined that infectious HCV particles contain disulfide-linked E1 and E2 oligomers and require the presence of reduced cysteines[33,34]. It is also widely reported that production of sE2 results in secretion of disulfide linked aggregates. Our own experiments have confirmed this result and have even found that monomeric sE2 can form disulfide-linked oligomers after extended periods of refrigeration (data not shown). Future efforts to crystallize E2 will be more likely to succeed once an appropriately folded conformation of E2 or an E1-E2 complex is isolated.

6.6 The future of antiviral therapy for *Flaviviridae*

There are intriguing economical and philosophical questions regarding the utility of antiviral therapies that target specific *Flaviviridae* proteins. The existence of approved vaccines for YFV and JEV[35] is likely to limit efforts by pharmaceutical companies to focus efforts on these viruses. Few other arthropod-borne flaviviruses represent global health threats except for DV, which infects ~50 million people annually[36]. As there are no

approved vaccines or specific treatments for DV infection, it is one of the only flaviviruses likely to be a target for design of specific antivirals.

Hepatitis C chronically infects roughly 170 million people, however the number of annual incidences has declined by ~90% since 1990 due to screening of donated blood and organs. The decline in new infections, ~50% success rate of existing therapies and delayed onset of symptoms make HCV a unique case for pharmaceutical development. Essentially, there exists a massive population of infected individuals but minimal spread of the virus, prompting the urgent need for treatments that augment the effectiveness of the current regimen. If infected individuals may be cured before the onset of damaging symptoms, a massive public health crisis could be averted. Vaccination against DV and HCV has been unsuccessful, possibly due to antibody-dependent enhancement linked to heterologous DV infection[37] and extensive genetic variability of HCV[38], so future development of antiviral compounds or therapeutic antibodies remains a priority.

Several recent discoveries, however, may lead to the effective control of *Flaviviridae*. Antibodies or compounds that target host receptors and broad-spectrum antiviral compounds are two promising strategies. Preventing interaction with required host factors is advantageous in that it circumvents the issue of viral diversity. Extensive characterization of HCV cellular receptors has provided several potential candidates for such an approach. Indeed, antibodies that bind CD81[39], SR-BI[40] and CLN1[41] and a compound that targets SR-BI[42] each are able to inhibit HCV infection of hepatocytes. Furthermore, *Plasmodium falciparum* utilizes both CD81 and SR-BI for invasion of hepatocytes[43,44], suggesting molecules that target this entry pathway may be broadly applicable. While no required receptor for members of the flavivirus genus has been

identified, the successful inhibition of HCV infection by these methods should encourage future searches.

Several broad-spectrum antiviral compounds that neutralize enveloped viruses have also been identified. One example of such an agent, LJ001, inhibits infection of cells by flaviviruses, paramyxoviruses and filoviruses amongst others and is believed to function by binding viral membranes to disrupt fusion[45]. Another molecule, squalamine, inhibits DV2 and Hepatitis B Virus infection in vitro and YFV and MCMV in vivo by neutralizing the negative charge of host membranes in a manner that is believed to inhibit viral replication[46]. An especially promising drug, T-705 (Farapirivir) protects mice from lethal infection with influenza A viruses and is currently in phase II clinical trials[47].

The failure to develop several vaccines for many important human viruses illuminates the need for detailed understanding of the structure and entry of *Flaviviridae.* Extensive characterization of these processes has led to the discovery of many new viral and cellular proteins amenable to targeting by antibodies or pharmacological agents. Therapies that use a multi-pronged approach to boost the immune response, disrupt receptor interactions and directly target viral components are foreseeable in the near future and may help to eradicate these difficult to treat pathogens.

6.7 References

1. Calisher, C.H. *et al.* Antigenic relationships between flaviviruses as determined by cross-neutralization tests with polyclonal antisera. *J. Gen. Virol* **70 (Pt 1)**, 37-43 (1989).
2. Kanai, R. *et al.* Crystal Structure of West Nile Virus Envelope Glycoprotein Reveals Viral Surface Epitopes. *J. Virol.* **80**, 11000-11008 (2006).
3. Nybakken, G.E., Nelson, C.A., Chen, B.R., Diamond, M.S. & Fremont, D.H. Crystal Structure of the West Nile Virus Envelope Glycoprotein. *J. Virol.* **80**, 11467-11474 (2006).
4. Kaufmann, B. *et al.* Neutralization of West Nile virus by cross-linking of its surface proteins with Fab fragments of the human monoclonal antibody CR4354. *Proceedings of the National Academy of Sciences* doi:10.1073/pnas.1011036107
5. Lee, J.W.-M., Chu, J.J.-H. & Ng, M.-L. Quantifying the specific binding between West Nile virus envelope domain III protein and the cellular receptor alphaVbeta3 integrin. *J. Biol. Chem* **281**, 1352-1360 (2006).
6. Chu, J.J.H. *et al.* Inhibition of West Nile virus entry by using a recombinant domain III from the envelope glycoprotein. *J. Gen. Virol.* **86**, 405-412 (2005).
7. Kuhn, R.J. *et al.* Structure of dengue virus: implications for flavivirus organization, maturation, and fusion. *Cell* **108**, 717-725 (2002).
8. Nybakken, G.E. *et al.* Structural basis of West Nile virus neutralization by a therapeutic antibody. *Nature* **437**, 764-769 (2005).
9. Thompson, B.S. *et al.* A therapeutic antibody against west nile virus neutralizes infection by blocking fusion within endosomes. *PLoS Pathog* **5**, e1000453 (2009).

10. Sabo, M.C. *et al.* Neutralizing monoclonal antibodies against hepatitis C virus E2 protein bind discontinuous epitopes and inhibit infection at a postattachment step. *J. Virol.* **85**, 7005-7019 (2011).
11. Scarselli, E. *et al.* The human scavenger receptor class B type I is a novel candidate receptor for the hepatitis C virus. *EMBO J.* **21**, 5017-5025 (2002).
12. Bartosch, B. *et al.* An interplay between hypervariable region 1 of the hepatitis C virus E2 glycoprotein, the scavenger receptor BI, and high-density lipoprotein promotes both enhancement of infection and protection against neutralizing antibodies. *J. Virol.* **79**, 8217-8229 (2005).
13. Owsianka, A.M. *et al.* Identification of conserved residues in the E2 envelope glycoprotein of the hepatitis C virus that are critical for CD81 binding. *J. Virol.* **80**, 8695-8704 (2006).
14. Heinz, F.X. *et al.* The flavivirus envelope protein E: isolation of a soluble form from tick-borne encephalitis virus and its crystallization. *J. Virol* **65**, 5579-5583 (1991).
15. Grove, J. *et al.* Identification of a residue in hepatitis C virus E2 glycoprotein that determines scavenger receptor BI and CD81 receptor dependency and sensitivity to neutralizing antibodies. *J. Virol.* **82**, 12020-12029 (2008).
16. Li, L. *et al.* The flavivirus precursor membrane-envelope protein complex: structure and maturation. *Science* **319**, 1830-1834 (2008).
17. Rey, F.A., Heinz, F.X., Mandl, C., Kunz, C. & Harrison, S.C. The envelope glycoprotein from tick-borne encephalitis virus at 2 A resolution. *Nature* **375**, 291-298 (1995).

18. Modis, Y., Ogata, S., Clements, D. & Harrison, S.C. A ligand-binding pocket in the dengue virus envelope glycoprotein. *Proceedings of the National Academy of Sciences of the United States of America* **100**, 6986 -6991 (2003).
19. Modis, Y., Ogata, S., Clements, D. & Harrison, S.C. Variable Surface Epitopes in the Crystal Structure of Dengue Virus Type 3 Envelope Glycoprotein. *J. Virol.* **79**, 1223-1231 (2005).
20. Bressanelli, S. *et al.* Structure of a flavivirus envelope glycoprotein in its low-pH-induced membrane fusion conformation. *EMBO J.* **23**, 728-738 (2004).
21. Modis, Y., Ogata, S., Clements, D. & Harrison, S.C. Structure of the dengue virus envelope protein after membrane fusion. *Nature* **427**, 313-319 (2004).
22. Nayak, V. *et al.* Crystal structure of dengue virus type 1 envelope protein in the postfusion conformation and its implications for membrane fusion. *J. Virol.* **83**, 4338-4344 (2009).
23. Zhang, Y., Kaufmann, B., Chipman, P.R., Kuhn, R.J. & Rossmann, M.G. Structure of immature West Nile virus. *J. Virol* **81**, 6141-6145 (2007).
24. Zhang, Y. *et al.* Structures of immature flavivirus particles. *EMBO J.* **22**, 2604-2613 (2003).
25. Yu, I.-M. *et al.* Structure of the Immature Dengue Virus at Low pH Primes Proteolytic Maturation. *Science* **319**, 1834-1837 (2008).
26. Mukhopadhyay, S., Kim, B.-S., Chipman, P.R., Rossmann, M.G. & Kuhn, R.J. Structure of West Nile virus. *Science* **302**, 248 (2003).
27. Cherrier, M.V. *et al.* Structural basis for the preferential recognition of immature flaviviruses by a fusion-loop antibody. *EMBO J* **28**, 3269-3276 (2009).

28. Pokidysheva, E. *et al.* Cryo-EM reconstruction of dengue virus in complex with the carbohydrate recognition domain of DC-SIGN. *Cell* **124**, 485-493 (2006).
29. Zhang, X. *et al.* Near-atomic resolution using electron cryomicroscopy and single-particle reconstruction. *Proceedings of the National Academy of Sciences* **105**, 1867 - 1872 (2008).
30. Junjhon, J. *et al.* Influence of pr-M cleavage on the heterogeneity of extracellular dengue virus particles. *J. Virol* **84**, 8353-8358 (2010).
31. Kwong, P.D. *et al.* Structure of an HIV gp120 envelope glycoprotein in complex with the CD4 receptor and a neutralizing human antibody. *Nature* **393**, 648-659 (1998).
32. Krey, T. *et al.* The Disulfide Bonds in Glycoprotein E2 of Hepatitis C Virus Reveal the Tertiary Organization of the Molecule. *PLoS Pathog* **6**, (2010).
33. Vieyres, G. *et al.* Characterization of the envelope glycoproteins associated with infectious hepatitis C virus. *J. Virol.* **84**, 10159-10168 (2010).
34. Fraser, J., Boo, I., Poumbourios, P. & Drummer, H.E. Hepatitis C virus (HCV) envelope glycoproteins E1 and E2 contain reduced cysteine residues essential for virus entry. *J. Biol. Chem.* **286**, 31984-31992 (2011).
35. Coller, B.-A.G. *et al.* Advances in flavivirus vaccine development. *IDrugs* **13**, 880-884 (2010).
36. Guzman, M.G. *et al.* Dengue: a continuing global threat. *Nat. Rev. Microbiol.* **8**, S7-16 (2010).
37. Mady, B.J., Erbe, D.V., Kurane, I., Fanger, M.W. & Ennis, F.A. Antibody-dependent enhancement of dengue virus infection mediated by bispecific antibodies against cell

surface molecules other than Fc gamma receptors. *J. Immunol.* **147**, 3139-3144 (1991).

38. Rispeter, K. *et al.* Hepatitis C virus variability: sequence analysis of an isolate after 10 years of chronic infection. *Virus Genes* **21**, 179-188 (2000).
39. Meuleman, P. *et al.* Anti-CD81 antibodies can prevent a hepatitis C virus infection in vivo. *Hepatology* **48**, 1761-1768 (2008).
40. Catanese, M.T. *et al.* High-avidity monoclonal antibodies against the human scavenger class B type I receptor efficiently block hepatitis C virus infection in the presence of high-density lipoprotein. *J. Virol.* **81**, 8063-8071 (2007).
41. Fofana, I. *et al.* Monoclonal anti-claudin 1 antibodies prevent hepatitis C virus infection of primary human hepatocytes. *Gastroenterology* **139**, 953-964, 964.e1-4 (2010).
42. Syder, A.J. *et al.* Small molecule scavenger receptor BI antagonists are potent HCV entry inhibitors. *J. Hepatol.* **54**, 48-55 (2011).
43. Silvie, O. *et al.* Hepatocyte CD81 is required for Plasmodium falciparum and Plasmodium yoelii sporozoite infectivity. *Nat. Med.* **9**, 93-96 (2003).
44. Yalaoui, S. *et al.* Scavenger receptor BI boosts hepatocyte permissiveness to Plasmodium infection. *Cell Host Microbe* **4**, 283-292 (2008).
45. Wolf, M.C. *et al.* A broad-spectrum antiviral targeting entry of enveloped viruses. *Proc. Natl. Acad. Sci. U.S.A.* **107**, 3157-3162 (2010).
46. Zasloff, M. *et al.* Squalamine as a broad-spectrum systemic antiviral agent with therapeutic potential. *Proc Natl Acad Sci U S A* **108**, 15978-15983 (2011).

47. Kiso, M. *et al.* T-705 (favipiravir) activity against lethal H5N1 influenza A viruses. *Proceedings of the National Academy of Sciences* **107**, 882 -887 (2010).

Appendix 1:

Neutralizing Monoclonal Antibodies against Hepatitis C Virus E2 Protein Bind Discontinuous Epitopes and Inhibit Infection at a Post-Attachment Step

The research within this appendix consists of data that are published in the *Journal of Virology.*

Sabo, MS, Luca, VC, Prentoe, J, Blight, KJ, Lemon, S, Ball, JK, Bukh, J, Evans, M, Fremont, DH, Diamond, MS. 2011. Neutralizing Monoclonal Antibodies against Hepatitis C Virus E2 Protein Bind Discontinuous Epitopes and Inhibit Infection at a Post-Attachment Step.

My personal contributions to this manuscript were: i) Cloning, purification and expression of soluble E2 ii) Design, cloning and expression of genotype yeast displayed E2 from genotype 1-6 and C-terminal E2 truncations iii) Preliminary staining of yeast displayed E2 C-terminal truncations and genotypes 3-6 with the panel of hybridoma supernatants. Writing of the manuscript and the majority of experiments were carried out by Michelle Sabo.

A1.1 Abstract

The E2 glycoprotein of hepatitis C virus (HCV) mediates viral attachment and entry into target hepatocytes and elicits neutralizing antibodies in infected patients. To characterize the structural and functional basis of HCV neutralization, we generated a novel panel of 78 monoclonal antibodies (MAbs) against E2 proteins from genotypes 1a and 2a HCV strains. Using high-throughput focus-forming reduction or luciferase-based neutralization assays with chimeric infectious HCV containing structural proteins from both genotypes, we defined eight MAbs that significantly inhibited infection of the homologous HCV strain in cell culture. Three of these bound E2 proteins from strains representative of HCV genotypes 1-6, and one MAb, H77.39, neutralized infection of strains from five of these genotypes. The two most potent neutralizing MAbs in our panel, H77.39 and J6.36, inhibited infection at an early post-attachment step. Receptor binding studies demonstrated that H77.39 inhibited binding of soluble E2 protein to both CD81 and SR-B1, whereas J6.36 blocked attachment to SR-B1 and modestly reduced binding to CD81. Using yeast surface display, we localized epitopes for the neutralizing MAbs on E2. One of the strongly inhibitory MAbs, J6.36, showed markedly reduced binding when amino acids within the first hypervariable region (HVR1) and at a site ~200 residues away were changed, suggesting binding to a discontinuous epitope. Collectively, these studies help to define the structural and functional complexity of antibodies against HCV E2 protein with neutralizing potential.

A1.2 Acknowledgements

This work was supported by a grant from the Washington University Institute of Clinical and Translational Science (to M.S.D. and D.H.F) and an NRSA Pre-doctoral fellowship from NIDDK (F30 DK088385 to M.C.S). S.H. is a pre-doctoral trainee and was supported in part by an U.S. Public Health Service Institutional Research Training Award (AI07647). M.E. is supported in part by the Pew Charitable Funds and the NIAID (R00 AI077800). This study also was supported by a Ph.D. stipend from the Faculty of Health Sciences, University of Copenhagen (J.P.), and research grants from the Lundbeck Foundation (J.B.).

A1.3 Introduction

Hepatitis C virus (HCV) is a blood-borne, hepatotropic virus that infects ~170 million people worldwide. Approximately 70% of infected individuals progress to chronic liver disease, which carries an increased risk of cirrhosis and hepatocellular carcinoma[1]. In general, treatment of chronic HCV is complicated by resistance due to extensive genetic diversity. HCV has been classified into seven major genotypes, which differ by ~30% at the nucleotide level[2], and this positive-sense, single-stranded RNA virus has a capacity for rapid evolution of variant viruses during persistent infection. The current treatment, pegylated IFN-a_{2a} and ribavirin, has variable side effects and response rates depending on the virus and host genotype[3]. No vaccine is currently available, and pre-clinical development has been hampered by a lack of understanding of which conserved epitopes on the HCV structural proteins should be targeted.

HCV contains a ~9.6kb RNA genome that is translated as a single polyprotein and then cleaved by viral and host proteases into structural proteins (core, E1, E2), p7, and nonstructural proteins (NS2, NS3, NS4A, NS4B, NS5A, and NS5B)[4]. Viral attachment and entry is mediated by the envelope glycoproteins, E1 and E2. Four attachment or entry receptors that are required for infection of hepatocytes have been identified including CD81[5], scavenger-receptor B1 (SR-B1)[6], and the tight junction proteins claudin-1 (CLDN1)[7], and occludin (OCLN)[8]. The importance of E2 binding to the large extracellular loop of CD81 has been established in vitro[5,9–12], and interactions between E2 hypervariable region 1 (HVR1) and SR-B1 have been reported[6,13,14]. The structural basis of binding of E2 to its cognate cell attachment factors, however, is poorly understood, in part because high-resolution structures of the HCV glycoproteins or intact virion have not been solved.

The role of the humoral immune response in controlling HCV infection in patients remains controversial, as patients with persistent infection develop high-titer antibodies that do not appear to clear infection[1]. Nonetheless, there are emerging data that classes of monoclonal and polyclonal antibodies against HCV have protective activity. Binding to CD81 by soluble forms of E2 (sE2, truncated proximal to the transmembrane domain) is inhibited by antibodies that also neutralize infection of pseudotyped HCV particles (HCVpp) derived from the structural proteins of multiple genotypes[15,16]. Perhaps more convincing, experiments in chimpanzees and chimeric mice have shown that passive transfer of anti-E2 antibodies protects against infection[17–19], and immunization with E1-E2 virus-like particles and E2 glycoprotein in chimpanzees induces protective antibodies[18,20,21]. Moreover, in a comprehensive study of neutralizing MAbs derived from

infected patients, MAbs that bound regions comprised of amino acid residues 396–424, 436–447 and 523–540 on E2 neutralized HCVpp derived from multiple genotypes[18]. Thus, anti-E2 antibodies apparently can restrict HCV infection, although the exact steps (attachment, entry, or fusion) in the viral entry process that are inhibited and the corresponding E2 binding epitopes have not been elucidated.

To gain more insight into the molecular and structural basis of anti-E2 antibody neutralization of HCV infection, we generated a panel of 78 mouse monoclonal antibodies (MAbs) against soluble, recombinant E2 proteins derived from genotypes 1a (H77 strain) and 2a (J6 strain) HCV strains. These MAbs were analyzed for inhibitory activity against infectious HCV in cell culture and assessed for mechanism of action with respect to inhibition of ligand binding on the cell surface. By combining this functional analysis with a high-throughput yeast surface display mapping strategy, we identified neutralizing MAbs that bound to distinct regions of E2, including MAbs that recognized determinants with discontinuous epitopes with primary sequences greater than 150 amino acids apart. These experiments suggest that neutralizing MAbs blocking distinct stages of the HCV cell entry process recognize discontinuous epitopes on the E2 protein.

A1.4 Results

MAb generation. Previous studies have demonstrated that HCV-specific monoclonal and polyclonal antibodies, particularly those that recognize the E2 protein, can control HCV infection in vitro and in vivo[17,18,20,37–39]. However, only a few of these antibodies have been characterized for their ability to inhibit at different stages of HCV infection or mapped to epitopes at the amino acid level. To better define the structural

basis of antibody neutralization of HCV, we generated a new panel of anti-HCV MAbs by immunizing BALB/c mice with soluble, recombinant E2 protein that was expressed in insect cells and derived from either genotype 1a (H77 strain, amino acids 384-664) or genotype 2a (J6 strain, amino acids 385-664) viruses. After five independent splenocyte-myeloma cell fusions, we subcloned 37 MAbs from genotype 1a-immunized mice and 41 MAbs from genotype 2a-immunized mice, all with reactivity against the E2 structural glycoprotein of HCV.

Neutralizing activity of anti-E2 MAbs. To study the inhibitory capacity of genotype 1a MAbs in cell culture, we utilized an H77-JFH1 chimeric infectious virus that contains genotype 1a core-NS2 sequence in the JFH1 background, with a compensatory Q221L mutation in NS3 (pHJ3-5)[23,24]. For high-throughput screening, we adapted a focus-forming unit (FFU) assay with Huh-7.5 cells such that infectious foci were scored objectively on an ELISPOT reader and the reduction in number of FFU was assessed after pre-incubation of virus with individual MAbs (**Fig 1A**). We performed a single endpoint focus reduction neutralization test (FRNT) using neat antibody supernatant (~10 mg/ml) and identified 13 MAbs that inhibited infection by 40% or greater (**Fig 1B**). Candidate neutralizing MAbs were purified by immunoaffinity chromatography and tested for inhibitory activity with a more complete dose-response curve (**Fig 1C)**. We confirmed that five MAbs (H77.16, H77.28, H77.31, H77.39 and H77.56) had reproducible neutralizing activity, and determined the concentration of MAb at which 50% of foci were inhibited (EC50 value) (**Fig 1C**). Of these MAbs, H77.16 and H77.39 showed the greatest inhibitory activity, with EC50 values of ~3.4 μg/ml and ~1.1 μg/ml, respectively.

To evaluate the neutralizing activity of MAbs generated against E2 derived from the genotype 2a HCV strain, we utilized a genotype 2a J6/JFH1/JC1 infectious chimera of HCV that contains a Renilla-luciferase reporter gene inserted immediately upstream of NS2A cleavage site[22]. All 41 MAbs that bound the genotype 2a E2 protein were purified and assessed for inhibitory activity over a broad range of concentrations to determine the concentration of antibody that reduced luciferase expression by 50% (EC50 value) (data not shown). We identified two antibodies, J6.36 and J6.103 that efficiently neutralized infection, (**Fig 1D**) with J6.36 having an EC50 value below 2 mg/ml. Notably, no significant difference in inhibitory potency of a given neutralizing MAb was observed when the luciferase and FRNT assays were directly compared (data not shown).

Cross-reactivity of anti-E2 MAbs. HCV is comprised of six epidemiological important genotypes with ~70% nucleotide identity[2]. A better understanding of the specific epitopes that are conserved and recognized by inhibitory antibodies may facilitate the design of future vaccines. To begin to address this, we assessed how genotype variation affected MAb reactivity using recombinant E2 proteins displayed on yeast (1a, H77; 2a, J6; 3a, UKN3a; 4a, UKN4a; 5a, SA13; and 6a, UKN6) and neutralization capacity with chimeric HCV strains (1a, H77; 2a, J6; 3a, S52; 4a, ED43; 5a, SA13; and 6a, HK6a) containing the non-structural proteins (NS3-NS5B) of the genotype 2a JFH1 strain and structural proteins, p7, and NS2 from strains representative of HCV genotypes 1-6.

*(a) Binding to different HCV genotypes***.** The ectodomain of E2 from individual strains corresponding to HCV genotypes 1-6 was expressed on the surface of yeast, incubated with MAbs, and analyzed for binding by flow cytometry. Four of the eight

neutralizing MAbs were broadly cross-reactive and recognized all five (H77.16, H77.36, and H77.39) or four of the five (H77.56) heterologous genotypes (**Fig 2 and Table 1**). Three of the neutralizing MAbs (H77.31, J6.36, and J6.103) bound to yeast expressing only the homologous E2.

(b) Cross-neutralizing potential of MAbs. As MAb binding capacity to recombinant viral structural proteins does not always directly correlate with neutralizing potential[40], we evaluated the inhibitory activity of several of the cross-reactive MAbs against HCV virus of other genotypes. Initially, single endpoint focus reduction assays were performed with high concentrations (50 mg/ml) of purified MAbs generated against genotype 1a or genotype 2a that cross-reacted with genotype 2a or genotype 1a E2, respectively (**Fig 3A and 3B**). Of the cross-reactive MAbs generated against genotype 1a E2, only H77.39 neutralized the genotype 2a virus. Of the cross-reactive MAbs generated against genotype 2a E2, only J6.27 inhibited genotype 1a HCV infection (**Fig 3B and 3C**). This was surprising because J6.27 lacked neutralizing activity against the genotype 2a strain against which it was generated (**Fig 3C**); this pattern of enhanced neutralizing activity of cross-reactive antibodies against the heterologous virus also has been observed with MAbs against distantly related flaviviruses[41,42]. H77.39 inhibited the genotype 2a virus with an EC50 value of ~5 mg/ml (**Fig 3D**), which was comparable to that observed with the genotype 1a virus (see **Fig 1C**). We subsequently tested whether H77.39 neutralized infection of a panel of chimeric viruses that expressed structural proteins from the remaining heterologous HCV genotypes. H77.39 dose-dependently inhibited HCV infection of genotypes 3a, 4a, and 5a but showed reduced activity against a virus containing structural proteins of genotype 6a (**Fig 3E**).

Mechanism of MAb neutralization. Antibody neutralization may involve different stages of viral infection including attachment, internalization, or fusion[43]. To begin to understand how our inhibitory MAbs blocked infection, we performed pre- and post-attachment neutralization assays and binding studies to the CD81 and SR-B1 receptors.

(a) *Pre- and post-attachment assays.* To identify the stage of infection at which MAbs neutralize infection, we adapted a pre- and post-attachment inhibition assay originally developed for flaviviruses[44–46]. Purified anti-E2 MAb was incubated with virus before or after attachment at 4°C to Huh-7.5 cells, and infection was measured by a single endpoint focus reduction assay. Of the nine neutralizing MAbs tested, two (H77.39, and J6.36) significantly reduced infection compared to the negative control MAb (WNV E16) when added after viral absorption to a cell monolayer, suggesting blockade of a post-attachment step (**Fig 4A-D**). Interestingly, both anti-CD81 and anti-SR-B1 MAbs also inhibited infection after viral adsorption, confirming previous results in Huh-7.5 cells which suggested that HCV binds to CD81 and SR-B1 after initial attachment[47,48]. Inhibition of infection at a post-attachment step by H77.39 was confirmed by performing more complete dose-response curve analysis (**Fig 4E**).

(b) MAb inhibition of sE2 binding to receptors. Given that anti-CD81, anti-SR-B1, and several anti-E2 MAbs all blocked after HCV attached to Huh-7.5 cells, it was difficult to discern whether some antibodies blocked binding to individual HCV receptors. To address this, we developed a binding assay for soluble E2 (sE2) to CHO cells that ectopically expressed human CD81 or SR-B1. CHO cells were transduced with a lentiviral vector encoding CD81 or SR-B1 fused to GFP. Surface staining of intact cells

with anti-CD81 and anti-SR-B1 MAbs confirmed high-level receptor expression (**Fig 5A**), as did analysis of cells for GFP fluorescence (data not shown). Binding of genotype 1a (**Fig 5B**) and genotype 2a (**Fig 5C**) sE2 to CD81 and SR-B1 expressing CHO cells (solid histograms), but not control CHO cells (outlined histograms) was confirmed by flow cytometry. To determine whether sE2-CD81/SR-B1 receptor interactions could be disrupted by anti-E2 MAbs, neutralizing or control (anti-WNV E16) MAbs were pre-incubated with sE2, added to wells containing CHO cells expressing CD81 or SR-B1, and loss of binding was assessed by flow cytometry (**Fig 5D**). The neutralizing MAb H77.39 significantly blocked (>70%, $P < 0.01$) sE2 binding to both CD81 and SR-B1. In comparison, H77.31 also reduced binding of sE2 to both receptors, although inhibition of SR-B1 binding was more modest (~40%, $P = 0.04$) compared to that seen with CD81 (>80%, $P = 0.003$). Conversely, J6.36 efficiently inhibited sE2-SR-B1 binding (>80%, $P = 0.0002$) yet only modestly (~50%, $P < 0.05$) diminished sE2-CD81 binding. H77.16 and J6.103 blocked sE2 binding to only a single receptor, with both efficiently reducing (>75%, $P = 0.0005$) binding to SR-B1 (**Fig 5D**). Three neutralizing MAbs, H77.28, H77.56, and J6.27, did not inhibit significantly sE2 attachment to either CD81 or SR-B1, suggesting that these may block an alternate attachment or entry step (**Fig 5E**).

Epitope localization of MAbs. To correlate the function of the anti-E2 MAbs with structure of the HCV E2 protein, we localized their epitopes using a previously validated yeast surface display mapping assay[31,41,45]. Initially, COOH-terminal truncated versions of E2, based on those described previously[34], were displayed on the surface of yeast and MAbs were tested for immunoreactivity by flow cytometry (**Fig 6 and Table S1**). Neutralizing MAbs showed different requirements for binding. H77.16, H77.39, J6.36,

and J6.103 bound to a region bracketed by amino acids 384-520 of genotype 1a and 384-518 of genotype 2a E2 (designated "region I"), whereas H77.28, H77.31, and J6.27 required amino acids 521-605 of genotype 1a or 519-603 of genotype 2a E2 (designated "region II") for binding. In contrast, MAb H77.56 required the full E2 ectodomain (1-664), suggesting that it interacts with amino acids 606-664 alone or requires a conformation of E2 that this region stabilizes. MAbs that neutralized efficiently at a post-attachment step, H77.39 and J6.36, both bound to region I of E2.

To localize MAb epitopes more clearly, we used error-prone PCR mutagenesis and yeast surface display to create a library of H77 and J6 E2 variants to define individual amino acid binding residues of neutralizing and non-neutralizing MAbs. Yeast that lost expression of individual MAb epitopes were sorted by flow cytometry and plasmids were recovered, sequenced, and tested for reactivity against a select panel of MAbs (**Fig 7 and Tables 2 and 3**).

H77.39, the most potent and highly cross-neutralizing MAb, showed markedly reduced binding when residues N415 and N417 of E2 were changed (**Fig 7A and Table 2**). Two neutralizing MAbs (J6.36, and J6.103) required a pair of mutations for significant loss of binding. J6.36 and J6.103 lost binding with changes in HVR1 and a more distal region of E2; mutation of residues G406, F403, or a combined mutation at residues G397 and R572 abrogated MAb binding. Single mutations of G397 and R572, however, did not affect binding (**Fig 7B and Table 3**). Similarly, H77.16 showed weakly reduced binding when a serine was introduced at residue G406 (**Fig 7A**), but complete loss of binding when residue G530 was altered in combination with G406S. However,

complete loss of H77.16 binding also was observed when residue G406 was mutated to an aspartic acid residue.

The neutralizing MAbs that were quantitatively weaker in our neutralization assays, H77.31 and J6.27, showed decreased binding when residues in the putative CD81 binding region (amino acids 523-535[49]) were changed. H77.31 binding to E2 on yeast was lost when residues W529, G530, and D533 were mutated, whereas J6.27 binding was abolished when amino acids A524 and W529 were altered. The remaining two weakly neutralizing MAbs (H77.28 and H77.56) showed reduced binding with changes at residues R543 and C552, respectively (**Fig 7A and Tables 2 and 3**).

Some non-neutralizing MAbs also were mapped. Several non-neutralizing MAbs (H77.27, H77.36, J6.2, J6.6, J6.15, J6.39, and J6.85) shared residues that impacted binding of H77.31 or J6.27 (**Tables 2 and 3**), and a few (J6.2, J6.6, J6.40, and J6.101) had total or partial loss of binding to residue G406, which was identified as an important recognition residue for the neutralizing MAbs H77.16, J6.36 and J6.103. In addition to G406, J6.2, J6.40 and J6.101 recognition was also affected by mutation of residue H617, thus defining another discontinuous epitope, albeit one that is not apparently involved in neutralization (**Fig 7 and Tables 2 and 3**). Additional residues that uniquely affected binding by non-neutralizing MAbs included G470 (H77.14 and H77.23), Y443 (J6.60), and H617 (J6.30).

A1.5 Discussion

In this study, we generated a novel panel of 78 MAbs against the E2 proteins of HCV genotypes 1a and 2a, analyzed them functionally for inhibition of HCV infection, and localized epitopes using yeast surface display of truncated and substituted forms of the E2 protein. We defined MAbs that mapped to distinct regions of E2, neutralized infection at different stages, and differentially affected CD81 and SR-B1 engagement. Our mapping data also suggests a tertiary interaction between the HVR1 and the COOH-terminal membrane proximal regions of E2, which provides new insight into the quaternary structural aspects of neutralization by functionally relevant antibodies.

Prior mapping studies of anti-E2 MAbs have utilized peptide binding[10,50], phage display[51], alanine scanning mutagenesis of recombinant E1-E2 [18,37,39,52] or E2[53], or generation of neutralization escape mutants[54] to localize antibody binding sites. In comparison, we used a forward genetic mutational approach coupled with yeast surface display to identify mutants in the context of the entire ectodomain of E2 protein in an unbiased manner. Three of our nine neutralizing MAbs required amino acid mutations greater than 100 amino acids apart in the linear sequence for loss of binding, suggesting that discontinuous regions of E2 come together to create functionally important antibody epitopes. H77.16 showed a loss-of-binding phenotype when mutations in the HVR1 (G406S) and the more COOH-terminal residue (G530A) were paired, suggesting that H77.16 binds a conformational epitope. Although complete loss of binding could be achieved with a single less conserved mutation (G406D), the more conserved G406S change required a second mutation at a discontinuous site (G530) for loss-of-binding. This finding, which suggests that the HVR1 interacts with more COOH-terminal

residues, is consistent with MAb competition studies with recombinant proteins that suggested that amino acids 396-424, 436-447, and 523-540 comprise an antigenic region (designated "antigenic region-3") within E2[18], and with sequencing results of MAb AP33 escape variants, which identified non-contiguous amino acid residues (N415 and E655) as factors in the loss of neutralization phenotype[54]. Additionally, these data support the recently described model of HCV E2 based on the three domain structure of class II E proteins in *Flaviviridae* and *Togaviridae*, which predicts that the HVR1 proximally apposes the proposed HCV Domain I (D1)[55] (**Fig 8B**).

Two other neutralizing MAbs, H77.31 and J6.27, also recognized residues within the third segment of antigenic region-3 (A524, W529, G530 and D533) but did not show a loss-of-binding phenotype when amino acids within segment 1 (396-424) were changed. These two MAbs less potently neutralized infection and were less cross-reactive. In comparison, human anti-HCV MAbs (A8, 1:7, and CBH5) that share epitopes in this region[37,56] have been characterized as inhibitory and cross-reactive (**Table 4**). Although further analysis is required, the differences in function of the mouse and human MAbs could be related to affinity or possibly, that the human MAbs bind additional sites and do not exclusively recognize the linear epitope centered at residues G523-D535, as was suggested in previous studies[15,56].

The neutralizing MAbs J6.36 and J6.103 also mapped to a discontinuous epitope, requiring residues within the HVR1 (G397, F403, and G406) and the more COOH-terminal residue R572. Although neutralizing MAbs (9/27[10,57] and AP213[51]) have been mapped to the HVR1, to our knowledge, MAbs that bind residues at or near R572 have not been identified. The MAb 9/27 does not block binding of sE2 to CD81[10,57] although it

did inhibit HCV VLPs interaction with CD81[16], suggesting that it also may recognize a conformational or possibly oligomeric epitope.

The MAb in our study with the greatest inhibitory activity, H77.39, localized to two amino acids, N415 and N417, that are highly conserved among all HCV genotypes[58,59]. N415 and N417 were defined previously as possible binding residues for MAbs AP33 and 3/11[39,54,58] (**Table 4**). Residue N417 comprises part of a highly conserved N-linked glycosylation site[60,61] that is implicated in obscuring antibody-mediated neutralization[59]. H77.39, as well as AP33 and 3/11, are thus unique in mapping to an N-linked glycan that is paradoxically hypothesized to impair antibody recognition.

To relate binding epitopes to function, MAbs were tested for their ability to inhibit sE2 engagement with the HCV cognate receptors CD81 and SR-B1. The MAbs J6.36, J6.103, and H77.16, which recognized residues within the HVR1 as well as the more COOH-terminal region, blocked sE2-SR-B1 binding[6,13,14]. These results are consistent with data suggesting the HVR1 participates in SR-B1 binding, and that the HVR1-specific MAb 9/27 inhibits sE2-SR-B1 interactions[6,14]. Although J6.36 did not map to any of the predicted CD81 binding residues[49], it partially inhibited binding to CD81. J6.36 could map to additional amino acid residues (within the CD81 binding site) not identified in our study or steric hindrance could mediate this partial inhibition. In the recently modeled E2 structure[55], the J6.36 interaction residues lie in proximity to the HCV D1, which is predicted to contain key CD81 binding residues[49,55] (**Fig 8B**). Conversely, H77.31, which potently inhibited CD81 binding and maps to residues (W529, G530) involved in CD81 binding[49] partially inhibited SR-B1 engagement despite a lack of contact residues in the HVR1. The inability of J6.103 to inhibit binding to CD81

despite localizing to the same residues as J6.36 could be explained by overlapping but not identical MAb footprints or perhaps differences in affinity of interaction.

Only one MAb, H77.39, potently inhibited sE2 binding to both CD81 and SR-B1. Interestingly, H77.39 did not map to residues within known SR-B1 or CD81 binding regions, suggesting that it may recognize a site that once occupied, can sterically prevent receptor engagement. This concept is supported by studies showing that N415 and N417 can obscure the CD81 and SR-B1 binding sites[58,59]. Finally, the E2 model recently proposed by Krey et al predicts that residues N415-N417 lie at the junction of the HVR1 and D1 (**Fig 8B**), in proximity to both HVR1 and the CD81 binding residues located within *C* and *D* loops of D1[49,55].

Pre- and post-attachment neutralization studies provided additional insight into the relative potency of MAbs. Studies with distantly related Flaviviruses have shown that MAbs inhibiting at a post-attachment step tend to have greater inhibitory activity in vitro and in vivo because they require reduced virion occupancy for neutralization[31,45,46,62,63]. Indeed, our two most potent MAbs, H77.39 and J6.36, neutralized infection in the post-attachment assay. Nevertheless, J6.103 shared apparent binding epitopes with J6.36, yet did not neutralize efficiently when added after attachment. This discrepancy may be explained by J6.36 having additional amino acid contacts not identified in our study.

MAb binding to conserved residues may not directly predict cross-binding or cross-neutralizing capabilities[36,40]. Despite mapping to highly conserved residues, MAbs H77.31, J.36 and J6.103 failed to cross-react with any other strains tested, and J6.27 was cross-reactive with only two of the strains tested. In comparison, MAb H77.16 was highly cross-reactive, but still did not neutralize heterologous strains. In contrast, H77.39

cross-reacted with genotypes 1-6 and neutralized chimeric virus representative of all strains except genotype 6. The inability of H77.39 to neutralize the genotype 6 chimeric virus may be explained by the presence of a mutation in one of the recognition residues, N417T[64]. This mutation is rare in natural HCV isolates[49,58], but was required for adaptation of the HK6a/JFH1 chimera in vitro[64]. Mutations at N415 are rare[49,58] and attenuating in the context of HCV infection[54].

Generation of an HCV vaccine has been impeded by the lack of a structural understanding of the epitopes on E2 that should be targeted by inhibitory antibodies. Although direct structural confirmation is necessary, our data suggests the existence of discontinuous epitopes that are recognized by antibodies that inhibit CD81 and SR-B1 binding. The yeast surface display antibody mapping data also provides support for a recently proposed structural model of E2 in which the residues comprising the CD81 binding region lie within a single domain of b-pleated sheets that contains the HVR1 as an N-terminal extension[55]. The epitopes defined by the MAbs H77.16, J6.36, and J6.103 suggest that the HVR1 might lie in proximity to this domain, creating an conformational epitope (**Fig 8B**), which could be a useful target for vaccines and therapeutic antibodies.

A1.6 Materials and methods

Cells and viruses. Huh-7.5 cells were cultured in Dulbecco's Modified Eagle Medium (DMEM) supplemented with 10% fetal bovine serum (FBS) (Equitech), non-essential amino acids (Gibco), and antibiotics (penicillin G and streptomycin) at 37°C in a 5% CO_2 incubator. SF9 cells were cultured in Grace's Insect cell medium (Gibco) supplemented with 10% FBS at 28^{o}C. HI-5 cells were cultured in Ex-cell media (Gibco)

at 27°C. CHO cells were grown in Ham's F12 medium (Gibco) supplemented with 10% FBS (HyClone) at 37°C.

The genotype 2 J6/JFH1/JC1 HCV chimera that expresses luciferase[22] was a generous gift from Apath Inc. The HJ3-5 H77/JFH1 chimera, which expresses the core-NS2 segment of the genotype 1a polyprotein within a genotype 2a background has been described[23,24]. The genotype 1a H77/JFH1[25], genotype 2a J6/JFH1[26], genotype 3a S52/JFH1[27], genotype 4a ED43/JFH1[25], genotype 5a SA13/JFH1[28], and genotype 6a HK6a/JFH1[27] infectious HCV recombinants used in cross-neutralization studies also have been described.

To generate virus stocks from infectious cDNA clones, plasmids were linearized and RNA transcription was performed using the T7 DNA-dependent RNA polymerase (MEGAscript Kit, Ambion). Infectious HCV RNA (2 mg) was electroporated as described[26], and virus was harvested at 48, 72, and 96 hours, sterile filtered (0.2 mm filter, Corning Inc), and buffered with 10mM HEPES pH 7.2 (Mediatech, Inc.). Virus was stored at 4°C for up to 6 weeks protected from light or aliquotted at -80°C. Virus titration on Huh-7.5 cells was performed by $TCID_{50}$ assay as previously described[26].

Generation of CHO cells stably expressing HCV cell entry factors. Human SR-BI and CD81 genes were expressed in CHO cells via lentivirus transduction in the context of pTRIP, a self-inactivating lentiviral provirus that expresses no HIV proteins but instead employs an internal cytomegalovirus (CMV) promoter to express cloned genes. An intermediate plasmid, called TRIP-GFP-linker, was generated as a backbone into which SR-BI and CD81 were cloned (all entry factor templates were kindly provided by C. Rice, Rockefeller University, NY). TRIP-GFP-linker was generated by amplifying

the GFP sequence with the forward oligonucleotide 5'-CGC AAA TGG GCG GTA GGC GTG and reverse oligonucleotide 5'-CTC GAG CTA GTC GAC TTC GAA ACT AGT GCT AGC CCG CGG CTT GTA CAG CTC GTC CAT GCC. This PCR product was digested with restriction enzymes BamHI and XhoI and ligated into the TRIP-GFP plasmid digested with the same enzymes. The human SR-BI sequence was amplified with forward oligonucleotide 5'-CCG CGG ATG GGC TGC TCC GCC AAA GCG and reverse oligonucleotide 5'-GCT AGC CAG TTT TGC TTC CTG CAG CAC from the previously described TRIP-hu-SR-BI plasmid[8], to generate TRIP-GFP-hu-SR-BI-linker. This PCR product was digested with SacII and NheI and ligated into similarly digested TRIP-GFP-linker. The human CD81 sequence was amplified from an expression construct, TRIP-GFP-hu-CD81[6], with forward oligonucleotide 5'-GCT AGC ATG GGA GTG GAG GGC TGC ACC and reverse oligonucleotide 5'-ACT AGT GTA CAC GGA GCT GTT CCG GAT. This PCR product was digested with NheI and SpeI and ligated into similarly digested TRIP-GFP-linker, to generate TRIP-GFP-hu-CD81-linker.

Pseudoparticle production was performed as previously described by co-transfection of three plasmids encoding a TRIP provirus containing a transgene, HIV Gag-Pol, and the VSV-G glycoprotein. 293-T cells were seeded at 1.8 x 10^6 cells/well into a poly-L-lysine (Sigma)-coated six-well plate. Transfection was performed the next day using a total of 1.5 mg of DNA plasmid, with 6 ml of TransIT-LT1 transfection reagent (Mirus). Supernatants were collected 24, 48, and 72 h post-transfection, filtered (0.45-mm pore size), and mixed with 100 ml of 1 M HEPES buffer. All transductions were performed in the presence of 4 mg/ml Polybrene (Sigma). Receptor expression was verified by flow cytometry using the following protocol: cells were lifted using PBS

supplemented with 4 mM EDTA and 10% FBS, washed, and pelleted in a V-bottom plate. Cells (10^5) were incubated with either 20 mg/ml of mouse anti-hu-CD81 (BD Biosciences) or rabbit anti-hu-SR-B1 (Ab-Cam) for 30 minutes on ice, washed, and then incubated with goat anti-mouse IgG or goat anti-rabbit IgG secondary antibody conjugated to Alexa Fluor 647 (Molecular Probes). Cells were washed twice and receptor expression was analyzed on a FACSArray flow cytometer (Becton-Dickinson) using FloJo software (Tree Star).

Cloning, expression, and purification of recombinant HCV E2. The E2 protein ectodomain of strains H77 (aa 384-661)[29] or J6 (aa 385-661) was cloned into a baculovirus expression vector (pFastBac derivative) from plasmids containing the structural proteins of H77 (gift of M. Gale, Jr., University of Washington) or the infectious J6/JFH1/JC1[22] viral genome (gift of Apath, Inc). The baculovirus expression vector adds a honeybee melittin signal peptide at the NH_2 terminus and a thrombin-cleavable His_6 tag and stop codon at the COOH-terminus. Recombinant baculoviruses expressing HCV E2 ectodomains were generated as described previously[30], amplified in SF9 cells, and used for large scale infection of Hi-5 cells under serum-free conditions. Supernatant was concentrated and buffer exchanged into binding buffer (300 mM sodium citrate, 150 mM sodium chloride, 50 mM sodium phosphate pH 8.0) using a Centramate tangential flow concentrator. E2 was purified by sequential nickel-affinity and size-exclusion chromatography and monodispersed fractions of monomeric protein were collected and used for subsequent studies.

Generation, purification, and labeling of anti-HCV MAbs. MAbs were generated by five independent splenocyte-myeloma fusions as described[31]. Mice were

immunized via an intraperitoneal route with sE2 produced from either genotype 1a (H77) or 2a (J6) HCV strains after complexing with RIBI Adjuvant System (Corixa Corp) or complete Freund's adjuvant (Sigma Chemical). Mice were boosted between two and five times with homologous HCV sE2 protein complexed with either incomplete Freund's adjuvant (Sigma), RIBI Adjuvant System (Corixa), or Sigma Adjuvant system (Sigma), depending on commercial availability, until adequate titers (>1:2500 by ELISA) were achieved. Mice with the highest serum titers were boosted intravenously with purified sE2 (50 mg) three days prior to fusion of splenocytes with P3X63Ag8.53 myeloma cells[32]. Hybridomas producing anti-HCV E2 antibodies were identified after binding to *Saccharomyces cerevesiae* yeast expressing sE2 on their surface by flow cytometry, subcloned by limiting dilution, and isotyped by ELISA. For large-scale production, MAbs were generated from ascites or adapted to growth in Hybridoma Serum Free Media (Gibco) and purified using protein A or G affinity chromatography (Pierce). In some experiments, MAbs were labeled with Alexa Fluor 647 (Molecular Probes) or NHS-FITC (Pierce) MAb labeling kits according to the manufacturer's instructions.

Virus neutralization assays. Neutralization of HCV infection by viruses containing genotype 1a structural proteins (H77/JFH1) was assessed by a focus forming unit (FFU) assay. Serial dilutions of HCV-specific MAb, control MAb (WNV E16[31]), anti-human CD81 (clone JS81, BD Biosciences), or anti-human SR-B1 (clone 396, Ab-Cam) were pre-incubated with 2.4 x 10^2 FFU of virus for one hour at 37°C. Virus-MAb mixtures were added to Huh-7.5 cells (1.2 x 10^4 cells per well) in a 48-well tissue culture plate pre-coated with poly-L lysine (Sigma). After 72 hours, cells were fixed with methanol (0^oC), and incubated sequentially with a mouse anti-NS5A (APA-1, 40 ng/ml)[26]

(a generous gift of Apath, Inc.) and secondary goat anti-mouse HRP diluted 1:3000 (Sigma). FFU were visualized using the True Blue Peroxidase Reagent (KPL) and quantitated using an S5 Biospot Macroanalyzer (Cellular Technologies Ltd). EC50 values were determined using non-linear regression analysis (Graph Pad Prism 4).

Neutralization of the genotype 2a (J6/JFH1/JC1) HCV was assessed by luciferase assay. Serial dilutions of HCV-specific or control MAbs were pre-incubated with the J6/JFH1/JC1 virus that expresses luciferase (10^2 FFU) for one hour at 37°C and then added to Huh-7.5 cells (10^4 cells per well) in a 96-well black flat bottom polystyrene-treated microplate (Corning). After 48 hours, cells were lysed and luciferase was detected using the Renilla Luciferase Assay System (Promega) according to the manufacturer's instructions. EC50 values were determined using non-linear regression analysis (Graph Pad Prism 4).

Neutralization of chimeric viruses with genotype 1a-6a specific core-NS2 sequences was assessed by FFU assay with the following modifications: 50 to 400 $TCID_{50}$ of HCV were incubated 1 hour at 37°C with MAb H77.39 or an isotype control and then incubated with cells for 3 hours. After 48 hours, cells were immunostained for NS5A as previously described[33]. FFU counting was automated using ImmunoSpot Series 5 UV Analyzer[27]. Percent neutralization was calculated by relating FFU counts to mean of six-replicates incubated in the absence of antibody (virus only). Neutralization data were analyzed as variable slope dose-response curves using GraphPad Prism 4.0 and EC50 values were interpolated by the software.

Pre-and post virus attachment assays. To assess the ability of MAbs to inhibit H77/JFH1 virus at pre- and post-attachment steps, FFU assays were modified as follows. For the post-attachment assay, pre-chilled cells were incubated with 4.8 x 10^2 FFU of virus for one hour at 4°C. Cells were washed thrice with cold DMEM to remove unbound virus and MAbs (diluted to 50 mg/ml in media and pre-warmed at 37°C) were added and the cells shifted to 37°C. After one hour, a 1:1 MEM-methylcellulose overlay with 4% FBS was added to prevent viral spread. For the pre-attachment assay, 4.8 x 10^2 FFU of virus were pre-incubated with 50 mg/ml of media for one hour at 37°C and then added to pre-seeded Huh-7.5 cells.

To assess the ability of MAbs to inhibit J6/JFH1/JC1 at pre- and post-attachment steps, the luciferase assay was modified in the following manner. 48-well tissue culture plates were pre-coated with poly-L lysine (Sigma) and seeded with 1.2 x 10^4 cells per well. For the post-attachment assay, 4.8 x 10^2 FFU of virus was added to pre-chilled cells and "spinoculated" for 45 minutes at 400 x g at 4°C, followed by a 15 minute incubation at 4°C. Cells were washed and pre-warmed MAbs and methylcellulose were added as described above. For the pre-attachment assay, 4.8 x 10^2 FFU of virus were pre-incubated with 50 mg/ml of MAb for one hour at 37°C and then added to pre-seeded Huh-7.5 cells. Cells from both the pre-and post-attachment assay were lysed after 48 hours and transferred to a 96-well black-bottom plate and luciferase was detected using the Renilla Luciferase Assay System (Promega) according to the manufacturer's instructions.

Cross-reactivity and mapping analysis of MAbs using yeast surface display. To assess MAb cross-reactivity with other HCV genotypes, the ectodomain of the E2 genes

from genotype 1a (H77, amino acids 384 to 660), genotype 2a (J6, amino acids 385 to 664), genotype 3a (UKN 3A13.6, amino acids 385 to 667), genotype 4a (UKN 4.21.16, amino acids 392 to 663), genotype 5a (SA13 NIH, amino acids 384 to 663) and genotype 6a (UKN 6, amino acids 385 to 668) was amplified by PCR with BamH1 and XhoI sites for cloning added at the 5' and 3' ends, respectively. The PCR products were cloned as downstream fusion proteins to the Aga2 gene in the pYD1 vector (Invitrogen) for expression on the surface of yeast. To determine the relative binding regions on E2 of specific MAbs, COOH-terminal truncation constructs, based on previous studies[34] were generated for genotypes 1a and 2a corresponding to regions I (amino acids 384 to 520 in genotype 1a and 384 to 518 in genotype 2a) or I and II (amino acids 384 to 605 in genotype 1a and 384 to 603 in genotype 2a) and displayed on the surface of yeast.

Expression constructs were transformed into *Saccharomyces cerevisiae* strain EBY100[35] using the *S.c*. EasyComp transformation Kit (Invitrogen). Individual yeast colonies were grown to logarithmic phase at 30°C in tryptophan-free yeast selection media containing 2% glucose. Protein expression was induced by cultivating yeast for an additional 48 to 72 hrs in tryptophan-free media supplemented with 2% galactose at 20°C. Yeast cells were washed with PBS containing 1 mg/ml BSA (PBS/BSA) and incubated with 40 ml of MAb (neat supernatant or 20 mg/ml purified diluted in PBS) for 30 minutes on ice. Yeast were washed in PBS/BSA, incubated with goat anti-mouse IgG secondary antibody conjugated to Alexa Fluor 647 (Molecular Probes) for 30 minutes on ice, washed, and analyzed on a FACSArray flow cytometer (Becton-Dickinson) using FloJo software (Tree Star).

Random mutant libraries of E2 were generated from genotype 1a (H77 strain) and genotype 2a (J6 strain) genes by error-prone PCR using a GeneMorph II random mutagenesis kit (Stratagene). Libraries were ligated into the pYD1 vector and transformed into XL2-Blue ultracompetent cells (Stratagene) with ~5.7 x 10^5 and 5.5 x 10^5 transformants for genotypes 1a and 2a, respectively. Screening of the libraries for loss of binding variants was performed as described[31,36]. In brief, yeast expressing E2 variants that lost specific binding to individual MAbs were sorted using two-color flow cytometry. To eliminate mutations that abolished surface expression of E2, yeast were stained sequentially with the Alexa Fluor 647-conjugated individual MAb, followed by a FITC-conjugated oligoclonal pool of the cross-reactive MAbs J6.1, J6.2, J6.16, J6.39, J6.51, and J6.101 for the genotype 1a library and J6.2, J6.14, J6.15, J6.39, J6.51, and J6.99 for the genotype 2a library on ice for 30 minutes. Yeast that stained positively for the oligoclonal pool but negatively for the MAb of interest were collected, cultivated, and iteratively sorted. In some cases, sorting was performed using MACS LS magnetic columns (Miltenyi Biotech). In brief, ~10^7 yeast cells were pelleted and resuspended in MACS buffer (PBS + 0.5% BSA+ 2mM EDTA) containing a 1:50 dilution of a FITC-labeled MAb of interest for 30 minutes, washed, and then incubated with 10 ml of anti-FITC microbeads (Miltenyi Biotech) on ice for 15 minutes. Yeast were washed and passed over a MACS LS column and the flow-through collected. After four to five rounds, yeast were plated and individual colonies were tested for binding to individual MAbs by flow cytometery. For clones that lost binding to the desired MAb of interest, the plasmid was recovered using a Zymoprep yeast minipreop kit (Zymo Research), transformed into XL1-Blue competent *E. coli*, purified using a QIAprep spin miniprep kit

(Qiagen) and sequenced. In cases where more than one mutation was detected, site-specific mutagenesis using the Quick Change II Mutagenesis kit (Stratagene) was used to generate individual mutations within the E2 protein to define the mutant of interest.

Inhibition of CD81 and SR-B1 binding. To assess the ability of neutralizing MAbs to inhibit binding of sE2 to CD81 and SR-B1, 50 mg/ml of purified MAb was pre-incubated with 20 mg/ml H77 E2 or J6 sE2 for 30 minutes at 37C. CHO cells expressing HCV receptors were detached with PBS supplemented with 4 mM EDTA and 10% FBS, and washed three times in medium. Cells (10^5) were pelleted in a V-bottom plate, resuspended with MAb-protein mixture, and incubated on ice for 30 minutes. Cells were washed and then incubated with a pool of Alexa Flour 647 labeled anti-E2 MAbs (J6.1, J6.2, J6.39, J6.51, H77.30, and H77.34 for the detection of H77 E2; and J6.2, J6.39, J6.51, J6.60, and J6.101 for the detection of J6 E2) for 20 minutes on ice. Cells were washed twice and sE2 binding was analyzed on a FACSArray flow cytometer (Becton-Dickinson) using FloJo software (Tree Star).

Statistical analysis. All data was analyzed using Graphpad Prism software (version 4.0). For neutralization assays and receptor-binding assays, an unpaired t-test was used to determine statistical significance.

Table 1: Binding of MAbs to HCV E2 from different HCV genotypes

MAb	Binding to genotype[a]:					
	1a(H77)	2a(J6)	3a(UKN 3)	4a(UKN4)	5a(SA13)	6a(UKN6)
J6.1	+++	+++	+++	+++	+++	+++
J6.2	+	+++	+++	+++	−	−
J6.6	+	+++	+	−	−	−
J6.7	+++	+++	+++	+	+++	+++
J6.8	+	+++	−	−	−	−
J6.9	+++	+++	−	−	+++	−
J6.12	+++	+++	+++	+++	−	−
J6.13	−	+++	−	−	−	−
J6.14	+++	+++	+++	+	+	+++
J6.15	−	+++	+++	+++	+++	+++
J6.16	+++	+++	+++	−	+++	−
J6.21	+++	+++	−	−	−	−
J6.23	+	+++	−	−	−	−
J6.25	−	+++	−	−	−	−
J6.27	+++	+++	+++	−	−	−
J6.30	+++	+++	+++	+++	+++	+++
J6.33	+++	+++	+++	+++	+++	+++
J6.34	+++	+++	+	+	+++	+
J6.36	−	+++	−	−	−	−
J6.39	+++	+++	+++	−	−	−
J6.40	−	+++	+	−	−	−
J6.42	+	+++	+++	+++	−	−
J6.48	−	+++	−	−	−	−
J6.49	−	+++	−	−	−	−
J6.51	+	+++	+	+++	−	−
J6.56	+++	+++	+++	+	+++	+++
J6.58	+++	+++	+++	+/−	+++	−
J6.60	−	+++	−	−	−	+++
J6.62	+++	+++	+++	+	+++	+
J6.67	+++	+++	+	−	+++	−
J6.68	+	+++	−	−	−	−
J6.75	+++	+++	+++	+++	+++	+++
J6.76	−	+++	−	−	−	−
J6.81	+++	+++	+++	−	+++	−
J6.85	−	+++	+++	+++	+++	+++
J6.86	+	+++	+++	+++	−	−
J6.91	+	+++	−	−	−	−
J6.98	−	+++	+	+++	−	−
J6.99	−	+++	−	−	−	+
J6.101	+++	+++	+	+++	−	+++

MAb	Binding to genotype[a]:					
	1a(H77)	2a(J6)	3a(UKN 3)	4a(UKN4)	5a(SA13)	6a(UKN6)
J6.103	−	+++	−	−	−	−
H77.1	+++	−	−	−	−	−
H77.7	+++	+++	+++	+++	+++	+++
H77.8	+++	−	−	−	−	−
H77.9	+++	−	−	−	−	−
H77.11	+++	−	−	−	−	−
H77.12	+++	+++	−	−	+++	−
H77.13	+++	−	−	−	−	−
H77.14	+++	−	−	−	−	−
H77.16	+++	+++	+++	+++	+++	+++
H77.17	+++	−	−	−	−	−
H77.18	+++	−	−	−	+	−
H77.19	+++	−	−	−	−	−
H77.22	+++	−	−	−	−	−
H77.23	+++	−	−	−	−	−
H77.27	+++	+++	−	−	+	−
H77.28	+++	+++	−	−	+	−
H77.29	+++	+++	−	−	+	−
H77.30	+++	−	−	−	−	−
H77.31	+++	−	−	−	−	−
H77.32	+++	+	+++	−	+++	−
H77.33	+++	−	−	+++	−	−
H77.34	+++	−	−	−	−	−
H77.35	+++	−	−	−	−	−
H77.36	+++	+++	+++	+++	+++	+++
H77.37	+++	−	−	−	+++	−
H77.38	+++	−	−	−	−	−
H77.39	+++	+++	+++	+++	+++	+++
H77.42	+++	−	−	−	+	−
H77.43	+++	−	−	−	−	−
H77.44	+++	−	−	−	+++	−
H77.45	+++	−	−	−	−	−
H77.46	+++	−	−	−	+++	−
H77.47	+++	+++	−	−	−	−
H77.50	+++	−	−	−	−	−
H77.53	+++	−	−	−	+++	−
H77.55	+++	−	−	−	+++	−
H77.56	+++	+++	+++	+++	−	+++

↵a +++, strong binding (40 to 100%) to yeast expressing E2; +, weak binding (15 to 40%) to yeast expressing E2; −, no appreciable binding detected. The data are a summary of 3 to 5 independent experiments.

Table 2. Summary of MAb binding to genotype 1 mutants expressed on the surface of yeast

MAb	Binding[a]															
	G406D	G406S	N410Y	I411N	N415Y	T416I	N417T	G470A	W529R	G530A	G530D	D533N	R543G	C552S	G406S + G530A	G406D + G530D
H77.14	100	100	100	100	67	100	58	**<1**	100	91	100	100	66	100	100	100
H77.16	**<1**	58	**<1**	**<1**	76	97	100	100	100	97	100	100	100	100	**<1**	**<1**
H77.23	100	100	100	100	75	100	61	**<1**	100	100	100	100	89	100	100	100
H77.27	77	91	100	97	64	100	80	81	**<1**	**<1**	11	27	84	100	**<1**	**<1**
H77.28	96	100	100	74	38	96	57	74	100	61	100	76	**<1**	***>500***	100	100
H77.31	77	100	100	100	96	100	65	100	**<1**	**<1**	24	**<1**	100	100	**<1**	**<1**
H77.36	97	88	100	92	100	100	98	100	**1.2**	26	**<1**	80	100	100	21	**<1**
H77.39	100	100	100	100	**<1**	81	**<1**	61	100	100	100	100	50	100	100	100
H77.56	100	100	100	100	100	100	100	100	100	100	100	92	100	**9.5**	100	100

Values shown were obtained by dividing the total fluorescence product (percent positive population x mean fluorescence intensity) of a mutant for a given MAb by the total fluorescence product of the wild type E2 for a given MAb. This value was then divided by the total fluorescence product of a mutant for an oligoclonal pool of MAbs by the total fluorescence product of WT E2 for the olicoglonal pool (to control for E2 binding) and multiplied by 100. Values in bold indicate complete loss of binding, with reductions in MAb binding greater than or equal to 80% for a given mutation. Underlined values show partial loss of binding, with a reduction between 50 and 79%. The results are the average of three independent experiments for each mutant and each antibody. Poly-protein amino acid numbering was determined by alignment with the H77 strain using Sequence Location tool on the Los Alamos HCV database (http://hcv.lanl.gov/cgi-bin/LOCATE/locate.cgi)

Table 3: Summary of MAb binding to genotype 2 mutants expressed on yeast

MAb	Binding[a]										
	G397E	F403L	G406C	S440P	Y443C	A524V	W529C	E531V	R572S	H617L	G397E + R572S
J6.1	71	97	100	100	83	83	100	88	100	100	61
J6.2	71	100	**16**	100	93	73	**20**	68	42	**6**	56
J6.6	64	100	26	41	100	**6**	**4**	69	100	100	100
J6.15	100	100	100	75	85	66	**13**	34	100	100	79
J6.16	100	100	100	76	100	80	100	86	100	100	100
J6.27	74	67	100	90	95	**<1**	**<1**	77	83	100	80
J6.30	85	100	100	100	75	58	88	82	100	**3**	100
J6.36	100	**<1**	**<1**	60	95	80	100	100	100	100	**<1**
J6.39	94	91	100	100	83	100	**3**	63	100	100	81
J6.40	98	100	32	32	100	75	63	65	40	**15**	80
J6.60	51	58	100	**<1**	**<1**	65	90	81	70	73	77
J6.75	100	100	100	100	100	100	100	100	100	100	100
J6.85	100	100	100	100	91	72	**10**	27	100	100	80
J6.101	83	100	43	100	100	100	57	91	82	**3**	50
J6.103	100	**2**	**<1**	26	100	100	100	100	100	100	**<1**

Values shown were obtained by dividing the total fluorescence product (percent positive population x mean fluorescence intensity) of a mutant for a given MAb by the total fluorescence product of the wild type E2 for a given MAb. This value was then divided by the total fluorescence product of a mutant for an oligoclonal pool of MAbs by the total fluorescence product of WT E2 for the olicoglonal pool (to control for E2 binding) and multiplied by 100. Values in bold indicate complete loss of binding, with reductions in MAb binding greater than or equal to 80% for a given mutation. Underlined values show partial loss of binding, with a reduction between 50 and 79%. The results are the average of three independent experiments for each mutant and each antibody. Poly-protein amino acid numbering was determined by alignment with the H77 strain using Sequence Location tool on the Los Alamos HCV database (http://hcv.lanl.gov/cgi-bin/LOCATE/locate.cgi)

Table 4: Previously characterized anti-E2 MAbs with available mapping information

MAb name	Source of MAb	Binding residues	Neutralization of HCVpp	Neutralization of HCVcc
AP33	Mouse	L413, N415, G418, W420	Yes; all genotypes	Yes; >80% neutralization with 50 μg/ml MAb
3/11	Rat	N415, W420, H421	Yes; genotypes 1, 2, 4, 5, and 6 by >50%	ND[a]
9/27	Rat	396–407	Yes; genotype 1 by >99%	ND
11/20	Rat	436–447	Yes; genotype 1 by >99%	ND
7/16b	Rat	436–447	Yes; neutralized HCVpp representative of genotype 1 by >99%	ND
2/69a	Rat	432–443	Yes; genotype 1 by >99%	ND
2/64a	Rat	524–531	Yes; genotype 1 by 40%	ND
1/39	Rat	432–443	Yes; genotype 1 by 20%	ND
CBH-5	Human	G523, P525, G530, D535, N540	Yes; all genotypes >40%	Yes
CBH-7	Human	N540, W549	Yes; genotypes 1, 2 and 4 by >20%	Yes
HCV-1	HuMAb mice[b]	L413, W420	Yes; genotypes 1, 2, 3, and 4	ND
95-2	HuMAb mice	L413, W420	Yes; genotypes 1, 2, 3, and 4	ND
1:7	Human	G523, T526, Y527, W529, G530, D535	Yes; all genotypes	Yes
A8	Human	G523, T526, Y527, W529, G530, D535	Yes; all genotypes	Yes
AR2A	Human	N540A	Yes; genotypes 1, 2, 4, and 5	No
AR3A	Human	S424, G523, P525, G530, D535, N540	Yes; genotypes 1, 2, 4, and 5	Yes
AR3B	Human	S424, G530, D535	Yes; genotypes 1, 2, 4, and 5	Yes
AR3C	Human	S424, P525, G530, D535, N540	Yes; genotypes 1, 2, 4, and 5	Yes
AR3D	Human	S424, G530	Yes; genotypes 1, 2, 4, and 5	Yes
e137	Human	T416, W420, W529, G530, D535	Yes; genotypes 1, 2, and 4	Yes

[a] ND, not done.
[b] HuMAb mice are transgenic for human μ, γ1, and κ germ line genes.

Figure 1: Identification of neutralizing anti-E2 antibodies against HCV.

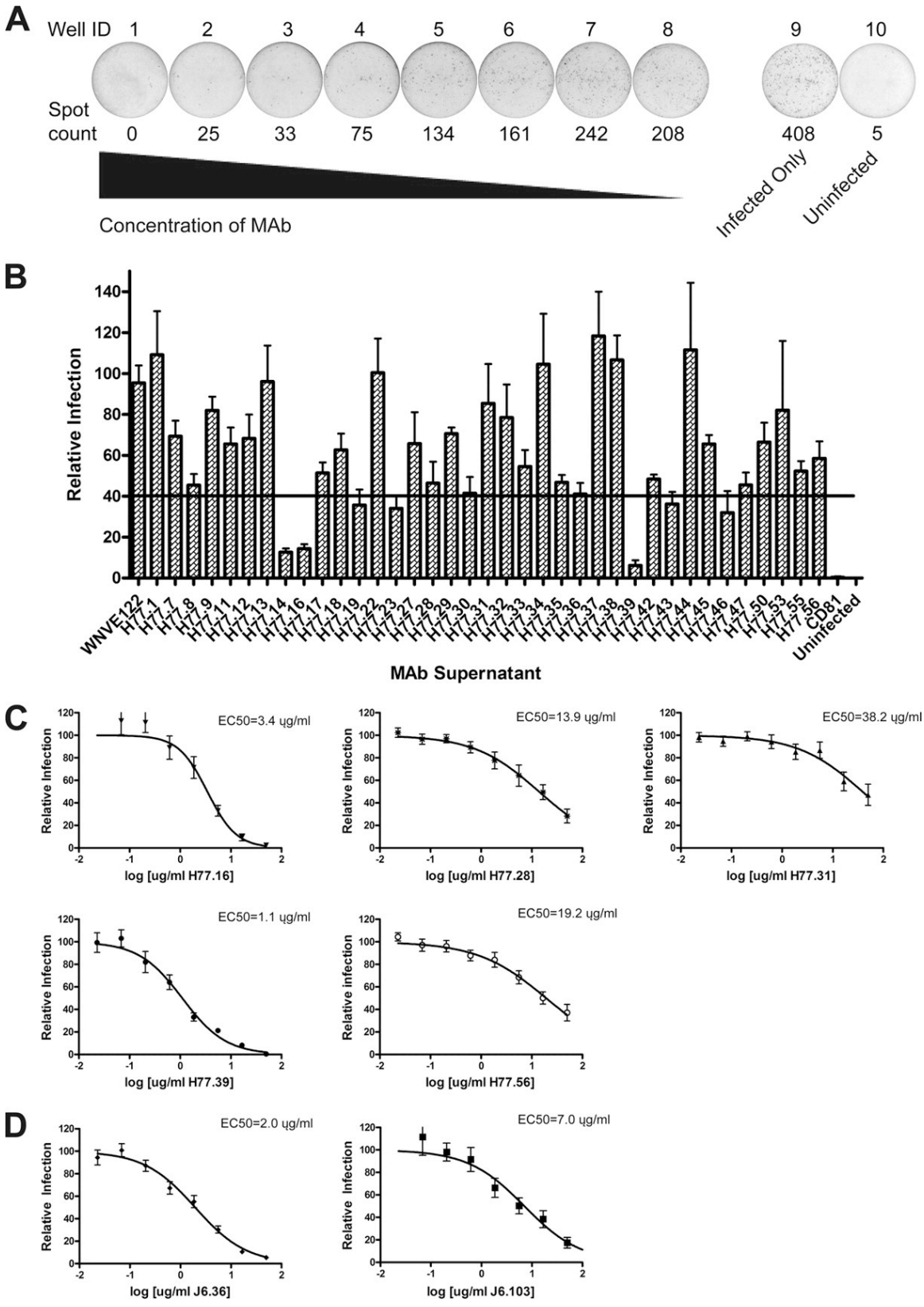

Figure 1 legend: Identification of neutralizing anti-E2 antibodies against HCV. A. Examples of MAb neutralization as judged by a reduction in the number of FFU using the Biospot Macroanalyzer. Spot counts are labeled below each well and well numbers are labeled above. Wells 1 through 8 represent decreasing (3-fold) concentrations of the neutralizing MAb H77.39 (starting concentration of 50 mg/ml). Well 9 shows infection in the absence of MAb, and well 10 is an uninfected well. Data are representative of three independent experiments performed in duplicate. **B.** MAb supernatant was mixed with the H77-JFH1 chimeric HCV for one 1 hour at 37°C and Huh-7.5 cells were infected. Three days later, neutralization was determined by FFU assay. MAb supernatants that decreased the number of FFU to 40% or less (below the solid black line) than the negative control MAb (anti-WNV E122) were purified for testing in full dose-response analysis. Data is pooled from three independent experiments performed in duplicate. **C**. Serial dilutions of genotype 1a specific purified MAbs were mixed with H77-JFH1 chimeric virus and neutralization was assessed. Efficient neutralization was observed for five (H77.16, H77.28, H77.31, H77.39 and H77.56) genotype 1a specific MAbs but not for the negative control MAb (data not shown). EC50 values were calculated after non-linear regression analysis. Data is pooled from of at least three independent experiments performed in duplicate. **D**. Increasing concentrations of purified genotype 2a specific MAbs (J6.36 and J6.103) were mixed with J6-JFH1-JC1-luciferase-expressing virus. At 48 hours, neutralization was assessed in Huh-7.5 cells by monitoring luciferase expression. EC50 values were calculated after non-linear regression analysis. Data is pooled from at least three independent experiments performed in duplicate. In this Figure, all error bars represent the standard error of the mean.

Figure 2: **Identification of MAbs that bind heterologous HCV genotypes using yeast display of E2 protein.**

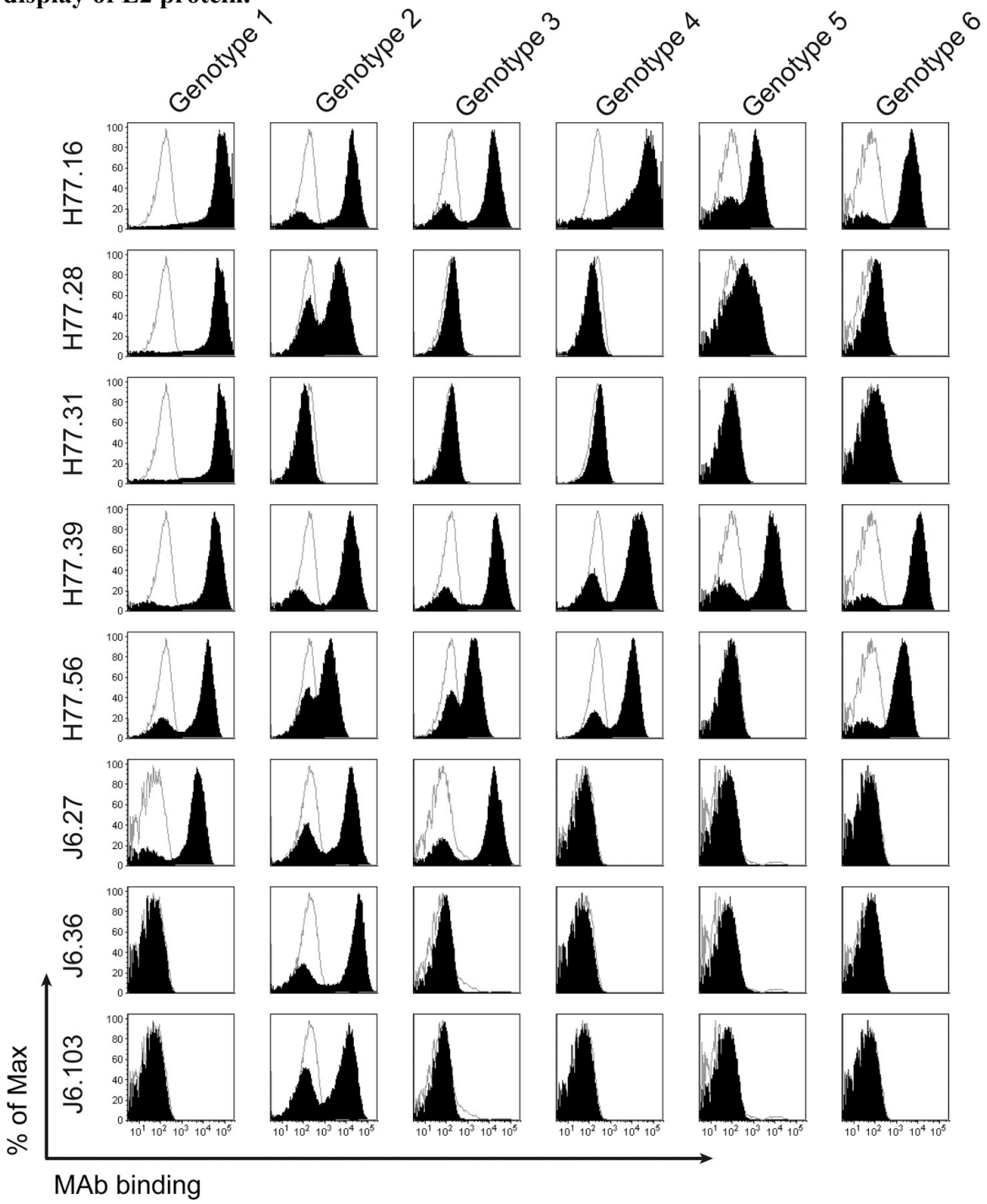

Figure 2 legend: **Identification of MAbs that bind heterologous HCV genotypes using yeast display of E2 protein.** The E2 ectodomain gene from six strains corresponding to HCV genotypes 1-6 was cloned into the PYD1 vector and expressed on the surface of yeast (see Materials and Methods). Yeast expressing HCV E2 were incubated with MAb supernatants and binding was assessed by flow cytometry. Representative histograms from all neutralizing MAbs (H77.16, H77.28, H77.31, H77.39, H77.56, J6.27, J6.36 and J6.103; solid black histograms) and negative control MAb (WNV E16; unfilled gray histograms) are depicted. Data is representative of three independent experiments.

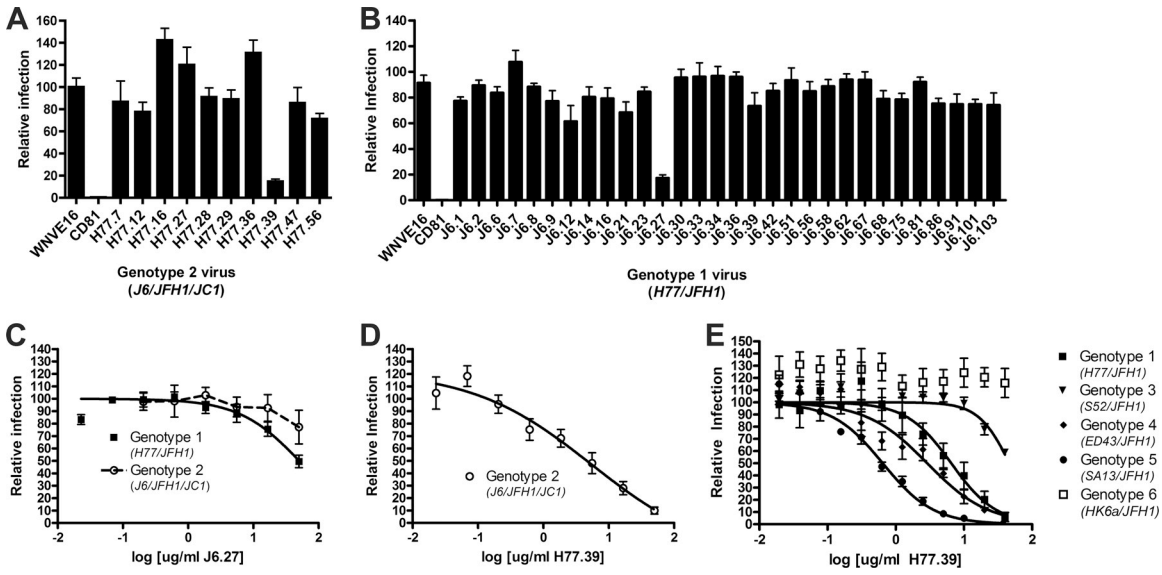

Figure 3: **MAb neutralization of heterologous HCV genotypes.** MAbs that were generated against (**A**) genotype 1a or (**B**) genotype 2a E2 proteins were tested for their ability to neutralize infection of virus from the heterologous genotype. Purified J6 or H77 MAbs (50 mg/ml) were pre-incubated at 37°C with H77-JFH1 (genotype 1a) or J6-JFH1-JC1 (genotype 2a) virus, respectively, and neutralization was assessed as described in Figure 1. **C-E**. EC50 analysis was performed with (**C**) J6.27 MAb and H77-JFH1 virus (■) or J6-JFH1-JC1 virus (○) or (**D**) H77.39 MAb and J6-JFH1-JC1 virus (○) or **(E)** H77.39 MAb and H77/JFH1 (■), J6/JFH1(▲), S52/JFH1(▼), ED43/JFH1(♦), SA13/JFH1(●) and HK6a/JFH1(□) chimeric viruses. Graphs represent pooled data from at least three independent experiments performed in duplicate (**A-D**) or two independent experiments performed in triplicate (**E**), and error bars represent the standard error of the mean.

Figure 4: Pre- or post-attachment neutralization.

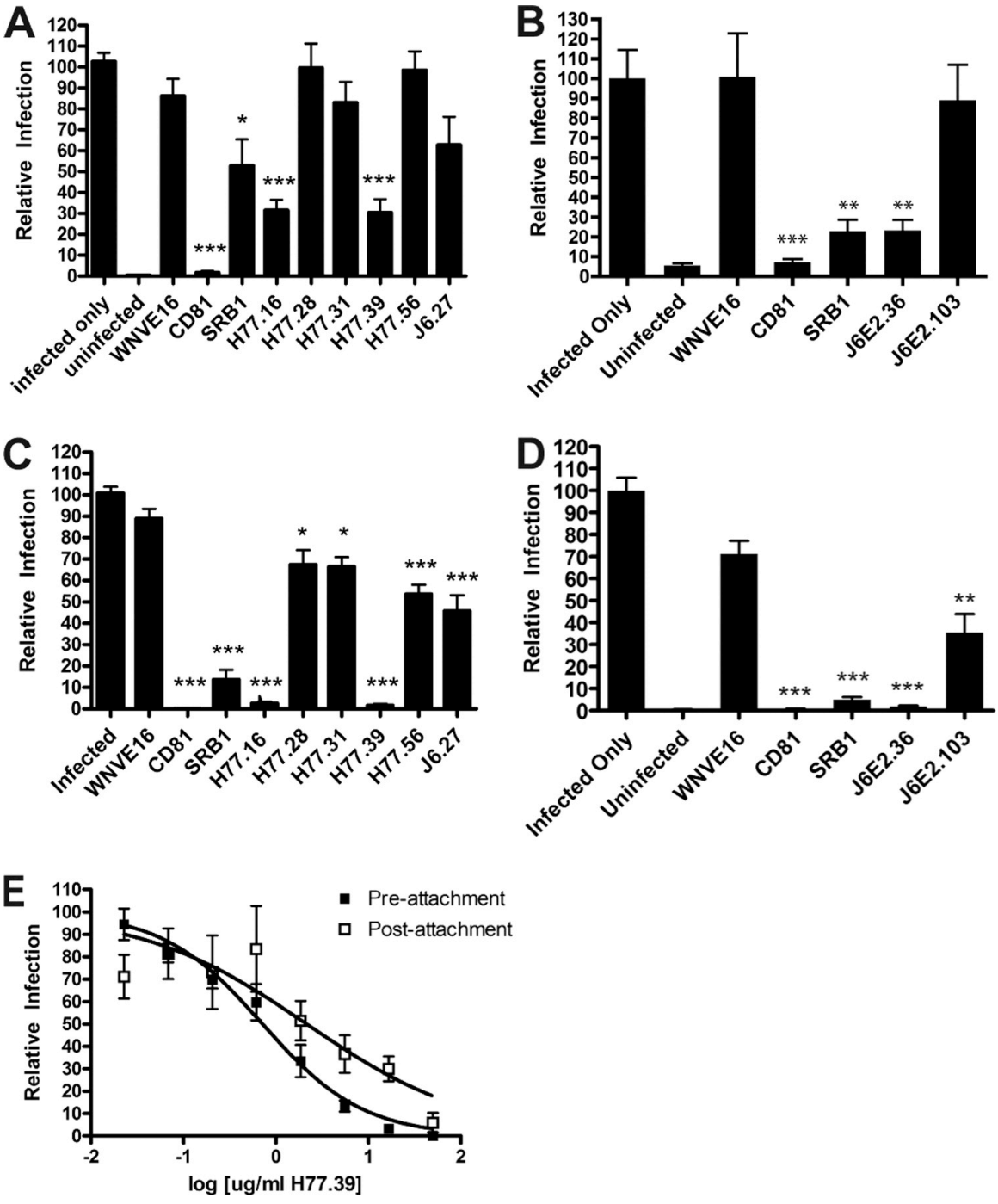

Figure 4 legend: Pre- or post-attachment neutralization. A-D. To determine whether MAbs neutralize HCV infection at a post-attachment step, Huh-7.5 cells were pre-chilled at 4°C and 480 FFU of (**A**) genotype 1a (H77-JFH1) or (**B**) genotype 2a (J6-JFH1-JC1) virus was added to each well for 1 hour at 4°C. After three washes with 4°C DMEM, saturating concentrations of MAbs (50 mg/ml) were added for 1 hour at 37°C and the neutralization assay completed. In comparison, a standard pre-incubation neutralization test was performed at 37°C, in which (**C**) genotype 1a virus or (**D**) genotype 2a virus and MAb were pre-incubated at 37°C prior to addition to cells. Data shown are the average of three independent experiments, with error bars representing standard error of the mean. Statistically significant difference in neutralization are compared to infection in the presence of a negative control MAb (WNV E16): *, $p < 0.05$; **, $p < 0.01$; and ***, $p < 0.001$. **E-F.** To confirm the ability of (**E**) H77.39 to neutralize infection at both pre-and post-attachment steps, a dose response curve was performed under both pre-and post-attachment conditions as described above using H77/JFH1 virus. Solid squares (■) represent pre-attachment data and clear squares (□) represent post-attachment data. Graphs represent pooled data from at least three independent experiments performed in duplicate, and error bars represent the standard error of the mean.

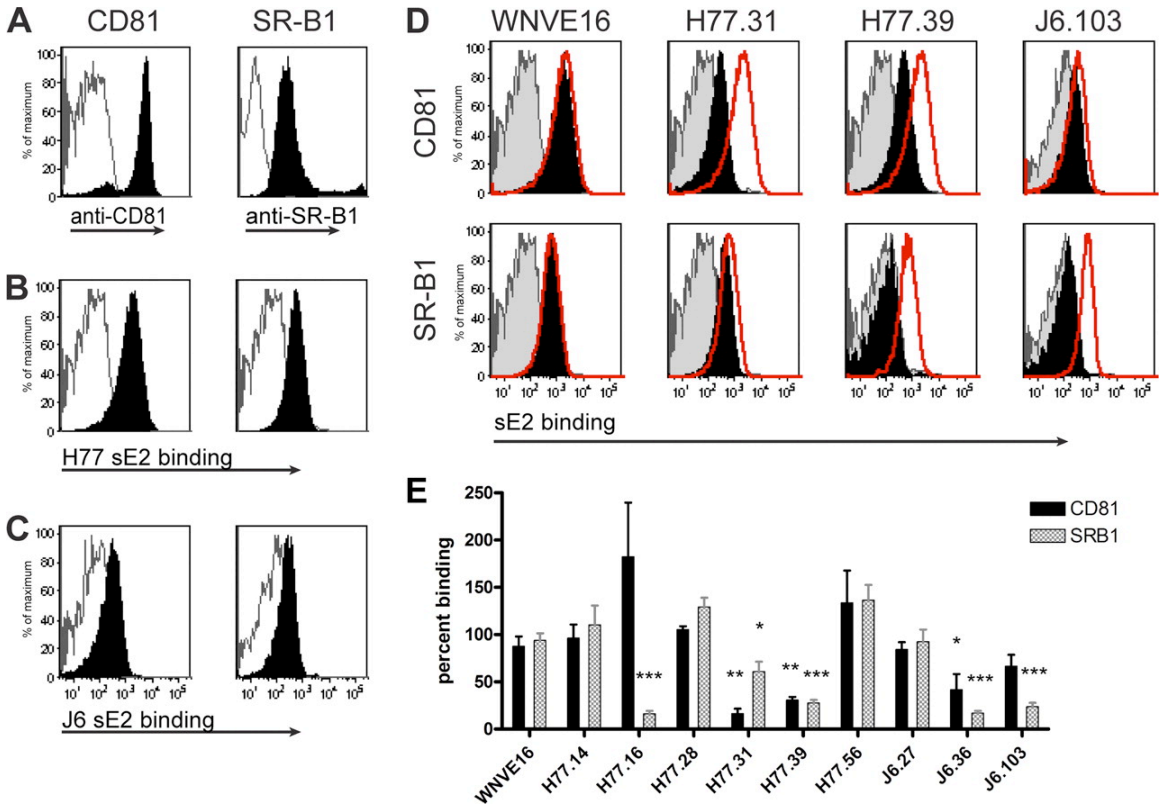

Figure 5: Inhibition of sE2 binding to CD81 and SR-B1 by neutralizing MAbs. A. Verification of ectopic CD81 and SR-B1 receptor expression on CHO cells. CHO-CD81 or CHO-SR-B1 cells were incubated with either mouse anti-hCD81 or rabbit-anti-hSR-B1 (black histograms) or an irrelevant MAb (unfilled gray histograms) for 30 minutes on ice. Cells were washed, incubated with the appropriate secondary antibodies, and processed by flow cytometry. **B-C.** Binding of (**B**) genotype 1a (H77) E2 or (**C**) genotype 2a (J6) E2 to CHO-CD81 and CHO-SR-B1 but not WT CHO cells. CHO-CD81 or CHO-SR-B1 (solid black histograms) or WT CHO (unfilled gray histograms) cells were incubated with sE2 and binding was assayed by flow cytometry. Data are representative of at least three independent experiments. **D.** Assessment of inhibition of sE2 binding to CHO-CD81 or CHO-SR-B1 cells by neutralizing MAbs. sE2 was pre-incubated with neutralizing MAbs, added to CHO cells, and binding detected by flow cytometry. Examples of MAbs that inhibit sE2 binding only to CD81 (H77.31), to both CD81 and SR-B1 (H77.39), or only to SR-B1 (J6.103), as well as a negative control MAb (WNV E16) are shown. Histograms are representative of three individual experiments. Solid black histograms represent sE2 binding in the presence of MAb, red histograms represent sE2 binding in the absence of MAb, and shaded gray histograms represent sE2 binding to CHO WT cells. **E**. Graphical representation of sE2 binding to CHO-CD81 and CHO-SR-B1 cells in the presence of neutralizing MAbs. Values were determined by dividing the fluorescence quotient (mean fluorescence intensity x percent positive cells) for E2 binding in the presence of a neutralizing MAb by the fluorescence quotient of sE2 binding to either CHO-CD81 or CHO-SR-B1 cells alone. Asterisks represent statistically significant difference in sE2 binding compared to the negative

control MAb, WNV E16: *, $p < 0.05$; **, $p < 0.01$; and ***, $p < 0.001$. Error bars represent the standard error of the mean. Data are pooled from three independent experiments.

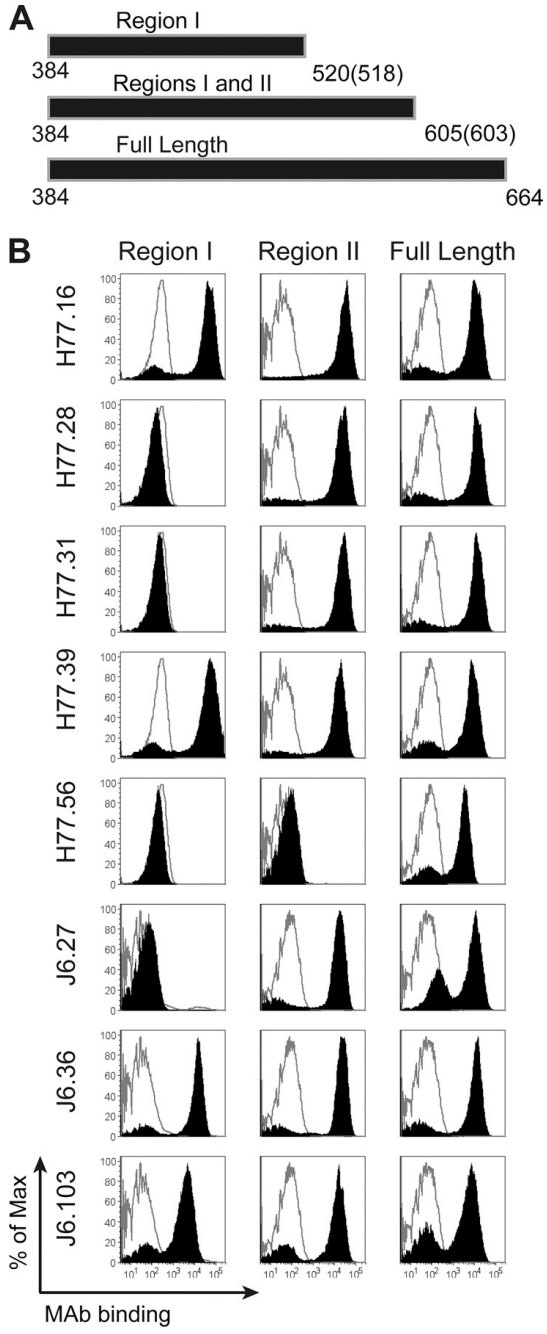

Figure 6: Mapping of anti-E2 antibodies using COOH-terminal truncation mutants. **A**. Scheme of E2 truncations used for mapping. cDNA containing region I (aa 384-520 and aa 384-518 in E2 of genotypes 1a and 2a, respectively) I and II (aa 384-605 and 384-603 in E2 of genotypes 1a and 2a, respectively), and the full length ectodomain (aa 384-664) were displayed on the surface of yeast. **B**. MAb supernatants were incubated with yeast and assessed for binding by flow cytometry**.** Neutralizing MAbs binding to regions I (H77.16, H77.39, J6.36, and J6.103), II (H77.28, H77.31, and J6.27), and III (H77.56) are shown. Solid black histograms depict binding of HCV-specific MAbs and gray, unfilled histograms represent binding of a negative control MAb (WNV E16). Histograms are representative of three independent experiments.

Figure 7: Epitope localization of anti-HCV MAbs.

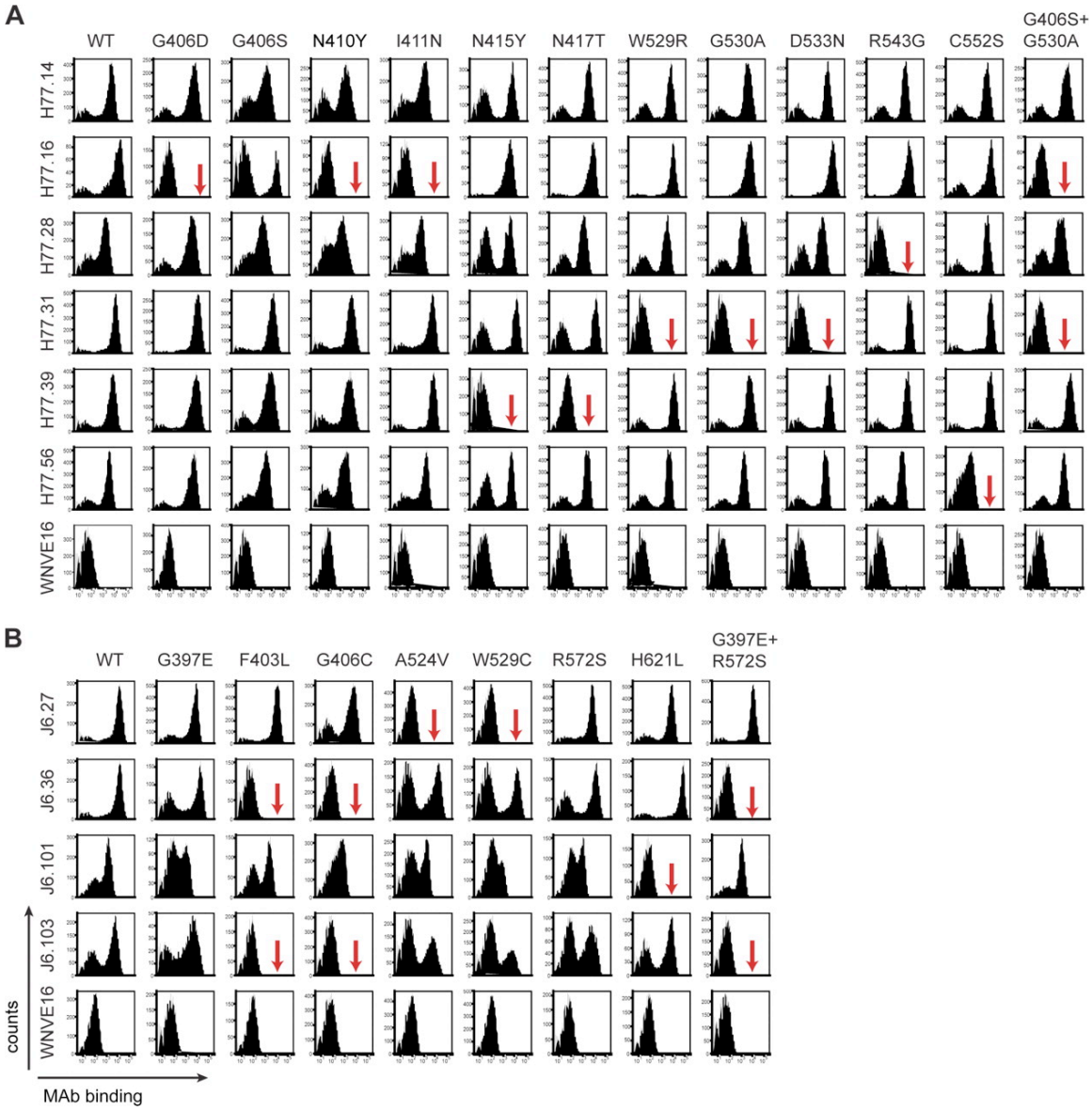

Figure 7 legend: Epitope localization of anti-HCV MAbs. Binding of neutralizing MAbs to yeast expressing E2 protein variants. **A**. Flow cytometry histograms of wild type and loss-of-binding genotype 1a E2 variants (G406D, G406S, N410Y, I411N, N415Y, N417T, W529R, G530A, D533N, R543G, C552S, and G406S + G530A). Representative histograms are shown for the MAbs H77.14, H77.16, H77.28, H77.31, H77.39, H77.56 xand WNV E16 (negative control) with WT H77 E2 and each of the variants. Data shown are representative of three independent experiments. Red arrows indicate >80% loss-of-binding of a specific MAb for a given variant. **B**. Flow cytometry histograms of wild type and loss-of-function genotype 2a E2 variants (G397E, F403L, G406C, A524V, W529C, R572S, H621L and G397E+R572S) with individual neutralizing MAbs. Representative histograms are shown for the MAbs J6.27, J6.36, J6.101, J6.103 and WNV E16 (negative control) with the wild type E2 and each of the variants. Data shown are representative of three independent experiments. Arrows indicate >80% loss-of-binding of a specific MAb for a given variant.

Figure 8: Localization of MAb binding residues on E2.

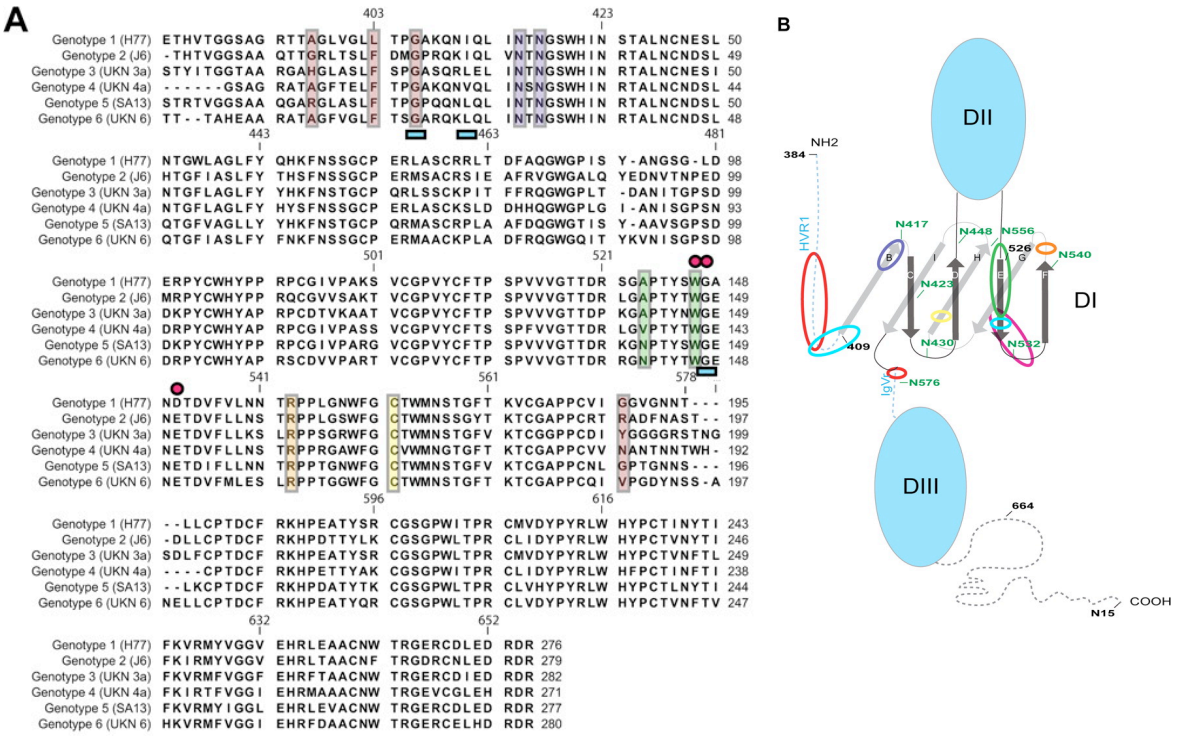

C

MAb	EC50 (ug/ml)	Cross-reactivity	Inhibition of SR-B1 binding	Inhibition of CD81 binding	E2 binding region	Loss of binding residues
H77.16	22.5	2, 3, 4, 5, 6	+++	-	I	G406, N410, I411, G406+G530
H77.28	13.9	2, 5	-	-	II	R543
H77.31	38.2	-	+	+++	II	W529, G530, D533
H77.39	1.09	2, 3, 4, 5, 6	+++	+++	I	N415, N417
H77.56	19.2	2, 3, 4, 6	-	-	Full-length	C552
J6.27	N/A	1, 3	-	-	II	A524, W529
J6.36	1.95	-	+++	+	I	F403, G406, G397+R572
J6.103	7.05	-	+++	-	I	F403, G406, G397+R572

Figure 8 legend: Localization of MAb binding residues on E2. **A**. Alignment of E2 sequences from HCV genotypes 1-6 with superimposed mapping of MAb binding residues. The sequences of E2 from strains representative of the different genotypes (genotype 1a, H77; genotype 2a; J6, genotype 3a, UKN 3; genotype 4a, UKN4a; genotype 5a, SA513; genotype 6a, UKN 6) were aligned and colored boxes and symbols were used to highlight neutralizing MAb binding residues as follows: red boxes, J6.36 and J6.103; purple boxes, H77.39; blue underscoring, H77.16; green boxes, J6.27; pink circles, H77.31; orange box, H77.28; yellow box, H77.56. **B.** Putative model of structure of the E2 protein with MAb binding regions highlighted. A scheme depicting a possible E2 structure was adapted from Krey et al. (36) to highlight regions involved in MAb recognition. N-linked glycosylation residues are labeled in green and amino acids numbered in black at intervals. b-sheets in D1 are labeled as previously described (36). MAb binding regions are highlighted by colored circles as follows: red circles, J6.36 and J6.103; purple circle, H77.39; light blue circles, H77.16; green circle, J6.27; pink circle, H77.31; orange circle, H77.28; yellow circle, H77.56. **C**. Summary of neutralizing MAbs described in this study. EC50 values (neutralization against homologous virus), cross-reactivity to E2 from different genotypes, inhibition of binding to CD81 and SR-B1, reactivity with different regions of E2, and loss of binding residues are listed. MAb names are color-coded to correspond to panels A and B.

A1.7 References

1. Bowen, D.G. & Walker, C.M. Adaptive immune responses in acute and chronic hepatitis C virus infection. *Nature* **436**, 946-952 (2005).
2. Bartenschlager, R., Frese, M. & Pietschmann, T. Novel insights into hepatitis C virus replication and persistence. *Adv. Virus Res.* **63**, 71-180 (2004).
3. Feld, J.J. & Hoofnagle, J.H. Mechanism of action of interferon and ribavirin in treatment of hepatitis C. *Nature* **436**, 967-972 (2005).
4. Lindenbach, B.D. & Rice, C.M. Unravelling hepatitis C virus replication from genome to function. *Nature* **436**, 933-938 (2005).
5. Pileri, P. *et al.* Binding of hepatitis C virus to CD81. *Science* **282**, 938-941 (1998).
6. Scarselli, E. *et al.* The human scavenger receptor class B type I is a novel candidate receptor for the hepatitis C virus. *EMBO J.* **21**, 5017-5025 (2002).
7. Evans, M.J. *et al.* Claudin-1 is a hepatitis C virus co-receptor required for a late step in entry. *Nature* **446**, 801-805 (2007).
8. Ploss, A. *et al.* Human occludin is a hepatitis C virus entry factor required for infection of mouse cells. *Nature* **457**, 882-886 (2009).
9. Drummer, H.E., Wilson, K.A. & Poumbourios, P. Identification of the hepatitis C virus E2 glycoprotein binding site on the large extracellular loop of CD81. *J. Virol.* **76**, 11143-11147 (2002).
10. Flint, M. *et al.* Characterization of hepatitis C virus E2 glycoprotein interaction with a putative cellular receptor, CD81. *J. Virol.* **73**, 6235-6244 (1999).

11. Higginbottom, A. *et al.* Identification of amino acid residues in CD81 critical for interaction with hepatitis C virus envelope glycoprotein E2. *J. Virol.* **74**, 3642-3649 (2000).
12. Petracca, R. *et al.* Structure-function analysis of hepatitis C virus envelope-CD81 binding. *J. Virol.* **74**, 4824-4830 (2000).
13. Bankwitz, D. *et al.* Hepatitis C virus hypervariable region 1 modulates receptor interactions, conceals the CD81 binding site, and protects conserved neutralizing epitopes. *J. Virol.* **84**, 5751-5763 (2010).
14. Bartosch, B. *et al.* Cell entry of hepatitis C virus requires a set of co-receptors that include the CD81 tetraspanin and the SR-B1 scavenger receptor. *J. Biol. Chem.* **278**, 41624-41630 (2003).
15. Allander, T. *et al.* Recombinant human monoclonal antibodies against different conformational epitopes of the E2 envelope glycoprotein of hepatitis C virus that inhibit its interaction with CD81. *J. Gen. Virol.* **81**, 2451-2459 (2000).
16. Owsianka, A., Clayton, R.F., Loomis-Price, L.D., McKeating, J.A. & Patel, A.H. Functional analysis of hepatitis C virus E2 glycoproteins and virus-like particles reveals structural dissimilarities between different forms of E2. *J. Gen. Virol.* **82**, 1877-1883 (2001).
17. Farci, P. *et al.* Prevention of hepatitis C virus infection in chimpanzees after antibody-mediated in vitro neutralization. *Proc. Natl. Acad. Sci. U.S.A.* **91**, 7792-7796 (1994).
18. Law, M. *et al.* Broadly neutralizing antibodies protect against hepatitis C virus quasispecies challenge. *Nat. Med.* **14**, 25-27 (2008).

19. Vanwolleghem, T. *et al.* Polyclonal immunoglobulins from a chronic hepatitis C virus patient protect human liver-chimeric mice from infection with a homologous hepatitis C virus strain. *Hepatology* **47**, 1846-1855 (2008).
20. Choo, Q.L. *et al.* Vaccination of chimpanzees against infection by the hepatitis C virus. *Proc. Natl. Acad. Sci. U.S.A.* **91**, 1294-1298 (1994).
21. Houghton, M. & Abrignani, S. Prospects for a vaccine against the hepatitis C virus. *Nature* **436**, 961-966 (2005).
22. Scheller, N. *et al.* Translation and replication of hepatitis C virus genomic RNA depends on ancient cellular proteins that control mRNA fates. *Proc. Natl. Acad. Sci. U.S.A.* **106**, 13517-13522 (2009).
23. Yi, M., Ma, Y., Yates, J. & Lemon, S.M. Trans-complementation of an NS2 defect in a late step in hepatitis C virus (HCV) particle assembly and maturation. *PLoS Pathog.* **5**, e1000403 (2009).
24. Ma, Y., Yates, J., Liang, Y., Lemon, S.M. & Yi, M. NS3 helicase domains involved in infectious intracellular hepatitis C virus particle assembly. *J. Virol.* **82**, 7624-7639 (2008).
25. Scheel, T.K.H. *et al.* Development of JFH1-based cell culture systems for hepatitis C virus genotype 4a and evidence for cross-genotype neutralization. *Proc. Natl. Acad. Sci. U.S.A.* **105**, 997-1002 (2008).
26. Lindenbach, B.D. *et al.* Complete replication of hepatitis C virus in cell culture. *Science* **309**, 623-626 (2005).

27. Gottwein, J.M. *et al.* Novel infectious cDNA clones of hepatitis C virus genotype 3a (strain S52) and 4a (strain ED43): genetic analyses and in vivo pathogenesis studies. *J. Virol.* **84**, 5277-5293 (2010).
28. Jensen, T.B. *et al.* Highly efficient JFH1-based cell-culture system for hepatitis C virus genotype 5a: failure of homologous neutralizing-antibody treatment to control infection. *J. Infect. Dis.* **198**, 1756-1765 (2008).
29. Kolykhalov, A.A. *et al.* Transmission of hepatitis C by intrahepatic inoculation with transcribed RNA. *Science* **277**, 570-574 (1997).
30. Hüssy, P., Schmid, G., Mous, J. & Jacobsen, H. Purification and in vitro-phospholabeling of secretory envelope proteins E1 and E2 of hepatitis C virus expressed in insect cells. *Virus Res.* **45**, 45-57 (1996).
31. Oliphant, T. *et al.* Development of a humanized monoclonal antibody with therapeutic potential against West Nile virus. *Nat. Med.* **11**, 522-530 (2005).
32. Diamond, M.S., Garcia-Aguilar, J., Bickford, J.K., Corbi, A.L. & Springer, T.A. The I domain is a major recognition site on the leukocyte integrin Mac-1 (CD11b/CD18) for four distinct adhesion ligands. *J. Cell Biol.* **120**, 1031-1043 (1993).
33. Gottwein, J.M. *et al.* Robust hepatitis C genotype 3a cell culture releasing adapted intergenotypic 3a/2a (S52/JFH1) viruses. *Gastroenterology* **133**, 1614-1626 (2007).
34. Martinez-Donato, G. *et al.* Expression and processing of hepatitis C virus structural proteins in Pichia pastoris yeast. *Biochem. Biophys. Res. Commun.* **342**, 625-631 (2006).

35. Feldhaus, M.J. *et al.* Flow-cytometric isolation of human antibodies from a nonimmune Saccharomyces cerevisiae surface display library. *Nat. Biotechnol.* **21**, 163-170 (2003).

36. Shrestha, B. *et al.* The development of therapeutic antibodies that neutralize homologous and heterologous genotypes of dengue virus type 1. *PLoS Pathog.* **6**, e1000823 (2010).

37. Johansson, D.X. *et al.* Human combinatorial libraries yield rare antibodies that broadly neutralize hepatitis C virus. *Proc. Natl. Acad. Sci. U.S.A.* **104**, 16269-16274 (2007).

38. Owsianka, A.M. *et al.* Broadly neutralizing human monoclonal antibodies to the hepatitis C virus E2 glycoprotein. *J. Gen. Virol.* **89**, 653-659 (2008).

39. Tarr, A.W. *et al.* Characterization of the hepatitis C virus E2 epitope defined by the broadly neutralizing monoclonal antibody AP33. *Hepatology* **43**, 592-601 (2006).

40. Brien, J.D. *et al.* Genotype-specific neutralization and protection by antibodies against dengue virus type 3. *J. Virol.* **84**, 10630-10643 (2010).

41. Oliphant, T. *et al.* Antibody recognition and neutralization determinants on domains I and II of West Nile Virus envelope protein. *J. Virol* **80**, 12149-12159 (2006).

42. Balsitis, S.J. *et al.* Lethal antibody enhancement of dengue disease in mice is prevented by Fc modification. *PLoS Pathog.* **6**, e1000790 (2010).

43. Pierson, T.C. & Diamond, M.S. Molecular mechanisms of antibody-mediated neutralisation of flavivirus infection. *Expert Rev Mol Med* **10**, e12 (2008).

44. Nybakken, G.E. *et al.* Structural basis of West Nile virus neutralization by a therapeutic antibody. *Nature* **437**, 764-769 (2005).

45. Sukupolvi-Petty, S. *et al.* Structure and function analysis of therapeutic monoclonal antibodies against dengue virus type 2. *J. Virol.* **84**, 9227-9239 (2010).
46. Vogt, M.R. *et al.* Human monoclonal antibodies against West Nile virus induced by natural infection neutralize at a postattachment step. *J. Virol.* **83**, 6494-6507 (2009).
47. Bertaux, C. & Dragic, T. Different domains of CD81 mediate distinct stages of hepatitis C virus pseudoparticle entry. *J. Virol.* **80**, 4940-4948 (2006).
48. Haberstroh, A. *et al.* Neutralizing host responses in hepatitis C virus infection target viral entry at postbinding steps and membrane fusion. *Gastroenterology* **135**, 1719-1728.e1 (2008).
49. Owsianka, A.M. *et al.* Identification of conserved residues in the E2 envelope glycoprotein of the hepatitis C virus that are critical for CD81 binding. *J. Virol.* **80**, 8695-8704 (2006).
50. Broering, T.J. *et al.* Identification and characterization of broadly neutralizing human monoclonal antibodies directed against the E2 envelope glycoprotein of hepatitis C virus. *J. Virol.* **83**, 12473-12482 (2009).
51. Vieyres, G., Dubuisson, J. & Patel, A.H. Characterization of antibody-mediated neutralization directed against the hypervariable region 1 of hepatitis C virus E2 glycoprotein. *J. Gen. Virol.* **92**, 494-506 (2011).
52. Perotti, M. *et al.* Identification of a broadly cross-reacting and neutralizing human monoclonal antibody directed against the hepatitis C virus E2 protein. *J. Virol.* **82**, 1047-1052 (2008).

53. Keck, Z.-Y. *et al.* Definition of a conserved immunodominant domain on hepatitis C virus E2 glycoprotein by neutralizing human monoclonal antibodies. *J. Virol.* **82**, 6061-6066 (2008).

54. Gal-Tanamy, M. *et al.* In vitro selection of a neutralization-resistant hepatitis C virus escape mutant. *Proc. Natl. Acad. Sci. U.S.A.* **105**, 19450-19455 (2008).

55. Krey, T. *et al.* The Disulfide Bonds in Glycoprotein E2 of Hepatitis C Virus Reveal the Tertiary Organization of the Molecule. *PLoS Pathog* **6**, (2010).

56. Hadlock, K.G. *et al.* Human monoclonal antibodies that inhibit binding of hepatitis C virus E2 protein to CD81 and recognize conserved conformational epitopes. *J. Virol.* **74**, 10407-10416 (2000).

57. Hsu, M. *et al.* Hepatitis C virus glycoproteins mediate pH-dependent cell entry of pseudotyped retroviral particles. *Proc. Natl. Acad. Sci. U.S.A.* **100**, 7271-7276 (2003).

58. Dhillon, S. *et al.* Mutations within a conserved region of the hepatitis C virus E2 glycoprotein that influence virus-receptor interactions and sensitivity to neutralizing antibodies. *J. Virol.* **84**, 5494-5507 (2010).

59. Helle, F. *et al.* Role of N-linked glycans in the functions of hepatitis C virus envelope proteins incorporated into infectious virions. *J. Virol.* **84**, 11905-11915 (2010).

60. Goffard, A. & Dubuisson, J. Glycosylation of hepatitis C virus envelope proteins. *Biochimie* **85**, 295-301 (2003).

61. Goffard, A. *et al.* Role of N-linked glycans in the functions of hepatitis C virus envelope glycoproteins. *J. Virol.* **79**, 8400-8409 (2005).

62. Pierson, T.C. *et al.* The stoichiometry of antibody-mediated neutralization and enhancement of West Nile virus infection. *Cell Host Microbe* **1**, 135-145 (2007).
63. Thompson, B.S. *et al.* A therapeutic antibody against west nile virus neutralizes infection by blocking fusion within endosomes. *PLoS Pathog.* **5**, e1000453 (2009).
64. Gottwein, J.M. *et al.* Development and characterization of hepatitis C virus genotype 1-7 cell culture systems: role of CD81 and scavenger receptor class B type I and effect of antiviral drugs. *Hepatology* **49**, 364-377 (2009).

Appendix Table 1: HCV E1&E2 constructs, purification and crystallization attempts.

Construct and polyprotein residues	Vector	Results and purification	Crystallization trials
H77E2 384-660	HTPbac-GFP	Secreted, nickel, SEC	alone +CD81-LEL +H77.16 +H77.34 +H77.16&H77.34 +H77.16, H77.34, chymo +H77.46 +H77.55
H77E2 384-660 C652S	HTPbac-GFP	Secreted, nickel, SEC	+deglyc +deglyc, chymo +deglyc, thrombin, H77.55, CD81 +H77.39 + deglyc, thrombin H77.55, H77.39
J6E2 385-660	HTPbac-GFP	Secreted, nickel, SEC	alone +E1frag +E1frag, CD81-LEL +CD81-LEL +J6.36
ΔHVR1 H77E2 384-386, 410-660	HTPbac-GFP	Secreted, nickel, SEC	
ΔHVR1 J6E2 384-386, 410-660	HTPbac-GFP	Secreted, nickel, SEC	
ΔHVR1 J6E2-cys 384-386, 410-652	HTPbac-GFP	Secreted, nickel, SEC	+deglyc, +deglyc+J6.36
H77E2 short 384-520	HTPbac-GFP	Secreted, misfolded	-
H77E2 med 384-605	HTPbac-GFP	Secreted, misfolded	-
J6E2 short 385-518	HTPbac-GFP	Secreted, misfolded	-
J6E2 med 385-603	HTPbac-GFP	Secreted, misfolded	-
H77E2 8cys 384-563	HTPbac-GFP	Secreted, misfolded	-
H77E2 10cys 384-580	HTPbac-GFP	Secreted, misfolded	-
ΔHVR1 H77E2 8cys 384-386, 410-580	HTPbac-GFP	Secreted, misfolded	-
ΔHVR1 H77E2 10cys 384-386, 410-563	HTPbac-GFP	Secreted, misfolded	-
H77E2 384-660	Pet21a(+)	Did not refold	-
J6E2 8cys 384-563	Pet21a(+)	Did not refold	-

J6E2 10cys 384-580	Pet21a(+)	Did not refold	-
J6E2 12cys 384-596	Pet21a(+)	Did not refold	-
J6E2 385-660	Pet21a(+)	Did not refold	-
J6E2 short 385-518	Pet21a(+)	Did not refold	-
J6E2 med 385-603	Pet21a(+)	Did not refold	-
J6E2 8cys 384-563	Pet21a(+)	Did not refold	-
J6E2 10cys 384-580	Pet21a(+)	Did not refold	-
J6E2 12cys 384-596	Pet21a(+)	Did not refold	-
J6E2 cys14-16 590-655	Pet21a(+)	Did not refold	-
J6E1 frag 191-262	Pet21a(+)	Refolded, disordered	-
J6E1 short 191-269	HTPbac-GFP	Secreted, misfolded	-
J6E1 long 191-334	HTPbac-GFP	Not secreted	-
Yeast constructs			
H77 E2	PYD1	Displayed	-
H77 E2 region 1	PYD1	Displayed	-
H77 E2 region 2	PYD1	Displayed	-
J6 E2	PYD1	Displayed	-
J6 E2 region 1	PYD1	Displayed	-
J6 E2 region 2	PYD1	Displayed	-
J6 E1 short 191-262	PYD1	Displayed	-
UKN 3a13.6 E2 385-667	PYD1	Displayed	-
UKN 4.21.16 E2 392-663	PYD1	Displayed	-
SA13 (5a) E2 384-663	PYD1	Displayed	-
UKN 6 E2 385-668	PYD1	Displayed	-

If a crystallization attempt is listed, this indicates the automated or manual setup of at least 192 sparse matrix conditions.

Legend:
+ thrombin: sE2 was incubated with 50U/mg thrombin overnight at 4 degrees
+ chmyo: 0.1% w/w chymotrypsin was added to the stock prior to screening
+ CD81-LEL: equimolar CD81-LEL was added to the stock prior to screening
+ E1 frag: equilmolar refolded E1 192-262 peptide was added to the stock
+ deglyc: E2 was pre-treated with Endo F1, Endo F3 and PngaseF as described in **4.6.3**
+ H77.XX or +J6.XX: E2 was complexed with sE2 prior to screening